# Identification and characterisation of the haematopoietic stem/progenitor cells at risk for leukaemia development following radiation exposure




A thesis submitted to the Division of Medical Sciences
of the University of Oxford
by

Tom Verbiest

for the Degree of Doctor of Philosophy

Trinity Term 2016

## Abstract

A variety of epidemiological studies have provided support for an increased leukaemia incidence following exposure to both high and low dose radiation. There is a close histopathological similarity between human and murine acute myeloid leukaemia with mouse models of the disease being most often used. We report here, for the first time, that allogeneic haematopoietic stem cells can compete for niches in the nonmyeloablated NSG bone marrow compartment and that the nonmyeloablated NSG bone marrow microenvironment is capable of supporting allogeneic long-term HSC engraftment and differentiation. Using this NSG transplantation model, we then provided evidence of a reduced contribution of low dose irradiated HSCs towards long-term haematopoiesis. We further report on the generation and characterisation of a novel Chr2MDR$^{mCh}$ mouse model where a construct positioned in the minimal deleted region following radiation exposure carries the fluorescent protein mCherry, which is expressed under control of the ubiquitous Rosa26 promoter. Crossing these mice with *Sfpi1*$^{GFP}$ mice allowed the early detection of an expanding haematopoietic clone which had lost mCherry fluorescence following radiation exposure (and so also the chromosome 2 homologue carrying the fluorescent construct and the *Sfpi1* gene). Finally, we report on a gender-dependent leukaemic progression and characterisation where 3 Gy irradiated male mice only present with acute myeloid leukemia and irradiated female mice mainly develop leukaemia with a lymphoid phenotype. In conclusion, the work in this thesis postulates data obtained from two novel mouse models and which could help to further identify key molecular mechanisms involved in leukaemia initiation and development.

## Preface

Some parts of chapter 1 were previously published as a review manuscript by myself, Dr Simon Bouffler, Professor Stephen Nutt and Dr Christophe Badie [Verbiest T, Bouffler S, Nutt S, Badie C (2015) PU.1 downregulation in murine radiation-induced acute myeloid leukaemia (AML): from molecular mechanism to human AML. Carcinogenesis. 36 (4): 413-419]. I was responsible for writing most of the manuscript with excellent guidance and editing by the other authors.

The longitudinal blood sampling data described in section 3.4 has been presented as a poster at the 2015 Public Health England National PhDs' Student Day and was awarded the first prize in the category 'Best poster presentation'.

All animal procedures performed in this doctoral project conformed to the UK Animals (Scientific Procedures) Act, 1986, Amendment Regulations 2012, and animal experimental protocols were reviewed and approved by the local Ethics Committee and the Home Office.

## Table of Contents

**ABSTRACT** ..... **II**

**PREFACE** ..... **III**

**TABLE OF CONTENTS** ..... **IV**

**LIST OF TABLES** ..... **VII**

**LIST OF FIGURES** ..... **VIII**

**LIST OF ABBREVIATIONS** ..... **XI**

**ACKNOWLEDGEMENTS** ..... **XIII**

**1. INTRODUCTION** ..... **2**

1.1. Radiation-induced leukaemia ..... 2

1.2. Murine modelling of radiation-induced leukaemia ..... 4

1.3. Cytogenetic aberrations following X-ray exposure ..... 4

1.4. *Sfpi1* exon 5 point mutation ..... 6

1.5. Target cells for rAML development ..... 9

1.6. PU.1 and haematopoietic cell fate ..... 12

1.7. Gene regulation by PU.1 ..... 14

1.8. PU.1 and myeloid leukaemia ..... 15

1.9. Relationship between murine rAML and human (t)AML ..... 16

1.10. Research objectives ..... 22

**2. METHODOLOGY** ..... **24**

2.1. Mouse models ..... 24

*2.1.1. NOD scid gamma mice* ..... *24*

*2.1.2. Sfpi1$^{GFP}$ transgenic mice* ..... *24*

*2.1.3. Chr2MDR$^{mCh}$ transgenic mice* ..... *24*

2.1.3.1. DNA isolation from ear clips ..... 26

2.1.3.2. PCR and agarose gel electrophoresis ..... 26

2.2. X-ray exposure ..... 27

2.3. Tissue harvest and cell preparation ..... 27

2.4. Immunomagnetic negative selection of haematopoietic stem and progenitor cells 28
2.5. Flow cytometry analysis and cell sorting ..... 28
2.6. Long-term transplantation assays ..... 29
2.7. Histology ..... 30
2.8. Suspension cultures ..... 30
2.9. Colony forming cell assay ..... 31
2.10. Mitochondrial stains ..... 31
*2.10.1. Mitochondrial mass ..... 31*
*2.10.2. Mitochondrial membrane potential ..... 32*
*2.10.3. Mitochondrial superoxide ..... 32*
2.11. Cell cycle analysis ..... 32
2.12. Gene expression analysis ..... 33
*2.12.1. RNA isolation ..... 33*
*2.12.2. Reverse transcription ..... 33*
*2.12.3. Multiplex quantitative real time-PCR ..... 34*
2.13. rAML induction and tissue preparation ..... 34
2.14. Immunophenotyping of rAMLs ..... 36
2.15. DNA isolation from rAML spleens and sequencing for *Sfpi1* and *Flt3* ..... 37
2.16. PCR for GFP construct detection in rAML samples ..... 38
2.17. Chromosome preparations ..... 39
2.18. Transplantation of leukaemic cells – 'passaging' ..... 39
2.19. Statistical analysis ..... 39
**3. RESULTS AND DISCUSSION ..... 41**
3.1. NSG mice are 'permissive' to allogeneic HSC transplantation without prior conditioning ..... 41
*3.1.1. Establishment of a novel transplantation model in unconditioned NSG mice ..... 42*
*3.1.2. Determination of donor contribution towards haematopoiesis in NSG mice ..... 44*
*3.1.3. Feasibility of transplantation following in vivo X-irradiation of donor HSCs ..... 48*
*3.1.4. Unconditioned NSG mice allow rAML passaging ..... 49*
*3.1.5. Discussion ..... 51*

3.2. Chr2MDR$^{mCh}$ mice express mCherry across HSCs and downstream haematopoietic lineages ..... 55

*3.2.1. Generation and maintenance of the Chr2MDR$^{mCh}$ reporter mouse model ..... 56*

*3.2.2. Characterisation and radiation response of Chr2MDR$^{mCh}$ mice ..... 58*

*3.2.3. Discussion ..... 74*

3.3. *In vivo* ionising radiation alters the transplantation potential, mitochondrial function and gene expression of murine HSCs ..... 81

*3.3.1. Both high and low dose ionising radiation exposure reduce the contribution of irradiated HSCs towards long-term haematopoiesis ..... 82*

*3.3.2. Mitochondrial function, gene expression and cell cycle of HSCs following in vivo radiation exposure ..... 91*

*3.3.3. Discussion ..... 100*

3.4. Murine radiation leukaemogenesis is a complex process with a variable rate of progression ..... 107

*3.4.1. Generation and characterisation of the Sfpi1$^{mCh/GFP}$ reporter mouse model ..... 108*

*3.4.2. Clonal expansion of chromosome 2 deleted WBCs following radiation exposure ... 111*

*3.4.3. rAML progression, presentation and characterisation is gender dependent ..... 125*

*3.4.4. Discussion ..... 152*

**4. GENERAL DISCUSSION AND CONCLUSION ..... 164**

4.1. General discussion ..... 164

4.2. Conclusion ..... 171

**5. FUTURE DIRECTIONS ..... 174**

**6. REFERENCES ..... 177**

**7. APPENDIX ..... 189**

## List of Tables

Table 1. Frequency of *Sfpi1* R235 point mutations in murine rAML ..... 7

Table 2. mCherry primer sequences ..... 26

Table 3. GFP primer sequences ..... 38

Table 4. Cell marker expression following radiation exposure ..... 69

Table 5. mCherry chimerism in secondary NSG mice ..... 89

Table 6. Summary of leukaemic mice described above ..... 151

Table 7. Spleen cell surface marker expression of leukaemic mice ..... 151

## List of Figures

Figure 1.1 Involvement of PU.1 in murine rAML and human primary AML ..... 20

Figure 2.1 Location of the ZFN target site and detailed view of primer locations..... 25

Figure 3.1 Flow cytometry analysis of NSG, NSG$^{GFP}$ and *Sfpi1*$^{GFP}$ peripheral blood WBCs..... 43

Figure 3.2 Immunomagnetic selection of haematopoietic stem and progenitor cells..... 45

Figure 3.3 Donor WBC chimerism following transplantation in unconditioned NSGs ..... 47

Figure 3.4 Immunophenotyping of NSG and NSG$^{AML}$ peripheral blood WBCs..... 50

Figure 3.5 Chr2MDR$^{mCh}$ mouse model characterisation ..... 59

Figure 3.6 Radiation response of Chr2MDR$^{mCh}$ haematopoietic stem and progenitor cells..... 61

Figure 3.7 Blood composition of Chr2MDR$^{mCh}$ mice following radiation exposure..... 64

Figure 3.8 Chr2MDR$^{mCh}$ mice show mCh- clonal expansion following radiation exposure..... 65

Figure 3.9 GFP and mCherry expression in CFC assays following radiation exposure..... 72

Figure 3.10 Unconditioned NSG mice are permissive to allogeneic HSC transplantation..... 83

Figure 3.11 Radiation-dependent changes in peripheral blood chimerism following transplantation of Chr2MDR$^{mCh}$ haematopoietic stem and progenitor cells..... 85

Figure 3.12 Changes in Sca1 and cKit expression following radiation exposure ..... 86

Figure 3.13 Expression of HSC cell surface markers in CBA/H and C57BL/6 mice..... 92

Figure 3.14 Changes in CD27+CD201+ cells following radiation exposure..... 94

Figure 3.15 Gene expression and cell cycle following radiation exposure ..... 98

Figure 3.16 Characterisation of *Sfpi1*$^{mCh/GFP}$ mice..... 110

Figure 3.17 Mixed lineage mCherry- clonal expansion in the peripheral blood WBCs..... 112

Figure 3.18 Lymphoid mCherry- clonal expansion in the peripheral blood WBCs ..... 113

Figure 3.19 Mixed lineage mCherry- clonal expansion in the haematopoietic stem and progenitor cell fraction of an irradiated *Sfpi1*$^{mCh/GFP}$ mouse ..... 115

Figure 3.20 Myeloid-biased mixed lineage mCherry- clonal expansion in the haematopoietic stem and progenitor cell fraction of an irradiated *Sfpi1*$^{mCh/GFP}$ mouse ..... 117

Figure 3.21 Lymphoid mCherry- clonal expansion in the haematopoietic stem and progenitor cell fraction of an irradiated *Sfpi1*$^{mCh/GFP}$ mouse..... 119

Figure 3.22 mCherry expression in the haematopoietic stem and progenitor cell fraction of a sham-irradiated *Sfpi1*$^{mCh/GFP}$ mouse..... 120

Figure 3.23 Cell surface marker expression of mCherry- WBCs..... 121

Figure 3.24 GFP expression is upregulated in peripheral blood WBCs following chromosome 2 deletion ..... 122

Figure 3.25 GFP expression is upregulated in bone marrow cells following chromosome 2 deletion ..... 123

Figure 3.26 No further increase of *Sfpi1*-GFP expression upon AML progression..... 126

Figure 3.27 Immunophenotyping of spleen cells obtained from mouse mCh46.1..... 128

Figure 3.28 mCh46.1 rAML characterisation ..... 129

Figure 3.29 Serial blood sampling of mouse mCh50 revealed changes in the FSC/SSC plot prior to AML presentation ..... 131

Figure 3.30 mCh50 rAML characterisation..... 133

Figure 3.31 Mixed lineage mCherry- clonal expansion in the peripheral blood WBCs of female mice..... 136

Figure 3.32 Lymhoid mCherry- clonal expansion in the peripheral blood WBCs of mouse mCh240 ..... 137

Figure 3.33 mCh240 rAML characterisation ..... 139

Figure 3.34 Decreased lymphocytes in the peripheral blood of mouse mCh68..... 141

Figure 3.35 mCh68 rAML characterisation..... 143

Figure 3.36 Tail vein blood sampling detects rapid WBC size change in mouse mCh27 ..... 145

Figure 3.37 mCh27 rAML characterisation..... 147

Figure 3.38 mCh82 rAML characterisation..... 150

Figure 3.39 Different pathways observed in male mice following radiation exposure ..... 161

Figure 3.40 Different pathways observed in female mice following radiation exposure..... 162

## List of Abbreviations

| | |
|---|---|
| **AML** | acute myeloid leukaemia |
| **APC** | allophycocyanin |
| **bp** | base pair |
| **CFC** | colony forming cell |
| **CFU** | colony forming unit |
| **CMP** | common myeloid progenitor |
| **CLP** | common lymphoid progenitor |
| **FBS** | foetal bovine serum |
| **FISH** | fluorescent in situ hybridisation |
| **FITC** | fluorescein isothiocyanate |
| **FSC/SSC** | forward scatter/side scatter |
| **GFP** | green fluorescent protein |
| **GMP** | granulocyte/macrophage progenitor |
| **HSPC** | haematopoietic stem and progenitor cell |
| **IMDM** | Iscove's Modified Dulbecco's Media |
| **IV** | intravenous |
| **IP** | intraperitoneal |
| **kb** | kilobase |
| **LSK** | Lin-Sca1+cKit+ |
| **LT-HSC** | long-term HSC |
| **MDR** | minimal deleted region |
| **MEP** | megakaryocyte/erythroid progenitor |
| **MP** | myeloid progenitors |
| **MPP** | multi-potent progenitors |

| | |
|---|---|
| **NSG** | NOD *scid* gamma |
| **PBS** | phosphate buffered saline |
| **PCR** | polymerase chain reaction |
| **PE** | phycoerythrin |
| **rAML** | radiation-induced AML |
| **RT** | room temperature |
| **SEM** | standard error of the mean |
| **tAML** | therapy-related AML |
| **TBM** | total bone marrow |
| **URE** | upstream regulatory element |
| **WBC** | white blood cell |
| **ZFN** | zinc finger nuclease |
| **7-AAD** | 7-amino-actinomycin D |

## Acknowledgements

I would like to express my sincere appreciation to all those who supported and guided me throughout this doctoral research project. In particular, I would like to thank my Public Health England supervisor Dr Christophe Badie for hosting me over the past three years in his research group at the 'Centre for Radiation, Chemical and Environmental Hazards' (Harwell, UK). He critically evaluated my results and hypotheses, and allowed me to share my data with various experts in the field of radiation leukaemogenesis at national and international meetings. I am also extremely grateful to my colleagues at Public Health England: Dr Rosemary Finnon, Dr Natalie Brown, Paul Finnon and Grainne Manning who greatly expanded my scientific reasoning and experimental skills. Similarly, I would like to express my special gratitude to my Oxford University supervisor Professor Peter O'Neill for the excellent guidance and continued feedback on my experimental work and academic progress. Above all, I would like to thank my parents for providing me with the opportunity to pursue my academic career abroad, and my girlfriend for supporting me in the sometimes difficult moments leading up to the submission of this doctoral thesis. Finally, I would like to thank Public Health England for providing me with a doctoral studentship which allowed me to carry out this project.

# CHAPTER 1

*Introduction*

# 1. Introduction

## 1.1. Radiation-induced leukaemia

Just over a decade following the discovery of X-rays by Wilhelm Roentgen in 1895, the first cases of leukaemia were suspected in medical radiation workers (Upton, 1986). Over the past 50 years, a variety of epidemiological studies provided further support for an increased leukaemia incidence following moderate to high dose radiation exposure. The two most widely studied human populations are the atomic bomb survivors and patients receiving radiotherapy as part of their treatment plan.

The continuing epidemiological survey of the Japanese atomic bomb survivors estimates that approximately 50% of all leukaemia cases are associated with radiation exposure. Over the last 15 years of this follow-up, acute myeloid leukaemia (AML) became the predominant radiation-associated leukaemia, accounting for approximately 80% of excess leukaemia cases (Hsu et al., 2013). Similarly, an increased incidence of leukaemia development was reported in patients who received thoracic radiotherapy for breast cancer (Yu et al., 2006; Kaplan et al., 2012) and patients who received pelvic radiotherapy for invasive tumours of the urogenital system (Travis et al., 2000; Wright et al., 2010; Radivoyevitch et al., 2016).

However, over the past three decades, low dose radiation exposure in humans increased two-fold, which can be mainly attributed to a six-fold increase in exposure from medical sources (Brenner and Hall, 2007). Recently, a variety of epidemiological studies of human cohorts exposed to low dose ionising radiation, provided clear evidence for a direct association between low dose radiation exposure and leukaemia.

Firstly, it was reported that the overall cancer incidence was 24% greater for people exposed to computed tomography scans in their childhood than for unexposed children. The incidence increased significantly for leukaemia and many types of solid cancer (Mathews et al., 2013). Another study into low dose medical radiation exposure reported that computed tomography scans in children delivering cumulative doses of approximately 50 mGy almost tripled the risk of developing leukaemia later in life (Pearce et al., 2012). Similarly, positive associations between protracted low dose radiation exposure and leukaemia have been reported for the Techa River Cohort (Krestinina et al., 2013) and radiation-monitored workers (Leuraud et al., 2015). Interestingly, a similar association has been postulated for human cohorts born in areas with high natural background radiation (Kendall et al., 2013; Spycher et al., 2015; Nikkilä et al., 2016).

Although a clear association between radiation exposure and leukaemia development is acknowledged, today, 80 years since two-time Nobel Prize winner Marie Curie died of radiation-induced leukaemia, the underlying mechanisms remain unidentified. Elucidating the cytogenetic and molecular alterations in murine radiation-induced AML (rAML) could provide further insight in the genetic basis of human radiation leukaemogenesis. In this introduction, we provide an overview on our current understanding of the involvement of the haematopoietic transcription factor *Sfpi1* in the initiation and development of murine rAML, and seek to further define its involvement in human primary and therapy-related AML.

## 1.2. Murine modelling of radiation-induced leukaemia

Since 99% of human protein-coding genes are shared with mice and given the power of murine genetic interventions (including gene knock-in/-out), the use of murine models remains the most representative option available to study the cytogenetic and molecular mechanisms underlying radiation leukaemogenesis. The CBA mouse inbred strain is regarded as the primary model in the study of rAML due to the very low background leukaemia incidence (i.e. less than 1 in 1,000 mice), the reproducible rAML induction in ~20% of mice exposed to a single acute 3 Gy whole-body X-irradiation, and the histopathological similarities with human myeloid leukaemia (Major, 1979). The CBA inbred strain originates from the cross of a Bagg albino female and a DBA male. Three rAML susceptible CBA substrains [CBA/H, MRC Harwell (UK); CBA/Ca, Institute of Animal Genetics (UK); CBA/Cne, ENEA Casaccia Laboratory (Italy)] have been extensively used in the study of radiation leukaemogenesis (Rithidech et al., 1999). Beside the CBA strain, three further mouse strains were previously described as moderately susceptible to rAML: the RF, SJL/J, and C3H/He strains (Rivina and Schiestl, 2013).

## 1.3. Cytogenetic aberrations following X-ray exposure

Twenty-four hours following a single acute exposure to 3 Gy whole-body X-irradiation (i.e. optimal rAML induction dose), all CBA/H mice exhibit bone marrow cells carrying chromosome 2 aberrations as assessed by G-banding, at an approximately 2-fold greater frequency in chromosome 2 compared with chromosomes 1 and 3 (Bouffler et al., 1997). Conversely, chromosomal aberration frequencies in chromosomes 1, 2 and 3 of non-susceptible mouse strains (such as C57BL/6 and AKR) are statistically identical

(Darakhshan et al., 2006). Over time, an increasing number of mice show clonal expansion of bone marrow cells with chromosome 2 aberrations. Twelve to eighteen months following radiation exposure, ~20% of the irradiated mice develop rAML (Bouffler et al., 1997). Leukaemic mice present in most cases with an increased white blood cell (WBC) count, hepato-/splenomegaly and myeloblastic infiltration of the bone marrow, liver and spleen (Major, 1979).

The first experimental murine rAML cases were described in the early 1930s (Krebs et al., 1930). However, it was not until 1977 that a partial deletion of one chromosome 2 homologue was reported as the characteristic finding in murine rAML cells (>85% of the rAML cases), irrespective of the radiation quality (high or low linear energy transfer)(Rithidech et al., 1993; Bouffler et al., 1996; Hirouchi et al., 2008; Steffen et al., 2013). Almost 20 years later, the loss of a putative tumour suppressor gene in the minimal deleted region (MDR) on chromosome 2 was postulated (Alexander et al., 1995), followed a few years later by the identification of the *Sfpi1* gene which encodes the transcription factor PU.1 (Silver et al., 1999). Fe-ion-irradiated mice initially showed two to three times more *Sfpi1* deleted cells than X- or γ-irradiated mice, but by 1 month post-irradiation, similar numbers were observed in both groups, indicating that although Fe-ions induce *Sfpi1* deletions more effectively, they also cause more damage to the cells than sparsely ionising radiation and eventually result in increased cell killing. rAML-resistant C57BL/6 mice had significantly fewer *Sfpi1* deleted cells compared with rAML-susceptible mice, and the deleted cells did not persist in the C57BL/6 mice, irrespective of the radiation quality (Peng et al., 2009). Genetic

background therefore seems to play an important role in radiation-induced leukaemogenesis.

Aside of a consistent partial chromosome 2 deletion, secondary chromosomal aberrations were reported in more than 30% of murine rAMLs: (i) loss/gain of the Y chromosome (Rithidech et al., 1993; Bouffler et al., 1996), (ii) loss/gain of chromosome 6 (Rithidech et al., 1993; Bouffler et al., 1996) and (iii) allelic loss on chromosome 4 (*Lyr2*/TLSR5)(Rithidech et al., 1993; Cleary et al., 2001). Most chromosome 2 deletions are extensive (>20 cM, representing 33% to 66% of chromosome 2), while most chromosome 4 deletions are relatively small (<10 cM; involving less than 10% of chromosome 4)(Cleary et al., 2001).

### 1.4. *Sfpi1* exon 5 point mutation

Interestingly, in ~85% of murine rAML cases with a chromosome 2 deletion, the remaining *Sfpi1* copy exhibits point mutations confined to a single CGC codon in exon 5, central to the DNA binding domain of the protein (Table 1; *Sfpi1* DNA sequence from the Mouse Genome Informatics [MGI] entry MGI:98282). The amino acid residue arginine 235 (known as R235) is replaced with cysteine (R235C; 62%), histidine (R235H; 9%), serine (R235S; 8%) or leucine (R235L; 2%). The first cytosine of the CGC sequence is often methylated (Cook et al., 2004; Steffen et al., 2013). Spontaneous deamination of 5-methylcytosine leads to a C to T transition via uracil formation and the replacement of thymine in one of the two daughter strands during the next replication round.

**Table 1. Frequency of *Sfpi1* R235 point mutations in murine rAML**

| Genetic background | AML-SG | Radiation quality | Gy | WT R235 CGC | R235C *T*GC | R235H C*A*C | R235L C*T*C | R235S *A*GC |
|---|---|---|---|---|---|---|---|---|
| CBA/H | 2 | X-ray | 3 Gy | 17% | nd | nd | nd | nd |
| C3H/He | 2 | X-ray | 3 Gy | 19% | 67% | 0 | 0 | 15% |
| | 2 | γ-ray | 3 Gy | 22% | 50% | 11% | 0 | 17% |
| (CBA/H × SJL) F1 | 2 | γ-ray | 3 Gy | 13% | 54% | 18% | 5% | 3% |
| CBA/CaJ | 2 | γ-ray | 2 Gy | 0 | 100% | 0 | 0 | 0 |
| | | | 3 Gy | 14% | 86% | 0 | 0 | 0 |
| CBA/H | 2 | neutron | 0.4 Gy | 44% | 56% | 0 | 0 | 0 |
| (CBA/H × C57BL/6) × CBA/H | 1.5 | X-ray | 3 Gy | 14% | 66% | 7% | 3% | 10% |
| (CBA/H × C57BL/6) F1 | 1 | X-ray | 3 Gy | 18% | nd | nd | nd | nd |
| (CBA/H × C57BL/Lia) F1 (C3H/He × C57BL/6J) F1 | 1 | X-ray | 3 Gy | 33% | 49% | 2% | 0 | 16% |
| (CBA/H × C57BL/6) × C57BL/6 | 0.5 | X-ray | 3 Gy | 89% | 0 | 0 | 0 | 11% |

nd, not determined; SG, susceptible genome

Similarly, the mutation spectrum of 24 human primary AML cases reported mainly transitions, with C to T transition as the most common single nucleotide mutation (Welch et al., 2012). To be noted, TET2, an important epigenetic regulator, which oxidates 5-methylcytosine, is often found mutated in human primary AML (Cancer Genome Atlas Research Network, 2013). Our group has recently sequenced exon 5 in a large murine rAML panel (more than 100 cases). Remarkably, no mutations could be found outside codon 235 (unpublished observations).

Recently, the R235 point mutation was reported as not being a major rate limiting step in murine rAML (Genik et al., 2014). There are data suggesting that this point mutation probably leads to complete abolition of PU.1 activity (Metcalf et al., 2006), and that mice carrying a deletion of the other allele might develop AML relatively soon after the

mutation is acquired. To verify this observation, it will be important to investigate AML frequency and latency in mice engineered to carry a R235 point mutation. It was also postulated that hemizygosity for one of the numerous genes located in the MDR could facilitate radiation leukaemogenesis (Genik et al., 2014). For example, the *DDB2* gene is present in the MDR and is involved in nucleotide excision repair. Nevertheless, this repair pathway is associated with the resolution of bulky adducts and pyrimidine dimerization, and not with abasic sites and damaged bases which are corrected by the base excision repair pathway, and its role in point mutagenesis has yet to be clarified.

The two-hit model of rAML involves a first irreversible mutational hit (i.e. interstitial deletion with loss of the *Sfpi1* gene on one chromosome 2 homologue) creating intermediate cells that have a growth advantage but which are not fully malignant. Subsequently, intermediate cells acquire a second mutational hit (i.e. point mutation in the remaining *Sfpi1* copy), resulting in the formation of a malignant cell which undergoes further clonal expansion and eventually develops into cancer (Dekkers et al., 2011). This two-hit model is supported by the finding that *Sfpi1* mutations are only observed in rAMLs with a partially deleted chromosome 2 homologue (Hirouchi et al., 2008; Steffen et al., 2013). However, our group recently reported the first rAML case harbouring a *Sfpi1* point mutation (R235H) without the accompanying chromosome 2 deletion (Brown et al., 2015). Whereas 87% of (CBA/H x SJL) F1 rAMLs (i.e. 2 rAML-susceptible genomes) harbour *Sfpi1* point mutations (Cook et al., 2004), only 67% of (CBA/H x C57BL/Lia) F1 rAMLs [i.e. one rAML-susceptible genome (CBA/H) and one rAML-resistant genome (C57BL/Lia)] harbour this point mutation (Suraweera et al., 2005). This percentage decreases even further when backcrossing (CBA/H x C57BL/6)

F1 mice to C57BL/6 (11%). Intriguingly, none of these 11% *Sfpi1* point-mutated rAMLs exhibited the most common C to T transition (Jawad et al., 2006). The type of R235 point mutation appears to differentially affect PU.1 mRNA levels in rAML cell lines. Whereas mRNA levels in R235S AMLs are similar to those observed in normal bone marrow, mRNA levels are 4-fold higher in R235C AMLs. Interestingly, PU.1 mRNA levels did not correspond to protein levels (i.e. no detectable protein levels in R235C and R235H AMLs). This discrepancy might be explained by a greater stability of the R235S protein, a differential regulation of mRNA translation, or be related to protein phosphorylation as serine 235 has been identified as a strong novel candidate phosphorylation site (Brown et al., 2011). Furthermore, the mutations were assessed as being deleterious to protein function by a range of bioinformatics approaches. In contrast, several PU.1 target genes (including *Flt3*, *GATA-1* and *c-Jun*) were downregulated, irrespective of the type of R235 mutation (Brown et al., 2011). While the fact that these are single base substitutions suggests that they are of spontaneous origin (Peng et al., 2009), it remains unknown at what time after irradiation these point mutations occur.

### 1.5. Target cells for rAML development

Little is currently known about the characteristics of the 'cell at risk' in radiation leukaemogenesis and it remains unknown whether the mutations leading to leukaemia occur in HSCs or haematopoietic progenitor cells. Adult HSCs reside primarily in the quiescent G0 phase of the cell cycle (Mohrin et al., 2010). Haematopoietic reconstitution following radiation exposure requires the release of the surviving HSCs from their quiescent state into the G1 phase of the cell cycle. Approximately 60% of

surviving HSCs actively cycle for more than 10 months following radiation exposure, with the number of cell divisions per surviving HSC reported ten times as high compared with unexposed mice (Ban and Kai, 2009). Upon entry into the G1 phase of the cell cycle, DNA damage is primarily repaired by error prone non-homologous end-joining, potentially promoting the formation of *de novo* mutations following DNA damage (Mohrin et al., 2010).

Similarly, the enhanced replicative stress contributes to premature HSC ageing and induction of HSC premature senescence in a ROS-dependent manner (Shao et al., 2014), hereby decreasing their DNA repair capacity and rendering them more prone to spontaneous mutations. This hypothesis is further supported by the finding of a common myeloid progenitor-like leukaemic stem cell (Lin-Sca1-cKit+CD34+) in a murine rAML model where it was postulated that, amid continuous cycling to reconstitute the CMP population, chromosome 2 deleted HSCs acquired additional aberrations, including point mutations of the remaining *Sfpi1* allele (Hirouchi et al., 2011).

The increased mutation rate with age might also play a role in the acquisition of secondary point mutations, hereby explaining the relatively long latency between exposure and rAML presentation (Steffen et al., 2013). In addition, PU.1 directly regulates the HSC cell cycle machinery by inhibition of cell cycle activators and induction of cell cycle inhibitors: loss of PU.1 autoregulation dysregulated the balanced cell cycle regulation, leading to excessive proliferation (Staber et al., 2013), thereby increasing the acquisition of point mutations, and eventually resulting in either exhaustion of the HSC pool or leukaemia.

Mitochondria are considered as the bioenergetic and biosynthetic organelles in the HSC, and can be affected by ionising radiation through various pathways. As the repair mechanisms of mitochondrial DNA are not as efficient as those found in the nucleus, mitochondrial DNA is regarded more susceptible to radiation-induced DNA damage than genomic DNA. Besides, mitochondrial DNA does not have histones, resulting in a decreased resistance to such insults and a higher mutation rate (Yakes and Van Houten, 1997). Exposure to ionising radiation has also been reported to generate both intracellular and mitochondrial oxidative stress. Interestingly, radiation-induced mitochondrial production of reactive oxygen species has been reported to be more influential in mediating cellular damage compared with reactive oxygen species produced in different parts of the cell (Azzam et al, 2012). Severe mitochondrial damage can trigger apoptosis or autophagy. Or in the event of lesser damage, result in mitochondrial fusion, hereby providing complementation between damaged mitochondria and supporting their functionality (Youle and van der Bliek, 2012). Exposure to ionising radiation has been reported to induce a 1.5- to 4-fold increase in mitochondrial mass, which supports a theory of increased mitochondrial fusion following radiation exposure (Nugent et al, 2007).

Recent advances in genetic engineering of mouse models allow tracking of cytogenetic alterations in living cells, from the time of irradiation and throughout tumour ontogenesis. In 2005, the Nutt laboratory generated a *Sfpi1*$^{GFP}$ reporter mouse strain containing an internal ribosome entry site GFP cassette adjacent to the *Sfpi1* gene within the radiation-induced MDR (Nutt et al., 2005). Therefore, green fluorescent protein (GFP) expression decreases (homozygous *Sfpi1*$^{GFP}$ mice) or disappears

(heterozygous *Sfpi1*$^{GFP}$ mice) following a radiation-induced interstitial chromosome 2 deletion, allowing this leukaemia initiating event to be detected by flow cytometry in live leukaemic cells (Olme et al., 2013b). Using fluorescent in situ hybridisation, our group previously demonstrated that interstitial chromosome 2 deletions are present in the HSC-enriched Lin- Sca1+ cKit+ subpopulation, but are not observed in the more differentiated lineage-negative cells (Olme et al., 2013a).

### 1.6. PU.1 and haematopoietic cell fate

Beyond its role as a tumour suppressor, PU.1 plays a vital role in commitment and maturation of the lymphoid and myeloid lineages. Analysis of *Sfpi1*$^{GFP}$ reporter mouse strains has revealed a dynamic regulation of PU.1 expression in adult haematopoietic cell lineages. All HSCs and common lymphoid progenitors (CLPs) express high levels of PU.1, with expression being reduced to a characteristic low level in early B-cell development. In contrast, two distinct PU.1 expressing subpopulations were identified within the common myeloid progenitors (CMPs). PU.1$^{high}$ CMPs were characterised as precursors of granulocyte/macrophage progenitors (GMPs), while the PU.1$^{low}$ CMPs were reported immediate precursors of the megakaryocyte/erythrocyte progenitors, confirming the hypothesis that downregulated PU.1 expression in CMPs restricts their differentiation to the erythroid and megakaryocytic lineages (Nutt et al., 2005). Small changes in PU.1 expression are also proposed to impact on cell fate decisions of the GMP through alterations in the PU.1 to CEBPA ratio: relatively high PU.1 commits GMPs towards a monocyte/macrophage fate, while increased CEBPA results in commitment towards granulocytes (Dahl et al., 2003). Similarly, lymphomyeloid

progenitors lengthen their cell cycle to allow PU.1 to accumulate to higher levels, which is functionally important for macrophage differentiation (Kueh et al., 2013).

The proximal promoter of *Sfpi1* contains, beside Oct-1, Sp1 and GATA-1 binding sites, binding sites for PU.1, suggesting autoregulation of its expression (Chen et al., 1995). Additional regulation is under control of a conserved distal regulatory enhancer (upstream regulatory element, URE) located -14 kilobase (kb) from the transcriptional start site (Okuno et al., 2005). Targeted deletion of the URE in mice (*Sfpi1*$^{ure/ure}$) reduced the PU.1 expression to approximately 20% of the wild-type level, leading to impaired maturation of myeloid progenitors (Rosenbauer et al., 2004). Molecular analysis of the URE revealed binding sites for various transcription factors, including Elf-1, NF-κB and PU.1 itself (Okuno et al., 2005; N. Bonadies et al., 2010; Staber et al., 2013).

In contrast to *Sfpi1*$^{ure/ure}$ mice, *Sfpi1*$^{-/-}$ embryos (expressing 0% of the wild-type PU.1 protein) die at day 18 of gestation, displaying a multilineage defect in the maturation of erythroblasts and the development of progenitors for granulocytes, monocytes, and B- and T-lymphocytes (Scott et al., 1994). When transplanted in lethally irradiated mice, embryonic stem cells of *Sfpi1*$^{-/-}$ mice contribute to the formation of erythrocytes, but not to cells of myeloid and lymphoid origin (Scott et al., 1997). Six months following transplantation of *Sfpi1*$^{-/-}$ foetal HSCs into lethally irradiated mice, haematopoiesis disappears completely, indicating the essential role of *Sfpi1* in HSC self-renewal. A second *Sfpi1*-deficient mouse model generated by the insertion of a Neomycin resistance cassette into exon 5, survives up to two weeks post-birth and is likely to be a severely hypomorphic allele (McKercher et al., 1996). This conclusion is

supported by the similar early lethality of two further PU.1-knock-down mouse models (*Sfpi1*$^{Blac/Blac}$ and *Sfpi1*$^{BN/BN}$ mice, expressing 2% and 20% of the wild-type PU.1 protein, respectively) generated by inserting a LacZ expression cassette into exon 1 of *Sfpi1* (Kamath et al., 2008).

Conditional deletion models have now overcome the limitations of the early lethality of *Sfpi1*-deficient mice. Inactivation of PU.1 in adult HSCs resulted in severely perturbed haematopoiesis, characterised by excess granulopoiesis and impaired production of other myeloid cells and lymphocytes as well as decreased ability to compete with wild-type HSCs (Dakic et al., 2005). Whereas a *Sfpi1*-knockout in myeloid progenitors inhibited their maturation but not their proliferation, neither maturation nor proliferation of B-cells were altered by a knockout in lymphoid progenitors (Iwasaki et al., 2005).

### 1.7. Gene regulation by PU.1

Recent studies have identified tens of thousands of PU.1 binding sites in the genome (Ghisletti et al., 2010; Heinz et al., 2010). Most of the sites are located in introns and distant intergenic regions, and possess chromatin signatures of enhancers. PU.1 also binds to 80% of promoters associated with actively transcribed genes. Ectopic binding of PU.1 in those studies has an instructive role in nucleosome remodelling, changing chromatin marks and establishing functional enhancers (Heinz et al., 2010). In this sense, PU.1 is considered to have a 'pioneer' role in establishing competence for genes to be regulated, in a positive or negative fashion, depending on the cross-talk with other transcription factors and co-factors. Prominent among the many known PU.1-

regulated genes, are those encoding cytokine receptors and integrins (Dakic et al., 2007; Turkistany and DeKoter, 2011).

PU.1 has long been recognised as a dose-dependent regulator of haematopoietic cell fate determination, but few dose dependent target genes have been reported to date. Examples of dose-sensitive genes include *Flt3*, whose expression is reduced in *Sfpi1*$^{+/-}$ progenitors (Carotta et al., 2010), and *Sfpi1*$^{Blac/Blac}$ and *Sfpi1*$^{BN/BN}$ mice that show a dose-dependent suppression of various T-cell and natural killer cell genes in interleukin-3 dependent myeloid cell lines (Kamath et al., 2008). A direct comparison of gene expression in adult HSCs derived from *Sfpi1*$^{ure/ure}$ and *Sfpi1*$^{-/-}$ [generated from a PU.1 conditional knockout strain (Metcalf et al., 2006)] mice would greatly add to our understanding of how PU.1 functions in a dose-dependent manner.

### 1.8. PU.1 and myeloid leukaemia

In keeping with the role of PU.1 as a suppressor of rAML, *Sfpi1*$^{ure/ure}$ mice or those resulting from the conditional deletion of the DNA binding Ets domain (exon 5) develop AML (Metcalf et al., 2006; Rosenbauer et al., 2004). For both models, approximately 95% of the mice develop AML in 8 months, a significant shortening compared with the 12-18 months latency period following radiation exposure. Leukaemia is observed even earlier (within 3 months) in (PU.1$^{ure/ure}$ x p53$^{-/-}$) F1 mice, only expressing 10% of wild-type PU.1 levels. This highly aggressive AML phenotype is attributed to further upregulation of MYB and miR-155 upon *p53* loss, resulting in additional downregulation of PU.1 (Basova et al., 2013). These data clearly indicate that the transcription factor PU.1 acts as a tumour suppressor. However, *Sfpi1* can also act as an oncogene in other contexts, since PU.1 overexpression inhibits erythroid

lineage maturation, eventually resulting in erythroleukaemia (Moreau-Gachelin et al., 1988).

### 1.9. Relationship between murine rAML and human (t)AML

Therapy-related AML (tAML) arises following exposure to chemo- and/or radiation therapy with an average latency period of five years, and is more frequently accompanied by unbalanced cytogenetic abnormalities compared with primary AML (75% vs 51%, respectively). The cytogenetic abnormalities 5q-/-5 and 7q-/-7 are often overrepresented in tAML. Among patients with a normal karyotype, a similar incidence of molecular abnormalities is observed in both primary AML and tAML (Kayser et al., 2011). A Danish tAML study predominantly observed *FLT3* mutations in patients who previously received radiotherapy and in those patients with a normal karyotype (Pedersen-Bjergaard et al., 2008). The most common aberrations were chromosome 5 and 7 deletions (50-60% of tAMLs), followed by *FLT3*-ITD and *TP53* point mutations in 20% of tAMLs. Interestingly, the genetic defects 5q-/-5 and 7q-/-7 were positively associated with *TP53* and *AML1* point mutations, respectively (Pedersen-Bjergaard et al., 2008). It is important to note that a comparison with murine rAML data is difficult as neither study distinguishes between tAML patients who received radiation therapy alone, chemotherapy alone or a combination of both. To overcome this limitation, our group is currently analysing samples of tAML patients who received radiation therapy alone and which should provide a better understanding of human tAML development following radiation therapy. Similarly, FISH analysis of Japanese AML patients revealed that those patients heavily exposed (>1Gy to the bone marrow) during the Hiroshima

atomic bombings had a higher incidence of chromosomes 5, 7, 13 and 20 deletions, compared with non-exposed Japanese AML patients (Nakanishi et al., 1999).

Recently, our group reported the presence of *Flt3*-ITD mutations in murine rAML (3/30 rAMLs)(Finnon et al., 2012). Remarkably, they were only found in rAML with an intact chromosome 2 and no *Sfpi1* point mutation, suggesting the involvement of *Flt3*-ITD and *Sfpi1* are mutually exclusive, and which is in agreement with published data from the Danish tAML study (Pedersen-Bjergaard et al., 2008). The observed murine *Flt3*-ITD mutations ranged in size from approximately 10 – 30 base pair (bp) and were, similar to those observed in human primary AML, inserted into the tyrosine-rich juxtamembrane domain.

Trisomy 8 is also observed in human primary and therapy-related AML (chromosome 8 is homologous to the murine chromosome 15). Half of the AML cases observed in PU.1$^{ure/ure}$ mice (4/7 AMLs) gained a chromosome 15 copy (Rosenbauer et al., 2004). The smallest region gained contains the proto-oncogene c-Myc. Interestingly, c-Myc expression was significantly elevated in PU.1-knockdown mice with AML (Rosenbauer et al., 2004). Similarly, c-Myc expression levels were significantly elevated in murine rAMLs with a partial chromosome 2 deletion, compared with rAMLs with an intact chromosome 2 (Hirouchi et al., 2008).

Consistent with murine data, heterozygous mutations and deletions of the *SPI1* locus (the human analogue of *Sfpi1*) have been described in human primary AML, although it is a rare event (Mueller et al., 2002). Heterozygous *SPI1* mutations were reported in 9/126 AMLs of a Japanese study (7%, with half of the cases comprising point mutations and the other half deletions). Mutated *SPI1* led to a reduced function of the

transcription factor and the median survival of patients with *SPI1* mutations was significantly shorter than patients without *SPI1* mutations. These mutations were predominantly found in undifferentiated and in (myelo)monocytic leukaemia subtypes, which is in line with the physiologic role of PU.1. Interestingly, they were not observed in leukaemic patients harbouring the chromosome translocations most commonly observed in primary AML, such as AML1-ETO and PML-RARA (Mueller et al., 2002). In contrast with the results of the Japanese AML study, investigations of North-American and European cohorts reported *SPI1* mutations in less than 1% of primary AML patients (Nicola Bonadies et al., 2010).

Four primary AML patients presented with a mutated NF-κB binding site in the URE of *SPI1* (N. Bonadies et al., 2010), thereby suppressing PU.1 mRNA expression. Another primary AML case harboured a deletion spanning at least 40 kb of the *SPI1* locus, including the URE region but no *CEBPA*, *FLT3* and *NPM1* mutations were detected. The PU.1 mRNA level was significantly lower compared with other AML patients and 10 times lower compared with unsorted bone marrow cells obtained from healthy individuals (Nicola Bonadies et al., 2010). Such minor deletions would escape detection by conventional sequencing techniques and may therefore further clarify the conflicting reports on the presence of *SPI1* mutations in human primary AML patients. As the mutations in the PU.1 DNA binding domain observed from human primary AML (Mueller et al., 2002) do not correspond to the residues mutated in murine rAML (Cook et al., 2004), it was speculated that *SPI1* point mutations might be more often associated with tAML. However, a small human tAML study (24 AML patients who had received therapy for a prior malignancy) did not report any *SPI1* mutations in the

coding, untranslated or promotor regions (Suraweera et al., 2005). To our knowledge, there are no studies reporting on *SPI1* mutations in tAML patients who received radiation therapy alone.

Although *SPI1* seems only infrequently mutated in human primary and therapy-related AML, several reports have highlighted downregulated *SPI1* gene/PU.1 mRNA expression in primary AML patients. Approximately half of primary AML patients (9/20 AMLs) had lower *SPI1* gene expression, compared with *SPI1* expression in HSCs from healthy donors (Steidl et al., 2006). Similarly, a Czech primary AML study reported decreased PU.1 mRNA levels in the majority of AML patients (27/36 AMLs)(Basova et al., 2013), which corresponds with our previous finding of decreased PU.1 mRNA levels in murine rAMLs with a wild-type *SPI1* allele (Olme et al., 2013b). Interestingly, *TP53* deletions were only observed in human primary AMLs with low PU.1 levels, and concomitantly with elevated MYB and miR-155 levels, directly linking *TP53* inactivation and a dysregulated MYB/miR-155/PU.1 pathway in human AML (Basova et al., 2013).

Transduction of human primary AML blasts with a lentivector encoding PU.1 increased the myelomonocytic marker expression and decreased proliferation rates together with increasing apoptosis, changes characteristic of restored differentiation in these myeloid leukaemic blasts (Durual et al., 2007). Similarly, all *trans* retinoic acid therapy leads to *in vivo* differentiation of acute promyelocytic leukaemia blasts through increased PU.1 activity (Mueller et al., 2006), resulting in complete remission in almost all leukaemic patients.

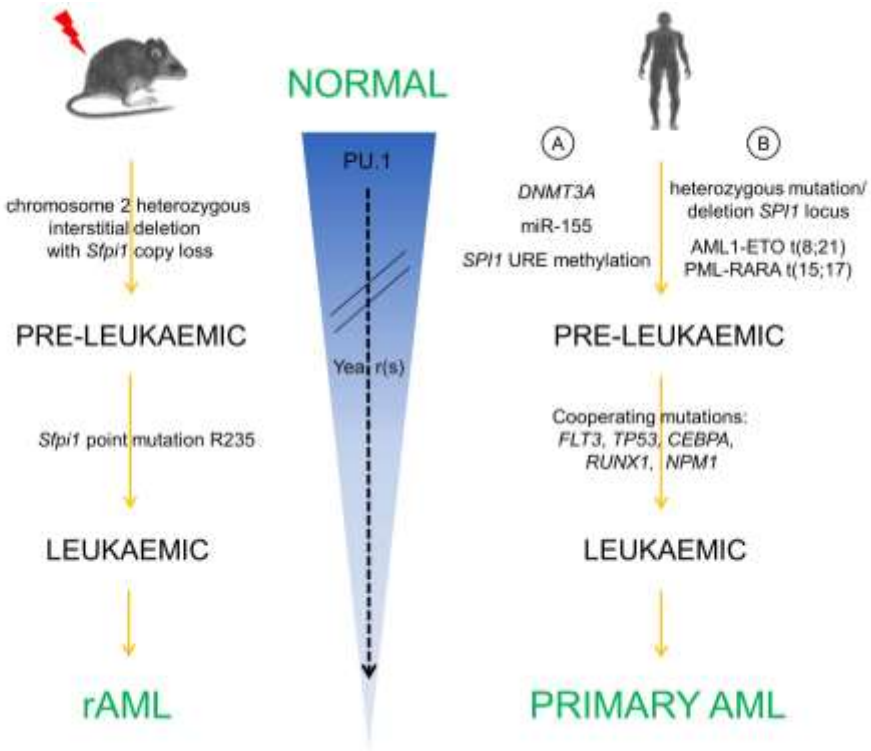



**Figure 1.1 Involvement of PU.1 in murine rAML and human primary AML**

In mice, exposure to ionising radiation induces a first mutational hit in haematopoietic cells (i.e. interstitial deletion of one *Sfpi1* gene on chromosome 2), creating intermediate cells that have a growth advantage but which are not fully malignant. Subsequently, these cells acquire a second mutational hit (i.e. point mutation in the remaining *Sfpi1* copy), resulting in the formation of a leukaemic cell which undergoes further clonal expansion and eventually leads to the development of rAML. In humans, no data is currently available on the involvement of PU.1 in tAML. However, various epigenetic (A) and genetic (B) modifications, contributing towards the formation of pre-leukaemic cells, have been linked with downregulation of PU.1 in human primary AML. These pre-leukaemic cells harbour some, but not all, of the mutations found in leukaemic cells (Corces-Zimmerman and Majeti, 2014). Numerous pre-leukaemic and leukaemic mutations contribute towards PU.1 downregulation in human primary AML, including the top three genes found mutated in human primary AML [*NPM1*, *FLT3*, and *DNMT3A* (Cancer Genome Atlas Research Network, 2013)]. Although the molecular targets seem to differ between species, it appears that a common PU.1 downregulation pathway is affected in murine rAML and human primary AML. Blue intensity indicates PU.1 expression/activity levels (dark equals high levels)(from Verbiest et al., 2015).

Various other mechanisms seem involved in PU.1 downregulation in human primary AML (Figure 1.1). Firstly, the formation of fusion proteins following chromosome translocations, including AML1-ETO in t[8;21] (Staber et al., 2014; Vangala et al., 2003)

and PML-RARA in t[15;17] (Staber et al., 2014; Walter et al., 2005), confers reduced PU.1 expression. Similarly, internal tandem duplications in the *FLT3* receptor tyrosine kinase suppress the PU.1 expression and function (Mizuki et al., 2003; Staber et al., 2014). Finally, with four of the top eight genes found mutated in human primary AML being epigenetic regulators, epigenetic silencing is most likely involved as well (Cancer Genome Atlas Research Network, 2013). This hypothesis is further supported by the findings that miR-155, a known regulator of PU.1 mRNA, is overexpressed in bone marrow samples of some primary AML subtypes (O'Connell et al., 2008), and that in high-risk myelodysplastic syndrome patients PU.1 downregulation is associated with DNA methylation of the PU.1 URE (Curik et al., 2012). In conclusion, although PU.1 is rarely directly mutated in human primary and therapy-related AML, it appears to be commonly downregulated through a series of indirect mechanisms.

## 1.10. Research objectives

The overall objective of the doctoral research presented here is to identify and characterise the haematopoietic stem and progenitor cells at risk for leukaemia development following radiation exposure.

The specific aims of this project are to:

- determine the feasibility of allogeneic HSC engraftment in highly immunodeficient NOD *scid* gamma mice without prior conditioning (i.e. exposed to a lethal dose of radiation to remove the host's bone marrow cells and avoid graft rejection), allowing low dose studies in a more biologically relevant microenvironment;
- generate and characterise a genetically engineered mouse model where the construct positioned in the MDR following radiation exposure carries the fluorescent protein mCherry which is expressed under control of the Rosa26 promoter, allowing detection of chromosome2/*Sfpi1* deletions in live haematopoietic cells;
- establish the effects of *in vivo* low and high dose ionising radiation exposure on murine HSCs and their contribution towards long-term haematopoiesis;
- assess the mitochondrial function of murine HSCs following *in vivo* radiation exposure;
- identify and sort live haematopoietic cells carrying the chromosome2/*Sfpi1* deletion, and investigate the key chromosomal and molecular mechanisms involved in leukaemia initiation and development in mice.

# CHAPTER 2

*Methodology*

# 2. Methodology

## 2.1. Mouse models

### 2.1.1. NOD *scid* gamma mice

Male eight week old NOD *scid* gamma (NSG) mice were obtained from Charles River (Margate, UK), housed in containment isolators and habituated for two weeks prior to experimental use. Mice were provided with sterile water and food *ad libitum* and subjected to a 12 h light/12 h dark cycle.

### 2.1.2. *Sfpi1*$^{GFP}$ transgenic mice

C57BL/6 mice expressing GFP as a reporter for *Sfpi1* were established at the Walter and Eliza Hall Institute of Medical Research (Melbourne, Australia) through the insertion of an IRES-GFP cassette in the 3' untranslated region of the gene under control of the *Sfpi1* promoter, resulting in a variable GFP expression throughout the different haematopoietic subpopulations (Nutt et al., 2005). Mice were rederived and backcrossed to a CBA/H background at the Mary Lyon Centre (MRC Harwell, UK) for ten generations before being used for experimental purposes. Mice were provided with water and food *ad libitum*.

### 2.1.3. Chr2MDR$^{mCh}$ transgenic mice

A Zinc Finger Nuclease (ZFN) pair targeting the insertion site (chr2: 92,823,765 - 92,823,766; ~1.7 Mb from *Sfpi1*), together with a Rosa26 donor vector, were microinjected into the nucleus of one-cell CBA embryos at SAGE® Labs (Boyertown, USA). Details of the insertion site on chromosome 2 and position of primers used for genotyping are presented in Figure 2.1. Mice were rederived at the Mary Lyon Centre (MRC Harwell, UK), and transferred to our facilities for breeding.

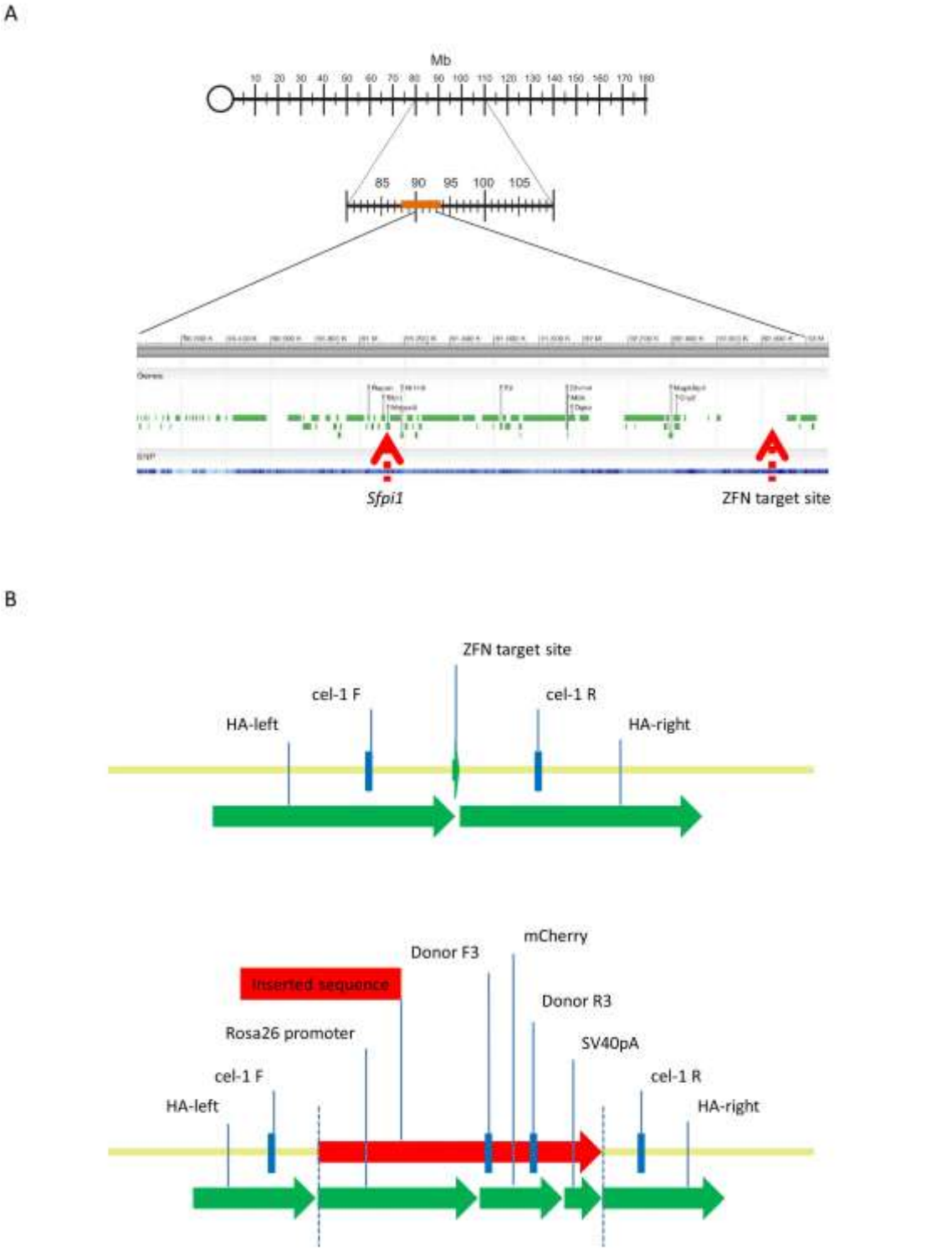



**Figure 2.1 Location of the ZFN target site and detailed view of primer locations**

(A) Both the *Sfpi1* gene (91,082,390 – 91,115,756 bp) and the ZFN target site (92,823,765 bp) are located within the MDR on chromosome 2 (MDR indicated in orange, modified from Brown et al., 2015). (B) The four primer binding sites (cel-1 F, cel-1 R, donor F3 and donor R3) and the ZFN target site are indicated.

#### 2.1.3.1. *DNA isolation from ear clips*

Genotyping was performed at weaning age by submerging ear clips overnight in 25 µl lysis buffer (1.25 µl 1 M Tris pH 8, 0.167 µl 3 M NaCl, 0.25 µl 10% sodium dodecyl sulfate, 20.9 µl $dH_20$, and 2.5 µl proteinase K). Following incubation, 20 µl $dH_20$ was added and centrifuged at 10,000 rpm for 5 min. Chelex 100 [12 µl; 0.5 g BT Chelex® 100 Resin (Bio-Rad, Hemel Hempstead, UK), 10 ml 10 mM Tris, 10 ml 0.1mM EDTA] was added to the supernatant, incubated at 37 °C for 30 min and 100 °C for 5 min, and centrifuged at 13,000 rpm for 5 min. Supernatant was stored at -20 °C until analysis. All reagents were obtained from Sigma-Aldrich (Dorset, UK), unless otherwise stated.

#### 2.1.3.2. *PCR and agarose gel electrophoresis*

Genotyping polymerase chain reaction (PCR) used 1 µl of extracted DNA in 24 µl PCR master mix [1.5 µl $H_20$, 2.5 µl 10 µM primer 'cel-1 F', 2.5 µl 10 µM primer 'cel-1 R', 2.5 µl 10 µM primer 'donor F3', 2.5 µl 10 µM primer 'donor R3', 12.5 µl Jumpstart™ Taq ReadyMix™ (Sigma-Aldrich)] and amplified at the following conditions: 5 min at 95 °C, then 35 cycles of (30 sec at 95 °C, 30 sec at 60 °C and 60 sec at 68 °C), followed by 5 min at 68 °C (Veriti® 96-well Thermal Cycler; Thermo Fisher Scientific, Paisley, UK). Primers were obtained from Integrated DNA Technologies (IDT, Leuven, Belgium) and primer sequences can be found in Table 2. PCR products were resolved on 1% agarose gels (75 V for 60 min) and gel images were obtained using a Gel Doc system (Bio-Rad).

**Table 2. mCherry primer sequences**

| | |
|---|---|
| cel-1 F | 5'-GTGACTCCCAACATCTGCCT-3' |
| cel-1 R | 5'-CTGCTTGCTTGCAGACTGAG-3' |
| donor F3 | 5'-AAGGGCGAGGAGGATAACAT-3' |
| donor R3 | 5'-CTTCAGCTTCAGCCTCTGCT-3' |

Band size: $Chr2MDR^{wt}$, 383 bp; $Chr2MDR^{mCh}$, 510 bp

## 2.2. X-ray exposure

Both *in vitro* and *in vivo* irradiations were performed at the Centre for Radiation, Chemical and Environmental Hazards (Public Health England, Harwell, UK) using the same X-ray source (AGO, Reading, UK; 250 kVp and 13 mA) with a dose rate of 4.9 mGy/min or 0.5 Gy/min (doses ≤100 mGy and doses >100 mGy, respectively). *In vitro* irradiations were performed at room temperature while cells were suspended in growth medium.

## 2.3. Tissue harvest and cell preparation

Mice were sacrificed using a rising concentration of $CO_2$, and upon dissection, blood was collected through cardiac puncture with a 0.5 ml insulin syringe and deposited into an EDTA blood collection tube (BD Biosciences, Oxford, UK). Red blood cells were lysed with lysis buffer (20:1; 20.75 g $NH_4$ Cl, 2.5 g NaH CO3 and 0.093 g $Na_2$ EDTA in 1,000 ml $dH_2O$) for 5 min at room temperature (RT), and washed in phosphate buffered saline (PBS). The spleen was removed and a sterile single cell suspension generated by disaggregation with an 18 G needle. The cell suspension was passed through a 40 micron cell strainer (BD Biosciences) and stored on ice until further processing.

Femurs, tibias, iliac crests and spine were removed, cleaned and crushed in a small volume Iscove's Modified Dulbecco's Media (IMDM) using a morter and pestle. A single cell bone marrow suspension was generated by disaggregation with an 18 G needle and passed through a 40 micron cell strainer. White blood cell, spleen cell and bone marrow cell number were determined using a Neubauer haemocytometer with 0.4% trypan blue to exclude dead cells. All reagents were obtained from Sigma-Aldrich, unless otherwise stated.

## 2.4. Immunomagnetic negative selection of haematopoietic stem and progenitor cells

A bone marrow cell suspension was prepared at 1 x $10^8$ cells/ml EasySep™ Buffer in a 5 ml Falcon™ polystyrene round-bottom tube (BD Biosciences). Both Normal Rat Serum and EasySep™ Mouse Hematopoietic Progenitor Cell Isolation Cocktail were added at 50 µl/ml of cells. Following incubation for 15 min on ice, EasySep™ Streptavidin™ RapidSpheres were added at 75 µl/ml of cells and incubated for another 10 min on ice. EasySep™ Buffer was added to bring the cell suspension up to a total volume of 2.5 ml and the tube was placed into the EasySep™ Magnet for 3 min at RT, after which the negative fraction containing the haematopoietic stem and progenitor cells (HSPCs) was poured off into a fresh tube. The cell number was determined using a Neubauer haemocytometer with 0.4% trypan blue. All reagents were obtained from Stem Cell Technologies, Grenoble, France, unless otherwise stated.

## 2.5. Flow cytometry analysis and cell sorting

Bone marrow cells were negatively selected for haematopoietic stem and progenitor cells by immunomagnetic negative selection, resuspended in EasySep™ Buffer and primary conjugated antibodies were added. The following antibodies conjugated with phycoerythrin (PE), PE-Cy5, PE-Cy7, fluorescein isothiocyanate (FITC), allophycocyanin (APC) or APCeFluor®780 were used: Sca1 (D7; Affymetrix, High Wycombe, UK), cKit (2B8; Affymetrix), CD27 (LG.3A10), CD48 (HM48-1; Affymetrix), CD127 (A7R34; Affymetrix), CD150 (TC15-12F12.2) and CD201 (RCR-16). Preincubation with unconjugated anti-FcRII/III (2.4G2; BD Biosciences) was used to reduce nonspecific binding. All reagents were purchased from BioLegend, unless otherwise stated, and diluted to the manufacturers' recommendations. Following incubation for 30 min on

ice, cells were washed twice in EasySep™ Buffer. Flow cytometry acquisition and sorting was performed using a MoFlo XDP (Beckman Coulter, High Wycombe, UK) equipped with four lasers [355nm (UV); 488nm (Blue); 561nm (Yellow-Green); 640nm (Red)] and analysed using Summit 5.4 software (Beckman Coulter)]. Single colour compensation controls were prepared for each fluorochrome (UltraComp eBeads®; Affymetrix). Cells were gated for size, shape and granularity, using forward and side scatter parameters. Regions were drawn around major populations of cells on a forward scatter/side scatter (FSC/SSC) dot plot. Dead cells, clumps and debris were excluded from further analysis. For dead cell exclusion, 7-amino-actinomycin D (7-AAD; BD Biosciences) was used.

### 2.6. Long-term transplantation assays

Bone marrow cells were harvested from 10 week old *Sfpi1*$^{GFP}$ or Chr2MDR$^{mCh}$ mice, followed by immunomagnetic negative selection of haematopoietic stem and progenitor cells and resuspension at the required concentration in 150 µl IMDM. Donor cells were injected using an insulin syringe (BD Biosciences) into the tail vein of restrained age-matched NSG mice (150 µl/NSG mouse). The exact cell number of injected cells varied per experiment and is stated in the relevant result section.

Five months following injection, tail veins of recipient NSG mice were punctured with an insulin syringe and blood collected using a heparinised capillary tube (Thermo Fisher Scientific), and transferred to a 0.2 ml eppendorf tube on ice (Starlab, Milton Keynes, UK). Red blood cells were lysed as previously described and $1.5 \times 10^5$ WBCs suspended in a 5 ml FACS tube (BD Biosciences) for analysis by flow cytometry.

Six months following injection, NSG recipients were sacrificed using a rising concentration of $CO_2$, and blood, spleen and bone marrow harvested and prepared as previously described (Section 2.3). Approximately $1.5 \times 10^5$ WBCs/sample (25 µl PBS/3% FBS) were aliquoted into FACS tubes. Cells were single labelled with antibodies (CD3-PE, B220-PE, Gr-1-PE or Mac1-PE; BD Biosciences) for 45 min on ice, and washed twice with PBS/1% FBS (1,200 rpm, 5 min, 4 °C) before analysis by flow cytometry.

### 2.7. Histology

Femurs were embedded in Tissue-Plus® (Scigen Scientific, Gardena, USA) and snap frozen using dry-ice and isopentane (Sigma-Aldrich). Cryosections (20 µm thickness) were fixed with 2% paraformaldehyde in PBS (VWR) for 10 min at RT, followed by three washes with PBS. Slides were incubated with 0.5% Triton X-100 (VWR) in PBS for 5 min at RT, followed by three washes with PBS and staining with a 300 nM DAPI solution (Thermo Fisher Scientific) for 15 min at RT. Following three washes with PBS, slides were mounted with SlowFade® Gold Antifade Mountant (Thermo Fisher Scientific) and visualised on an inverted Nikon Eclipse Ti-E inverted microscope with NIS-Elements imaging software (Nikon Instruments, Badhoevedorp, The Netherlands).

### 2.8. Suspension cultures

Following immunomagnetic negative selection of haematopoietic stem and progenitor cells (section 2.4), cells were seeded at the required concentration in StemSpan™ serum-free expansion medium with the addition of 50 ng/ml recombinant murine stem cell factor, 100 ng/ml recombinant human interleukin-11, 100 ng/ml recombinant human Flt3 Ligand, 40 µg/ml low density lipoprotein (Sigma-Aldrich), 100 U/ml penicillin (Thermo Fisher Scientific) and 100 µg/ml streptomycin (Thermo

Fisher Scientific) in 6-well plates and incubated at 37 °C/5% $CO_2$. All reagents were obtained from Stem Cell Technologies, unless otherwise stated.

### 2.9. Colony forming cell assay

Cultures were set up by addition of 400 µl haematopoietic stem and progenitor cell suspension (20,000 cells/ml IMDM) to 4 ml Methocult™ (Stem Cell Technologies) before transferring to 6-well plates using a 2.5 ml syringe and 18 G needle (1.1 ml/well, in triplicate, one well containing sterile water). Cultures were incubated at 37 °C/5% $CO_2$, and colonies counted on day 12 using an inverted microscope. The average colony count was calculated as the mean colony count of three wells.

### 2.10. Mitochondrial stains

Bone marrow cells were negatively selected for haematopoietic stem and progenitor cells by immunomagnetic negative selection 7 days following X-irradiation (0 – 3 Gy). Cells were resuspended in EasySep™ Buffer with primary conjugated antibodies for CD27 (LG.3A10) and CD201 (RCR-16) diluted to manufacturer's recommendations. Following incubation for 30 min on ice, cells were washed twice in EasySep™ Buffer (1,200 rpm for 5 min at 4 °C).

#### 2.10.1. Mitochondrial mass

Cells were resuspended at 1 x $10^6$ cells/ml Advanced RPMI 1640 and incubated with 100 nM MitoTracker® Green FM (Thermo Fisher Scientific; dissolved in DMSO) at 37 °C/5% $CO_2$ for 30 min. Cells were washed, resuspended in Advanced PRMI 1640 and stored on ice. Ten minutes before analysis by flow cytometry, cells were passed through a cell strainer and 7-AAD (5 µl/sample) was added.

### 2.10.2. Mitochondrial membrane potential

Cells were resuspended at 1 x $10^6$ cells/ml Advanced RPMI 1640 and incubated with 2 µM MitoProbe™ JC-1 cationic dye (Thermo Fisher Scientific; dissolved in DMSO) at 37 °C/5% $CO_2$ for 30 min. For the control tube, 50 µM carbonyl cyanide 3-chlorophenylhydrazone (CCCP; Thermo Fisher Scientific) was added simultaneously. Cells were washed, resuspended in EasySep™ Buffer and stored on ice. Ten minutes before analysis by flow cytometry, cells were passed through a cell strainer and 7-AAD (5 µl/sample) was added.

### 2.10.3. Mitochondrial superoxide

Cells were resuspended at 1 x $10^6$ cells/ml EasySep™ Buffer and incubated with 5 µM MitoSOX™ Red (Thermo Fisher Scientific; dissolved in DMSO) at 37 °C/5% $CO_2$ for 30 min. Cells were washed, resuspended in 0.5 ml EasySep™ Buffer and stored on ice. Ten minutes before analysis by flow cytometry, cells were passed through a cell strainer and 7-AAD (5 µl/sample) was added.

## 2.11. Cell cycle analysis

Following immunomagnetic negative selection of haematopoietic stem and progenitor cells (section 2.4), cells were incubated at 1 x $10^6$ cells/ml IMDM supplemented with 50 µg/ml verapamil (Sigma-Aldrich) and 10 µg/ml Hoechst33342 (Thermo Fisher Scientific) for 45 min at 37 °C/5% $CO_2$. Pyronin Y (1 µg/ml; Sigma-Aldrich) was added and incubated for a further 30 min. Cells were stained with Sca1 and cKit antibodies conjugated with PE-Cy7 and APCeFluor®780, respectively, for 30 min on ice. Cells were washed in EasySep™ Buffer, resuspended in 0.5 ml EasySep™ Buffer and 7-AAD (5 µl/sample) was added 10 min before analysis by flow cytometry.

## 2.12. Gene expression analysis

### 2.12.1. RNA isolation

RNA was extracted from freshly sorted cells using a modified Single Cell RNA Purification Kit (Norgen Biotek, Thorold, Canada). Cells were centrifuged at 200 *x g* for 10 min. Following addition of 350 µl Buffer RL to the pellet, cells were lysed by vortexing for 15 sec, followed by addition of 200 µl 100% ethanol. The vortexed lysate was transferred to a micro spin-column, centrifuged at 3,500 *x g* for 1 min and the flowthrough discarded. Following addition of 400 µl Wash Solution A to the column and centrifugation at 14,000 *x g* for 2 min, the flowthrough was discarded. RNase-free DNase I solution (100 µl) was added to the column and centrifuged at 14,000 *x g* for 1 min. The flowthrough was pipetted back onto the top of the column and incubated for 15 min at RT. The column was washed twice with 400 µl Wash Solution A and centrifuged at 14,000 *x g* for 1 min, followed by 2 min at 14,000 *x g* (each time discarding the flowthrough). Finally, Elution Solution A (20 µl) was added to the column and centrifuged at 200 *x g*, followed by 1 min at 14,000 *x g*. The RNA quantity of the eluate was measured by NanoDrop 2000 and the RNA quality was assessed by Tapestation 2200 (Agilent Technologies, Stockport, UK).

### 2.12.2. Reverse transcription

Reverse transcription reactions were performed using a High-Capacity cDNA Reverse Transcription Kit (Applied Biosystems, Foster City, USA) according to the manufacturer's protocol. In brief, 10 µl RNA sample (30ng RNA/sample) was added to 10 µl 2X reverse transcription master mix. Reactions were performed on a IQ5 Real-Time PCR detection system (Bio-Rad), using the following conditions: 25 °C for 10 min, 37 °C for 120 min and 85 °C for 5 min.

### 2.12.3. Multiplex quantitative real time-PCR

Real-time PCR was performed using a Rotor-Gene Q (Qiagen). Reactions were run in triplicate with primer and probe sets for target genes at 300 nM each and 2.5 µl cDNA in 30 µl reaction volume (PerfeCTa® MultiPlex qPCR SuperMix; Quanta Biosciences, Gaithersburg, USA). 3'6-Carboxyfluorescein (FAM), 6-Hexachlorofluorescein (HEX), Texas Red and CY5 (Eurogentec Ltd, Fawley, UK) were used as fluorochrome reporters for the hydrolysis probes analysed in multiplexed reactions. Cycling parameters were as follows: 2 min at 95 °C and 45 cycles of (10 sec at 95 °C and 60 sec at 60 °C). Data was collected and analysed using Rotor-Gene Q Series software by Grainne Manning. Gene target cycle threshold ($C_t$) values were normalised to an internal control (*Hypoxanthine-Guanine phosphoribosyltransferase 1; HPRT*). $C_t$ values were converted to transcript quantity using standard curves obtained by serial dilution of PCR-amplified DNA fragments of each gene and run in each reaction. The linear dynamic range of the standard curves covering six orders of magnitude (serial dilution from $3.2 \times 10^{-4}$ to $8.2 \times 10^{-10}$) gave PCR efficiencies between 93% and 103% for each gene with $R^2$ >0.998. Relative gene expression levels after irradiation were determined.

## 2.13. rAML induction and tissue preparation

Homozygous Chr2MDR$^{mCh}$ mice were crossed with homozygous *Sfpi1*$^{GFP}$ mice. The resulting offspring, termed *Sfpi1*$^{mCh/GFP}$ mice, had one chromosome 2 homologue carrying the Rosa26-mCherry construct, with the other homologue carrying the GFP construct. One hundred and one male *Sfpi1*$^{mCh/GFP}$ mice and 50 female *Sfpi1*$^{mCh/GFP}$ mice were given acute 3 Gy whole-body X-irradiation at 10 – 12 weeks of age with 10 female and 10 male *Sfpi1*$^{mCh/GFP}$ mice sham-exposed.

Tail vein blood samples were monthly analysed by flow cytometry starting at the time of exposure, allowing the detection of an expanding haematopoietic clone which has lost GFP or mCherry fluorescence (and so also the chromosome 2 homologue carrying the fluorescent construct). Mice were examined twice a day for outward physical signs of rAML (such as hunched posture, poor grooming, decreased activity and pallor) and euthanised with a rising concentration of $CO_2$. Animals found to display spleno- and/or hepatosplenomegaly upon dissection, or having increased WBC counts, were treated as potential rAMLs.

Blood smears were prepared by drawing a spreader at a $45^{o}$ angle just in front of a 5 µl blood droplet at the frosted end of a microscope slide (Thermo Fisher Scientific). Slides were allowed to air-dry on the bench for 24 h and stained as follows: 2 min in 100% methanol (Sigma-Aldrich), then 5 min in May-Grünwald (10 ml May-Grünwald's stain in 30 ml Giemsa buffer), followed by 30 min in Giemsa (0.5 ml Giemsa stain in 40 ml Giemsa buffer). Finally, slides were rinsed twice in Giemsa buffer for 5 min and dried on a hot plate before analysis by light microscopy. All reagents were purchased from VWR, Poole, UK, unless otherwise stated.

The weight of the spleen was recorded before using a scalpel to cut it into three transverse sections. The proximal part of the spleen was stored at -80 °C in 3 ml RNAlater (Ambion, Austin, USA) until required for DNA isolation (Section 2.15). The central part was touched with the cut surface against a microscope slide repeatedly to leave an imprint (slides were air-dried and stained as described above for blood smears) and then the piece of spleen was stored in 4% formaldehyde until histopathological processing and analysis. The distal part of the spleen was

disaggregated for analysis by flow cytometry (Section 2.14) and chromosome preparations for cytogenetics (Section 2.16).

rAML was diagnosed using the criteria described in the 'Bethesda proposals for classification of nonlymphoid hematopoietic neoplasms in mice' (Kogan et al., 2002). All cases defined as rAML had a rapid onset of outward physical signs, an increased WBC count and nonlymphoid immature forms/blasts made up ≥20% of WBCs in the peripheral blood. Furthermore, flow cytometric immunophenotyping confirmed the absence of maturity, and the presence of immaturity, cell surface markers.

### 2.14. Immunophenotyping of rAMLs

Spleen cells and WBCs were resuspended in EasySep™ Buffer and primary conjugated antibodies were added. The following PE-conjugated antibodies were used: Sca1 (E13-161.7; BioLegend, San Diego, USA), cKit (2B8; Abcam, Cambridge, UK), Flt3 (A2F10.1), Gr1 (1A8), Ly6c (HK1.4; Abcam), Mac1 (M1/70), CD31 (MEC13.3), CD3 (17A2) and B220 (RA3-6B2). Preincubation with unconjugated anti-FcRII/III (2.4G2) was used to reduce nonspecific binding. All reagents were purchased from BD Biosciences, unless otherwise stated, and diluted to the manufacturer's recommendations. Following incubation for 30 min on ice, cells were washed twice in EasySep™ Buffer. Acquisition was performed using a Guava® easyCyte Single Sample flow cytometer and analysed using InCyte™ software (Merck Millipore, Watford, UK). Cells were gated for size, shape and granularity, using forward and side scatter parameters. Regions were drawn around major populations of cells on a FSC/SSC dot plot. Events with low FSC/SSC were assumed to be dead cells and debris, and excluded from analysis.

### 2.15. DNA isolation from rAML spleens and sequencing for *Sfpi1* and *Flt3*

DNA was extracted from spleen tissue using a DNeasy® Blood & Tissue kit (Qiagen, Manchester, UK) with some modifications to the manufacturer's instructions. Eight mg of spleen was incubated at 56 °C in a microcentrifuge tube containing 180 µl Buffer ATL and 20 µl proteinase K. Upon complete lysation, 4 µl RNase A (Sigma-Aldrich) was added and incubated for 2 min at RT, followed by addition of 200 µl Buffer AL and 200 µl 100% ethanol (Sigma-Aldrich). The mixture was pipetted into a DNeasy Mini spin column and centrifuged at 6,000 *x g* for 1 min. Buffer AW1 (500 µl) was added to the spin column and centrifuged at 6,000 *x g* for 1 min, followed by adding 500 µl Buffer AW2 and centrifugation at 20,000 *x g* for 3 min. The spin column was transferred to a new microcentrifuge tube and the DNA eluted by adding 200 µl Buffer AE. Following incubation for 1 min at RT, the column was centrifuged at 6,000 *x g* for 1 min. DNA quantity was measured by NanoDrop 2000 (Thermo Fisher Scientific).

For the PCR reaction, we used 1 µl of extracted DNA (25 ng DNA/µl) in 9 µl PCR master mix [1 µl 10x PCR buffer, 2 µl 5x Q-solution, 1.6 µl 1.25 mM dNTP, 3.15 µl $dH_20$, 0.5 µl 10 µM primer 'Forward', 0.5 µl 10 µM primer 'Reverse', 0.25 µl *Taq* DNA Polymerase (Qiagen)] and amplified at the following conditions: 4 min at 95 °C, then 35 cycles of [30 sec at 95 °C (denaturation), 30 sec at 57 °C (annealing) and 30 sec at 72 °C (elongation)], followed by 10 min at 72 °C. *Sfpi1* point mutations were detected using PCR with primers designed to amplify the region covering exon 5 (F: 5'-GCGACATGAAGGACAGCATCT-3', R: 5'-TTTCTTCACCTCGCCTGTCT-3'). *Flt3*-ITD mutations were detected with primers designed to amplify the region covering exons 14 and 15 (F: 5'-CAATTTAGGTACGAGAGTCAGC-3', R: 5'-CTTTTAGCATCTTCACCGCCACC-3').

Size and integrity of the PCR product was assessed on a 1% agarose gel with 10 µl GelRed (Biotium, Fremont, USA). Samples were mixed with loading buffer (0.5% bromophenol blue, 40% sucrose in $dH_2O$; 1:5) and ran alongside a 1 kB ladder (Thermo Fisher Scientific) at 100 V for 1 h, before visualisation using a Gel Doc system. The PCR product concentration was determined by NanoDrop 2000. PCR product (1 ng/µl per 100 bp) and primers (3.2 pmol/µl) were sent for sequencing by Source BioScience (University of Oxford, UK). Sequencing files were analysed using Chromas 2.6 software (Technelysium Pty Ltd, Brisbane, Australia).

### 2.16. PCR for GFP construct detection in rAML samples

We used 1 µl extracted spleen DNA in 9 µl PCR mastermix [1 µl 10x buffer, 0.05 µl *Taq* DNA Polymerase, 0.5 µl 6.6 µM primer 'Fa', 0.5 µl 6.6 µM primer 'Fc', 0.5 µl 6.6 µM primer 'Rb', 0.08 µl 200 µM dNTPs and 6.37 µl $dH_2O$ (Qiagen)] and amplified at the following conditions: 5 min at 95 °C, then 45 cycles of (30 sec at 95 °C, 30 sec at 57 °C and 30 sec at 72 °C), followed by 10 min at 72 °C (Veriti® 96-well Thermal Cycler; Thermo Fisher Scientific, Paisley, UK). Primers were obtained from Integrated DNA Technologies (IDT, Leuven, Belgium) and primer sequences can be found in Table 3. PCR products were resolved on 1% agarose gels (80 V for 60 min) and gel images were obtained using a Gel Doc system (Bio-Rad).

**Table 3. GFP primer sequences**

| | |
|---|---|
| Fa | 5'-TGGCGCCTACCGGTGGATGTGG-3' |
| Fc | 5'-GTGCTTCCTTGGGAGTCTGGCGCT-3' |
| Rb | 5'-CTGTCTGCCACCACCTGCCTACATT-3' |

Band size: *Sfpi1*$^{wt}$, 680 bp; *Sfpi1*$^{GFP}$, 512 bp

### 2.17. Chromosome preparations

Spleen cells were cultured at 2 × $10^6$ cells/ml in 5 ml RPMI1640/20% FBS with addition of penicillin (100 U/ml), streptomycin (100 µg/ml), lipopolysaccharide (25 µg/ml) (Sigma-Aldrich) and Concanavalin A (4 µg/ml; Amersham Biosciences UK, Little Chalfont, UK) for 48 h at 37 °C/5% $CO_2$. Demecolcine (0.06 µg/ml; Sigma-Aldrich) was added and incubated for a further hour. Following incubation with 2 ml 0.075 M KCl (10 min at 37 °C), cells were fixed on ice [25 ml acetic acid (Sigma-Aldrich)/75 ml 100% methanol] and stored at -20 °C until slide preparations. All reagents were obtained from Thermo Fisher Scientific, unless otherwise stated.

### 2.18. Transplantation of leukaemic cells – 'passaging'

Six million spleen cells were resuspended in 300 µl IMDM and transplantated via intraperitoneal (IP) injection (150 µl per mouse) into eight week old NSG mice or unirradiated CBA/Ca mice (Envigo, Bicester, UK). Upon onset of outward physical signs, mice were processed as described in section 2.7.

### 2.19. Statistical analysis

IBM SPSS Statistics 22 (IBM, Portsmouth, UK) was used for statistical comparison between two groups using the two-tailed unpaired Student's t-test, and between more than two groups by analysis of variance (ANOVA). All data was expressed as mean values ± standard error of the mean (SEM). P values $<0.05$ were considered significant.

# CHAPTER 3

*Results and discussion*

## 3. Results and discussion

### 3.1. NSG mice are 'permissive' to allogeneic HSC transplantation without prior conditioning

Murine models are indispensable in studying radiation-induced acute myeloid leukaemogenesis with no *in vitro* system satisfactorily mimicking this process. For instance, the time from exposure to disease development is very long (i.e. 12 – 18 months post-irradiation; Major and Mole, 1978) and isolated haematopoietic stem cell culture systems cannot be maintained for the time required. Bone marrow transplantation assays have been extensively used to study the molecular and chromosomal processes in the haematopoietic system at early time points post-irradiation, and have been the gold standard to study HSCs and their long-term engraftment potential for many years (Mcculloch and Till, 1960). Here, the donor cells are transplanted into conditioned (i.e. radio-ablation of the bone marrow) recipient mice together with a limited number of helper cells (i.e. bone marrow cells required by the radio-ablated recipients until the donor HSCs have generated sufficient progeny).

However, one of the major limitations of the way bone marrow transplantation assays are currently performed, is the requirement of prior conditioning of the recipients, where host mice are exposed to lethal doses of X-irradiation (Olme et al., 2013a). This is a high risk procedure with a number of drawbacks (including gastrointestinal syndrome, bone marrow failure, premature ageing/death, radiation-induced cataract and hepatic neoplasia) not least of which is the profound alteration of the host's bone marrow microenvironment (Duran-Struuck and Dysko, 2009). Similarly, the high dose prior conditioning of recipients makes investigating the effect of low dose radiation exposure problematic.

### 3.1.1. Establishment of a novel transplantation model in unconditioned NSG mice

Recently, it was reported that an intrinsic defect in the maintenance of *scid* HSCs, the so-called 'bone marrow hematopoietic niche occupancy defect', facilitates allogeneic HSC transplantation without prior conditioning (Qing et al., 2012). Nevertheless, NOD-*scid* mice have a significantly altered life span due to the early development of thymic lymphomas, which compromises the ability to study the long-term fate of transplanted HSCs and their progeny in these recipient mice (Prochazka et al., 1992).

NOD *scid* gamma (NOD.Cg-*Prkdc*$^{scid}$ *Il2rg*$^{tm1Wjl}$/SzJ, NSG) mice are highly immunodeficient mice generated by crossing NOD-*scid* mice with mice bearing the X-linked B6.129S4-*Il2rg*$^{tm1Wjl}$/J allele: the NOD background contributes to innate immune deficiencies, the *scid* mutation prevents the maturation of lymphocytes and the *Il2rg* deficiency blocks natural killer cell development (Shultz et al., 2005). Interestingly, NSG mice are resistant to thymic lymphoma development, even following sublethal irradiation (Ishikawa et al., 2005). To this end, we investigated the ability of allogeneic bone marrow cells to achieve long-term engraftment in NSG mice without prior conditioning, and thus leaving the recipient's bone marrow microenvironment uncompromised.

The tracking of allogeneic bone marrow cells in NSG recipients required the presence of a marker allowing their detection; here we used cells of *Sfpi1*$^{GFP}$ mice, expressing GFP as a reporter for *Sfpi1* expression. The *Sfpi1*$^{GFP}$ mouse model contains a GFP construct which is under control of the *Sfpi1* promoter, resulting in a variable expression throughout the different haematopoietic subpopulations. Peripheral blood monocytes (Mac1+) have GFP$^{high}$ expression levels, whereas B-cells (B220+) have

GFP$^{low}$ expression levels, as analysed by flow cytometry (Figure 3.1, right panel). In contrast, peripheral blood T-cells (CD3+) do not express GFP (GFP$^{neg}$). Peripheral blood WBCs of non-transplanted NSG mice are GFP$^{neg}$ and mainly express Mac1+ (monocytes). T-cells (CD3+) and B-cells (B220+) are almost completely absent in the peripheral blood of non-transplanted NSG mice (Figure 3.1, left panel).

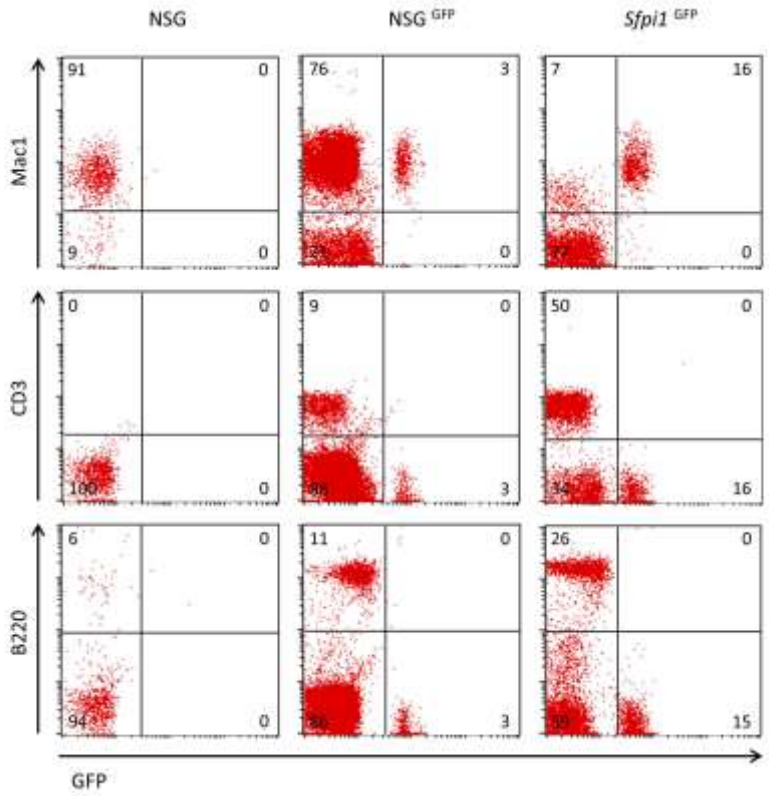



**Figure 3.1 Flow cytometry analysis of NSG, NSG$^{GFP}$ and *Sfpi1*$^{GFP}$ peripheral blood WBCs**

*Sfpi1*$^{GFP}$ haematopoietic stem and progenitor cells were IV transplanted into age-matched unconditioned NSG mice (4 NSG mice per group; 3 groups). Four months following injection, donor chimerism in the peripheral blood of recipients was analysed by flow cytometry. Representative peripheral blood flow cytometry analysis of a non-transplanted NSG mouse, a multilineage reconstituted NSG mouse, and a *Sfpi1*$^{GFP}$ mouse (left, middle and right panels, respectively). Mac1 is a marker expressed by monocytes, CD3 is expressed by T-cells, and B220 is expressed by B-cells.

### 3.1.2. Determination of donor contribution towards haematopoiesis in NSG mice

Bone marrow cells from 10 week old *Sfpi1*$^{GFP}$ mice were harvested, resuspended at the required concentration and injected via the tail vein into 4 age-matched NSG mice (5 x $10^6$ cells in 150 µl IMDM/NSG mouse). Five months following intravenous (IV) injection, NSG mice were sacrificed, and spleen and peripheral blood were collected to assess contribution of *Sfpi1*$^{GFP}$ donor cells towards long-term multilineage haematopoiesis. Half of the injected NSG mice presented with low levels of donor-derived lymphoid cells in the spleen (<5% B220+/GFP$^{low}$ and CD3+/GFP$^{neg}$), as analysed by flow cytometry. None of the NSG mice had donor-derived myeloid cells (Mac1+/GFP$^{high}$ or Gr1+/GFP$^{high}$) or lymphoid cells (B220+/GFP$^{low}$ or CD3+/GFP$^{neg}$) in the peripheral blood.

We hypothesised that injecting haematopoietic stem and progenitor cells [commonly referred to as Lineage negative (Lin-) cells], rather than total bone marrow cells, could potentially increase the ability of the donor cells to contribute towards long-term multilineage haematopoiesis in the unconditioned recipients. The use of immunomagnetic negative selection of haematopoietic stem and progenitor cells allowed us to significantly decrease the percentage of mature, lineage-committed bone marrow cells (such as granulocytes, lymphocytes and monocytes) and increase the percentage of haematopoietic stem and progenitor cells (such as cKit+ cells). The number of monocytes, granulocytes, erythroid cells and B-cells following immunomagnetic selection decreased with 98%, 99%, 92% and 75%, respectively. The number of cKit+ cells increased following immunomagnetic selection by 540% (Figure 3.2A).

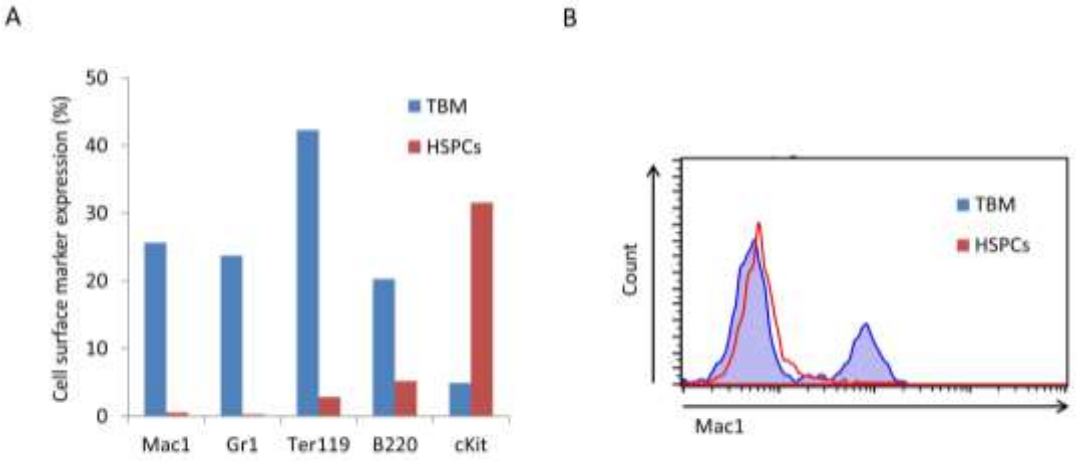



**Figure 3.2 Immunomagnetic selection of haematopoietic stem and progenitor cells**

*Sfpi1*$^{GFP}$ total bone marrow (TBM) cells were harvested from a 10 week old mouse and negatively selected for haematopoietic stem and progenitor cells (HSPCs) by immunomagnetic negative selection. (A) TBM cells (blue) and HSPCs (red) were labelled with Mac1, Gr1, Ter119, B220 and cKit antibodies conjugated with PE, followed by flow cytometry analysis for cell surface marker expression. (B) Flow cytometry histogram of representative Mac1 expression in TBM cells (blue) and HSPCs (red).

Bone marrow cells from 10 week old *Sfpi1*$^{GFP}$ mice were harvested and negatively selected for haematopoietic stem and progenitor cells by immunomagnetic selection, hereby depleting the bone marrow from mature, lineage-committed cells. Age-matched NSG mice were randomised into three experimental groups (4 NSG mice per group) prior to tail vein injection of (a) 1 x$10^5$, (b) 5 x $10^5$ or (c) 1 x $10^6$ haematopoietic stem and progenitor cells. Four months following IV injection, a tail vein blood sample was collected from each recipient to assess contribution of *Sfpi1*$^{GFP}$ donor cells towards long-term multilineage haematopoiesis in unconditioned NSG recipients.

Eleven out of twelve NSG mice presented with donor-derived lymphoid cells in the peripheral blood, both B-cells (B220+/GFP$^{low}$) and T-cells (CD3+/GFP$^{neg}$), as analysed by

flow cytometry (Figure 3.1, middle panel). The only NSG mouse which did not show any chimerism four months following transplantation was an NSG mouse injected with the lowest amount of cells (i.e. 1 x $10^5$ haematopoietic stem and progenitor cells). Five of the eleven chimeric NSG mice showed myeloid cell chimerism in the peripheral blood: one NSG mouse injected with 1 x$10^5$ cells (25%, 1/4), two NSG mice injected with 5 x$10^5$ cells (50%, 2/4) and two NSG mice injected with 1 x $10^6$ cells (50%, 2/4). Approximately 2% of myeloid cells in the recipients' peripheral blood were donor-derived ($GFP^{high}$). The highest donor WBC chimerism was observed in NSG mice injected with 5 x$10^5$ cells and 1 x $10^6$ cells. Donor WBC chimerism was calculated as the GFP+ lympho-/monocytes of the total lympho-/monocyte population (Figure 3.3, left panel).

One month following peripheral blood analysis, all mice were sacrificed, and donor chimerism in the spleen of NSG recipients was analysed by flow cytometry. Similarly to the results obtained from peripheral blood analysis, all eleven chimeric mice presented with donor-derived lymphoid cells in the spleen, both B-cells (B220+/$GFP^{low}$) and T-cells (CD3+/$GFP^{neg}$). The spleen weight of transplanted NSG mice was significantly higher compared with the spleen weight of control NSGs, with the highest spleen weights recorded for NSG mice injected with 5 x$10^5$ cells and 1 x $10^6$ cells (Figure 3.3, right panel). Upon analysis of the NSG bone marrow, both donor-derived lymphoid and myeloid cells were identified in NSG mice which showed multilineage reconstitution on peripheral blood analysis.

Given the fact that five months following transplantation, haematopoiesis is entirely dependent on long-term HSC activity (Marusyk et al., 2009), these results suggest that

the presence of multilineage reconstitution is most likely due to allogeneic HSC engraftment in these unconditioned NSG mice. It also indicates that *Sfpi1*$^{GFP}$ haematopoietic stem and progenitor cells can compete for the niches in the bone marrow compartment and that the NSG bone marrow microenvironment is capable of supporting HSC differentiation and development of mature, lineage-committed WBCs without prior conditioning.

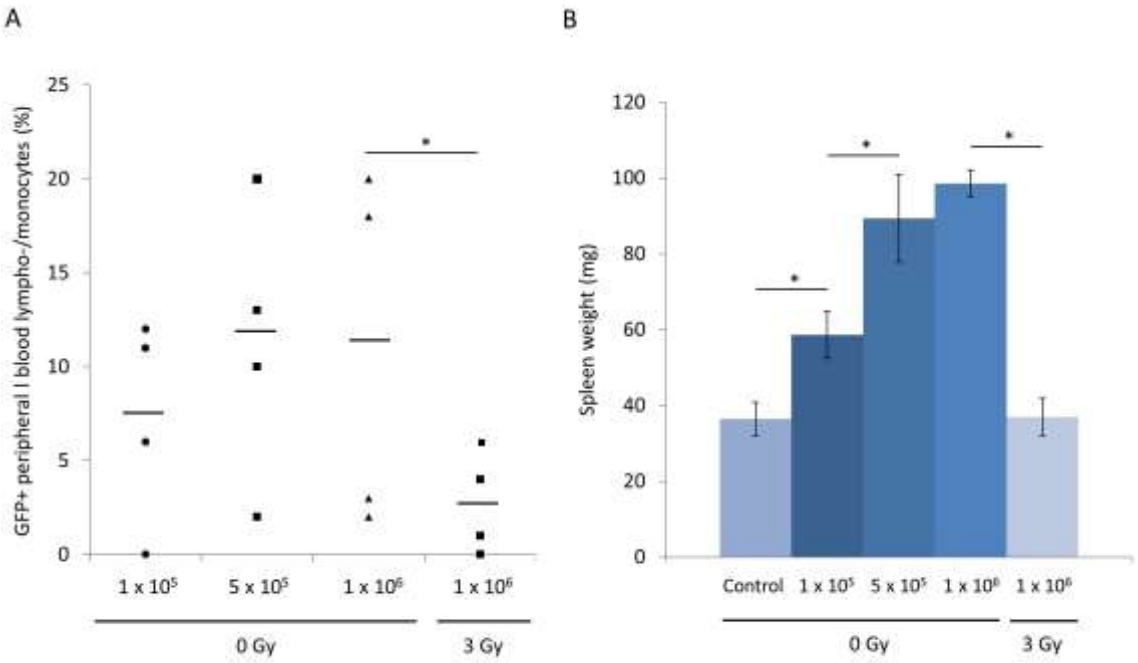



**Figure 3.3 Donor WBC chimerism following transplantation in unconditioned NSGs**

*Sfpi1*$^{GFP}$ haematopoietic stem and progenitor cells (1 x $10^5$, 5 x $10^5$, or 1 x $10^6$ cells/NSG mouse) were i.v. transplanted into age-matched NSG mice (4 NSG mice per group; 3 groups). A fourth group received a transplant of 1 x $10^6$ irradiated HSPCs/NSG mouse (3 Gy seven days prior to harvest; 4 NSG mice per group). (A) Four months following injection, donor chimerism in peripheral blood of NSG recipients was analysed by flow cytometry (each mouse is represented by an individual point; horizontal lines represent the average within the group). The percentage of GFP+ peripheral blood lympho-/monocytes is the GFP+ lympho-/monocytes portion of the total lympho-/monocytes population. (B) NSG spleen weights (mg) were recorded five months following transplantation (* P <0.05).

### 3.1.3. Feasibility of transplantation following *in vivo* X-irradiation of donor HSCs

Although we report here for the first time that unconditioned NSG mice have a similar intrinsic bone marrow haematopoietic niche occupancy defect as previously reported in NOD-*scid* mice (Qing et al., 2012), allowing allogeneic engraftment of non-irradiated haematopoietic stem and progenitor cells without prior conditioning, we hypothesised that the reduced 'fitness' of prior radiation exposure of donor haematopoietic stem and progenitor cells might be a limiting factor towards the success of this transplantation model.

Therefore, we sought to determine the ability of irradiated *Sfpi1*$^{GFP}$ haematopoietic stem and progenitor cells to contribute towards long-term multilineage haematopoiesis in unconditioned NSG mice. Two 10 week old *Sfpi1*$^{GFP}$ mice were 3 Gy irradiated seven days prior to harvest and immunomagnetic selection, followed by tail vein injection of $1 \times 10^6$ haematopoietic stem and progenitor cells into four age-matched NSG recipients. Five months following IV injection, three out of four injected NSG mice presented with donor-derived lymphoid cells in the spleen and peripheral blood, although overall WBC donor chimerism was four times lower compared with non-irradiated donor haematopoietic stem and progenitor cells (Figure 3.3, left panel).

In contrast with the multilineage chimerism observed following transplantation of non-irradiated cells, donor-derived myeloid cells were not observed in the peripheral blood of these NSG recipients. The spleen weight of NSG mice transplanted with irradiated haematopoietic stem and progenitor cells was not significantly higher compared with the spleen weight of control NSG mice (Figure 3.3, right panel).

### 3.1.4. Unconditioned NSG mice allow rAML passaging

To compare AML presentation in immunocompetent CBA/Ca mice and immunodeficient NSG mice, $3 \times 10^6$ 'AN9' or 'AN59' rAML spleen cells were resuspended in 150 µl IMDM and transplanted via IP injection (2 NSG mice per rAML spleen sample). Both 'AN9' and 'AN59' were historical rAMLs which were previously proven to successfully transplant into immunocompetent 129/Sv mice. Two months following injection, all NSG mice presented with outward physical signs of AML (such as hunched posture, poor grooming, decreased activity and pallor). Each leukaemic NSG mouse (referred to $NSG^{AML}$ hereafter) was sacrificed, and spleen and peripheral blood single cell suspensions were prepared.

The $NSG^{AML}$ WBC counts were markedly higher compared with the WBC count of control NSG mice ($9 \times 10^6$ cells/ml and $2 \times 10^6$ cells/ml, respectively). Upon examination of the $NSG^{AML}$ peripheral blood smears, only primitive large myeloblasts and no mature granulocytes were observed (Figure 3.4A, lower panel). In contrast, control NSG mice had only granulocytes in the peripheral blood (Figure 3.4A, upper panel).

Flow cytometric analysis of the $NSG^{AML}$ peripheral blood showed on the FSC/SSC dot plot that $NSG^{AML}$ peripheral blood WBCs were much larger and granular compared with control NSG WBCs (i.e. higher FSC and higher SSC values, respectively). Immunophenotyping of the $NSG^{AML}$ peripheral blood revealed that $NSG^{AML}$ WBCs expressed immaturity/progenitor cell surface markers (including cKit, Ly6c and CD31) and did not express mature, lineage-committed cell surface markers (including Mac1, Gr1, B220 and CD3), which is consistent with the immunophenotyping of the primary

rAMLs (Figure 3.4B, lower panels). Immunophenotyping of the control NSG peripheral blood revealed that control NSG WBCs only expressed mature, lineage-committed cell surface markers (including Mac1 and Gr1) and did not express immaturity/progenitor cell surface markers (including cKit, Ly6c and CD31; Figure 3.4B, upper panels)

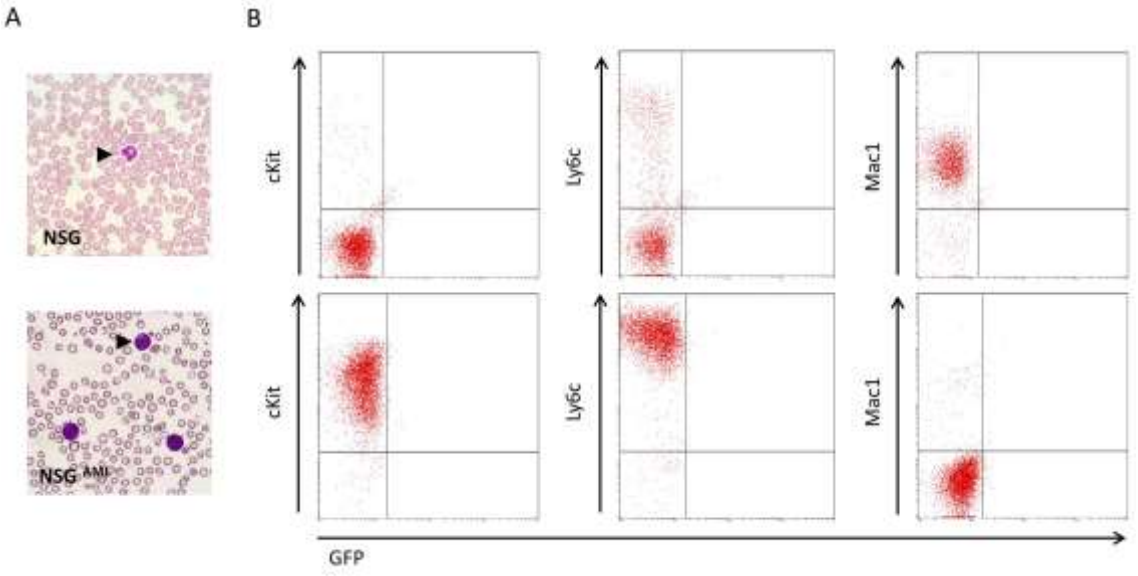



**Figure 3.4 Immunophenotyping of NSG and NSG$^{AML}$ peripheral blood WBCs**

NSG mice were IP injected with rAML spleen samples (2 NSG mice per rAML spleen sample), and spleen and peripheral blood cell suspensions were prepared upon presentation of outward physical signs of AML. (A) Representative photograph of control NSG and NSG$^{AML}$ peripheral blood smear (upper and lower panel, respectively). (B) WBC single cell suspensions were labelled with antibodies conjugated with PE, followed by flow cytometry analysis for cell surface marker expression. Representative dot plot of peripheral blood cell marker expression in control NSG and NSG$^{AML}$ mice (upper and lower panel respectively).

### 3.1.5. Discussion

Bone marrow transplantation assays are the gold standard to study HSCs and their transplantation potential, and up until today, we and other research groups have performed bone marrow transplantation assays following prior conditioning of the recipient mice (i.e. radio-ablation of the bone marrow). A commonly used conditioning dose in our laboratory is 8.5 Gy; a dose which completely myeloablates the bone marrow of CBA/H and CBA/Ca mice (Olme et al., 2013a) and would be lethal to the mouse if no subsequent transplantation of HSCs takes place. These immunocompetent mice have a functional immune system and would, without prior conditioning, reject the transplant. However, conditioning of recipients is a high risk procedure with a number of drawbacks (including gastrointestinal syndrome and bone marrow failure) not least of which is the profound alteration of the host's bone marrow microenvironment. The profound changes to the HSC niche following such high radiation exposure greatly compromise our ability to study low dose radiation exposure (≤100 mGy) and the effects on the HSCs and their contribution towards long-term haematopoiesis in a biologically relevant setting.

We hypothesised that the recently reported 'bone marrow haematopoietic niche occupancy defect' of *scid* HSCs (Qing et al., 2012) would allow allogeneic HSC transplantation into NSG mice without prior conditioning. NSG mice carry the same *scid* mutation and NSG mice should therefore be susceptible to transplantation without prior conditioning as well. Also, NSG mice do not develop thymic lymphoma (in contrast with *scid* mice), allowing a longer follow-up of transplanted cells and making it possible for serial transplantations to be undertaken (Prochazka et al., 1992).

The initial experiment, where we transplanted 5 x $10^6$ bone marrow cells in unconditioned NSG mice, resulted in very low levels of lymphoid spleen chimerism in only two out of four injected NSG mice, and no lymphoid and myeloid chimerism was observed in the peripheral blood five months following injection. Total bone marrow contains ~0.001% HSCs, so it can be assumed that each NSG mouse was transplanted with approximately 50 HSCs. We repeated the initial experiment but instead of injecting bone marrow cells, a more purified haematopoietic cell population was injected (i.e. haematopoietic stem and progenitor cells). Using immunomagnetic negative selection for haematopoietic stem and progenitor cells, we were able to deplete the mature, terminally-differentiated haematopoietic cells from the total bone marrow population and increase the percentage of progenitors in the transplant.

Five months following injection of haematopoietic stem and progenitor cells, the highest peripheral blood donor chimerism was observed in NSG mice injected with 5 x $10^5$ and 1 x $10^6$ haematopoietic stem and progenitor cells. The haematopoietic stem and progenitor cell population contains ~0.1% HSCs (up from ~0.001% in total bone marrow). In our experiment, we can therefore assume that each NSG mouse in these two groups was injected with ~500 and 1,000 HSCs, respectively. When donor haematopoietic stem and progenitor cells were irradiated prior to transplantation, we observed a decreased chimerism compared with transplantation of non-irradiated donor cells. As the overall transplanted cell number was exactly the same (i.e. 1 x $10^6$ haematopoietic stem and progenitor cells), we can conclude that the lower peripheral blood donor chimerism following irradiation is most likely due to the reduced fitness of the irradiated donor haematopoietic cells.

Several recent publications have studied human HSC engraftment in immunodeficient NSG mice, but to the authors' knowledge the engraftment potential of murine HSCs has not been described. Importantly, the percentage of *Sfpi1*$^{GFP}$ cell chimerism in the blood of adult nonmyeloablated NSG mice five months following engraftment of 1 x $10^6$ *Sfpi1*$^{GFP}$ haematopoietic stem and progenitor cells (approximately 1 x $10^3$ HSCs; 13%) was lower compared with the human cell chimerism level reported in the blood of 2.5 Gy myeloablated NSG mice eight weeks following engraftment of 5 x $10^4$ CD34+ human HSCs (22%)(Futrega et al., 2016). Our observed cell chimerism was similar to the human cell chimerism level reported in blood of newborn nonmyeloablated NSG mice twelve weeks following engraftment of 3 x $10^4$ CD34+ human HSCs, but lower compared with the human cell chimerism level reported in blood of adult nonmyeloablated NSG mice 12 weeks following engraftment of 3 x $10^4$ CD34+ human HSCs (18% and 41%, respectively)(Brehm et al., 2012). The authors did not observe a statistical difference in human cell chimerism levels in the blood of nonmyeloablated NSG mice compared with newborn or adult 1 Gy myeloablated NSG mice (Brehm et al., 2012). A more recent study reported a lower human cell chimerism level in blood of adult nonmyeloablated NSG mice 12 weeks following engraftment of 2.5 x $10^5$ CD34+ human HSCs (8%). In contrast with the previous studies, the authors did observe a significantly enhanced human cell chimerism level in the blood of 2.5 Gy myeloablated NSG mice compared with nonmyeloablated NSGs (approximately 60% and 8%, respectively)(McIntosh et al., 2015).

Given the fact that five months following transplantation, haematopoiesis is entirely dependent on long-term HSC activity (Marusyk et al., 2009), and following our

observation of both lymphoid and myeloid reconstitution five months following transplantation, we postulate that transplanted *Sfpi1*$^{GFP}$ HSCs can compete for niches in the nonmyeloablated NSG bone marrow compartment and that the nonmyeloablated NSG bone marrow microenvironment is capable of supporting allogeneic long-term HSC engraftment and differentiation.

### 3.2. Chr2MDR$^{mCh}$ mice express mCherry across HSCs and downstream haematopoietic lineages

The *Sfpi1*$^{GFP}$ mouse model, expressing GFP as a reporter for *Sfpi1* expression, has been previously used by our group with the aim of identifying live cells that have lost a copy of *Sfpi1* through flow cytometry analysis for reduced GFP expression levels (Olme et al., 2013b). However, initially it was designed by Nutt and colleagues in Australia to study the dynamic regulation of *Sfpi1* expression in the murine haematopoietic system (Nutt et al., 2005). *Sfpi1* is highly expressed in HSCs, CLPs, and a subset of CMPs. Therefore, all these cell types have GFP$^{high}$ expression. The CMPs can be further divided into two subpopulations based on their *Sfpi1* expression: the megakaryocyte/erythroid progenitors (MEPs; GFP$^{low}$) and the GMPs (GFP$^{high}$). GMPs are the precursors of the mature, terminally-differentiated monocytes and granulocytes, and both cell types require *Sfpi1* expression for their final differentiation and maturation, and hence have GFP$^{high}$ expression. On the other hand, the CLPs give rise to pro-B-cells and pro-T-cells: *Sfpi1* expression is partially downregulated upon differentiation and maturation towards B-cells (GFP$^{low}$) or completely downregulated upon commitment towards T-cell differentiation (GFP$^{neg}$).

Overall, the major drawback of the *Sfpi1*$^{GFP}$ mouse model for our use in transplantation studies, is that the GFP construct is under control of the *Sfpi1* promoter, resulting in a variable GFP expression throughout the different haematopoietic subpopulations. Therefore, once transplanted *Sfpi1*$^{GFP}$ HSCs give rise to less primitive, lineage-committed lymphoid cell types, the GFP expression is lost (T-cells) or reduced (B-cells), and the cells can no longer be tracked without cell surface marker analysis by flow cytometry.

### 3.2.1. Generation and maintenance of the Chr2MDR$^{mCh}$ reporter mouse model

To allow tracking of allogeneic haematopoietic cells in NSG recipients and to overcome the variable reporter expression in the haematopoietic cells, a constitutively expressed marker was required. Therefore, a genetically engineered mouse model was developed where a construct, positioned in the chromosome 2 MDR following radiation exposure, carries the fluorescent protein gene *mCherry*. mCherry is expressed under control of the ubiquitous Rosa26 promoter, resulting in a constitutive expression of mCherry in all haematopoietic cells (from primitive HSCs to mature, terminally-differentiated lymphocytes and granulocytes). The insertion site on chromosome 2 was selected at 92,823,765 – 92,823,766 bp, which is approximately 1.7 Mb away from *Sfpi1*. Using Zinc Finger Nuclease technology, transgenic one-cell embryos were generated at SAGE® Labs (Boyertown, USA), followed by rederivation at MRC Harwell (UK) and establishment of a breeding colony at our animal facilities.

A recent screen of ninety-seven radiation-induced AML spleen samples using array comparative genomic hybridization allowed our group to redefine the chromosome 2 MDR following radiation exposure to 5.5 Mb of chromosome 2 (Brown et al., 2015). Hereby, the MDR was reduced to a much smaller region, spanning from 88,090,995 bp to 93,545,541 bp. Since both *Sfpi1* (located at 91,082,390 bp) and the Rosa26-mCherry construct (located at 92,823,765 bp) are located within the MDR (Figure 2.1), we hypothesised that upon an interstitial deletion of chromosome 2 following radiation exposure, we would be able to detect a loss in mCherry expression, as the chromosome 2 homologue carrying the Rosa26-mCherry construct would be lost as well.

It was of utmost importance to confirm that a loss of mCherry fluorescence in any haematopoietic cells would be solely due to an interstitial chromosome 2 deletion and simultaneous loss of the Rosa26-mCherry construct. To this end, mCherry could not be silenced upon commitment to any specific haematopoietic cell type (as observed in the *Sfpi1*$^{GFP}$ T-cells who have GFP$^{neg}$ expression); hence we chose a promotor which is constitutively active (rather than the *Sfpi1* promotor which has a variable expression depending upon the differentiation stage of the haematopoietic cell). Similarly, as the peak incidence of rAML is approximately 9 – 12 months following radiation exposure, and as mice are usually not exposed before the age of 10 – 12 weeks, we had to confirm that mCherry fluorescence would be expressed at the same level throughout life and would not be silenced following dozens of division rounds to give rise to daughter haematopoietic cells.

### 3.2.2. Characterisation and radiation response of Chr2MDR$^{mCh}$ mice

To assess the constitutive expression of mCherry in all haematopoietic cell types (from primitive HSCs to mature, terminally-differentiated lymphocytes and granulocytes), we first analysed the peripheral blood from young adult Chr2MDR$^{wt}$ and Chr2MDR$^{mCh}$ mice by flow cytometry (8 – 12 weeks old). Chr2MDR$^{wt}$ mice were siblings of Chr2MDR$^{mCh}$ mice and were generated by crossing heterozygous Chr2MDR$^{mCh}$ mice with heterozygous Chr2MDR$^{mCh}$ mice (a heterozygous Chr2MDR$^{mCh}$ mouse has one chromosome 2 homologue harbouring the Rosa26-mCherry construct, whereas the other chromosome 2 homologue does not harbour the construct, and hence is not fluorescent). As *Sfpi1*$^{wt}$ mice do not harbour the Rosa26-mCherry construct, all *Sfpi1*$^{wt}$ peripheral blood WBC cell types did not express mCherry (both myeloid and lymphoid). In contrast, mCherry was ubiquitously and constitutively expressed across all myeloid Chr2MDR$^{mCh}$ peripheral blood WBCs, both monocytes (Mac1+) and granulocytes (Gr1+)(approximately 17% of peripheral blood WBCs were of myeloid origin). Similarly, in the lymphoid lineage of Chr2MDR$^{mCh}$ peripheral blood WBCs, both B-cells (B220+) and T-cells (CD3+) had mCherry expression (Figure 3.5A, upper panels). As mature red blood cells (i.e. erythrocytes) do not express mCherry due to nuclear expulsion before reaching full maturity, peripheral blood was treated with RBC lysis buffer before analysis by flow cytometry. Similarly, we analysed the different spleen WBC cell types of young adult Chr2MDR$^{mCh}$ WBCs, and found similar mCherry expression levels compared with those observed in the peripheral blood of those animals (Figure 3.5A, lower panels). Notably, fewer myeloid cells were observed in the spleen compared with the peripheral blood (6% and 17%, respectively).

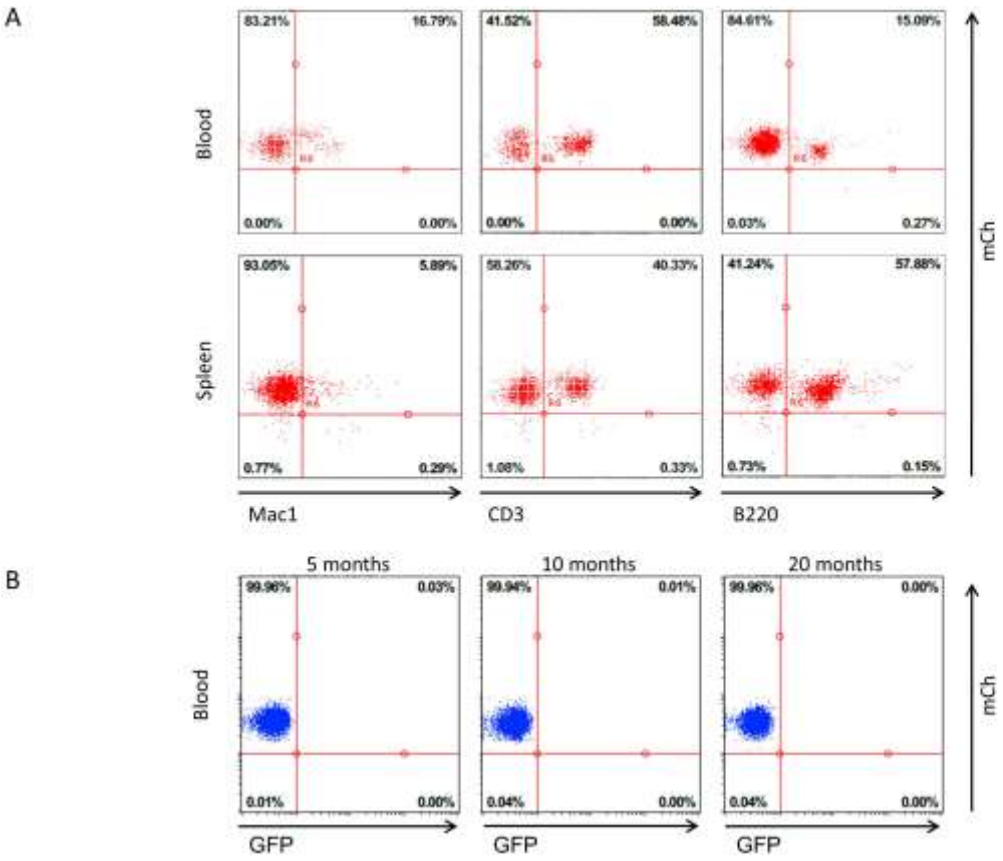



**Figure 3.5 Chr2MDR$^{mCh}$ mouse model characterisation**

(A) Blood and spleen were harvested from three young adult Chr2MDR$^{mCh}$ mice and single cell WBC suspensions were prepared. Cell suspensions were labelled with Mac1, CD3, and B220 antibodies conjugated with PE, followed by flow cytometry analysis for mCherry and cell surface marker expression. (B) Serial tail vein blood sampling was performed for life span (5 female and 5 male mice) and mCherry expression analysed by flow cytometry. Representative dot plot are shown.

To assess mCherry expression in peripheral blood at different stages throughout life (i.e. haematopoietic progeny generated from young versus older HSCs), and to exclude that mCherry is silenced when mice age, we collected tail vein blood samples throughout the life of five female and five male Chr2MDR$^{mCh}$ mice. As demonstrated above, all WBC cell types of 10 week old Chr2MDR$^{mCh}$ mice expressed mCherry. Serial blood sampling of ageing mice confirmed that mCherry expression is retained throughout life (Figure 3.5B) and these mice have a similar life span as *Sfpi1*$^{wt}$ mice (i.e.

20 months). As we had determined that mCherry is expressed across all haematopoietic cell types, and that mCherry expression is retained throughout life, we then investigated the effect of radiation on cell division of Chr2MDR$^{mCh}$ haematopoietic cells. Bone marrow was harvested from 10 week old Chr2MDR$^{mCh}$ mice and negatively selected for haematopoietic stem and progenitor cells, followed by overnight incubation in suspension cultures (200,000 cells/2 ml Stemspan™). Cultures were irradiated the following morning with a range of doses (0.1 – 3 Gy) and cell number was assessed daily. Sham-irradiated haematopoietic stem and progenitor cells showed exponential growth (a four-fold increase in cell number after 3 days). Low dose radiation exposure (i.e. 100 mGy) did not alter the growth potential. For dose higher than 100 mGy, a dose-dependent cell number reduction was observed, with doses of 2 Gy and 3 Gy highly compromising the cell division potential of the haematopoietic stem and progenitor cells (Figure 3.6A). Overall, this suggests that Chr2MDR$^{mCh}$ haematopoietic cells have a similar radiation response in suspension cultures compared to wild-type haematopoietic cells. We also investigated the effect of radiation on the colony forming potential of the Chr2MDR$^{mCh}$ haematopoietic stem and progenitor cells. Bone marrow was harvested from 10 week old Chr2MDR$^{mCh}$ mice, followed by immunomagnetic selection for haematopoietic stem and progenitor cells. Colony forming cell (CFC) assays were set-up in triplicate and irradiated the following morning (0.1 – 3 Gy). Plates were incubated for a further ten days before colonies (>50 cells/colony) were counted by light microscopy (Figure 3.6B, colony forming unit-granulocyte/macrophage). The plating efficiency for haematopoietic stem and progenitor cells was 6% (i.e. for every ~20 cells seeded, one cell was able to form a colony following ten days incubation in semisolid medium).

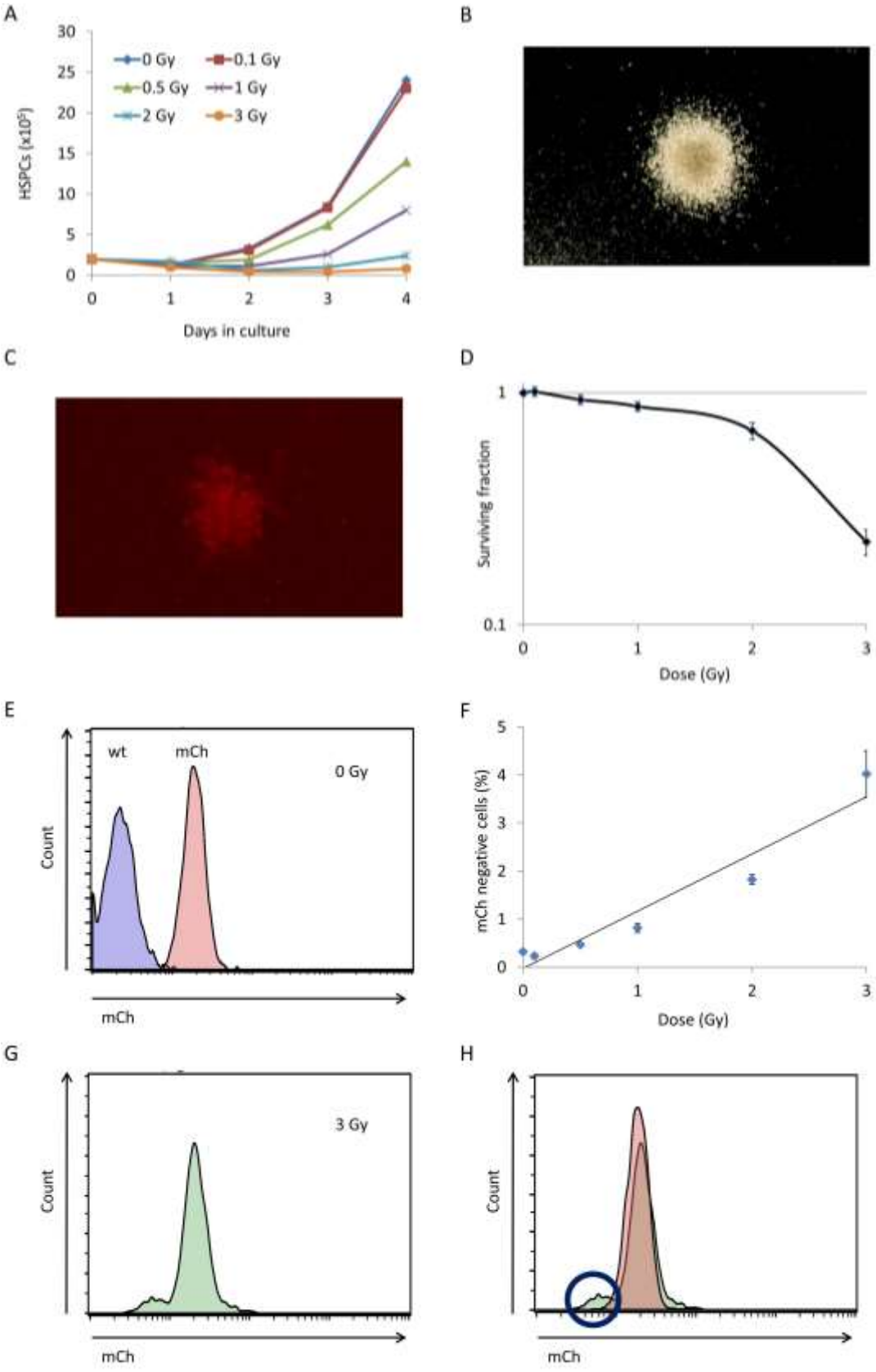



**Figure 3.6 Radiation response of Chr2MDR$^{mCh}$ haematopoietic stem and progenitor cells**

(A) Haematopoietic stem and progenitor suspension cultures showed a dose-dependent growth reduction following radiation exposure. (B) Clonogenic survival was assessed using the CFC assay (light microscopic colony forming unit, CFU; B). (C) Fluorescent image of a Chr2MDR$^{mCh}$ CFU (D) A dose-dependent reduction in colony formation was observed following radiation exposure. (E) mCherry expression of *Sfpi1*$^{wt}$ versus Chr2MDR$^{mCh}$ haematopoietic stem and progenitor cells. (F) Twenty-four hours following radiation exposure, mCherry expression of Chr2MDR$^{mCh}$ haematopoietic stem and progenitor cells was assessed by flow cytometry (3 independent replicates). (G/H) Following 3 Gy radiation exposure, approximately 4% of haematopoietic stem and progenitor cells had lost mCherry fluorescence [marked by circle; generated by overlay of mCherry sham-irradiated (red) and mCherry 3 Gy irradiated (green) histograms].

Although low dose radiation exposure (100 mGy) did not significantly reduce the colony formation of the haematopoietic stem and progenitor cells, we did observe a dose-dependent reduction in colony formation following high dose radiation exposure; with 2 Gy reducing the surviving fraction to 68% (Figure 3.6D).

We then investigated the effect of radiation exposure on mCherry expression in haematopoietic stem and progenitor cells. Bone marrow was harvested from 10 week old Chr2MDR$^{mCh}$ mice and negatively selected for haematopoietic stem and progenitor cells, followed by overnight incubation in suspension cultures (300,000 cells/2 ml Stemspan™). Cultures were irradiated the following morning, and analysed for mCherry expression by flow cytometry 24 hours following radiation exposure (0.1 – 3 Gy). Using *Sfpi1*$^{wt}$ haematopoietic stem and progenitor cells, it was possible to establish a clear cut-off for mCherry expression (Figure 3.6E). Low dose radiation exposure (100 mGy) did not alter the percentage of mCherry negative cells (i.e. cells which presumably lost the chromosome 2 homologue carrying the Rosa26-mCherry construct). A dose-dependent increase in mCherry negative cells was observed, with a maximum of 4% of haematopoietic stem and progenitor cells having lost mCherry expression following 3 Gy radiation exposure (Figure 3.6F/G/H).

Chr2MDR$^{mCh}$ haematopoietic stem and progenitor cells which do not express mCherry following radiation exposure, presumably lost the chromosome 2 homologue carrying the Rosa26-mCherry construct. As *Sfpi1* also resides in the MDR following radiation exposure, this would entail that these cells have lost one copy of *Sfpi1* and only have one *Sfpi1* copy left on the remaining chromosome 2 homologue. Having detected Chr2MDR$^{mCh}$ haematopoietic stem and progenitor cells which did not express mCherry 24 hours following 3 Gy *in vitro* radiation exposure, and as the chromosome 2 hemizygous interstitial deletion is considered to be the initiating step in radiation leukaemogenesis, we wanted to further characterise these cells having lost mCherry expression by expanding them in CFC assays.

To this end, we exposed 10 week old Chr2MDR$^{mCh}$ mice to 0 or 3 Gy *in vivo* radiation exposure and sacrificed them at 1 and 2 months post-irradiation (2 mice per condition; 6 mice in total). Bone marrow was harvested, followed by immunomagnetic selection for haematopoietic stem and progenitor cells. CFC assays were set-up in triplicate and incubated for twelve days before colonies were sampled and analysed for mCherry expression by flow cytometry (Figure 3.6C, fluorescent image of Chr2MDR$^{mCh}$ CFU). At 1 month post-irradiation, 250 colonies were sampled and all retained mCherry expression. Similarly, all 250 colonies sampled from CFC assays set-up 2 months following radiation exposure, had retained mCherry expression. Also, flow cytometry analysis of the peripheral blood and spleen of the 3 Gy exposed mice was unable to identify WBCs which had lost mCherry expression.

Interestingly, following staining of the peripheral blood with antibodies identifying T-cells, B-cells and monocytes, a significant decrease in the percentage of T-cells (and

concomitant increase in the percentage of B-cells and monocytes) was observed following radiation exposure, possibly indicating a reduced ability of the thymus to produce new T-cells (Figure 3.7).

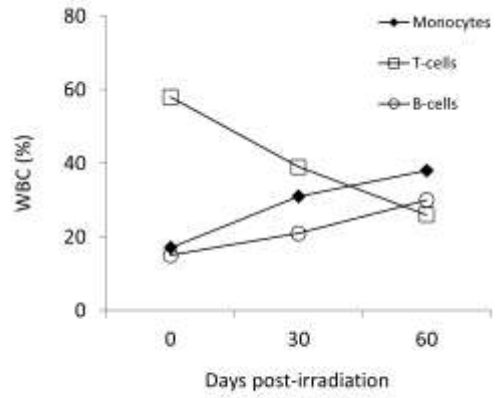



**Figure 3.7 Blood composition of Chr2MDR$^{mCh}$ mice following radiation exposure**

Chr2MDR$^{mCh}$ mice were exposed to 3 Gy *in vivo* X-irradiation and sacrificed one and two months following radiation exposure (2 mice per condition; 6 mice in total). For each mouse, peripheral blood WBC cell suspensions were labelled with Mac1 (monocytes), CD3 (T-cells), and B220 (B-cells) antibodies conjugated with PE, followed by flow cytometry analysis for cell surface marker expression.

Although we could not identify haematopoietic stem and progenitor cells which had lost mCherry expression at 1 month and 2 months following 3 Gy *in vivo* radiation exposure, we hypothesized it could take multiple months for these cells to expand and become detectable in the haematopoietic system. To this end, we exposed 10 week old Chr2MDR$^{mCh}$ mice to 0 or 3 Gy *in vivo* radiation exposure and sacrificed the mice twelve months following radiation exposure (2 mice in the sham-irradiated group and 4 mice in the 3 Gy irradiated group; 6 mice in total; Figure 3.8).

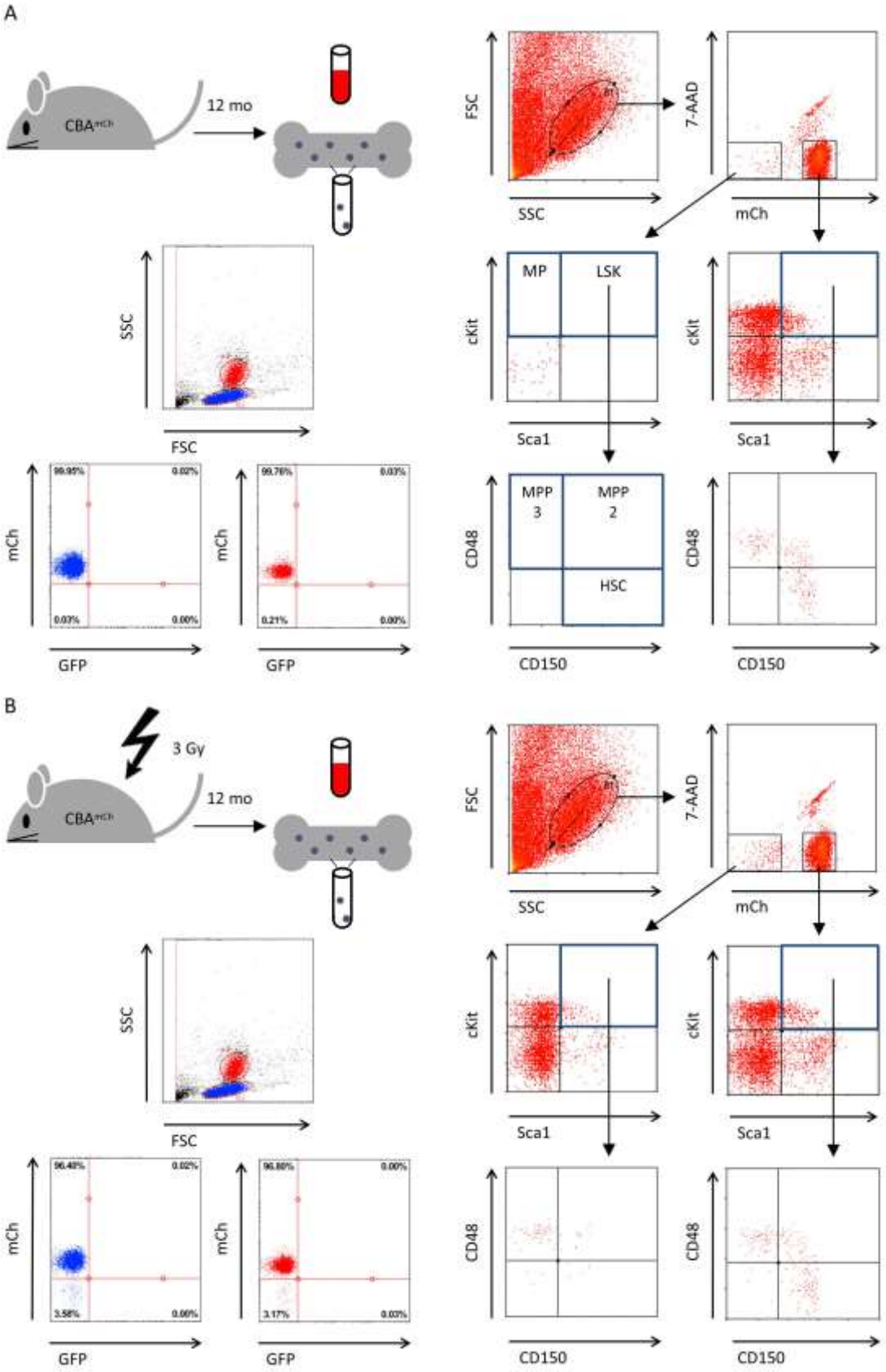



**Figure 3.8 Chr2MDR$^{mCh}$ mice show mCh- clonal expansion following radiation exposure**

Chr2MDR$^{mCh}$ mice were exposed to 0 or 3 Gy *in vivo* X-irradiation and sacrificed 12 months following radiation exposure (2 mice in the sham-irradiated group and 4 mice in the 3 Gy irradiated group; 6 mice in total). Peripheral blood WBC cell suspensions were prepared, followed by flow cytometry analysis for mCherry expression. Bone marrow was harvested and negatively selected for haematopoietic stem and progenitor cells. Cell suspensions were labelled with Sca1, cKit, CD48 and CD150 antibodies conjugated with different fluorophores, followed by flow cytometry analysis for mCherry and cell surface marker expression. Representative dot plots of sham-irradiated and 3 Gy irradiated mice (A and B, respectively).

Upon analysis of the peripheral blood of the sham-irradiated Chr2MDR$^{mCh}$ mice, all WBCs had retained mCherry expression (Figure 3.8A, left panel). Bone marrow of these mice was harvested, followed by immunomagnetic selection for haematopoietic stem and progenitor cells. Cell suspensions were labelled with Sca1, cKit, CD48 and CD150 antibodies conjugated with different fluorophores, followed by flow cytometry analysis for mCherry and cell surface marker expression. We used SLAM (i.e. CD48 and CD150) markers to identify the different haematopoietic stem and progenitor cell types. The multi-potent progenitors 1 (MPP1) and long-term HSCs (LT-HSCs, i.e. the most primitive haematopoietic stem and progenitor cells) are within a specific subset of the Lin-Sca1+cKit+ (LSK) cells: the CD48-CD150+ subpopulation. The MPP2 and MPP3 are also within the LSK cells, but have CD48+CD150+ and CD48+CD150- expression, respectively (Figure 3.8A, right panel). Myeloid progenitors (MPs) are found within the Sca1-cKit+ population. Within the haematopoietic stem and progenitor cell fraction, 4% of cells stained positive for 7-AAD and 95.1% of cells expressed mCherry (Figure 3.8A, right panel). Of those mCherry+ cells, 3% were LSK, 42.4% were MPs and 48.3% were Sca1-cKit-. Within the mCherry+LSK population, 44.7% were LT-HSCs/MPP1, 22.4% were MPP2 and 32.2% were MPP3. Only 0.9% of the haematopoietic stem and progenitor cell fraction had no mCherry expression and all were Sca1-cKit-.

In contrast, analysis of the peripheral blood of Chr2MDR$^{mCh}$ mice which were sacrificed 12 months following 3 Gy *in vivo* radiation exposure, revealed that three out of four mice had mCherry- WBCs (2.1% of peripheral blood WBCs had lost mCherry expression; Figure 3.8B, left panel). Bone marrow of these mice was also harvested, followed by immunomagnetic selection of haematopoietic stem and progenitor cells. Lin- cell suspensions were stained with Sca1, cKit, CD48 and CD150 antibodies, then analysed flow cytometry for mCherry and cell surface marker expression.

Within the haematopoietic stem and progenitor cell fraction of these 3 Gy irradiated mice, 4% of cells stained positive for 7-AAD and 92.9% of cells expressed mCherry (Figure 3.8B, right panel). Of those mCherry+ cells, 2.6% were LSK, 31.3% were MPs and 58% were Sca1-cKit-. Within the mCherry+LSK population, 42.2% were LT-HSCs/MPP1, 18.6% were MPP2 and 35.2% were MPP3. Approximately 2.3% of the haematopoietic stem and progenitor cell fraction was mCherry-. Although the majority of those cells were Sca1-cKit- (77.6%) and MPs (17.1%), some mCherry-haematopoietic stem and progenitor cells (1.7%) were LSK. Within the mCherry-LSK population, the expression of SLAM markers varied highly between mice. The vast majority of cells of the mouse represented in Figure 3.8B were MPP3 (73.3%) and MPP2 (17.4%). Only 5.81% of mCherry-LSK cells were found within the LT-HSCs/MPP1 compartment. The majority of mCherry-LSK cells for mouse 2 were LT-HSCs/MPP1 (45.5%) and MPP2 (34.5%), only 16.4% were MPP3. The mCherry-LSK cells of the third mouse were mainly LT-HSCs/MPP1 (66.4%) and MPP2 (26.7%), only 6.1% were MPP3. These LT-HSCs/MPP1 with no mCherry expression (i.e. mCherry-LSKCD48-CD150+) were then sorted (5 cells for mouse 1, 25 cells for mouse 2 and 87 cells for mouse 3)

and seeded in semisolid medium. Ten days following incubation, no colonies were detectable for any of the three mice.

As it was previously reported that following radiation exposure, cKit expression is transiently downregulated and Sca1 expression transiently upregulated with peak changes obtained two days following 3 Gy *in vivo* radiation exposure (Simonnet et al., 2009), and as we observed a reduced percentage of MPs in the haematopoietic stem and progenitor cell fraction 12 months following radiation exposure compared with sham-irradiated mice, we decided to analyse the changes in Sca1 and cKit expression at time points more closely following the radiation exposure. To this end, we exposed six male 10 week old Chr2MDR$^{mCh}$ mice to 0 or 3 Gy *in vivo* radiation exposure and sacrificed the mice 1 day and 7 days following radiation exposure (2 mice per condition). Bone marrow of these mice was harvested, followed by immunomagnetic selection for haematopoietic stem and progenitor cells. Cell suspensions were stained with Sca1 and cKit antibodies, followed by flow cytometry analysis for mCherry and cell surface marker expression.

Within the haematopoietic stem and progenitor cell fraction of the sham-irradiated mice, 5.8% of cells stained positive for 7-AAD and 92.8% of cells expressed mCherry. Of those mCherry+ cells, 1% were LSK cells and 27.5% were MPs. Only 1.4% of the haematopoietic stem and progenitor cell fraction was mCherry- and all mCherry- cells were Sca1-cKit-. In contrast, within the haematopoietic stem and progenitor cell fraction of the mice sacrificed 1 day following 3 Gy radiation exposure, the fraction of cells staining positive for 7-AAD had increased approximately two-fold compared with the sham-irradiated haematopoietic stem and progenitor cells (10.6% and 5.8%,

respectively) and 87.4% of cells expressed mCherry. Although the LSK fraction did not change (1.3% of mCherry+ cells were LSK), the MP fraction decreased two-fold compared with sham-irradiated haematopoietic stem and progenitor cells (13.8% and 27.5%, respectively). Interestingly, the Sca1+cKit-fraction increased three-fold compared with sham-irradiated haematopoietic stem and progenitor cells (13.6% and 4%, respectively; Table 4). Only 2% of the haematopoietic stem and progenitor cell fraction was mCherry- and all mCherry- cells were Sca1-cKit-.

However, seven days following 3 Gy radiation exposure, the haematopoietic stem and progenitor cell fraction of cells staining positive for 7-AAD had decreased again to levels similar compared with the sham-irradiated haematopoietic stem and progenitor cells (4.5% and 5.8%, respectively) and 93.8% of cells expressed mCherry. Within the mCherry+ fraction, 0.5% of cells were LSK. The MP fraction had increased again to levels similar compared with the sham-irradiated haematopoietic stem and progenitor cells (33% and 27.5%, respectively). Similarly, the Sca1+cKit- fraction decreased again to levels similar compared with the sham-irradiated haematopoietic stem and progenitor cells (3.5% and 4%, respectively; Table 4). Only 1.7% of the haematopoietic stem and progenitor cell fraction was mCherry- and all mCherry- cells were Sca1-cKit-.

**Table 4. Cell marker expression following radiation exposure**

| | **0 Gy** | **3 Gy 1d** | **3 Gy 7d** |
|---|---|---|---|
| **Sca1+** | 4% | 13.6% | 3.5% |
| **Sca1-** | 96% | 86.4% | 96.5% |
| **cKit+** | 28.5% | 15% | 33.5% |
| **cKit-** | 71.5% | 85% | 66.5% |

Overall, we observed an increased Sca1 expression and decreased cKit expression 1 day following radiation exposure. These changes in cell marker expression were transient, as at 7 days following radiation exposure, the Sca1 expression had decreased, and the cKit expression increased, to levels observed in sham-irradiated mice.

Finally, in all the above-mentioned experiments, heterozygous Chr2MDR$^{mCh}$ mice were used (i.e. one chromosome 2 carries the Rosa26-mCherry construct and the other is wild-type). Therefore, when the chromosome 2 deletion takes place on the chromosome 2 homologue carrying the Rosa26-mCherry construct, we would observe a loss of mCherry expression. However, if the deletion takes place on the wild-type homologue, the mCherry expression would remain unchanged and therefore, the deletion would not be detected. We tested the possibility of using homozygous Chr2MDR$^{mCh}$ mice in these experiments. However, as the mCherry expression histogram plots of cells harvested from heterozygous and homozygous Chr2MDR$^{mCh}$ mice partially overlap, it would be impossible to detect when cells from homozygous Chr2MDR$^{mCh}$ mice lose one fluorescent chromosome 2 homologue and retain the other. To overcome the issue of deletions of the wild-type chromosome 2 being undetectable, we crossed homozygous Chr2MDR$^{mCh}$ mice with homozygous *Sfpi1*$^{GFP}$ mice. The resulting offspring, termed *Sfpi1*$^{mCh/GFP}$ mice, had one chromosome 2 carrying the Rosa26-mCherry construct, with the other carrying the GFP construct. Therefore, whichever chromosome 2 is deleted, we would observe a change in fluorescence: either a loss of mCherry expression or a loss of GFP expression.

To this end, bone marrow from two male 10 week old *Sfpi1*$^{mCh/GFP}$ mice was harvested, followed by immunomagnetic selection for haematopoietic stem and progenitor cells. CFC assays were set-up in triplicate and incubated for twelve days before colonies were sampled and analysed for mCherry expression and GFP expression by flow cytometry (Figure 3.9A). Colonies were labelled with Mac1, B220 and CD3 antibodies conjugated with PE. Approximately 250 colonies were sampled, and each analysed colony expressed Mac1 cell surface marker expression, indicating that the cells in these colonies had a myeloid cell surface marker phenotype. However, the colonies did not have any B220 or CD3 expression, indicating that these cells did not have a lymphoid cell surface marker phenotype. All analysed colonies had both mCherry expression and GFP expression, making it a suitable model to investigate the chromosome 2 deletions following radiation exposure, as either GFP expression or mCherry would be lost following a radiation-induced interstitial deletion of one chromosome 2 homologue.

Therefore, bone marrow from two male 10 week old *Sfpi1*$^{mCh/GFP}$ mice was harvested, followed by immunomagnetic selection for haematopoietic stem and progenitor cells. CFC assays were set-up in triplicate and the following morning cultures were *in vitro* irradiated with a range of doses (0 – 3 Gy). Twelve days later, 100 colonies were sampled for each dose and analysed for loss of mCherry expression or GFP expression by flow cytometry (Figure 3.9B). Interestingly, all analysed colonies retained mCherry expression and GFP expression, irrespective of the radiation dose.

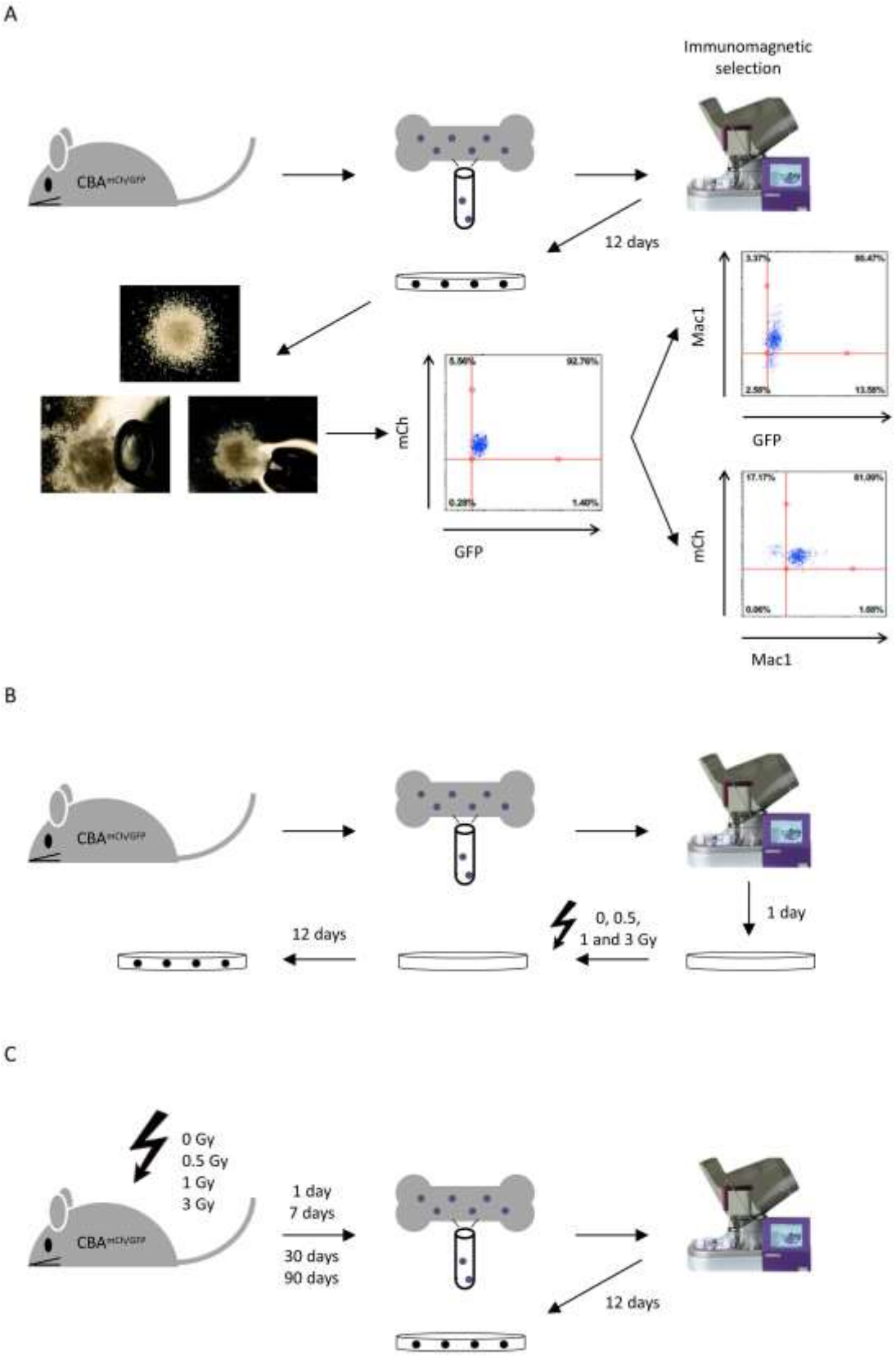



**Figure 3.9 GFP and mCherry expression in CFC assays following radiation exposure**

Homozygous Chr2MDR$^{mCh}$ mice were crossed with homozygous *Sfpi1*$^{GFP}$ mice. The resulting offspring, termed *Sfpi1*$^{mCh/GFP}$, had one chromosome 2 homologue carrying the Rosa26-mCherry construct, with the other homologue carrying the GFP construct. Bone marrow was harvested from sham-irradiated (A/B; 2 mice per experiment) or irradiated (C; 1 mouse per dose and per time-point; 16 mice overall) 10 week old *Sfpi1*$^{mCh/GFP}$ mice, followed by immunomagnetic selection for haematopoietic stem and progenitor cells. CFC assays were set-up in triplicate, and sham-irradiated (A/C) or irradiated (B) the following morning. Cultures were incubated for twelve days before colonies were sampled and analysed for loss of mCherry expression or GFP expression by flow cytometry. Colonies were labelled with Mac1, CD3, B220 antibodies conjugated with PE, followed by flow cytometry analysis for cell surface marker expression.

As we could not observe colonies which had lost mCherry expression or GFP expression following *in vitro* radiation exposure of CFC assays, we hypothesised that we might observe loss of fluorescence expression following *in vivo* radiation exposure. To this end, we exposed male 10 week old *Sfpi1*$^{mCh/GFP}$ mice to *in vivo* radiation exposure (0 - 3 Gy) and sacrificed the mice 1 day, 7 days, 1 month and 3 months later. Bone marrow was harvested, followed by immunomagnetic selection for haematopoietic stem and progenitor cells. CFC assays were set-up in triplicate and incubated for twelve days before 100 colonies were sampled for each radiation dose and each time-point, and analysed for loss of mCherry expression or GFP expression by flow cytometry (Figure 3.9C). Similarly to what was observed following *in vitro* radiation exposure, all analysed colonies retained mCherry expression and GFP expression, irrespective of the radiation dose or time-point.

### 3.2.3. Discussion

We reported in the first section of this chapter that allogeneic HSCs can compete for niches in the nonmyeloablated NSG bone marrow compartment and that the nonmyeloablated NSG bone marrow microenvironment is capable of supporting allogeneic long-term HSC engraftment and differentiation. Donor haematopoietic stem and progenitor cells were harvested from *Sfpi1*$^{GFP}$ mice, and expressed GFP under control of the *Sfpi1* promotor. However, once *Sfpi1*$^{GFP}$ haematopoietic cells reached the mature, terminally-differentiated lymphocytic stage, GFP expression was reduced (i.e. B-cells) or completely lost (i.e. T-cells), making it difficult to track and study these cells without cell surface marker analysis by flow cytometry. Therefore, we engineered a novel genetic mouse model, Chr2MDR$^{mCh}$ mice, where the fluorescent reporter mCherry is under the ubiquitous expression of the Rosa26 promotor.

The insertion site of the Rosa26-mCherry construct was chosen specifically to be located within the MDR following radiation exposure, so that in the event of an interstitial chromosome 2 deletion occuring in a haematopoietic cell, the Rosa26-mCherry construct would be deleted simultaneously, allowing us to detect the deletion as a loss of mCherry expression. Therefore, it was of utmost importance to confirm that mCherry was expressed in all haematopoietic cell types, and not only in a subset of cells (as in *Sfpi1*$^{GFP}$ mice). We first confirmed that young adult Chr2MDR$^{mCh}$ mice express mCherry across all terminally-differentiated haematopoietic cell types, both myeloid and lymphoid lineages. We also confirmed through serial blood sampling of ageing Chr2MDR$^{mCh}$ mice that when Chr2MDR$^{mCh}$ HSCs age and undergo multiple cell divisions to generate daughter haematopoietic cells, mCherry was still expressed.

If a HSC or haematopoietic progenitor had lost the Rosa26-mCherry construct at a specific point in time, we would have been able to detect this as an expanding clone of mCherry- haematopoietic cells. For example, in the case the construct had been lost in a HSC, we would have detected mCherry- granulocytes, monocytes and lymphocytes, whereas if the construct had been lost in a GMP, we would have only observed mCherry- granulocytes and monocytes in the peripheral blood, as lymphocytes would have retained mCherry expression.

We also assessed the effect of radiation exposure on mCherry expression in haematopoietic cells. A dose-dependent increase in mCherry- haematopoietic stem and progenitor cells was observed 24 hours following *in vitro* radiation exposure (StemSpan™ suspension cultures). It is noteworthy that without radiation exposure approximately 0.3% of cells had no mCherry expression. However, it was previously reported that, using FISH with a probe specific for *Sfpi1* loss, 0.85% of sham-irradiated CBA/H bone marrow cells showed *Sfpi1* loss (Peng et al., 2009). Twenty-four hours following 3 Gy *in vitro* radiation exposure, we observed that approximately 4% of cells had no mCherry expression. As these haematopoietic stem and progenitor cells were harvested from heterozygous Chr2MDR$^{mCh}$ mice (i.e. one chromosome 2 homologue carries the Rosa26-mCherry construct and the other homologue is wild-type), we can extrapolate that, in theory, we might have missed half of the chromosome 2 deletions (in case the deletion took place on the wild-type, non-fluorescent chromosome 2 homologue), and that the total of haematopoietic stem and progenitor cells which lost a chromosome 2 copy was approximately 8%. A similar level of *Sfpi1* loss was reported 24 hours following 3 Gy *in vivo* radiation exposure [approximately 8.67% of bone

marrow cells had *Sfpi1* loss 24 hours following radiation exposure, as assessed by FISH (Peng et al., 2009)].

As we observed an increased percentage of mCherry- haematopoietic stem and progenitor cells following *in vitro* radiation exposure, we then wanted to further investigate this following *in vivo* radiation exposure. Interestingly, one month following 3 Gy radiation exposure of Chr2MDR$^{mCh}$ mice, we observed a clear decrease in the number of T-cells in the peripheral blood, which decreased even further two months following radiation exposure. In contrast, the percentage of B-cells and monocytes increased following radiation exposure. It has been previously described that cancer patients treated with radiotherapy, develop a similar T-lymphopenia and B-lymphocytosis which was attributed to a reduced ability of the thymus to produce new T-cells (Fuks et al., 1976). However, we did not observe mCherry- cells in the peripheral blood and spleen of these mice. CFC assays were then set-up using haematopoietic stem and progenitor cells isolated from these mice. Interestingly, all analysed colonies expressed mCherry, both at one and two months following radiation exposure. It was surprising to us not to detect mCherry- colonies (as each colony is derived from one single 'haematopoietic stem and progenitor cell', all cells in the colony would be clones of this cell). It was previously reported that one month following 3 Gy *in vivo* radiation exposure, approximately 10% of bone marrow cells had lost *Sfpi1*, analysed by FISH (Peng et al., 2009). As we used heterozygous Chr2MDR$^{mCh}$ mice, in theory, we would not detect 50% of the chromosome 2 deletions (as those occurring on the wild-type, non-fluorescent chromosome 2 homologue would not change the fluorescence of the cell). Therefore, we would still expect to detect 5% of colonies to have lost mCherry

expression. It could be possible that mCherry- haematopoietic stem and progenitor cells require a micro-environment which is only found in the bone marrow haematopoietic niche, and therefore these cells cannot form colonies *in vitro*. The semisolid medium we used in this experiment has been formulated to support optimal growth of murine granulocyte-macrophage progenitor cells, and contains growth factors such as recombinant mouse stem cell factor, recombinant mouse interleukin 3, recombinant human interleukin 6 and recombinant human erythropoietin. Possibly, mCherry- cells are at a growth disadvantage and are incapable of forming colonies.

It was previously reported that, nine to twelve months following radiation exposure, 50% of exposed mice have a clonal expansion of bone marrow cells with chromosome 2 aberrations (Bouffler et al., 1997). Therefore, we repeated the above-mentioned experiment but sacrificed Chr2MDR$^{mCh}$ mice only at twelve months following radiation exposure. Upon analysis of the peripheral blood of the sham-irradiated mice, all WBCs had retained expression. Interestingly, analysis of the bone marrow compartment revealed that 1% of haematopoietic stem and progenitor cells had no mCherry expression. Similar background levels of *Sfpi1* loss in bone marrow cells have been reported in CBA/Ca mice 365 days following sham-irradiation [0.83% of bone marrow cells showed *Sfpi1* loss, as analysed by FISH (Peng et al., 2009)]. Staining with Sca1 and cKit antibodies (i.e. cell surface markers only expressed by primitive haematopoietic cells), showed that all mCherry- haematopoietic stem and progenitor cells were Sca-cKit-, indicating these cells most likely belonged to the more lineage-committed haematopoietic lineages rather than the haematopoietic stem cell population.

In contrast, three out of four Chr2MDR$^{mCh}$ mice sacrificed twelve months following 3 Gy *in vivo* radiation exposure, presented with mCherry- cells in the peripheral blood. Similarly, in the bone marrow, the percentage of mCherry- haematopoietic stem and progenitor cells increased to 2.3%, compared with 0.9% in sham-irradiated mice. The vast majority of mCherry- cells were Sca1-cKit-. However, 1.7% of mCherry- haematopoietic stem and progenitor cells were LSK. Within this mCherry-LSK population, the use of SLAM markers allowed, aside of mCherry- MPP2s and MPP3s, the identification of mCherry- HSCs/MPP1, albeit in very small numbers. These mCherry- HSCs/MPP1 were subsequently cultured in semisolid medium but failed to generate any colonies. Within the mCherry+ cell population, the number of LSK cells was not markedly lower compared with sham-irradiated mice (2.6% and 3%, respectively). However, the Sca1-cKit- cells increased compared with sham-irradiated mice (58% and 48.3%, respectively). Similarly, the percentage of MPs decreased significantly (31.3 and 44.7%, respectively), indicating a reduced number of MPs are present in these irradiated mice twelve months following 3 Gy *in vivo* radiation exposure.

As we were able to identify mCherry- HSCs and MPPs in the haematopoietic stem and progenitor cell fraction twelve months following 3 Gy *in vivo* radiation exposure, we then investigated if we could identify mCherry- HSCs and MPPs shortly following radiation exposure. We sacrificed Chr2MDR$^{mCh}$ mice one and seven days following 3 Gy radiation exposure, but could not identify any mCherry- HSCs or MPPs. However, we did observe an increase in Sca1 expression and a decrease in cKit expression of haematopoietic stem and progenitor cells one day following radiation exposure.

Similar changes have been reported at two days following 3 Gy *in vivo* radiation exposure (Simonnet et al., 2009). Interestingly, at 7 days following radiation exposure, Sca1 and cKit expression had returned to normal levels, indicating these changes in cell surface marker expression are transient rather than permanent.

All the above-mentioned experiments were performed with heterozygous Chr2MDR$^{mCh}$ mice. The disadvantage of using these mice was, that in half of haematopoietic cells, a chromosome 2 deletion would occur on the wild-type, non-fluorescent chromosome 2 homologue and would therefore not be detected as a loss in fluorescence. To overcome this shortcoming, we crossed homozygous Chr2MDR$^{mCh}$ mice with homozygous *Sfpi1*$^{GFP}$ mice, resulting in offspring with one chromosome 2 homologue carrying the Rosa26-mCherry construct and the other homologue carrying the GFP construct. The haematopoietic stem and progenitor cells of the *Sfpi1*$^{mCh/GFP}$ mice were then used in CFC assays. Interestingly, twelve days following *in vitro* radiation exposure, we could not identify colonies that had lost mCherry expression or GFP expression, irrespective of the radiation dose. We also sacrificed *Sfpi1*$^{mCh/GFP}$ mice at 1 day, 1 week, 1 month and 3 months following radiation exposure (0 – 3 Gy) followed by seeding the cells in CFC assays, hypothesising we might be able to detect colonies following *in vivo* radiation exposure. It was previously reported that three months following 3 Gy *in vivo* radiation exposure, approximately 5.4% of bone marrow cells had lost *Sfpi1*, as analysed by FISH (Peng et al., 2009). However, we did not identify a single colony that had lost mCherry expression or GFP expression, both short- and long-term following radiation exposure.

It was an interesting finding that all CFC colonies of *in vivo* exposed mice retained both mCherry expression and GFP expression. As we demonstrated before, both sham-irradiated and 3 Gy irradiated mice had approximately 1% mCherry- haematopoietic stem and progenitor cells in the bone marrow, as analysed by flow cytometry. Therefore, we would anticipate to observe at least 1% of all colonies to have lost mCherry expression or GFP expression. However, our findings are in agreement with previously published data where chromosome 2 deletions were not detected in Lin- cells 7 days following 3 Gy *in vitro* radiation exposure, as analysed by FISH, and was possibly attributed to the fact that culturing for 7 days inadvertently selected for cells that are not damaged. Similarly, chromosome 2 deletions were not detected in CFU-S12 assays were myeloablated mice were injected with 3 Gy *in vivo* exposed TBM cells (Olme et al., 2013a). In this study, the TBM cells were harvested and injected 7 days and 10 months following radiation exposure, and individual spleen colonies were dissected out 12 days after transplantation.

We briefly considered the possibility that the Rosa26-mCherry construct was not located within the MDR following radiation exposure, and would therefore not be deleted in the event of an interstitial chromosome 2 deletion. As we confirmed the presence of the construct by PCR, and as we were able to detect substantial numbers of mCherry- haematopoietic stem and progenitor cells, including HSCs and MPPs, twelve months following *in vivo* radiation exposure, we were confident we could rule out this possibility.

### 3.3. *In vivo* ionising radiation alters the transplantation potential, mitochondrial function and gene expression of murine HSCs

A variety of epidemiological studies provided clear support for an increased leukaemia incidence following moderate to high radiation exposure. The continuing epidemiological survey of the atomic bomb survivors estimates that approximately 50% of all leukaemia cases observed in survivors exposed to doses higher than 5 mGy, are associated with radiation exposure (Hsu et al., 2013). Similarly, patients who received radiotherapy as part of their treatment plan have an elevated risk of leukaemia (Travis et al., 2000; Wright et al., 2010). However, over the past 30 years, low dose radiation exposure increased two-fold, mainly attributed to a six-fold increase in exposure from medical sources (e.g. computed tomography, nuclear medicine and radiography)(Brenner and Hall, 2007). Recent epidemiological studies reported positive associations between protracted low dose radiation exposure and leukaemia, both in radiation-monitored workers (Leuraud et al., 2015) and in patients exposed to computed tomography during childhood or adolescence (Pearce et al., 2012; Mathews et al., 2013).

Our findings reported in section 3.1 indicate that allogeneic HSCs can compete for niches in the nonmyeloablated NSG bone marrow compartment and that the nonmyeloablated NSG BM microenvironment is capable of supporting allogeneic long-term HSC engraftment and differentiation. Using this novel NSG transplantation model, we undertook to study the effects of high and low dose *in vivo* radiation exposure on the long term fate of HSCs, without the requirement of prior radio-ablation of the recipient, and thus leaving the recipient's bone marrow microenvironment uncompromised.

### 3.3.1. Both high and low dose ionising radiation exposure reduce the contribution of irradiated HSCs towards long-term haematopoiesis

Following the development of the Chr2MDR$^{mCh}$ mice described in section 3.2, where mCherry is expressed under control of the Rosa26 promotor, resulting in a constitutively expression across all haematopoietic cell types, and following the subsequent characterisation of these mice and their response to radiation response, we decided to use the Chr2MDR$^{mCh}$ mice in subsequent experiments rather than the *Sfpi1*$^{GFP}$ mice, where *Sfpi1* is under control of the *Sfpi1* promotor, resulting in a variable expression across the haematopoietic cells.

Bone marrow cells from male 10 week old Chr2MDR$^{mCh}$ mice were harvested 7 days following radiation exposure (0, 0.01, 0.1, 1 or 3 Gy; cells of three donor mice were pooled per dose), followed by immunomagnetic selection for haematopoietic stem and progenitor cells, hereby depleting the bone marrow from mature, lineage-committed cells. Age-matched NSG mice were randomised into five experimental groups (5 NSG mice per group) prior to tail vein injection of 1 x$10^6$ haematopoietic stem and progenitor cells per NSG mouse. Six months following IV transplantation, NSG mice were sacrificed, and peripheral blood was collected to assess contribution of Chr2MDR$^{mCh}$ donor cells towards long-term multilineage haematopoiesis in unconditioned NSG recipients (Figure 3.10A).

All five NSG mice injected with sham-irradiated haematopoietic stem and progenitor cells, presented with donor-derived lymphoid cells in the peripheral blood, both B-cells (B220+/mCherry+) and T-cells (CD3+/mCherry+), in contrast to the peripheral blood of unconditioned NSG mice which lacked B-cells (B220-) and T-cells (CD3-)(Figure 3.10B, right and left panels, respectively).

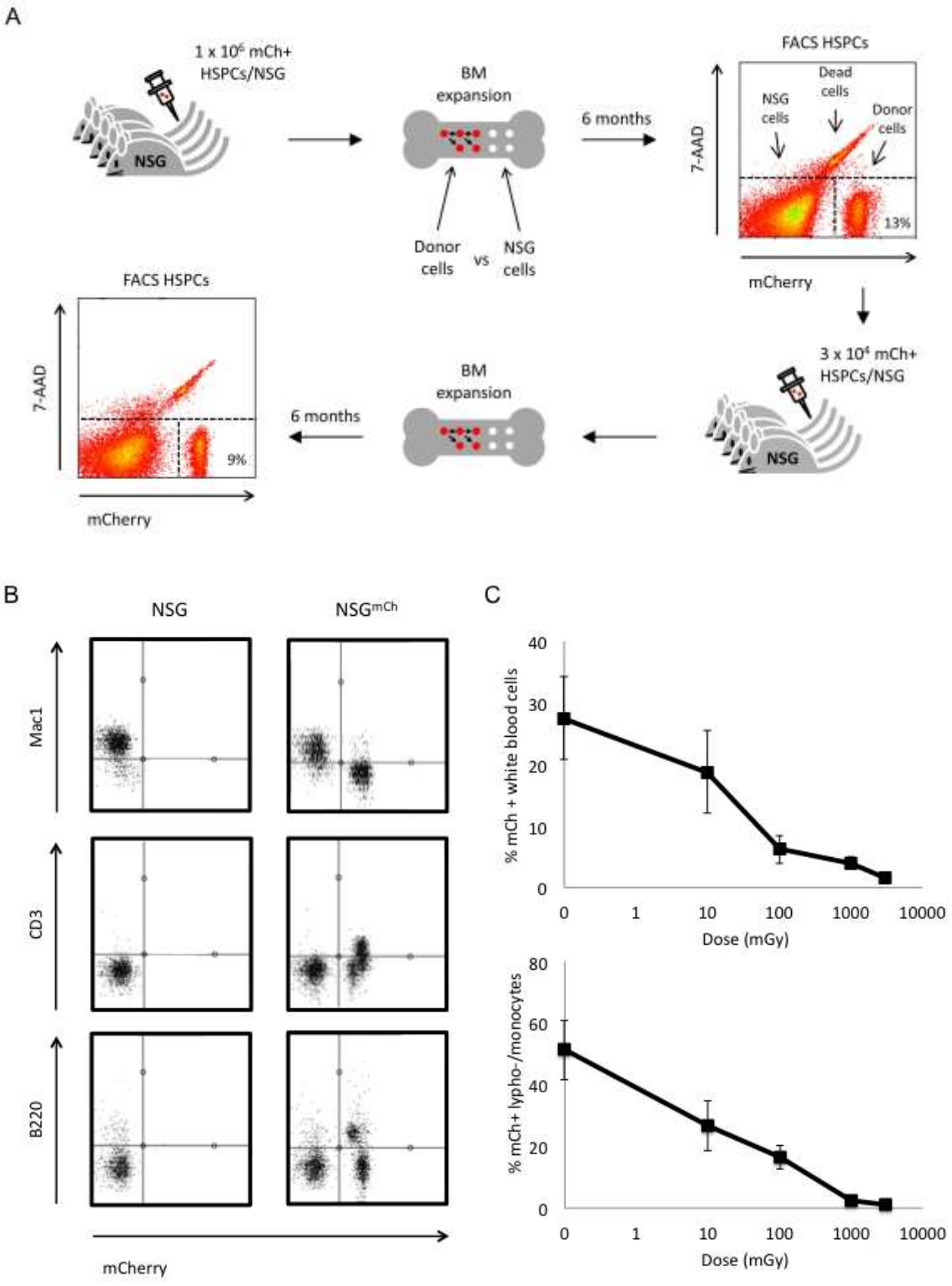



**Figure 3.10 Unconditioned NSG mice are permissive to allogeneic HSC transplantation**

(A) Six months following tail vein injection of Chr2MDR$^{mCh}$ haematopoietic stem and progenitor cells (exposed to 0, 0.01, 0.1, 1 or 3 Gy seven days prior to injection; cells of three donor mice were pooled per dose; 4 NSG mice per dose), NSG mice were

sacrificed, followed by immunomagnetic selection of haematopoietic stem and progenitor cells, and analysis of donor chimerism in the bone marrow and peripheral blood by flow cytometry. mCherry+Sca1+ haematopoietic stem and progenitor cells were reinjected into secondary NSG recipients. Six months later, donor chimerism in the peripheral blood and haematopoietic stem and progenitor cells was analysed by flow cytometry. (B) Representative multilineage NSG peripheral blood chimerism (B-cells, B220+/mCherry+; T-cells, CD3+/mCherry+; monocytes and granulocytes, Mac1+/mCherry+) six months following primary transplantation. (C) Donor chimerism in peripheral blood of NSG mice injected with sham-irradiated or irradiated Chr2MDR$^{mCh}$ haematopoietic stem and progenitor cells six months following primary transplantation.

In addition, all five NSG mice showed myeloid cell chimerism (approximately 8% of granulocytes and monocytes in the recipients' peripheral blood were donor-derived, Mac1+/mCherry+), and 13% of haematopoietic stem and progenitor cells in these NSG mice' was donor-derived. Similar to NSG mice transplanted with sham-irradiated cells, all twenty NSG mice injected with irradiated haematopoietic stem and progenitor cells (0.01 – 3 Gy), presented six months following transplantation with mCherry+ lympho-/monocytic cells in the peripheral blood (B-cells, T-cells and monocytes; Figure 3.10C, lower panel). A significant decrease in mCherry+ lympho-/monocytic cells was observed in NSG mice injected with 0.01 Gy irradiated haematopoietic stem and progenitor cells, compared with NSG mice injected with sham-irradiated cells (29% and 50.9%, respectively). Chimerism levels decreased even further in NSG mice injected with cells exposed to higher doses of irradiation. When looking at individual haematopoietic cell types, a dose-dependent decrease of B-cell and T-cell lymphoid cell chimerism was observed following radiation exposure (Figure 3.11A, upper and lower panel, respectively). Similarly, a dose-dependent decrease was observed for monocytes and granulocytes chimerism following radiation exposure (Figure 3.11B, upper and lower panel, respectively).

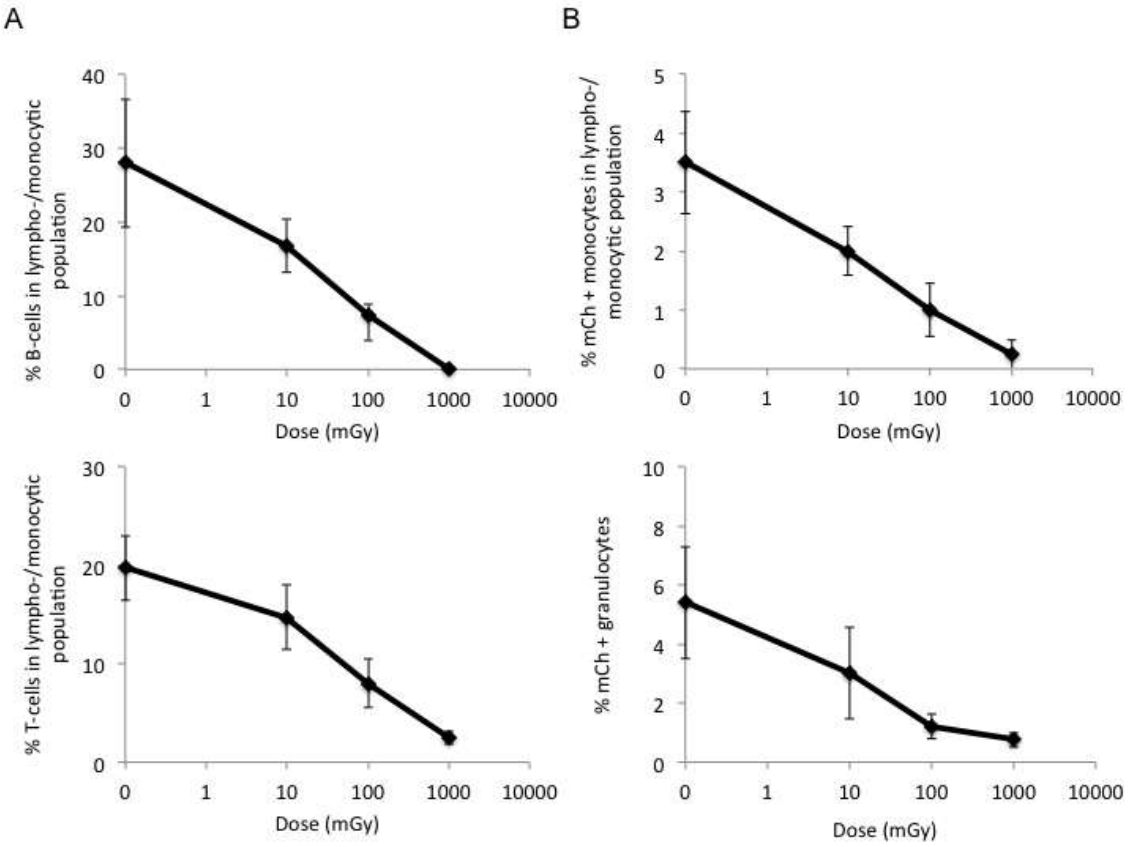



**Figure 3.11 Radiation-dependent changes in peripheral blood chimerism following transplantation of Chr2MDR$^{mCh}$ haematopoietic stem and progenitor cells**

Six months following tail vein injection of Chr2MDR$^{mCh}$ haematopoietic stem and progenitor cells (exposed to 0, 0.01, 0.1, 1 or 3 Gy seven days prior to injection; cells of three donor mice were pooled per dose; 4 NSG mice per dose), NSG mice were sacrificed, followed by analysis of donor chimerism in the peripheral blood by flow cytometry. Peripheral blood WBC cell suspensions were labelled with antibodies for B220, CD3 and Mac1 conjugated with PE. Peripheral blood B-cell and T-cell chimerism (A) and myeloid chimerism (B) were calculated.

Subsequently, we also analysed the bone marrow chimerism levels. To this end, bone marrow of the primary NSG mice was harvested and pooled per radiation dose, followed by immunomagnetic selection for haematopoietic stem and progenitor cells. Cell suspensions were stained with Sca1, cKit, CD48 and CD150 antibodies, followed by flow cytometry analysis for mCherry and cell surface marker expression.

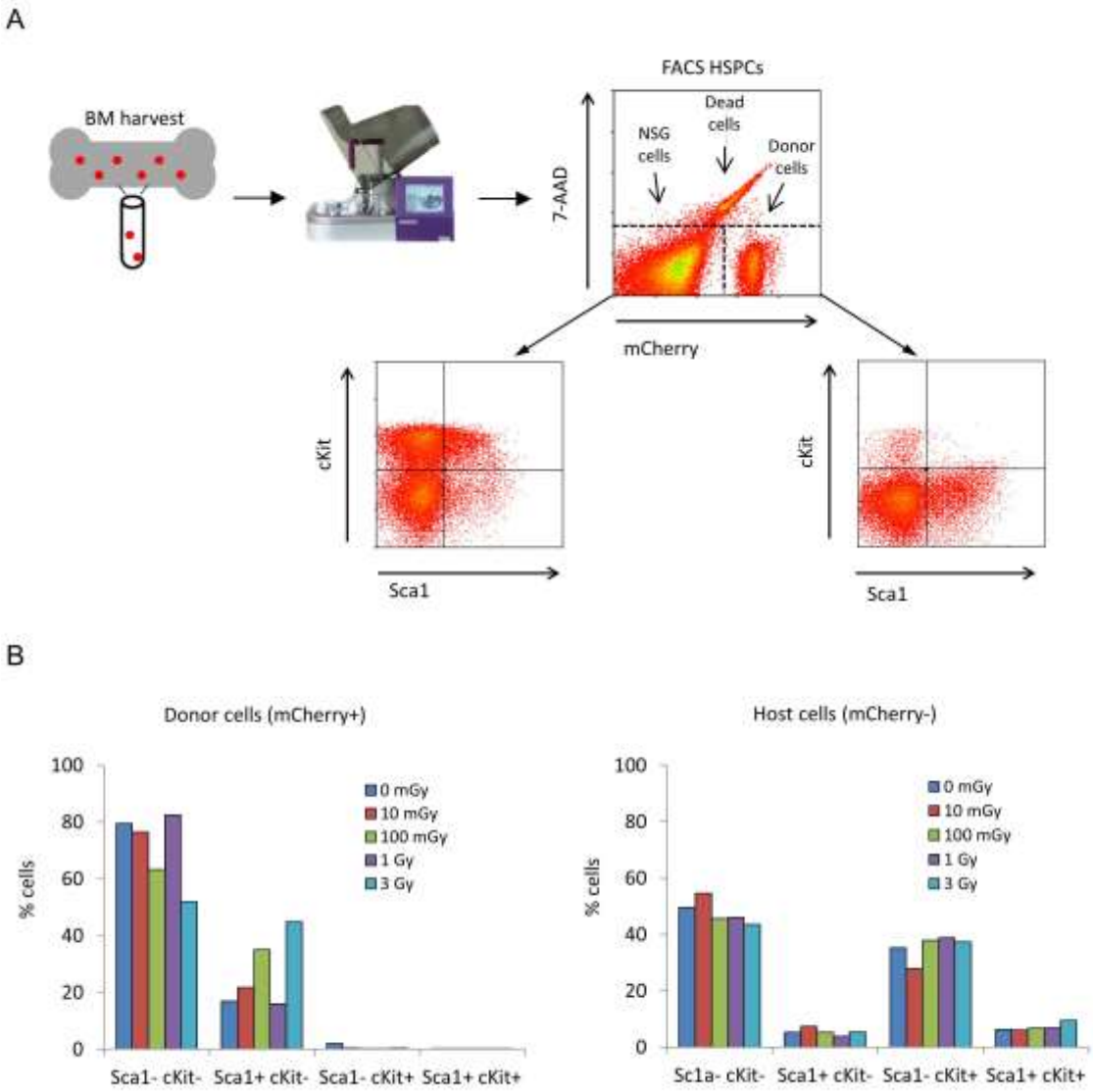



**Figure 3.12 Changes in Sca1 and cKit expression following radiation exposure**

Six months following tail vein injection of Chr2MDR$^{mCh}$ haematopoietic stem and progenitor cells (exposed to 0, 0.01, 0.1, 1 or 3 Gy seven days prior to injection; cells of three donor mice were pooled per dose; 4 NSG mice per dose), NSG mice were sacrificed, followed by analysis of donor chimerism in the haematopoietic stem and progenitor cells by flow cytometry. Cell suspensions were labelled with antibodies for Sca1 and cKit. (A) Representative dot plot of haematopoietic stem and progenitor cell fraction. (B) Quantification of the percentage of cells expressing a particular cell surface marker.

Analysis of the haematopoietic stem and progenitor cell fraction of NSG mice injected with sham-irradiated haematopoietic stem and progenitor cells, showed that approximately 13% of these cells expressed mCherry (Figure 3.12A).

Interestingly, the expression of Sca1 and cKit differed highly between mCherry+ cells (i.e. Chr2MDR$^{mCh}$ donor cells) and mCherry- cells (i.e. NSG cells). Whereas 5.3% of mCherry- cells were LSK, only 0.51% of mCherry+ cells were LSK (Figure 3.12A). Within the LSK fraction, the percentage of HSCs/MPP1 was markedly lower in mCherry-LSK cells compared with mCherry+LSK cells (1.6% and 12.8%, respectively). The number of MPs (i.e. Sca1-cKit+ cells) was markedly lower in mCherry- cells compared with mCherry+ cells (2.8% and 39.5, respectively). Contrastingly, the percentage of Sca1+cKit- was markedly higher in mCherry- cells compared with mCherry+ cells (16.8% and 5.3%, respectively). Overall, this indicated a lower cKit expression and higher Sca1 expression in mCherry+ cells compared with mCherry- cells (Figure 3.12A).

This change became even more apparent when comparing Sca1 expression of mCherry+ haematopoietic stem and progenitor cells obtained from NSG mice injected with irradiated haematopoietic stem and progenitor cells. Sca1 expression increased further with dose, from 15.7% Sca+cKit- in 0 Gy to 41.4% Sca+cKit- cells in 3 Gy (Figure 3.12B, left panel). However, Sca1 and cKit had stable expression levels in mCherry- cells, indicating that this dose-dependent change in Sca1 expression is possibly attributable to the radiation exposure of mCherry+ haematopoietic stem and progenitor cells prior to transplantation (Figure 3.12B, right panel). It was also noted that within the mCherry+ cell fraction, the percentage Sca1-cKit+ cells decreased from 2.6% in sham-irradiated NSGs to 0.2% in irradiated NSGs, irrespective of dose

(Figure 3.12B, left panel), a change which was not observed in mCherry- cells. Finally, the mCherry+ haematopoietic stem and progenitor cell fraction six months following primary transplantation was 13%, 16.9%, 10.1%, 7.2% and 3.6% (NSG mice injected with 0, 0.01, 0.1, 1 and 3 Gy irradiated cells, respectively).

mCherry+Sca1+ haematopoietic stem and progenitor cells were subsequently sorted for each individual radiation dose, and reinjected into secondary NSG mice, except for 3 Gy cells where insufficient cells could be harvested from the primary NSG mice. Each secondary NSG mouse was injected with 3 x $10^4$ mCherry+Sca1+ haematopoietic stem and progenitor cells (Figure 3.10A). Six months following secondary transplantation, all except one NSG mouse had mCherry+ cells in the peripheral blood. The only mouse which did not show chimerism was a secondary NSG injected with cells harvested from primary NSG mice injected with sham-irradiated cells, possibly due to a failed injection.

Although the same number of mCherry+Sca1+ haematopoietic stem and progenitor cells was injected for each radiation dose (i.e. 3 x $10^4$ cells/secondary NSG mouse), the mCherry+ chimerism levels six months following transplantation into secondary NSG mice varied with radiation dose. The highest mCherry+ chimerism level was detected in the peripheral blood of the secondary NSG mouse which was injected with mCherry+Sca1+ cells obtained from primary NSG mice transplanted with sham-irradiated cells (6.7%; Table 5). Closely followed by chimerism levels in secondary NSG mice which were injected with mCherry+Sca1+ cells obtained from primary NSG mice transplanted with 0.01 Gy irradiated cells (0.3%, 0.9%, 1.4% and 6.5% mCherry+ WBCs in secondary NSG A, B, C and D, respectively; Table 5).

Peripheral blood mCherry+ chimerism levels decreased even further in secondary NSG mice which were injected with mCherry+Sca1+ cells obtained from primary NSG mice transplanted with 0.1 Gy irradiated cells (0.6%, 1.8% and 4.4% mCherry+ WBCs in secondary NSG A, B and C, respectively) and 1 Gy irradiated cells (0.4% and 0.5% mCherry+ WBCs in secondary NSG A and B, respectively; Table 5).

**Table 5. mCherry chimerism in secondary NSG mice**

| Dose (Gy) | NSG number | % mCh+ WBCs | % mCh+ granul | % mCh+ HSPCs |
|---|---|---|---|---|
| **0** | A | 6.7 | 0.5 | nd |
| | B | 0 | 0 | nd |
| **0.01** | A | 0.3 | 0 | nd |
| | B | 0.9 | 0 | nd |
| | C | 1.4 | 0.3 | 7.8 |
| | D | 6.5 | 1.8 | 9.0 |
| **0.1** | A | 0.6 | 0 | nd |
| | B | 1.8 | 0 | nd |
| | C | 4.4 | 0 | nd |
| **1** | A | 0.4 | 0 | nd |
| | B | 0.5 | 0 | nd |

nd, not determined

mCherry+ myeloid chimerism was only observed in secondary NSG mice which were injected with mCherry+Sca1+ cells obtained from primary NSG mice transplanted with 0 Gy irradiated cells (0.5% of granulocytes were mCherry+) and 0.01 Gy irradiated cells (secondary NSG A and B did not have myeloid chimerism, however in secondary NSG C and D, 0.3% and 1.8% of granulocytes were mCherry+; Table 5). Secondary NSG mice which were injected with mCherry+Sca1+ cells obtained from primary NSG mice transplanted with 0.1 Gy irradiated cells and 1 Gy irradiated cells did not show mCherry+ myeloid chimerism six months following secondary transplantation. As the number of sorted mCherry+ Sca1+ cells from the primary NSG mice varied per

radiation dose, the number of injected secondary NSG mice varied depending on the total number of cells sorted, but each secondary NSG was injected with 3 x $10^4$ mCherry+Sca1+ haematopoietic stem and progenitor cells.

The bone marrow of two secondary NSG mice was harvested (i.e. secondary NSG mice which were injected with mCherry+Sca1+ cells obtained from primary NSG mice transplanted with 0.01 Gy irradiated cells), followed by immunomagnetic selection for haematopoietic stem and progenitor cells. Cell suspensions were labelled with Sca1 and cKit antibodies, followed by flow cytometry analysis for mCherry and cell surface marker expression. The secondary NSG mouse with the highest peripheral blood WBC chimerism had 9% mCherry+ haematopoietic stem and progenitor cells, and the majority of mCherry+ cells were Sca1+ (86.1%). The other secondary NSG mouse had 7.8% mCherry+ haematopoietic stem and progenitor cells, and the majority of mCherry+ cells were Sca1+ (94.3%). The mCherry+ haematopoietic stem and progenitor cells in both secondary NSG mice did not express cKit.

### 3.3.2. Mitochondrial function, gene expression and cell cycle of HSCs following *in vivo* radiation exposure

As we described in the previous section, a dose-dependent reduction in chimerism levels could be observed in unconditioned NSG mice six months following transplantation of irradiated haematopoietic stem and progenitor cells (both low and high dose radiation exposure). Given the fact that five months following transplantation, haematopoiesis is entirely dependent on long-term HSC activity (Marusyk et al., 2009), our results suggested that the presence of multilineage reconstitution is most likely due to allogeneic HSC engraftment in these unconditioned NSG mice. To begin to define how these reduced chimerism levels are induced following low dose radiation exposure, we committed to investigating the HSC fraction at the time of transplantation (i.e. seven days following radiation exposure).

Commonly used cell surface markers to isolate HSCs within the haematopoietic stem and progenitor cell fraction, are Sca1, cKit, CD48 and CD150 (i.e. LSKCD48-CD150+)(Kiel et al., 2005). However, it has been previously reported that for various murine strains, including CBA/H and BALB/c mice, the haematopoietic cells have low Sca1 expression (Spangrude and Brooks, 1993). To this end, we harvested the bone marrow of four male 10 week old mice [two Chr2MDR$^{mCh}$ mice (i.e. CBA/H background) and two C57BL/6 mice], followed by immunomagnetic selection of haematopoietic stem and progenitor cells. Cells were labelled with Sca1, cKit, CD27 and CD201 antibodies. In Chr2MDR$^{mCh}$ mice, the LSK population was five-fold smaller compared with age-matched C57BL/6 mice (0.9% and 4.5% of haematopoietic stem and progenitor cells are LSK, respectively; Figure 3.13A).

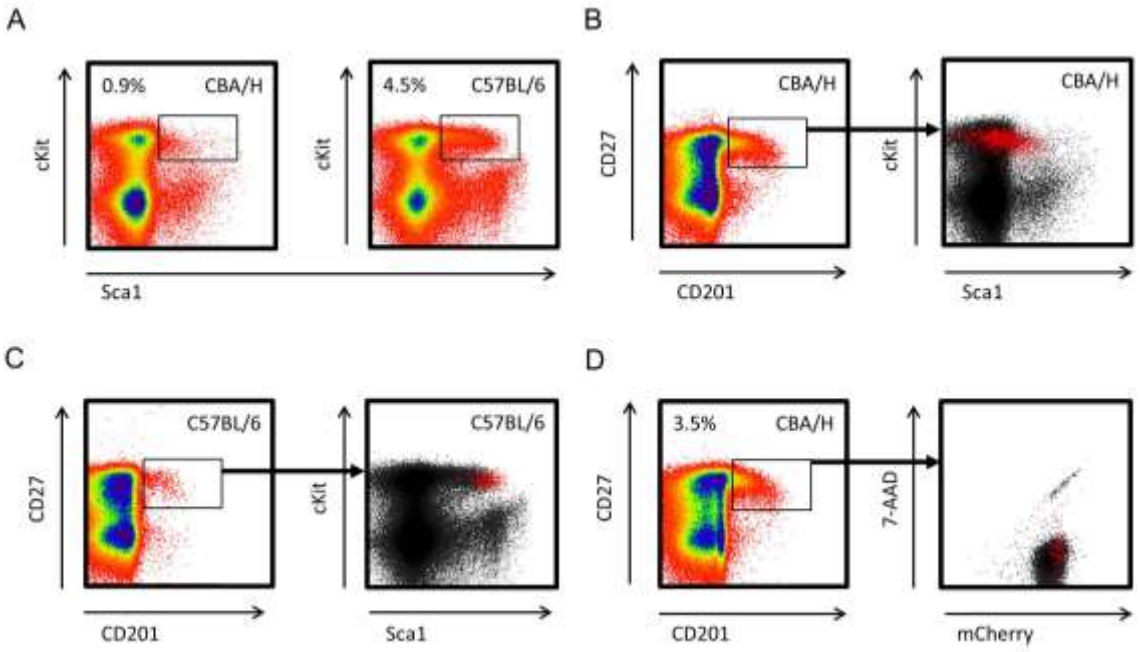



**Figure 3.13 Expression of HSC cell surface markers in CBA/H and C57BL/6 mice**

Bone marrow cells were harvested from male 10 week old CBA/H and C57BL/6 mice (two Chr2MDR$^{mCh}$ mice (i.e. CBA/H background) and two C57BL/6 mice), followed by immunomagnetic selection of haematopoietic stem and progenitor cells. (A) Cells were labelled with Sca1, cKit, CD27 and CD201 antibodies. The LSK population in CBA/H mice is five-fold smaller compared with C57BL/6 mice (0.9% and 4.5% of Lin- cells are LSK, respectively). (B/C) The CD27+CD201+ population partially or completely overlaps the Sca1+cKit+ population. (D) CBA/H HSCs (i.e. CD27+CD201+ haematopoietic stem and progenitor cells) constitutively express mCherry.

A recent study postulated that staining bone marrow cells with CD27 and CD201 antibodies, rather than Sca1 and cKit antibodies, allows a more efficient isolation of HSCs in murine strains with phenotypically low Sca1 expression (Vazquez et al., 2015). Whereas the CD27+CD201+ partially overlapped the Sca1+cKit+ population in Chr2MDR$^{mCh}$ mice, it completely overlapped the Sca1+cKit+ population in C57BL/6 mice (Figure 3.13B and C, respectively). By isolating CD27+CD201+ haematopoietic stem and progenitor cells, the Chr2MDR$^{mCh}$ HSC yield increased approximately four-fold compared with Sca1+cKit+ gating (3.5% vs 0.9%, respectively; left panels of Figure

3.13D and A, respectively). The CD27+CD201+ population is considered to contain the vast majority of LT-HSCs (Vazquez et al., 2015), and all these cells expressed mCherry (CD27+CD201+ haematopoietic stem and progenitor cells in red; Figure 3.13D right panel). We then sorted the CD27+CD201+ haematopoietic stem and progenitor cells from Chr2MDR$^{mCh}$ mice and initiated CFC assays in triplicate (500 cells/1.1 ml Methocult™). Ten days following incubation, the average colony count was 90 colonies per well (i.e. 18% plating efficiency). This four-fold higher plating efficiency (compared with the 6% plating efficiency observed for unsorted haematopoietic stem and progenitor cells, section 3.2.2) indicates that CD27+CD201+ haematopoietic stem and progenitor cells have a more primitive phenotype.

As indicated above, we committed to further investigate the haematopoietic stem and progenitor cell fraction at the time of transplantation. To this end, bone marrow cells from male 10 week old Chr2MDR$^{mCh}$ mice were harvested seven days following radiation exposure (0 Gy, 5 mGy, 10 mGy, 100 mGy or 1 Gy), followed by immunomagnetic selection of haematopoietic stem and progenitor cells. Cells were labelled with CD27 and CD201 anitbodies (Figure 3.14A). From each donor mouse, the following bones were collected: spine, iliac crests, femurs and tibias. Although the number of bone marrow cells harvested did not differ significantly between groups, the number of haematopoietic stem and progenitor cells was significantly different between sham-irradiated and irradiated mice (Figure 3.14B and C, respectively)(1 mouse per radiation dose, 8 independent replicates; 40 mice in total).

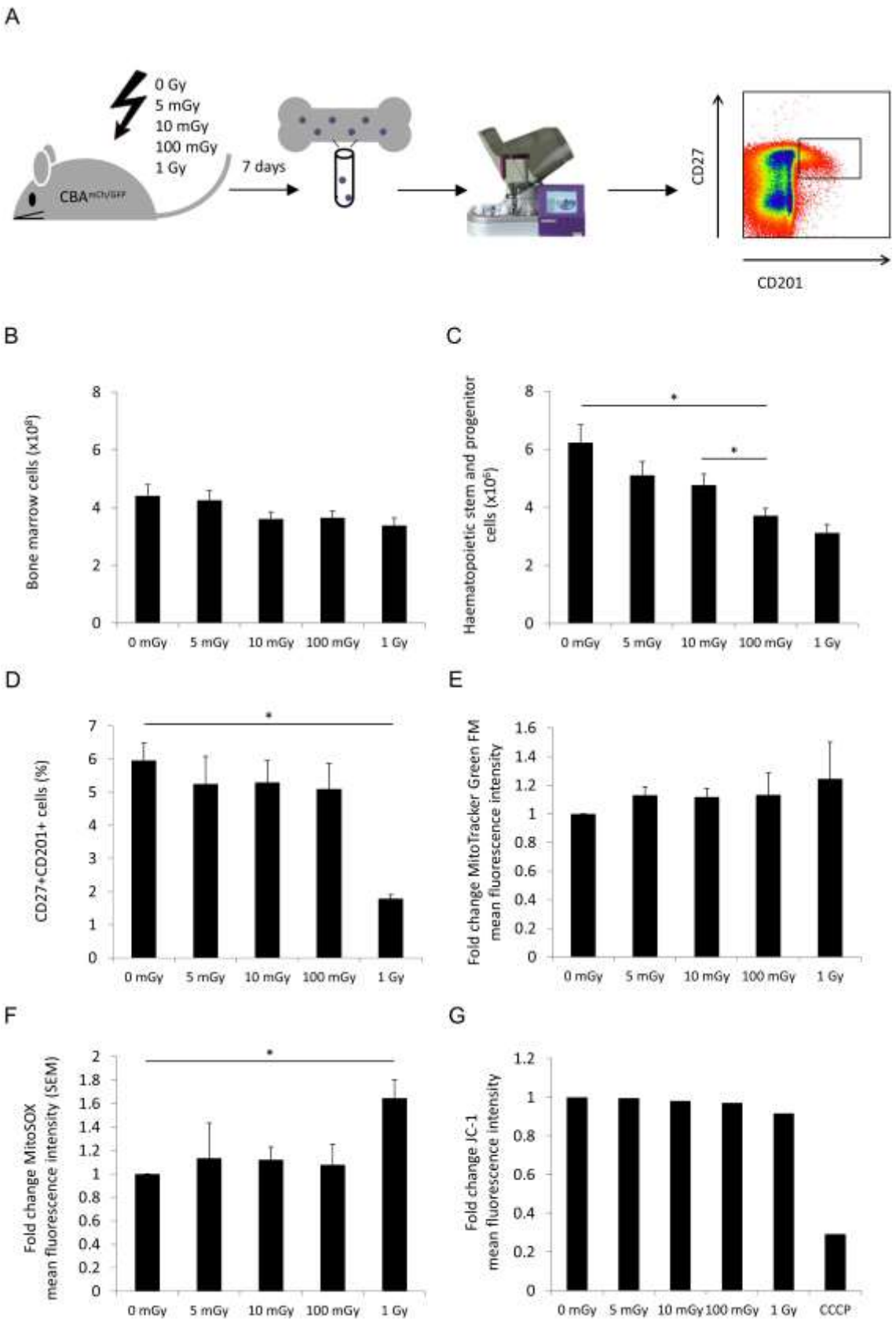



**Figure 3.14 Changes in CD27+CD201+ cells following radiation exposure**

(A) Bone marrow cells were harvested from male 10 week old Chr2MDR$^{mCh}$ mice seven days following radiation exposure (0 – 1 Gy), followed by immunomagnetic selection of haematopoietic stem and progenitor cells. Cells were labelled with CD27 and CD201 antibodies. (B/C) The number of bone marrow cells and haematopoietic stem and progenitor cells was compared between groups (1 mouse per radiation dose, 8 independent replicates; 40 mice in total). (D) The percentage of CD27+CD201+ cells was determined by flow cytometry (1 mouse per radiation dose, 8 independent replicates; 40 mice in total). (E/F/G) Mitochondrial status of CD27+CD201+ cells was assessed by three different flow cytometry assays: MitoTracker Green FM (1 mouse/dose/experiment, 5 mice per experiment, 3 independent experiments), MitoSOX (1 mouse/dose/experiment, 5 mice per experiment, 3 independent experiments) and JC-1 (1 mouse/dose/experiment, 5 mice per experiment, 1 independent experiment), and is displayed as fold change in mean fluorescence intensity. CCCP, a mitochondrial uncoupler, was used as positive control (* P <0.05).

The number of haematopoietic stem and progenitor cells in 100 mGy irradiated mice was significantly lower compared with sham-irradiated mice (3.7 x $10^6$ cells and 6.2 x $10^6$ cells, respectively; Figure 3.14C). However, the percentage of CD27+CD201+ cells in the haematopoietic stem and progenitor cell fraction did not differ significantly between groups, except in 1 Gy irradiated mice (6% and 1.9%, sham-irradiated and 1 Gy irradiated mice, respectively; Figure 3.14D). As the percentage of CD27+CD201+ haematopoietic stem and progenitor cells did not differ significantly between groups exposed to low dose irradiation, we could conclude that each transplant contained the same number of HSCs, and therefore, the decreased chimerism levels six months following transplantation could not be explained by numerical HSC changes at the time of transplantation.

Recently, it was reported that, following low dose *in vivo* radiation exposure for 30 consecutive days, increased mitochondrial ROS levels could be detected 3 months after the last exposure (Guo et al., 2015). Therefore, we investigated whether the mitochondrial function of the HSC fraction at the time of transplantation was altered and whether these changes could contribute to the reduced chimerism levels six

months following radiation exposure. To this end, bone marrow cells from male 10 week old Chr2MDR$^{mCh}$ mice were harvested seven days following radiation exposure (0 Gy, 5 mGy, 10 mGy, 100 mGy and 1 Gy), followed by immunomagnetic selection of haematopoietic stem and progenitor cells. Cells were labelled with CD27 and CD201 anitbodies, stained with mitochondrial probes [MitoTracker Green FM, MitoSOX Red (i.e. a mitochondrial superoxide-sensitive fluorophore) or JC-1 (i.e. a membrane potential-dependent mitochondrial dye)], and analysed by flow cytometry. The MitoTracker reagent passively diffuses across the plasma membrane and accumulates in active mitochondria, hereby providing an indication of the mitochondrial mass. However, the HSC mitochondrial mass did not differ between radiation doses (1 mouse/dose/experiment, 5 mice per experiment, 3 independent experiments; Figure 3.14E). The MitoSOX Red reagent selectively targets the mitochondria, and once inside, it is rapidly oxidised by superoxide. Although HSC mitochondrial superoxide levels did not change following low dose radiation exposure, they increased 1.7-fold following high dose exposure compared with sham-irradiation (1 mouse/dose/experiment, 5 mice per experiment, 3 independent experiments; Figure 3.14F). Mitochondrial membrane potential was assessed with JC-1 staining but did not differ between radiation doses (1 mouse/dose/experiment, 1 experiment; Figure 3.14G). CCCP, a mitochondrial uncoupler, was used as positive control.

Similar to the assessment of the HSC mitochondrial function, we investigated whether altered *Gadd45* or *Sfpi1* gene expression could be detected at the time of transplantation and whether these changes could contribute to the reduced chimerism levels six months following radiation exposure. To this end, bone marrow cells from

male 10 week old Chr2MDR$^{mCh}$ mice were harvested seven days following radiation exposure (0 Gy, 5 mGy, 10 mGy, 100 mGy and 1 Gy), followed by immunomagnetic selection of haematopoietic stem and progenitor cells. Cells were labelled with CD27 and CD201 anitbodies, and CD27+CD201+ haematopoietic stem and progenitor cells were sorted (Figure 3.15A).

As previously reported in the literature (Wingert et al., 2016), *Gadd45* expression was markedly upregulated in CD27+CD201+ cells two hours following 1 Gy *in vitro* radiation exposure (i.e. four-fold). However, the expression remained unchanged in CD27-CD201- and CD27+CD201- cells (Figure 3.15B, 1 experiment). In contrast, seven days following *in vivo* radiation exposure, we did not observe significant changes in *Gadd45* expression (Figure 3.15C; 1 mouse/dose/experiment, 5 mice per experiment, 3 independent experiments). However, a trend towards a dose-dependent *Gadd45* downregulation was identified. In contrast, *Sfpi1* expression was weakly downregulated at two hours following 1 Gy *in vitro* radiation exposure (Figure 3.15D; 1 experiment). Although, seven days following *in vivo* radiation exposure, *Sfpi1* expression did not differ significantly between radiation doses, a similar trend towards a dose-dependent downregulation was observed (Figure 3.15E; 1 mouse/dose/experiment, 5 mice per experiment, 3 independent experiments).

Finally, it was previously reported that the percentage of quiescent LSK cells was significantly lower in mice up to 15 months following *in vivo* radiation exposure, compared with sham-irradiated mice (Chua et al., 2012). Therefore, we assessed the cell cycle status of the LSK cells seven days following radiation exposure.

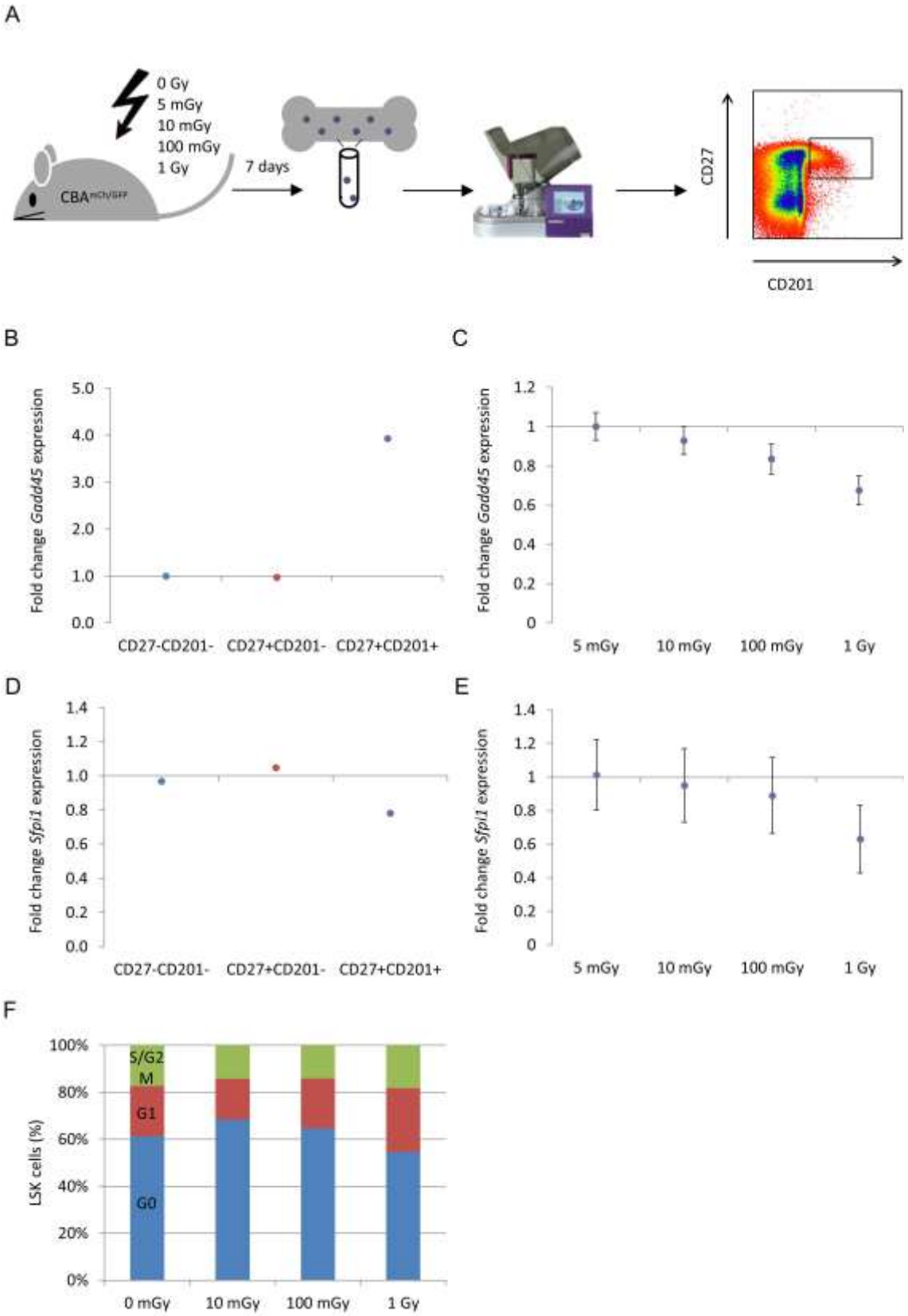



**Figure 3.15 Gene expression and cell cycle following radiation exposure**

(A) Bone marrow cells were harvested from male 10 week old Chr2MDR$^{mCh}$ mice seven days following radiation exposure (0 – 1 Gy), followed by immunomagnetic selection of haematopoietic stem and progenitor cells. Cells were labelled with CD27 and CD201 antibodies, and CD27+CD201+ haematopoietic stem and progenitor cells were sorted. (B) *Gadd45* expression in CD27+CD201+ cells 2 hours following 1 Gy *in vitro* radiation exposure by quantitative realtime-PCR. (C) *Gadd45* expression in CD27+CD201+ cells seven days following *in vivo* radiation exposure (0 – 1 Gy; 1 mouse/dose/experiment, 5 mice per experiment, 3 independent experiments) by quantitative realtime-PCR. (D) *Sfpi1* expression in CD27+CD201+ cells 2 hours following 1 Gy *in vitro* radiation exposure by quantitative realtime-PCR. (E) *Sfpi1* expression in CD27+CD201+ cells seven days following *in vivo* radiation exposure (0 – 1 Gy; 1 mouse/dose/experiment, 5 mice per experiment, 3 independent experiments) by quantitative realtime-PCR. (F) Cell cycle analysis of LSK cells seven days following radiation exposure (0 – 1 Gy; 1 mouse/dose/experiment, 5 mice per experiment, 1 independent experiment) by Hoechst33342 and PyroninY staining.

Cells were stained with Hoechst33342 and Pyronin Y, labelled with Sca1 and cKit anitbodies, and analysed by flow cytometry. Although the majority of LSK cells were quiescent (G0, 60%), approximately 20% of LSK cells was in the G1 phase of the cell cycle and 20% was in the S/G2/M phase. No cell cycle changes could be detected at seven days following *in vivo* radiation exposure (Figure 3.15F; 1 mouse/dose/experiment, 5 mice per experiment, 1 independent experiment).

### 3.3.3. Discussion

It is widely accepted that exposure to high dose radiation leads to an increased risk of developing leukaemia later in life (Shore, 2014). However, a variety of low dose epidemiological studies report that low dose radiation exposure is positively associated with leukaemia (Pearce et al., 2012; Mathews et al., 2013; Leuraud et al., 2015). To this end, we investigated the effects of low and high dose *in vivo* radiation exposure on the long-term fate of HSCs by transplanting Chr2MDR$^{mCh}$ haematopoietic stem and progenitor cells in unconditioned NSG mice. We reported in section 3.1 that allogeneic HSCs can compete for niches in the unconditioned NSG bone marrow compartment and that the unconditioned NSG BM microenvironment is capable of supporting allogeneic long-term HSC engraftment and differentiation. We hypothesised that studying the effects of low dose radiation exposure on HSC transplantation is more appropriate in unconditioned recipients (rather than myeloablated recipients) as the recipient's bone marrow microenvironment remains uncompromised, and thus allows a more biologically relevant investigation of the effects of low dose radiation exposure.

We showed that six months following transplantation of sham-irradiated Chr2MDR$^{mCh}$ haematopoietic stem and progenitor cells, all NSG mice showed multilineage mCherry chimerism in the peripheral blood (27% mCherry+ WBCs). Given the fact that five months following transplantation, haematopoiesis is entirely dependent on long-term HSC activity (Marusyk et al., 2009), we postulate that transplanted Chr2MDR$^{mCh}$ HSCs were able to compete for niches in the nonmyeloablated NSG bone marrow compartment and that the nonmyeloablated NSG bone marrow microenvironment is capable of supporting allogeneic long-term HSC engraftment and differentiation.

The percentage of Chr2MDR$^{mCh}$ cell chimerism we observed in the peripheral blood of adult nonmyeloablated NSG mice six months following transplantation of 3.5 x $10^4$ Chr2MDR$^{mCh}$ CD27+CD201+ cells (27%) was similar to the human cell chimerism level reported in the blood of 2.5 Gy myeloablated NSG mice 8 weeks following engraftment of 5 x $10^4$ CD34+ human cells (22%)(Futrega et al., 2016). Our observed cell chimerism was higher compared with the human cell chimerism level reported in blood of newborn nonmyeloablated NSG mice 12 weeks following engraftment of 3 x $10^4$ CD34+ human HSCs, but lower compared with the human cell chimerism level reported in blood of adult nonmyeloablated NSG mice 12 weeks following engraftment of 3 x $10^4$ CD34+ human HSCs (18% and 41%, respectively)(Brehm et al., 2012). The authors did not observe a statistical difference in human cell chimerism levels in the blood of nonmyeloablated NSG mice compared with newborn or adult 1 Gy myeloablated NSG mice (Brehm et al., 2012). A more recent study reported a much lower human cell chimerism level in blood of adult nonmyeloablated NSG mice 12 weeks following engraftment of 2.5 x $10^5$ CD34+ human HSCs (8%). In contrast with the previous studies, the authors did observe a significantly enhanced human cell chimerism level in the blood of 2.5 Gy myeloablated NSG mice compared with nonmyeloablated NSG mice (approximately 60% and 8%, respectively)(McIntosh et al., 2015).

When transplanting Chr2MDR$^{mCh}$ haematopoietic stem and progenitor cells which were irradiated seven days prior to harvest (0.01 – 3 Gy), we observed a dose-dependent reduction in the peripheral blood mCherry chimerism six months following transplantation, both for low (100 mGy) and high dose (1 Gy and 3 Gy) exposed cells,

indicating a reduced contribution of donor HSCs towards long-term haematopoiesis following radiation exposure.

Analysis of the haematopoietic stem and progenitor cell fraction of NSG mice injected with sham-irradiated haematopoietic stem and progenitor cells, revealed that 13% of cells expressed mCherry. Whereas mCherry+ cells had higher Sca1 expression compared with mCherry- cells (16.8% and 5.3%, respectively), they had lower cKit expression compared with mCherry- cells (2.8% and 39.5%, respectively). Interestingly, Sca1 expression was further upregulated in a dose-dependent manner (41.4% mCherry+Sca1+ cells in NSG mice which were injected with 3 Gy irradiated cells). However, Sca1 and cKit had stable expression levels in mCherry- cells, indicating that this dose-dependent upregulation of Sca1 expression is possibly attributable to the radiation exposure of the mCherry+ haematopoietic stem and progenitor cells prior to transplantation. These Sca1 and cKit changes are somewhat similar to what we reported in section 3.2.2, where cKit downregulation and Sca1 upregulation could be observed 24 hours following 3 Gy *in vivo* radiation exposure. However these changes in Sca1 and cKit expression could no longer be detected seven days following radiation exposure.

mCherry+ Sca1+ haematopoietic stem and progenitor cells were sorted from the haematopoietic stem and progenitor cell fraction for each individual radiation dose, and reinjected into secondary NSG mice. Six months following secondary transplantation, all but one secondary NSG showed reconstitution. Although the same number of mCherry+ Sca1+ haematopoietic stem and progenitor cells was injected for each radiation dose (i.e. 3 x $10^4$ cells/secondary NSG mouse), the mCherry+ chimerism

levels six months following transplantation into secondary NSG mice varied with radiation dose. In contrast with the peripheral blood chimerism levels observed after the first round of transplantation, we only observed myeloid chimerism in the peripheral blood of secondary NSG mice which were injected with mCherry+Sca1+ cells obtained from primary NSG mice transplanted with low dose irradiated cells (0 Gy and 0.01 Gy), but not in the peripheral blood of secondary NSG mice which were injected with mCherry+Sca1+ cells obtained from primary NSG mice transplanted with 0.1 Gy or 1 Gy irradiated cells, indicating that, although more than twelve months following radiation exposure, we can still detect that irradiated HSCs have a reduced contribution towards long-term haematopoiesis.

We next aimed to identify the underlying mechanisms of the reduced chimerism levels following low dose radiation exposure. Given the fact that the peripheral blood WBCs observed six months following radiation exposure must originate from transplanted HSCs (Marusyk et al., 2009), we committed to in detail investigate the HSC fraction at the time of transplantation. As *Sfpi1*$^{mCh}$ mice have a CBA/H background, and as it has been previously reported that this strain has phenotypically low Sca1 expression (Spangrude and Brooks, 1993), we investigated whether any other markers existed for HSC isolation. Last year, it was then postulated that in strains with phenotypically low Sca1 expression, CD27 and CD201 allowed a more efficient isolation of HSCs in these strains (Vazquez et al., 2015). Using these markers, rather than Sca1 and cKit, we were able to increase the HSC yield per Chr2MDR$^{mCh}$ mice by four times.

Having identified the HSCs within the haematopoietic stem and progenitor cell fraction, we then investigated whether the number of HSCs varied per radiation dose,

and therefore could contribute towards the lower chimerism levels six months following radiation exposure. Although the number of bone marrow cells harvested did not differ significantly between groups, the number of haematopoietic stem and progenitor cells was significantly different between sham-irradiated and irradiated mice. However, the percentage of CD27+CD201+ cells in the haematopoietic stem and progenitor cell fraction did not differ significantly between groups, except in 1 Gy irradiated mice. Therefore, as the percentage of CD27+CD201+ haematopoietic stem and progenitor cells did not differ significantly between groups exposed to low dose irradiation, we could conclude that each transplant contained the same number of HSCs, and thus the decreased chimerism levels six months following transplantation could not be explained by numerical HSC changes at the time of transplantation.

In subsequent experiments, it will be of importance to determine the number of mCherry+ HSCs six months following transplantation. If a dose-dependent reduction in the number of mCherry+ HSCs can be detected at six months, a compromised HSC homing could be at the basis of our observation of reduced chimerism following low dose radiation exposure. However, if a similar number of mCherry+ HSCs can be detected six months following transplantation, independent of the radiation dose, a radiation-induced intrinsic HSC defect is more likely. For example, total body irradiation has previously been linked to sustained damage to HSCs, including impaired self-renewal and myeloid skewing (Shao et al., 2014).

Our next step was to investigate changes taking place at a HSC cellular level. To this end, we assessed the mitochondrial function, *Gadd45* and *Sfpi1* gene expression, and the cell cycle at the time of transplantation. Firstly, we used three flow cytometry

mitochondrial probes: MitoTracker Green FM (i.e. an indicator of mitochondrial mass), MitoSOX Red (i.e. a mitochondrial superoxide-sensitive fluorophore) and JC-1 (i.e. a membrane potential-dependent mitochondrial dye). We did not observe dose-dependent changes to the mitochondrial mass or membrane potential at the time of transplantation. Similar to the increased mitochondrial ROS levels detected in murine LSK cells three months following 1.5 Gy *in vivo* radiation exposure (Guo et al., 2015), we observed a 1.7-fold increase in mitochondrial superoxide levels seven days following 1 Gy *in vivo* radiation exposure. However, we did not identify increased levels in HSCs seven days following low dose radiation exposure, indicating that mitochondrial ROS production did not conritbute towards lower chimerism levels six months following low dose *in vivo* radiation exposure. Secondly, we assessed *Gadd45* and *Sfpi1* gene expression at the time of transplantation. It has been previously reported that *Gadd45* expression is upregulated in HSCs four hours following radiation exposure, inducing HSC differentiation by activating p38 MAPK signalling and reducing their self-renewal ability (Wingert et al., 2016). Although we observed a similar upregulation two hours following 1 Gy *in vitro* radiation exposure, we did not observe changes in *Gadd45* expression at seven days following low and high dose *in vivo* radiation exposure. Similarly, we did not observe a significant change in *Sfpi1* gene expression. Finally, although it was previously reported that the percentage of quiescent LSK cells was significantly lower several months following high dose *in vivo* radiation exposure (Chua et al., 2012), no cell cycle changes could be detected in LSK cells at seven days following *in vivo* radiation exposure.

In conclusion, we observed decreased peripheral blood and haematopoietic stem and progenitor cell chimerism six months following low and high dose *in vivo* radiation exposure and transplantation into unconditioned NSG mice. However, we were unable to identify changes in HSC mitochondrial function, HSC *Gadd45* and *Sfpi1* gene expression or LSK quiescence at the time of transplantation, and therefore, we could not identify the underlying mechanisms contributing to the reduced chimerism level following low dose radiation exposure.

### 3.4. Murine radiation leukaemogenesis is a complex process with a variable rate of progression

It has been widely accepted that exposure to high dose ionising radiation significantly increases the leukaemia incidence. The two most widely studied human populations are the atomic bomb survivors and patients receiving radiotherapy as part of their treatment plan (Hsu et al., 2013; Wright et al., 2010, respectively). However, the underlying mechanisms remain unidentified. The use of murine models remains the most representative option available to study the cytogenetic and molecular mechanisms underlying radiation leukaemogenesis.

The CBA mouse strain is regarded as the primary model in the study of rAML. Firstly, CBA mice do 'not' develop spontaneous AML (background incidence <1/1,000), and therefore, we can assume that when irradiated mice are diagnosed with AML, radiation is the causative agent. Secondly, they have a highly reproducible rAML induction in 15-20% of mice exposed to a single acute 3 Gy whole body X-irradiation (12 – 18 months following radiation exposure). Finally, there are many histopathological similarities with human myeloid leukaemia (Major, 1979).

An interstitial deletion of one chromosome 2 homologue is a characteristic molecular finding in 80% of murine rAMLs (Rithidech et al., 1993), with the MDR harbouring the haematopoietic transcription factor *Sfpi1* (Alexander et al., 1995). Interestingly, in ~85% of these rAML cases, the remaining *Sfpi1* copy exhibits a point mutation confined to a single CGC codon in exon 5, central to the DNA binding domain of the protein (Cook et al., 2004). These biallelic *Sfpi1* aberrations support a two-hit model in murine radiation leukaemogenesis.

### 3.4.1. Generation and characterisation of the *Sfpi1*$^{mCh/GFP}$ reporter mouse model

As described in section 3.2, we designed a novel Chr2MDR$^{mCh}$ mouse model where a Rosa26-mCherry construct was inserted on chromosome 2 within the MDR following radiation exposure. mCherry expression was under control of the Rosa26 promotor, resulting in constitutively expressed mCherry across all haematopoietic cell types, from HSCs to terminally-differentiated lymphocytes and monocytes. We hypothesised that, upon an interstitial deletion of chromosome 2 following radiation exposure, we would be able to detect a loss in mCherry expression, as the chromosome 2 homologue carrying the Rosa26-mCherry construct would be lost as well.

However, the mCherry expression profile of homozygous and heterozygous Chr2MDR$^{mCh}$ mice partially overlaps, and therefore, we would not be able to identify a hemizygous chromosome 2 deletion in homozygous Chr2MDR$^{mCh}$ mice. Similarly, in 50% of the cases, a hemizygous chromosome 2 deletion in heterozygous Chr2MDR$^{mCh}$ mice would not be detected (if the deletion takes place on the wild-type, non-fluorescent chromosome 2 homologue).

To overcome these limitations, we crossed homozygous Chr2MDR$^{mCh}$ mice with homozygous *Sfpi1*$^{GFP}$ mice. The resulting offspring, termed *Sfpi1*$^{mCh/GFP}$ mice, had one chromosome 2 homologue carrying the Rosa26-mCherry construct, with the other homologue carrying the GFP construct. Therefore, whichever chromosome 2 homologue is deleted, we would observe a change in fluorescence: either a loss of mCherry expression or a loss of GFP expression. The main reason to use the existing *Sfpi1*$^{GFP}$ mouse model (rather than generating another mouse model where a fluorescent marker is constitutively expressed), is that GFP is under control of the *Sfpi1*

promotor. To date, it remains to be elucidated which changes take place on the remaining chromosome 2 homologue, and therefore, we could detect if GFP expression changes upon deletion of the chromosome 2 homologue carrying the Rosa26-mCherry construct.

Before we could investigate the effect of radiation exposure on mCherry and GFP expression, we had to determine if any physiological GFP and mCherry fluctuations occurred in *Sfpi1*$^{mCh/GFP}$ mice. To this end, male *Sfpi1*$^{mCh/GFP}$ mice were tail vein bled from 10 weeks of age, and peripheral blood was analysed for mCherry and GFP expression by flow cytometry. A follow-up blood sample was taken every month until mice had to be humanly euthanised (Figure 3.16). At ten weeks of age, all peripheral blood WBCs expressed mCherry. As GFP is under control of the *Sfpi1* promotor, and as *Sfpi1* needs to be downregulated upon commitment to the lymphoid lineage, peripheral blood lymphocytes did not express GFP (i.e. mCherry+GFP-). Myeloid cells however require *Sfpi1* for their terminal differentiation and maturation, and therefore, monocytes and granulocytes express GFP (i.e. mCherry+GFP+). Interestingly, the percentage of mCherry+GFP- peripheral blood WBCs decreased as *Sfpi1*$^{mCh/GFP}$ mice aged. Concomitantly, the percentage of mCherry+GFP+ peripheral blood WBCs increased with age, indicating an increased percentage of myeloid cells in the peripheral blood as mice age. As mCherry is under control of the Rosa26 promotor, mCherry was expressed at the same level when mice age, and no mCherry- cells could be detected in the peripheral blood of ageing mice, indicating that the Rosa26-mCherry construct remained present and active throughout life. *Sfpi1*$^{mCh/GFP}$ mice had a similar average life span as wild-type CBA mice (i.e. 21 months).

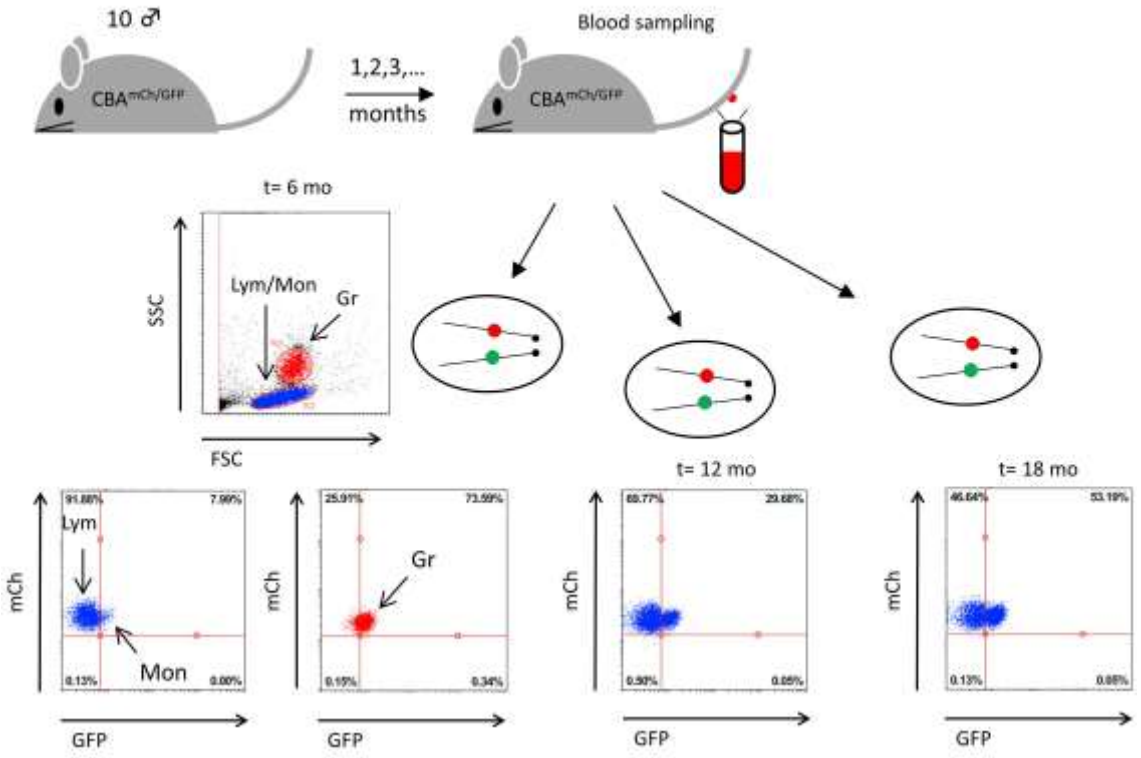



**Figure 3.16 Characterisation of *Sfpi1*$^{mCh/GFP}$ mice**

Ten male 10 week old *Sfpi1*$^{mCh/GFP}$ mice were sham-irradiated. Tail vein blood samples were collected monthly, and analysed for mCherry and GFP expression by flow cytometry. 'Lym' for lymphocytes (mCherry+GFP-), 'Mon' for monocytes (mCherry+GFP+) and 'Gr' for granulocytes (mCherry+GFP+).

### 3.4.2. Clonal expansion of chromosome 2 deleted WBCs following radiation exposure

As we confirmed that *Sfpi1*$^{mCh/GFP}$ mice express mCherry throughout life and that no mCherry- WBC clonal expansion can be observed in the peripheral blood when sham-irradiated mice age, we investigated the effect of radiation exposure on mCherry and GFP expression of *Sfpi1*$^{mCh/GFP}$ mice. To this end, we exposed one hundred male 10 week old *Sfpi1*$^{mCh/GFP}$ mice to a single acute 3 Gy whole body X-irradiation. As stipulated in the '*Bethesda proposals for classification of non-lymphoid haematopoietic neoplasms in mice*', one approach to evaluate mice for haematologic disease, is to observe mice daily, and bleed them monthly (Kogan et al., 2002). Therefore, we collected tail vein blood samples of these mice at one month following 3 Gy *in vivo* radiation exposure, and analysed mCherry and GFP expression by flow cytometry. A follow-up blood sample was collected every month until mice presented with outward physical signs of rAML (such as hunched posture, poor grooming, decreased activity and pallor) or until they had to be euthanised because of poor condition. As 37 of the 100 irradiated male *Sfpi1*$^{mCh/GFP}$ mice were still alive at the time of analysis, the data presented here will be derived from the 64 mice that had been diagnosed with rAML or had to be humanely euthanised. Those mice which had to be humanely sacrificed, were mainly diagnosed with hepatic neoplasia and Harderian gland neoplasia.

All *Sfpi1*$^{mCh/GFP}$ mice had mCherry- peripheral blood WBCs at 1 month following radiation exposure (<0.5% of WBCs). At 9 months following radiation exposure, 27% of mice had mCherry- clonal expansion detectable in the peripheral blood (>1% mCherry- WBCs, 16/59 mice) and clonal expansion was of mixed lineage origin (i.e. myeloid and lymphoid mCherry- cells; Figure 3.17).

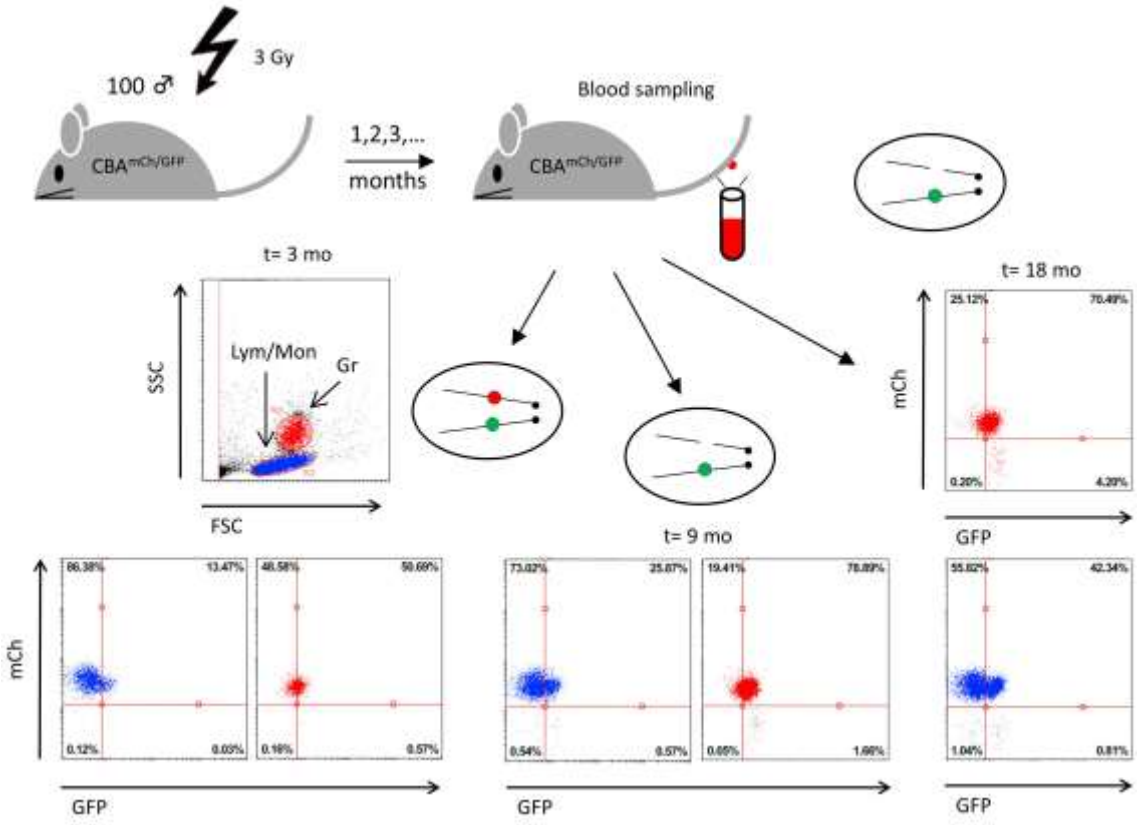



**Figure 3.17 Mixed lineage mCherry- clonal expansion in the peripheral blood WBCs**

One hundred male 10 week old *Sfpi1*$^{mCh/GFP}$ mice were exposed to a single acute 3 Gy whole body X-irradiation. Tail vein blood samples were collected at one month following radiation exposure, and analysed for mCherry and GFP expression by flow cytometry. A follow-up blood sample was collected every month until mice presented with outward physical signs of rAML or until they had to be euthanised because of poor condition. Representative flow cytometry data of a mouse with mixed lineage mCherry- clonal expansion in the peripheral blood WBCs.

The percentage of mice with mCherry- clonal expansion had increased by 12 months following radiation exposure (34%, 17/50). At 15 and 18 months, 46% and 71 % of mice had mCherry- clonal expansion detectable in the peripheral blood (17/37 and 12/17, respectively). Although *Sfpi1*$^{mCh/GFP}$ mice which presented with mCherry- clonal expansion at 9 and 12 months following radiation exposure, had clonal expansion of mixed lineage origin (i.e. myeloid and lymphoid mCherry- cells), 41% of mice which presented with mCherry- clonal expansion at 15 and 18 months following radiation

exposure, had clonal expansion of lymphoid origin only (7/17 and 5/12 mice with mCherry- clonal expansion, respectively; Figure 3.18). At the time of death, 37.5% of *Sfpi1*$^{mCh/GFP}$ mice did not show mCherry- clonal expansion (24/64), 33% presented with mCherry- clonal expansion of mixed lineage origin (21/64), 16% presented with mCherry- clonal expansion of lymphoid origin (10/64) and 17% were potential leukaemic mice (i.e. hepatosplenomegaly on necropsy and increased WBC count; 11/64).

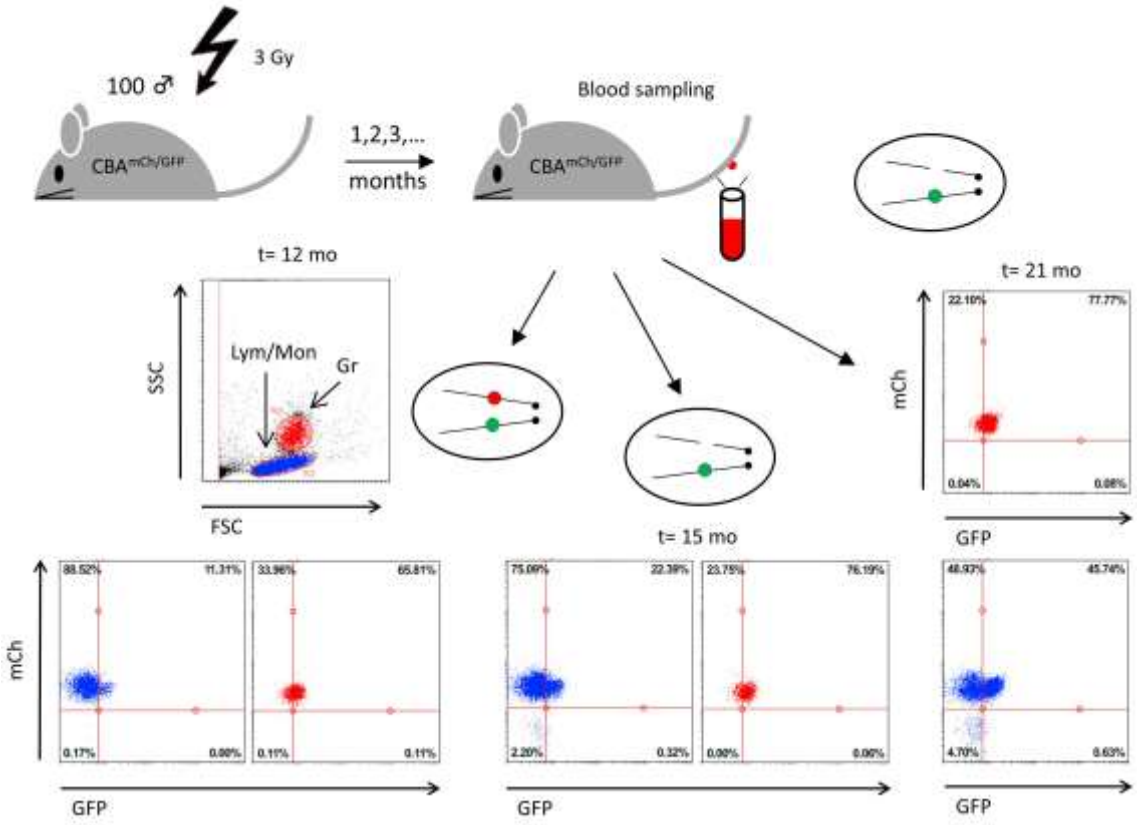



**Figure 3.18 Lymphoid mCherry- clonal expansion in the peripheral blood WBCs**

One hundred male 10 week old *Sfpi1*$^{mCh/GFP}$ mice were exposed to a single acute 3 Gy whole body X-irradiation. Tail vein blood samples were collected at one month following radiation exposure, and analysed for mCherry and GFP expression by flow cytometry. A follow-up blood sample was collected every month until mice presented with outward physical signs of rAML or until they had to be euthanised because of poor condition. Representative flow cytometry data of a mouse with lymphoid mCherry- clonal expansion in the peripheral blood WBCs.

As the majority of *Sfpi1*$^{mCh/GFP}$ mice presented with mCherry- clonal expansion in myeloid and lymphoid peripheral blood WBCs, we hypothesised that an interstitial deletion of chromosome 2 (and a concomitant loss of the Rosa26-mCherry construct) had occurred in a HSC. To this end, one of the *Sfpi1*$^{mch/GFP}$ mice was sacrificed upon detection of mixed lineage mCherry- clonal expansion in the peripheral blood WBCs (Figure 3.19A). Bone marrow was harvested, followed by immunomagnetic selection of haematopoietic stem and progenitor cells. Cells were labelled with Sca1, cKit, CD48, CD150 and CD127 antibodies, and analysed for mCherry and cell surface marker expression by flow cytometry. Peripheral blood analysis showed that 5% of granulocytes were mCherry-, 2.7% of monocytes were mCherry- and 3.3% of lymphocytes were mCherry- (Figure 3.19A).

Analysis of the haematopoietic stem and progenitor cells revealed that 11.2% was mCherry-. Within the mCherry- fraction, most cells were Sca1-cKit- and Sca1-cKit+ (71.9% and 26.4%, respectively). However, 0.8% of mCherry- cells were LSK, and within the mCherry- LSK fraction, 54.7% of cells were CD48-CD150+ (i.e. LT-HSCs/MPP1), indicating that this mouse harboured HSCs which had lost the chromosome 2 homologue carrying the Rosa26-mCherry construct (Figure 3.19B). Similarly, mCherry- myeloid progenitors (i.e. mCherry-Sca1-cKit+ cells) were identified (26.4% of the mCherry- fraction). The expression of interleukin-7 receptor alpha-chain (CD127) is limited to common lymphoid progenitors and other downstream lymphoid progenitors (Akashi et al., 2000). Within the mCherry- haematopoietic stem and progenitor cells, 4% of cells expressed CD127 (compared with 5.8% in mCherry+ haematopoietic stem and progenitor cells; Figure 3.19C).

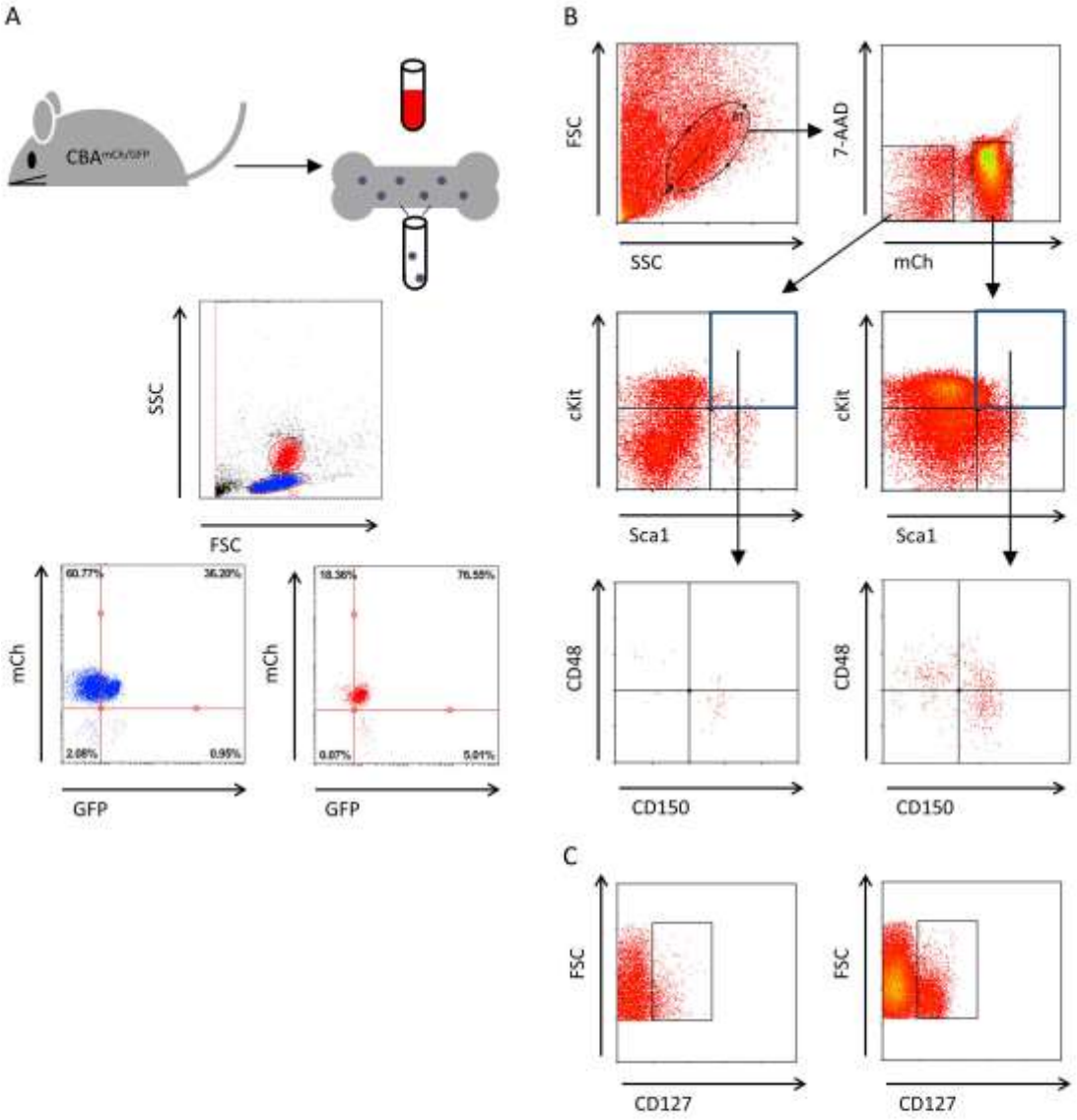



**Figure 3.19 Mixed lineage mCherry- clonal expansion in the haematopoietic stem and progenitor cell fraction of an irradiated *Sfpi1*$^{mCh/GFP}$ mouse**

(A) A male *Sfpi1*$^{mch/GFP}$ mouse which was exposed to a single acute 3 Gy whole body X-irradiation at 10 weeks of age, was sacrificed upon detection of mixed lineage mCherry- clonal expansion in the peripheral blood WBCs. (B) Bone marrow was harvested, followed by immunomagnetic selection of haematopoietic stem and progenitor cells. Cells were labelled with Sca1, cKit, CD48, CD150 and CD127 antibodies, and analysed for mCherry and cell surface marker expression by flow cytometry. (C) CD127 expression in mCherry- and mCherry+ haematopoietic stem and progenitor cells (left and right panel, respectively).

Not every *Sfpi1*$^{mCh/GFP}$ mice which presented with mixed lineage mCherry- clonal expansion in the peripheral blood, had an equal level of mCherry- lymphoid and myeloid cells. To this end, one of the *Sfpi1*$^{mch/GFP}$ mice was sacrificed upon detection of myeloid-biased mixed lineage mCherry- clonal expansion in the peripheral blood WBCs (Figure 3.20A). Bone marrow was harvested, followed by immunomagnetic selection of haematopoietic stem and progenitor cells. Cells were labelled with Sca1, cKit, CD48, CD150 and CD127 antibodies, and analysed for mCherry and cell surface marker expression by flow cytometry. Peripheral blood analysis showed that 15.3% of granulocytes were mCherry-, 16.5% of monocytes were mCherry- and 1.6% of lymphocytes were mCherry- (Figure 3.20A).

Analysis of the haematopoietic stem and progenitor cells revealed that 57.6% was mCherry-. Within the mCherry- fraction, almost all cells were Sca1- (99.7%). However, 0.2% of mCherry- cells were LSK, and within the LSK fraction, 31.3% of mCherry-LSK cells were CD48-CD150+ (i.e. LT-HSCs/MPP1), indicating that this mouse harboured HSCs which had lost the chromosome 2 homologue carrying the Rosa26-mCherry construct (Figure 3.20B). The remaining mCherry-LSK cells were mainly CD48+CD150+ (i.e. MPP2, 40.9%) and CD48+CD150- (i.e. MPP3, 24.7%) cells. Similarly, mCherry- myeloid progenitors (i.e. mCherry- Sca1-cKit+ cells) were identified. Within the mCherry- haematopoietic stem and progenitor cells, only 0.7% of cells expressed CD127 (compared with 7.6% in mCherry+ haematopoietic stem and progenitor cells; Figure 3.20C), indicating that the vast majority of mCherry- haematopoietic stem and progenitor cells had a myeloid phenotype.

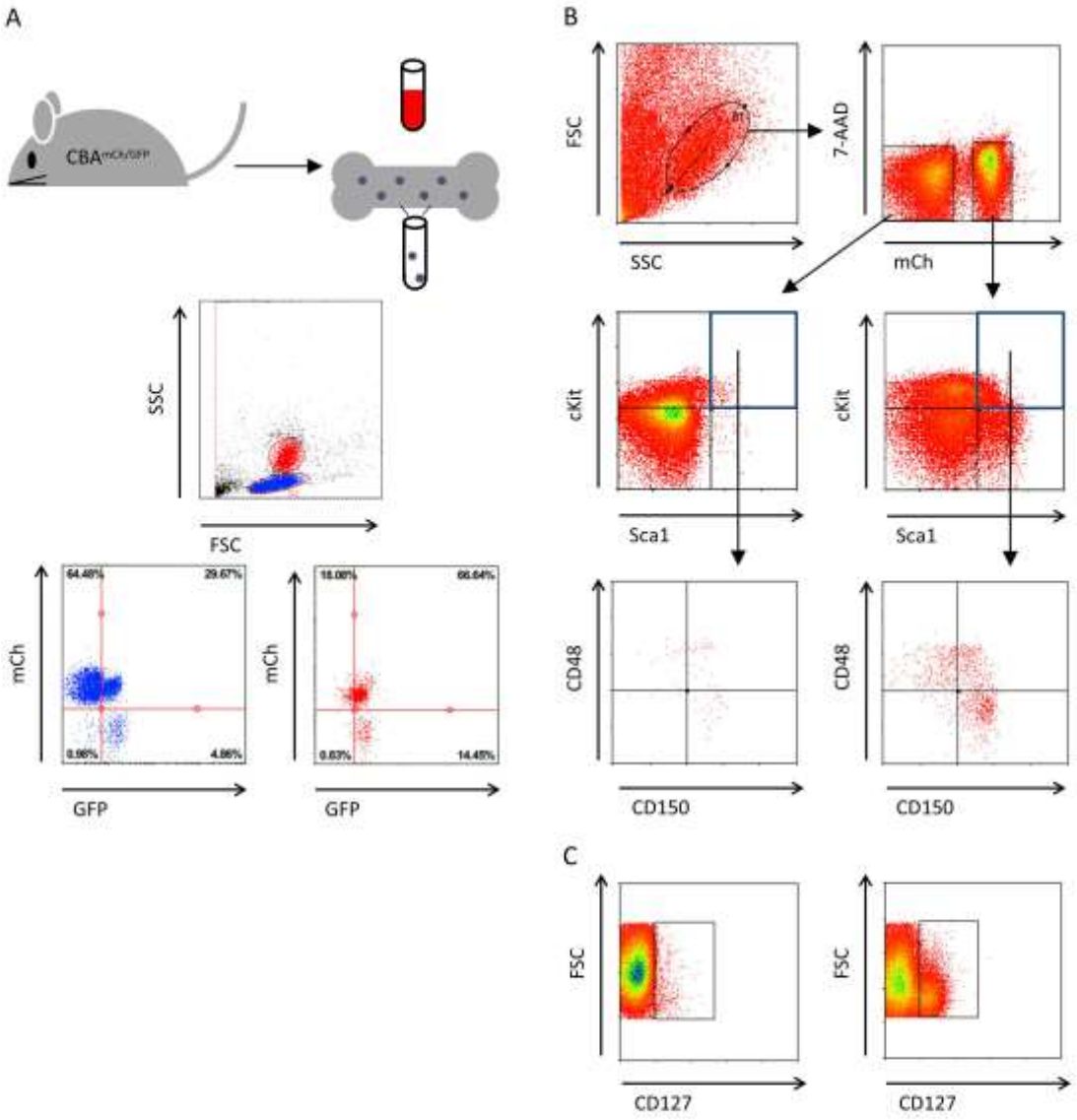



**Figure 3.20 Myeloid-biased mixed lineage mCherry- clonal expansion in the haematopoietic stem and progenitor cell fraction of an irradiated *Sfpi1*$^{mCh/GFP}$ mouse**

(A) A male *Sfpi1*$^{mch/GFP}$ mouse which was exposed to a single acute 3 Gy whole body X-irradiation at 10 weeks of age, was sacrificed upon detection of myeloid mCherry- clonal expansion in the peripheral blood WBCs. (B) Bone marrow was harvested, followed by immunomagnetic selection of haematopoietic stem and progenitor cells. Cells were labelled with Sca1, cKit, CD48, CD150 and CD127 antibodies, and analysed for mCherry and cell surface marker expression by flow cytometry. (C) CD127 expression in mCherry- and mCherry+ haematopoietic stem and progenitor cells (left and right panel, respectively).

Interestingly, at 15 months following radiation exposure, 40% of mice which presented with mCherry- clonal expansion in the peripheral blood WBCs, had mCherry- clonal expansion of lymphoid origin only. To this end, one of the *Sfpi1*$^{mch/GFP}$ mice was sacrificed upon detection of lymphoid mCherry- clonal expansion in the peripheral blood WBCs (Figure 3.21A). Bone marrow was harvested, followed by immunomagnetic selection of haematopoietic stem and progenitor cells. Cells were labelled with Sca1, cKit, CD48, CD150 and CD127 antibodies, and analysed for mCherry and cell surface marker expression by flow cytometry. Peripheral blood analysis showed that 36.5% of lymphocytes were mCherry-. However, all monocytes and granulocytes were mCherry+ (Figure 3.21A). Analysis of the haematopoietic stem and progenitor cells revealed that only 1.9% was mCherry-. Within the mCherry- fraction, almost all cells were Sca1-cKit- (95.7%; Figure 3.21B). Within the mCherry- haematopoietic stem and progenitor cells, 10.6% of cells expressed CD127 (compared with 8.3% in mCherry+ haematopoietic stem and progenitor cells; Figure 3.21C), indicating a mCherry- lymphoid phenotype.

We then had to confirm that the haematopoietic stem and progenitor cell changes described above, are only seen in mice following radiation exposure. To this end, one of the sham-irradiated *Sfpi1*$^{mch/GFP}$ mice was sacrificed at 27 months of age. Bone marrow was harvested, followed by immunomagnetic selection of haematopoietic stem and progenitor cells. Cells were labelled with Sca1, cKit, CD48, CD150 and CD127 antibodies, and analysed for mCherry and cell surface marker expression. Peripheral blood analysis showed that all peripheral blood WBCs retained mCherry expression (Figure 3.22A).

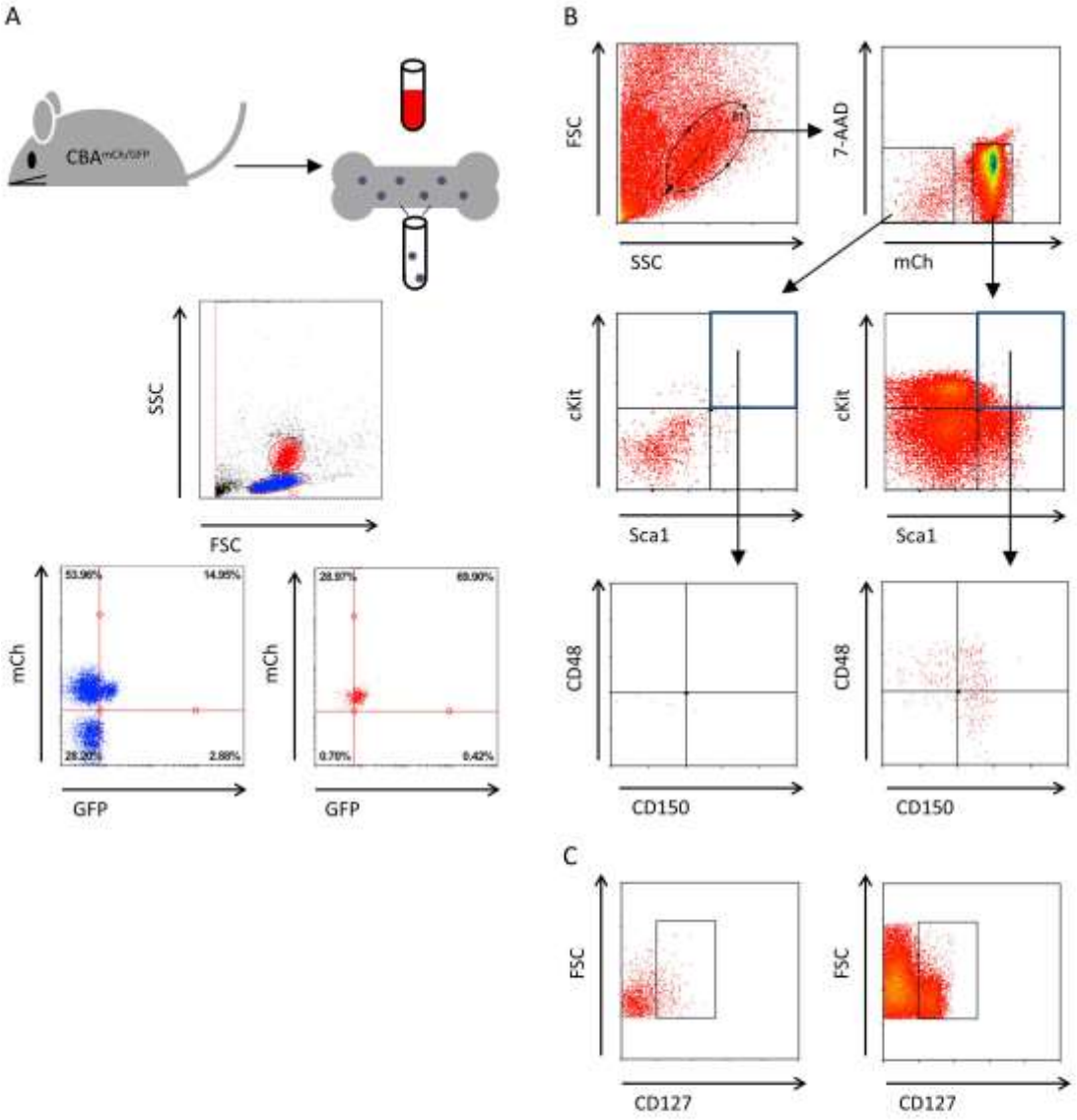



**Figure 3.21 Lymphoid mCherry- clonal expansion in the haematopoietic stem and progenitor cell fraction of an irradiated *Sfpi1*$^{mCh/GFP}$ mouse**

(A) A male *Sfpi1*$^{mch/GFP}$ mouse which was exposed to a single acute 3 Gy whole body X-irradiation at 10 weeks of age, was sacrificed upon detection of lymphoid mCherry- clonal expansion in the peripheral blood WBCs. (B) Bone marrow was harvested, followed by immunomagnetic selection of haematopoietic stem and progenitor cells. Cells were labelled with Sca1, cKit, CD48, CD150 and CD127 antibodies, and analysed for mCherry and cell surface marker expression by flow cytometry. (C) CD127 expression in mCherry- and mCherry+ haematopoietic stem and progenitor cells (left and right panel, respectively).

Analysis of the haematopoietic stem and progenitor cells of this sham-irradiated mouse, revealed that only 1.1% was mCherry-, and that within the mCherry- fraction, all cells were Sca1-cKit- (99.9%; Figure 3.22B).

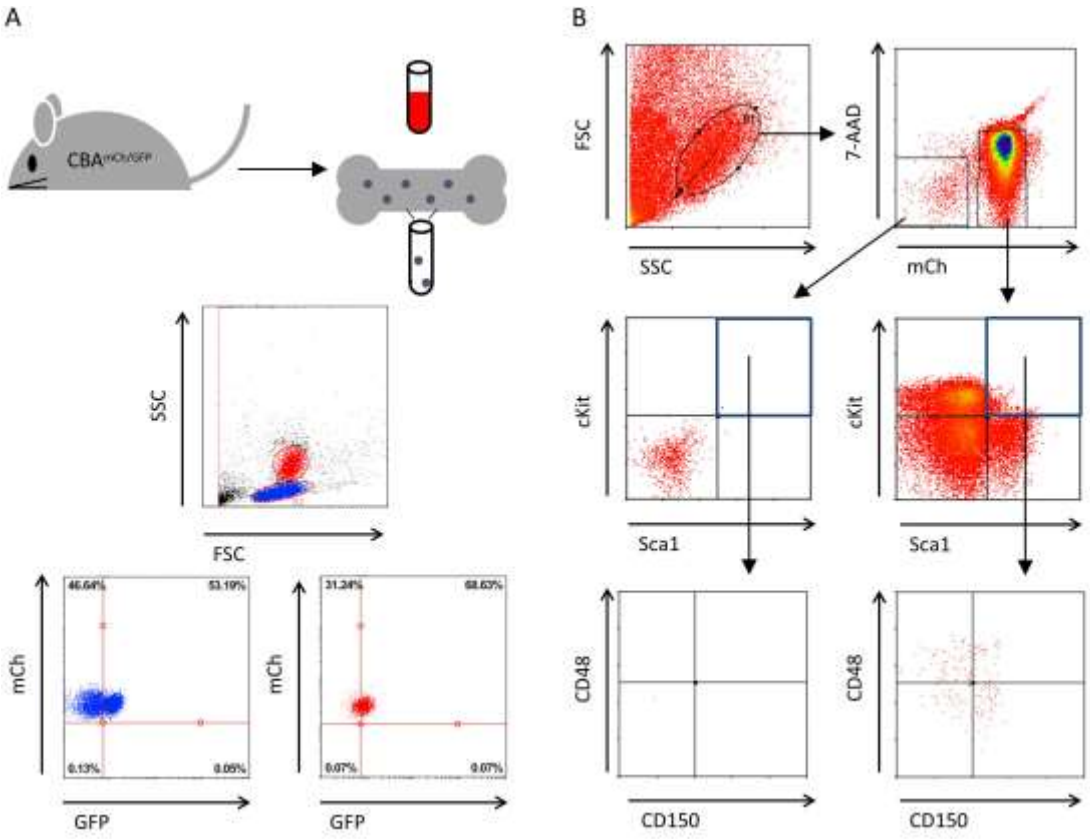



**Figure 3.22 mCherry expression in the haematopoietic stem and progenitor cell fraction of a sham-irradiated *Sfpi1*$^{mCh/GFP}$ mouse**

(A) A sham-irradiated *Sfpi1*$^{mch/GFP}$ mouse was sacrificed at 27 months of age, and peripheral blood WBCs were analysed for mCherry and GFP expression by flow cytometry. (B) Bone marrow was harvested, followed by immunomagnetic selection of haematopoietic stem and progenitor cells. Cells were labelled with Sca1, cKit, CD48, CD150 and CD127 antibodies, and analysed for mCherry and cell surface marker expression by flow cytometry.

We next assessed the cell surface marker expression of mCherry- peripheral blood WBCs. To this end, we labelled the peripheral blood WBCs of two *Sfpi1*$^{mch/GFP}$ mice (one mouse with myeloid-biased mixed lineage mCherry- clonal expansion and one mouse with lymphoid mCherry- clonal expansion) with Mac1, B220, CD3, Sca1 and cKit antibodies conjugated with PE, and analysed mCherry and cell surface marker expression by flow cytometry. In the mouse with a myeloid-biased mixed lineage mCherry- clonal expansion, the majority of mCherry- WBCs were monocytes (mCherry-Mac1+, Figure 3.23A). In the mouse with a lymphoid mCherry- clonal expansion, the vast majority of cells were B-cells (Figure 3.23B). In both mice, mCherry- cells did not express CD3, Sca1 and cKit.

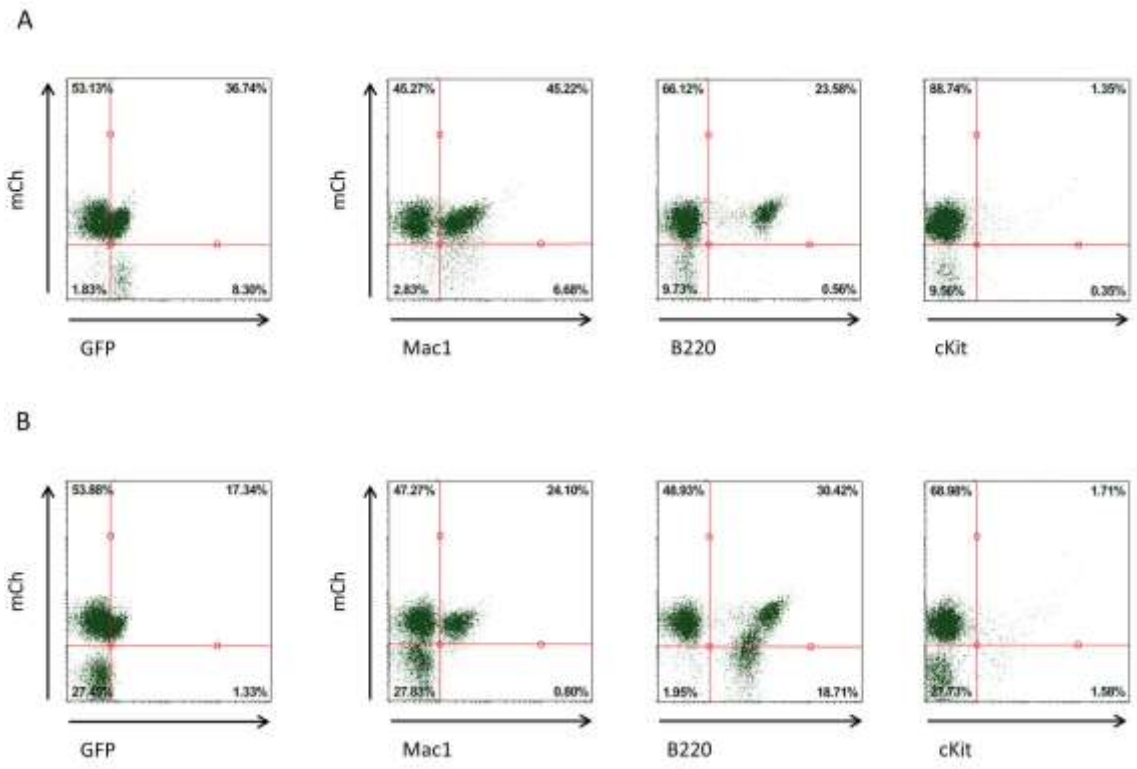



**Figure 3.23 Cell surface marker expression of mCherry- WBCs**

Peripheral blood of *Sfpi1*$^{mch/GFP}$ mice with myeloid-biased mixed lineage (A) and lymphoid (B) mCherry- clonal expansion was labelled with Mac1, B220 and cKit antibodies conjugated with PE, and analysed mCherry and cell surface marker expression by flow cytometry.

As we were interested to determine the changes in *Sfpi1* expression following an interstitial chromosome 2 deletion, we assessed GFP expression in mCherry- peripheral blood WBCs. To this end, the peripheral blood of a *Sfpi1*$^{mCh/GFP}$ mouse with mCherry- clonal expansion was analysed for mCherry and GFP expression by flow cytometry (Figure 3.24A). When comparing GFP expression between mCherry- and mCherry+ granulocytes, it was clear that chromosome 2 deleted WBCs (i.e. mCherry-) had a continuous 1.4-fold higher GFP expression (Figure 3.24B). Interestingly, mean GFP fluorescence in mCherry+ WBCs increased with time (Figure 3.24C, yellow line).

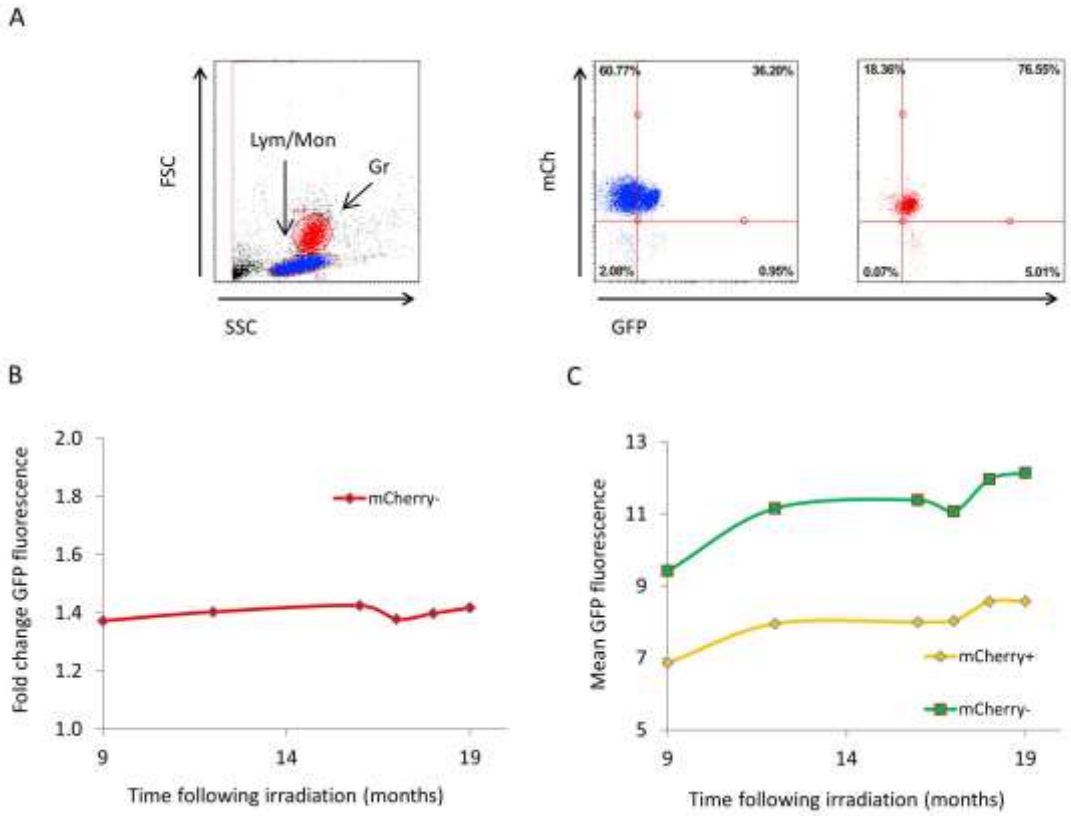



**Figure 3.24 GFP expression is upregulated in peripheral blood WBCs following chromosome 2 deletion**

(A) Peripheral blood of a *Sfpi1*$^{mCh/GFP}$ mouse with mCherry- clonal expansion was analysed for mCherry and GFP expression by flow cytometry. (B) Fold change GFP expression in mCherry- granulocytes was analysed by flow cytometry and assessed over time. (C) GFP expression of mCherry- granulocytes and mCherry+ granulocytes was analysed by flow cytometry and compared over time.

Remarkably, GFP expression was significantly increased in mCherry- peripheral blood WBCs of each *Sfpi1*$^{mCh/GFP}$ mouse with mixed lineage mCherry- clonal expansion (1.4-fold higher compared with mCherry+ peripheral blood WBCs; Figure 3.25A). We also wanted to assess changes in GFP expression in mCherry- haematopoietic stem and progenitor cells. To this end, GFP expression of haematopoietic stem and progenitor cells from a *Sfpi1*$^{mCh/GFP}$ mouse with mCherry- clonal expansion in peripheral blood WBCs and a *Sfpi1*$^{GFP}$ mouse was analysed by flow cytometry (Figure 3.25C and D, respectively). Similar to what we had observed in mCherry- peripheral blood WBCs of *Sfpi1*$^{mCh/GFP}$ mice, GFP expression was higher in mCherry- haematopoietic stem and progenitor cells, compared with mCherry+ haematopoietic stem and progenitor cells (Figure 3.25D).

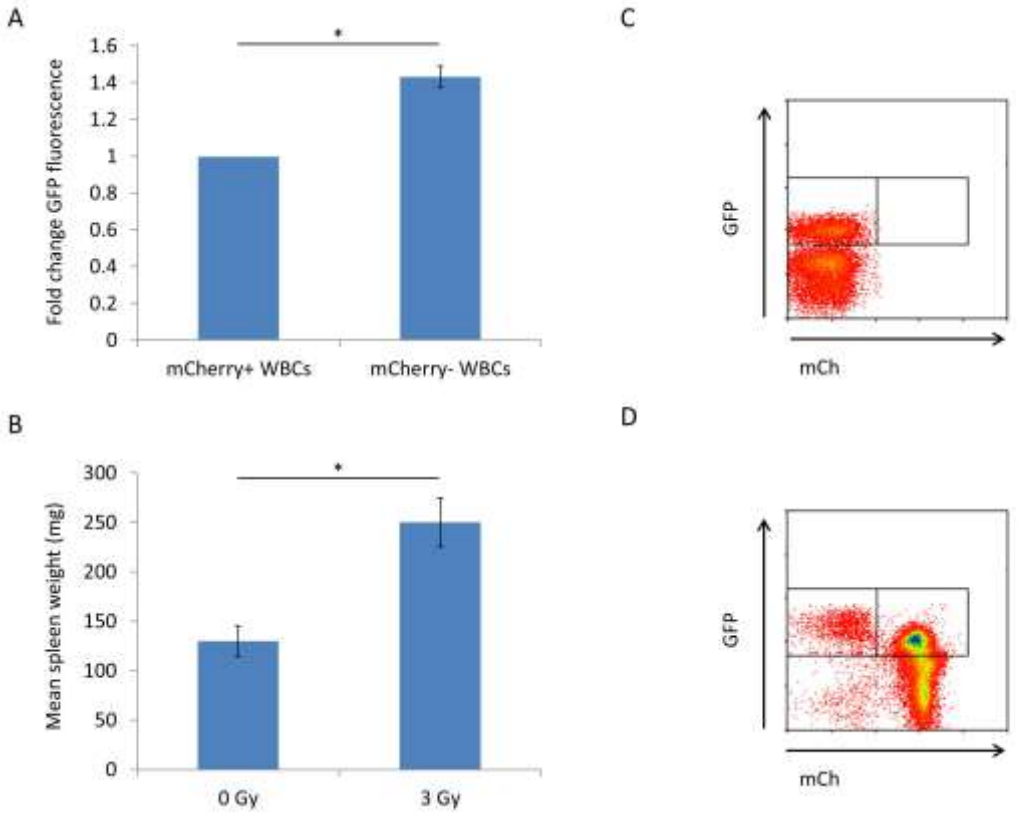



**Figure 3.25 GFP expression is upregulated in bone marrow cells following chromosome 2 deletion**

(A) Peripheral blood of *Sfpi1*$^{mCh/GFP}$ mice with mCherry- clonal expansion (10 mice) was analysed for mCherry and GFP expression by flow cytometry, and fold change GFP expression in mCherry- granulocytes was assessed. (B) Spleen weights of sham-irradiated *Sfpi1*$^{mCh/GFP}$ mice (5 mice) and irradiated (5 mice) *Sfpi1*$^{mCh/GFP}$ mice with a mCherry- clonal expansion in peripheral blood WBCs was analysed at time of sacrifice. (C/D) GFP expression of haematopoietic stem and progenitor cells from a sham-irradiated *Sfpi1*$^{GFP}$ mouse and a *Sfpi1*$^{mCh/GFP}$ mouse with mCherry- clonal expansion in peripheral blood WBCs was analysed by flow cytometry (* P <0.05).

Interestingly, at the time of sacrifice, spleen weights of irradiated *Sfpi1*$^{mCh/GFP}$ mice with a mCherry- clonal expansion in peripheral blood WBCs were consistently higher than spleen weights of sham-irradiated *Sfpi1*$^{mCh/GFP}$ mice (Figure 3.25B).

### 3.4.3. rAML progression, presentation and characterisation is gender dependent

In the previous section, we described the experiment where we exposed male 10 week old *Sfpi1*$^{mCh/GFP}$ mice to a single acute 3 Gy whole body X-irradiation. By monthly tail vein blood sampling, we demonstrated that following deletion of one chromosome 2 homologue (i.e. mCherry expression loss detectable in peripheral blood WBCs) *Sfpi1* expression is upregulated (i.e. GFP expression upregulated 1.4-fold). This *Sfpi1* upregulation indicates that a feedback mechanism is in place, as the *Sfpi1* promotor on the intact chromosome 2 homologue most likely senses this drop, and induces its own upregulation. We can detect this increase in *Sfpi1* promotor activity as the GFP construct is under control of the *Sfpi1* promotor (in contrast with mCherry expression being under control of the ubiquitous Rosa26 promotor).

However, in some *Sfpi1*$^{mCh/GFP}$ mice, this feedback mechanism seems to become dysregulated, resulting in the mice developing AML. We will further explain the underlying mechanism by looking into detail at *Sfpi1*$^{mCh/GFP}$ mouse mCh46.1. At six months following radiation exposure, peripheral blood analysis showed that 1.3% of granulocytes was mCherry- and 0.9% of monocytes was mCherry- (Figure 3.26A). Three months later, the percentage of mCherry- granulocytes and mCherry- monocytes had increased (2.7% and 5%, respectively; Figure 3.26A). Interestingly, at six months following radiation exposure, GFP expression in mCherry- granulocytes had decreased slightly compared with GFP expression in mCherry- granulocytes at four months (1.34- and 1.40-fold higher compared with mCherry+ granulocytes, respectively; Figure 3.26B).

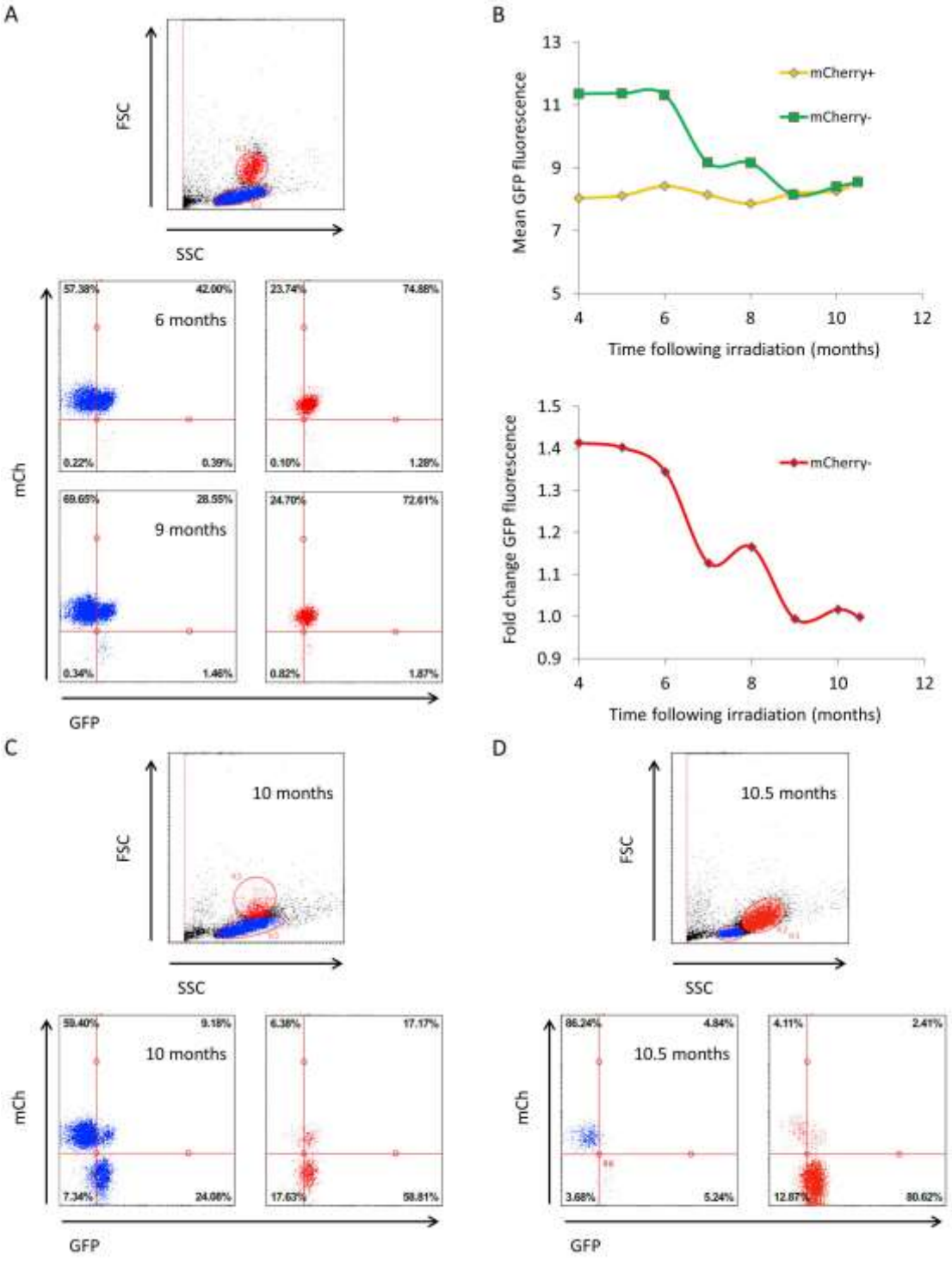



**Figure 3.26 No further increase of *Sfpi1*-GFP expression upon AML progression**

(A) Tail vein blood samples were collected monthly from *Sfpi1*$^{mCh/GFP}$ mouse mCh46.1 and mCherry and GFP expression were analysed by flow cytometry. (B) GFP expression between mCherry- granulocytes and mCherry+ granulocytes was analysed by flow cytometry and compared over time. (C/D) Flow cytometry data of peripheral blood WBCs of mouse mCh46.1 at 10 and 10.5 months following radiation exposure. mCherry and GFP expression were analysed by flow cytometry.

GFP upregulation in mCherry- granulocytes decreased even further over the next few months, and at nine months following radiation exposure, GFP expression was no longer increased compared with mCherry+ granulocytes (Figure 3.26B). Although the GFP expression of mCherry- granulocytes had returned to normal levels at nine months, the FSC/SSC plot did not show any change in WBC size or granularity (Figure 3.26A). One month later, the percentage of mCherry- granulocytes and monocytes had increased further, and a change in the FSC/SSC plot could be detected (i.e. merging of the granulocytes and monocytes; Figure 3.26C). Two weeks later (i.e. 10.5 months following radiation exposure), the mouse presented with outward physical signs of rAML (i.e. hunched posture, decreased activity and pallor) and peripheral blood analysis showed a homogenous population on the FSC/SSC plot and 93.5% of these cells were mCherry-, but still expressed GFP (Figure 3.26D), indicating that these cells had lost the chromosome 2 homologue carrying the Rosa26-mCherry construct and retained the chromosome 2 homologue carrying the GFP construct.

This mouse was then sacrificed and hepatosplenomegaly was detected upon opening the abdominal cavity (spleen weight 880 mg). The spleen was extracted and a single cell spleen suspension prepared, after which cells were labelled with antibodies. The rAML antibody panel contained nine different antibodies: for immaturity/progenitor cell surface markers (i.e. Sca1, cKit, Ly6c and CD31), for mature, lineage-committed cell surface markers (i.e. Mac1, Gr1, B220 and CD3), and for the Flt3 cell surface marker. mCherry, GFP and cell surface marker expression were analysed by flow cytometry. Similar to flow cytometry data from the peripheral blood, although all spleen cells had lost mCherry expression, they still expressed GFP (Figure 3.27). Immunophenotyping of

the spleen cells of this mouse showed that mCherry-GFP+ spleen cells expressed immaturity cell surface markers, including cKit, Ly6c and CD31. On the other hand, these cells did not express mature, lineage-committed cell surface markers, such as B220 (Figure 3.27)(summarised in Table 6 and Table 7, at the end of this section).

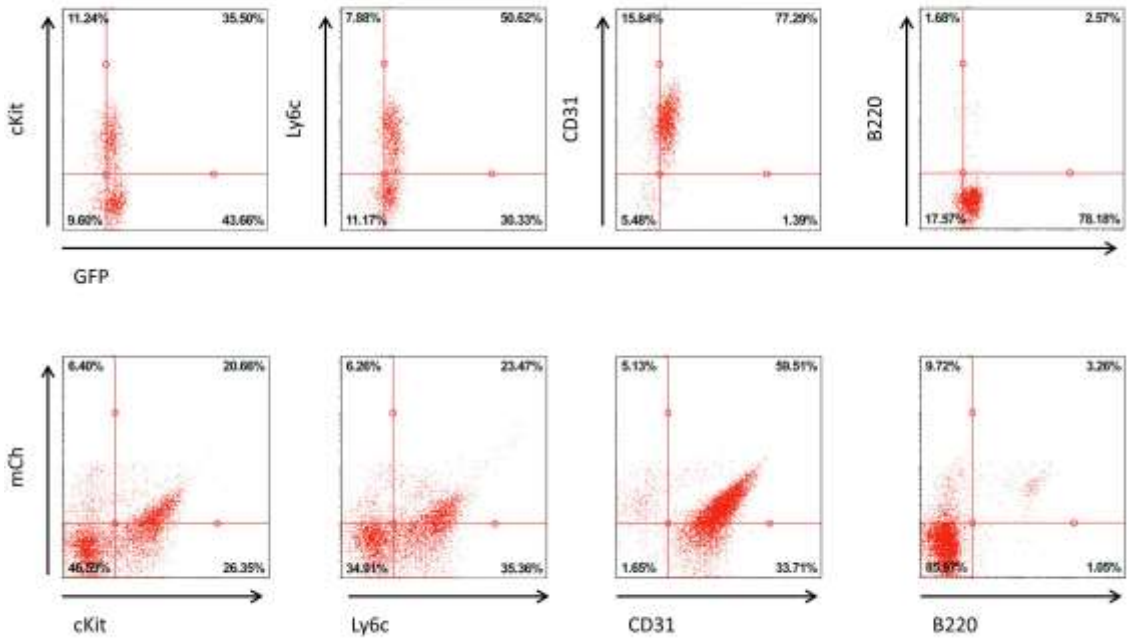



**Figure 3.27 Immunophenotyping of spleen cells obtained from mouse mCh46.1**

At ten and a half months following radiation exposure, *Sfpi1*$^{mch/GFP}$ mouse mCh46.1 presented with outward physical signs of rAML and was sacrificed. A single cell spleen suspension was prepared, and cells were labelled with antibodies conjugated with PE. mCherry, GFP and cell surface marker expression were analysed by flow cytometry.

To assess the point mutation status of the remaining *Sfpi1* copy (i.e. the second mutational hit), we isolated DNA from the spleen and amplified exon 5 of the *Sfpi1* gene by PCR. The PCR product was sent for sequencing and sequencing files were analysed using Chromas 2.6 software. The mCh46.1 DNA sequence revealed a **T**GC sequence (compared with a **C**GC sequence in a sham-irradiated mouse; Figure 3.28A).

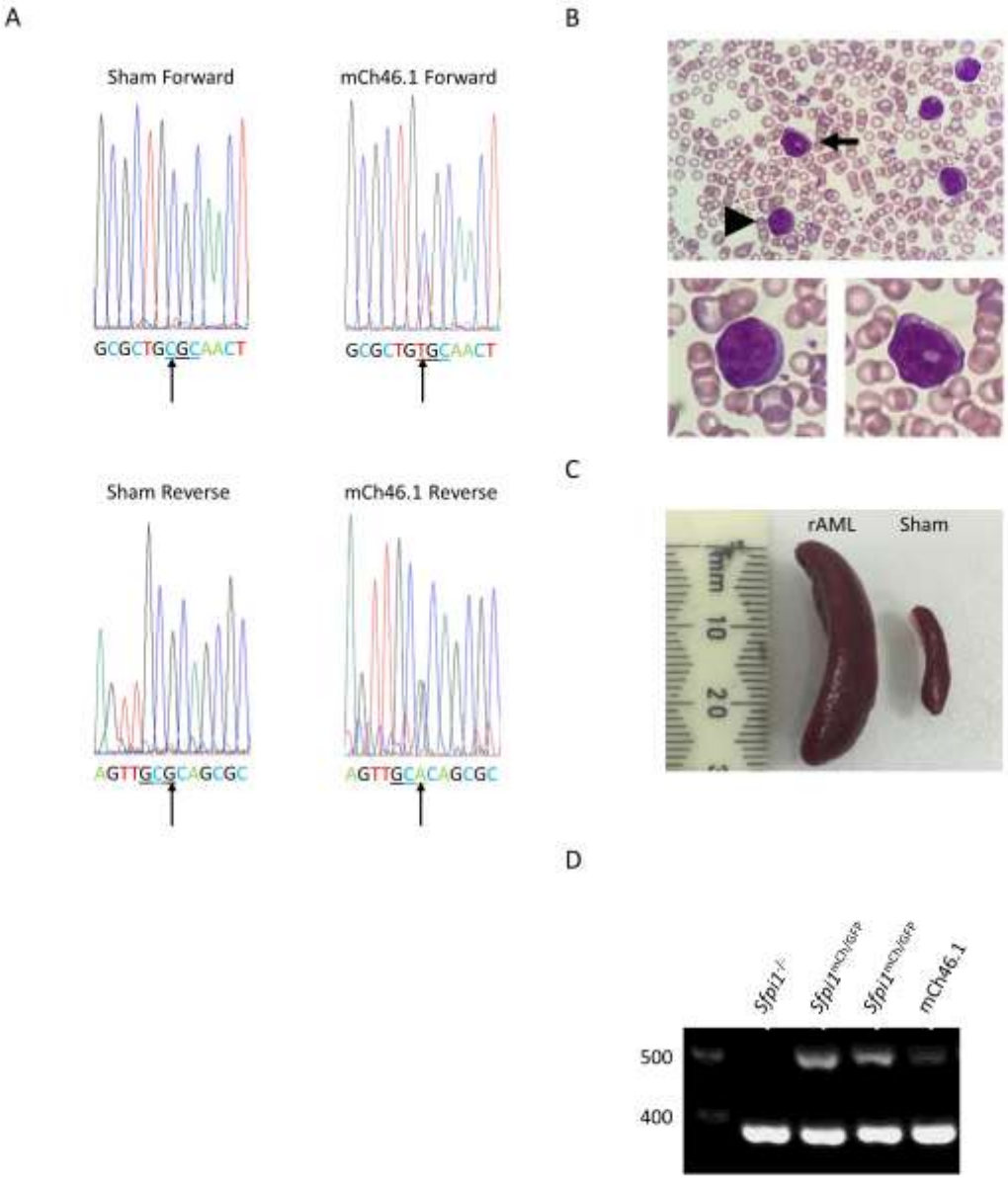



**Figure 3.28 mCh46.1 rAML characterisation**

*Sfpi1*$^{mch/GFP}$ mouse mCh46.1 was sacrificed upon presentation of outward physical signs of rAML. (A) DNA was isolated from the spleen and exon 5 of the *Sfpi1* gene was amplified by PCR. The PCR product was sent for sequencing by Source BioScience (University of Oxford, UK). Sequencing files were analysed using Chromas 2.6 software. The exon 5 *Sfpi1* DNA sequence of a sham-irradiated and mCh46.1 mouse is zoomed in on the CGC codon known to exhibit a point mutation (left panels and right panels, respectively; point mutation are always confined to the underlined CGC codon and the arrow indicates the point mutation in mCh46.1 where C is substituted for T, compared with the non-mutated CGC codon in a sham-irradiated mouse). (B) Peripheral blood smear. (C) Photograph of the spleen of mCh46.1 and a sham-irradiated mouse (left and right, respectively). (D) DNA was isolated from the spleen and a PCR was performed amplifying the region containing the Rosa26-mCherry construct. The PCR product was run on an agarose gel (control DNA was obtained from a wild-type mouse and two sham-irradiated *Sfpi1*$^{mch/GFP}$ mice).

This point mutation replaced the amino acid residue arginine 235 (R235) with cysteine (R235C). A peripheral blood smear was also prepared. Following May-Grünwald-Giemsa staining, slides were observed by light microscopy (Figure 3.28B). Nucleated cells were two-fold larger than red blood cells and had a blastic appearance. An undifferentiated blast cell with several nucleoli is indicated by an arrowhead and is enlarged at the bottom left (Figure 3.28B). A neutrophilic myelocyte with a typical ringed nucleus is indicated by an arrow and is enlarged at the bottom right (Figure 3.28B).

DNA isolated from the spleen was also used in a PCR to amplify the region containing the Rosa26-mCherry construct. Whereas DNA obtained from *Sfpi1*$^{-/-}$ mice (i.e. mice not carrying the construct) only revealed a wild-type allele (383 bp; Figure 3.28D, left lane), DNA obtained from sham-irradiated *Sfpi1*$^{mCh/GFP}$ mice revealed both the Rosa26-mCherry allele (510 bp) and wild-type allele (Figure 3.28D, two middle lanes). As anticipated from the flow cytometry data, DNA obtained from the mouse mCh46.1 revealed only a wild-type allele (and a faint Rosa26-mCherry allele, most likely due to contaminating non-AML DNA present in the leukaemic spleen; Figure 3.28D, right lane), indicating that the spleen cells had lost the Rosa26-mCherry construct. In summary, mouse mCh46.1 was diagnosed with rAML and had a latency of 10.5 months following radiation exposure. The chromosome 2 homologue carrying the Rosa26-mCherry construct was deleted, and the remaining chromosome 2 homologue retained the GFP construct but had a point mutation in exon 5 of the *Sfpi1* gene.

Similar to what we described for mouse mCh46.1 which developed myeloid leukaemia where the Rosa26-mCherry construct was deleted, *Sfpi1*$^{mCh/GFP}$ mice can also develop leukaemia following loss of the GFP construct on the other chromosome 2 homologue. We will discuss this further by looking into detail at *Sfpi1*$^{mCh/GFP}$ mouse mCh50. At 14 months following radiation exposure, peripheral blood analysis showed that 0.5% of granulocytes was mCherry-, 0.5% of monocytes was mCherry- and 0.6% of lymphocytes was mCherry- (Figure 3.29A). One month later, the number of granulocytes had decreased and the number of mCherry+GFP- cells in the lympho-monocytic population had increased from 67.5% to 77% (Figure 3.29B). Interestingly, a change in the FSC/SSC plot could be detected (i.e. merging of the granulocytes and monocytes; Figure 3.29B), changes similar to those observed in mCh46.1 (Figure 3.26).

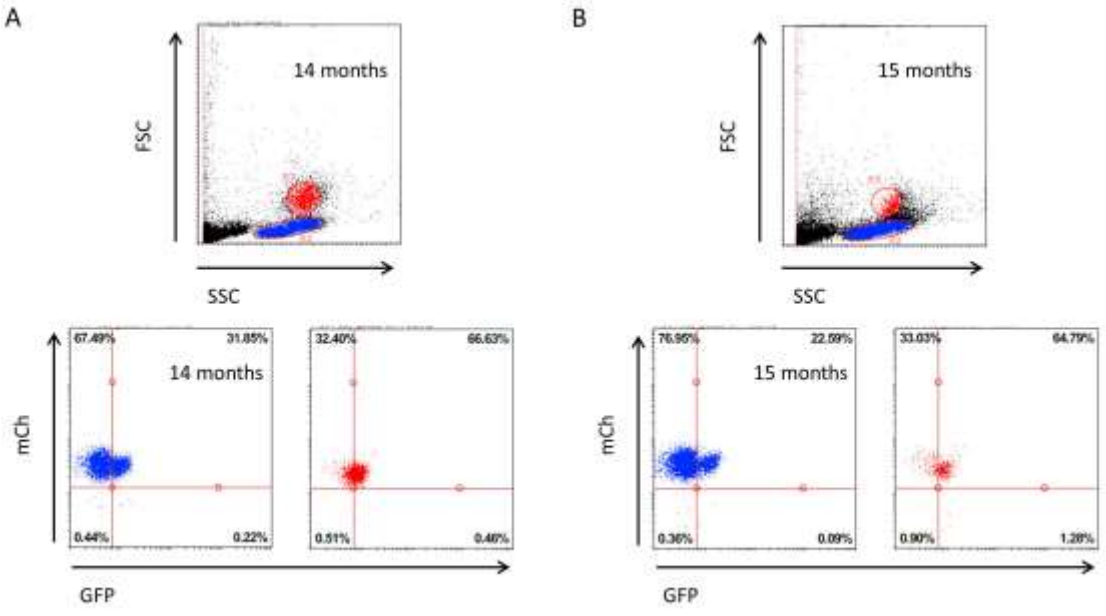



**Figure 3.29 Serial blood sampling of mouse mCh50 revealed changes in the FSC/SSC plot prior to AML presentation**

Tail vein blood samples were collected from *Sfpi1*$^{mCh/GFP}$ mouse mCh50 at 14 and 15 months following radiation exposure and mCherry and GFP expression were analysed by flow cytometry (A and B, respectively).

Three weeks later (i.e. 15.5 months following radiation exposure), the mouse presented with outward physical signs of rAML (i.e. hunched posture and decreased activity). This mouse was then sacrificed and hepatosplenomegaly was detected upon opening the abdominal cavity (spleen weight 900 mg). The spleen was extracted and a single cell spleen suspension prepared, after which cells were labelled with antibodies conjugated with PE, and mCherry, GFP and cell surface marker expression analysed by flow cytometry. Although all spleen cells had lost GFP expression, they still expressed mCherry (Figure 3.30A), indicating that these cells had lost the chromosome 2 homologue carrying the GFP construct and retained the chromosome 2 homologue carrying the Rosa26-mCherry construct. Immunophenotyping of the spleen cells of this mouse showed that mCherry+GFP- spleen cells expressed immaturity cell surface markers, including cKit, Ly6c and CD31. On the other hand, these cells did not express mature, lineage-committed cell surface markers, such as Mac1 (Figure 3.30A) (summarised in Table 6 and Table 7, at the end of this section).

To assess the point mutation status of the *Sfpi1* copy on the remaining chromosome 2 homologue carrying the Rosa26-mCherry construct, we isolated DNA from the spleen and amplified exon 5 of the *Sfpi1* gene by PCR. The mCh50 DNA sequence revealed a C**A**C sequence (compared with a C**G**C sequence in a sham-irradiated mouse; Figure 3.30B). This point mutation replaced the amino acid residue arginine 235 (R235) with histidine (R235H). A peripheral blood smear was also prepared. Nucleated cells were two-fold larger than red blood cells and had a blastic appearance. An undifferentiated blast cell with several nucleoli is indicated by an arrow and is enlarged at the bottom right (Figure 3.30C).

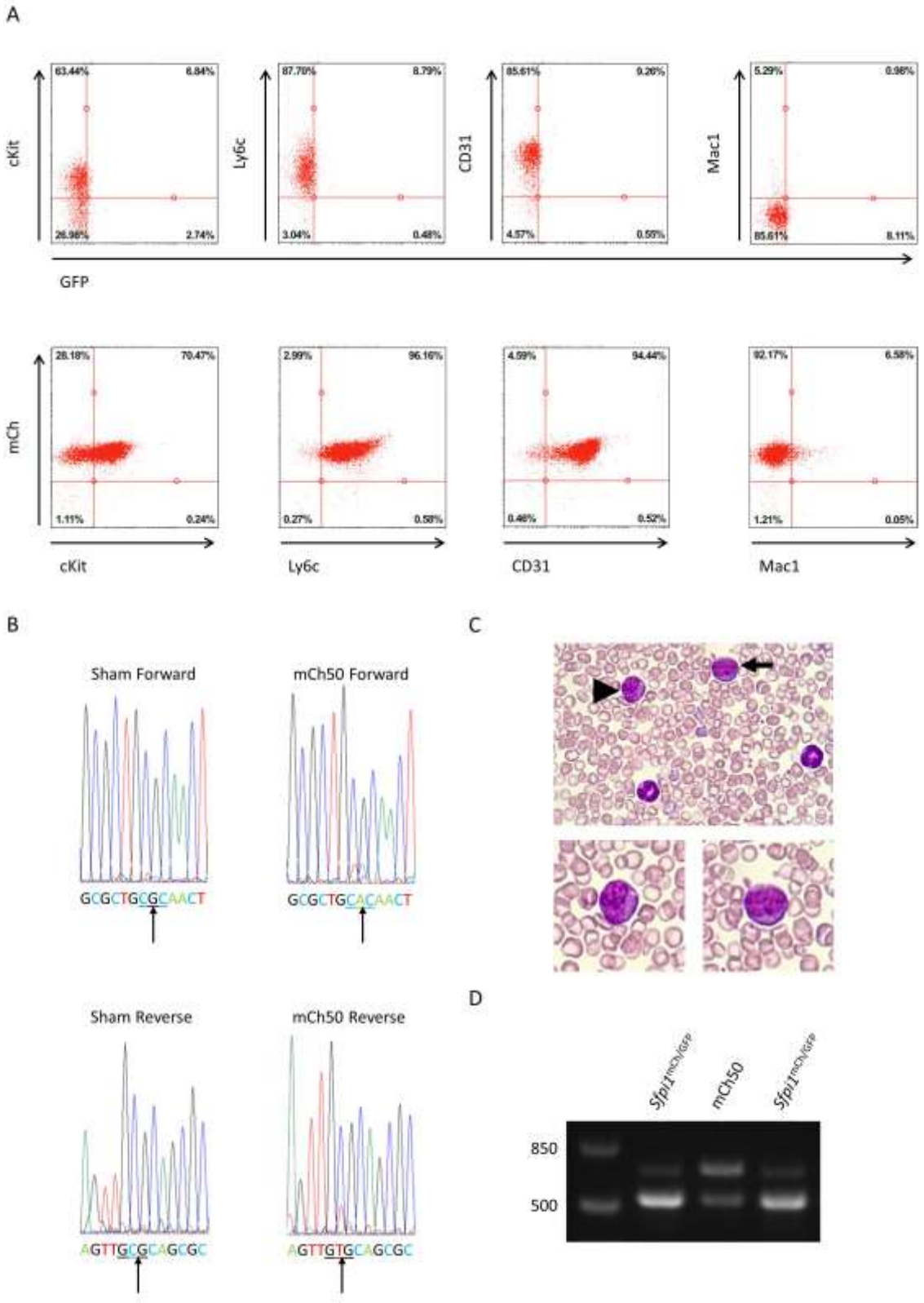



**Figure 3.30 mCh50 rAML characterisation**

At fifteen and a half months following radiation exposure, *Sfpi1*$^{mch/GFP}$ mouse mCh50 presented with outward physical signs of rAML and was sacrificed. (A) A single cell spleen suspension was prepared, and cells were labelled with antibodies conjugated with PE. mCherry, GFP and cell surface marker expression were analysed by flow

cytometry. (B) DNA was isolated from the spleen and exon 5 of the *Sfpi1* gene was amplified by PCR. The PCR product was sent for sequencing by Source BioScience (University of Oxford, UK). Sequencing files were analysed using Chromas 2.6 software. The exon 5 *Sfpi1* DNA sequence of a sham-irradiated and mCh50 mouse is zoomed in on the CGC sequence known to exhibit a point mutation (left panels and right panels, respectively; point mutation are always confined to the underlined CGC sequence and the arrow indicates the point mutation in mCh50 where G is substituted for A, compared with the non-mutated CGC in a sham-irradiated mouse). (C) Peripheral blood smear. (D) DNA was isolated from the spleen and a PCR was performed amplifying the region containing the GFP construct. The PCR product was run on an agarose gel (control DNA was obtained from two sham-irradiated *Sfpi1*$^{mch/GFP}$ mice).

DNA isolated from the spleen was also used in a PCR to amplify the region containing the GFP construct. DNA obtained from sham-irradiated *Sfpi1*$^{mCh/GFP}$ mice revealed both the GFP allele (512 bp) and wild-type allele (680 bp; Figure 3.30D, left and right lanes). As anticipated from the flow cytometry data, DNA obtained from mouse mCh50 revealed a reduced intensity of the GFP allele and an increased intensity of the wild-type allele (the presence of a faint GFP allele can most likely be explained by contaminating non-AML DNA present in the leukaemic spleen; Figure 3.30D, middle lane), indicating that the leukaemic spleen cells had lost the GFP construct. In summary, mouse mCh50 was diagnosed with rAML and had a latency of 15.5 months following radiation exposure. The chromosome 2 homologue carrying the GFP construct was deleted, and the remaining chromosome 2 homologue retained the Rosa26-mCherry construct but had a point mutation in exon 5 of the *Sfpi1* gene.

Thus far, we reported on the rAML induction experiment where we exposed male 10 week old *Sfpi1*$^{mCh/GFP}$ mice to a single acute 3 Gy whole body X-irradiation, and that some of these mice develop myeloid leukaemia with an average latency of 13 months follow radiation exposure. However, we wanted to assess whether female mice develop leukaemia following radiation exposure as well (the vast majority of rAML induction experiments used only male mice). To this end, we exposed fifty female 10 week old *Sfpi1*$^{mCh/GFP}$ mice to a single acute 3 Gy whole body X-irradiation. Tail vein blood samples of these mice were collected at one month following radiation exposure, and mCherry and GFP expression were analysed by flow cytometry. A follow-up blood sample was collected every month until mice presented with outward physical signs of rAML (such as hunched posture, poor grooming, decreased activity and pallor) or until they had to be euthanised because of poor condition (Figure 3.31). As two of the fifty irradiated female *Sfpi1*$^{mCh/GFP}$ mice were still alive at the time of analysis, the data presented here will be derived from the forty-eight mice that had been sacrificed. Those mice which had to be humanely sacrificed, were mainly diagnosed with hepatic neoplasia and ovarian cysts/uterine hyperplasia.

At 12 months following radiation exposure, 35% of female mice had mCherry- clonal expansion detectable in the peripheral blood (>1% mCherry- WBCs, 15/43 mice), and in most mice, mCherry- clonal expansion was of mixed lineage origin (i.e. myeloid and lymphoid mCherry- cells; Figure 3.31). However, 5 out of these 15 mice had mCherry- clonal expansion which was of lymphoid origin only. The percentage of female mice with mCherry- clonal expansion had increased further by 15 months following radiation exposure (58%, 21/36).

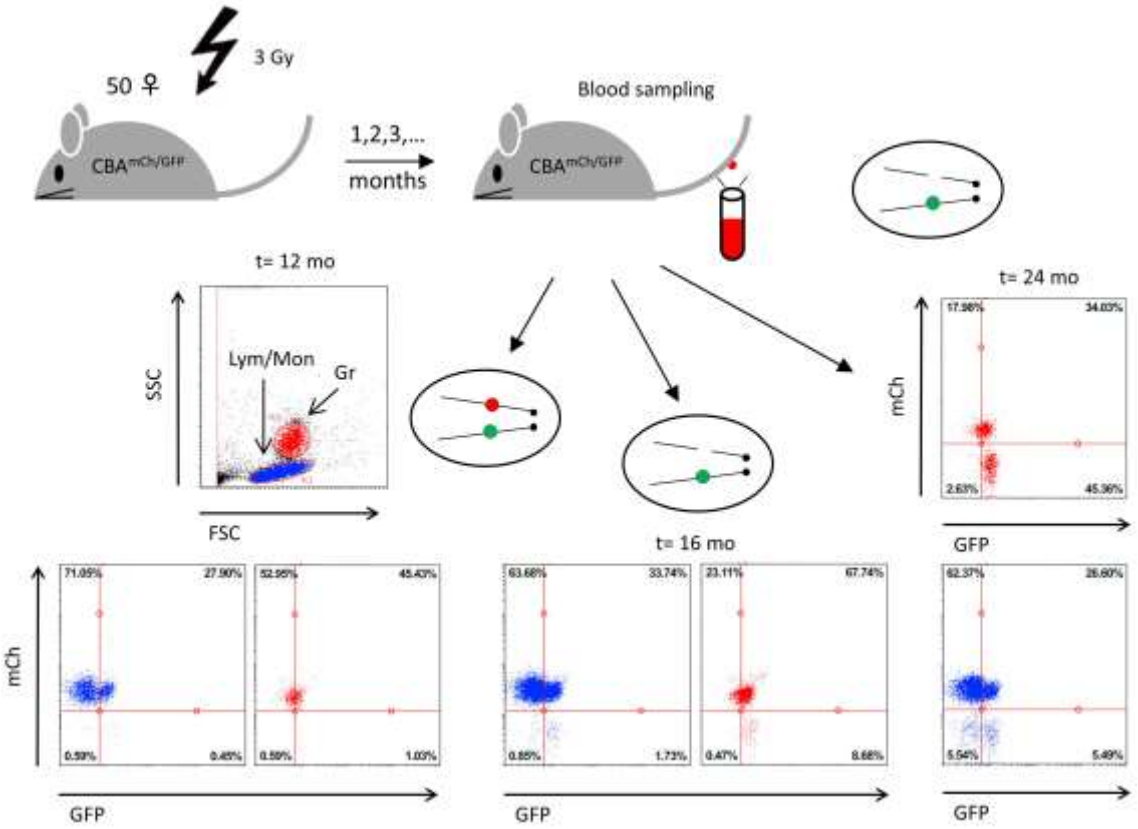



**Figure 3.31 Mixed lineage mCherry- clonal expansion in the peripheral blood WBCs of female mice**

Fifty female 10 week old *Sfpi1*$^{mCh/GFP}$ mice were exposed to a single acute 3 Gy whole body X-irradiation. Tail vein blood samples were collected at one month following radiation exposure, and analysed for mCherry and GFP expression by flow cytometry. A follow-up blood sample was collected every month until mice presented with outward physical signs of rAML or until they had to be euthanised because of poor condition. Representative flow cytometry data of a female mouse with mixed lineage mCherry- clonal expansion in the peripheral blood WBCs.

At 18 and 21 months, 73% and 100% of female mice had mCherry- clonal expansion detectable in the peripheral blood (16/22 and 8/8, respectively). Interestingly, with time, lymphoid mCherry- clonal expansion became predominant. Whereas it was only 33% of female mice with mCherry- clonal expansion who had lymphoid mCherry- clonal expansion, this percentage increased to 67% at 15 months (14/21), 75% at 18 months (12/16), to reach 100% of female mice with mCherry- clonal expansion having lymphoid mCherry- clonal expansion at 18 months following exposure (8/8).

We will discuss this further by looking into detail at female *Sfpi1*$^{mCh/GFP}$ mouse mCh240. At 13 months following radiation exposure, peripheral blood analysis showed that 1.9% of lymphocytes was mCherry-. All monocytes and granulocytes expressed mCherry (Figure 3.32A). One month later, the percentage of mCherry- lymphocytes had increased to 16.7% mCherry- lymphocytes (Figure 3.32B). Interestingly, at 15 and 16 months, the percentage of mCherry- lymphocytes had increased further and a change in the FSC/SSC plot could be detected (i.e. merging of the granulocytes and monocytes; Figure 3.32B), changes similar to those observed in mCh46.1 and mCh50.

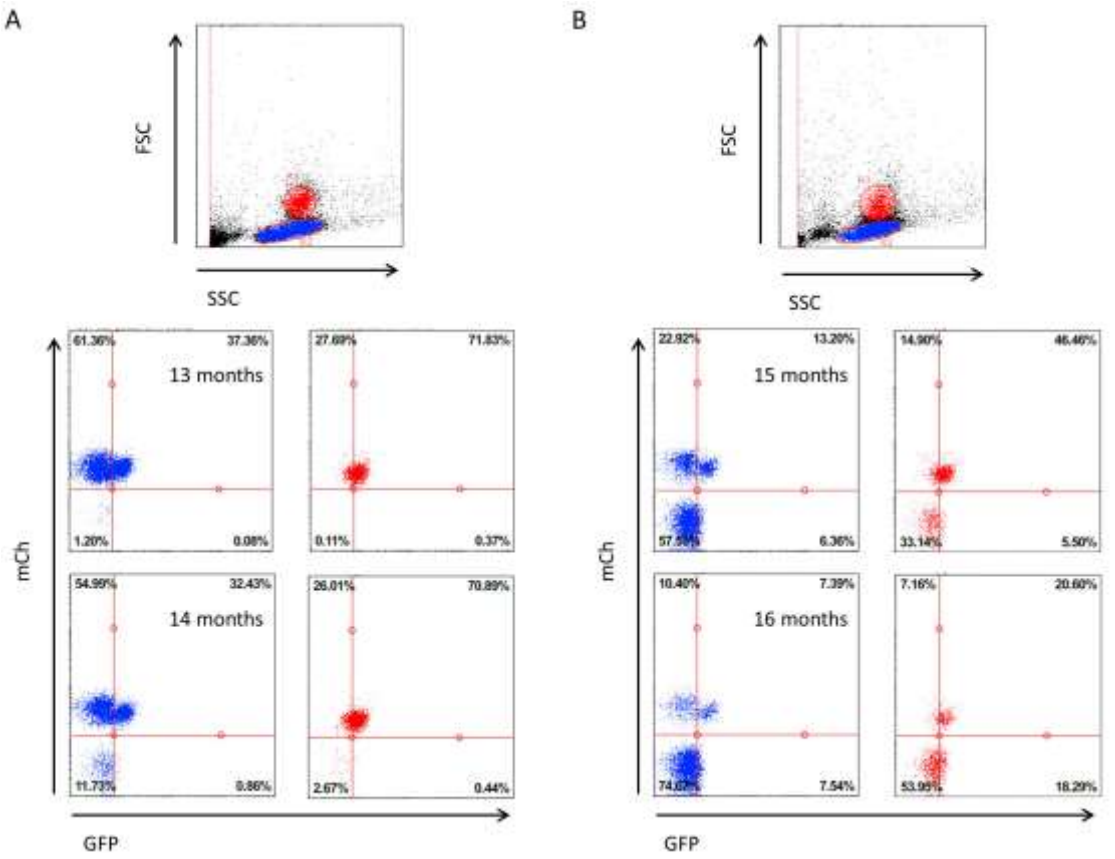



**Figure 3.32 Lymhoid mCherry- clonal expansion in the peripheral blood WBCs of mouse mCh240**

Tail vein blood samples were collected from *Sfpi1*$^{mCh/GFP}$ mouse mCh240 at 13, 14, 15 and 16 months following radiation exposure, and mCherry and GFP expression were analysed by flow cytometry (A/B).

Four weeks later (i.e. 17 months following radiation exposure), the mouse presented with outward physical signs of AML (i.e. decreased activity and pallor). This mouse was then sacrificed and hepatosplenomegaly was detected upon opening the abdominal cavity (spleen weight 640 mg). The spleen was extracted and a single cell spleen suspension prepared, after which cells were labelled with antibodies conjugated with PE, and mCherry, GFP and cell surface marker expression analysed by flow cytometry. Similar to flow cytometry data from the peripheral blood, all spleen cells had lost mCherry expression, and also did not express GFP (Figure 3.33A). Immunophenotyping of the spleen cells of this mouse showed that mCherry-GFP- spleen cells did not express all expected immaturity cell surface markers. Whereas it expressed CD31, it did not express cKit and Ly6c. On the other hand, these cells did not express mature, lineage-committed cell surface markers (CD3-, Mac1- and Gr1-), except for intermediate B220 expression (Figure 3.33A)(summarised in Table 6 and Table 7, at the end of this section).

To assess the point mutation status of the *Sfpi1* copy on the remaining chromosome 2 homologue carrying the GFP construct, we isolated DNA from the spleen and amplified exon 5 of the *Sfpi1* gene by PCR. The mCh240 DNA sequence revealed that the CGC sequence was not mutated (compared with a sham-irradiated mouse; Figure 3.33B). A peripheral blood smear was also prepared. Nucleated cells were 1.5-fold larger than red blood cells and had a homogeneous appearance. The vast majority of cells had a round nucleus and a very high nucleus to cytoplasm ratio (indicated by an arrowhead, Figure 3.33C). Occasionally, a larger version of these cells could be identified (indicated by an arrow, Figure 3.33C).

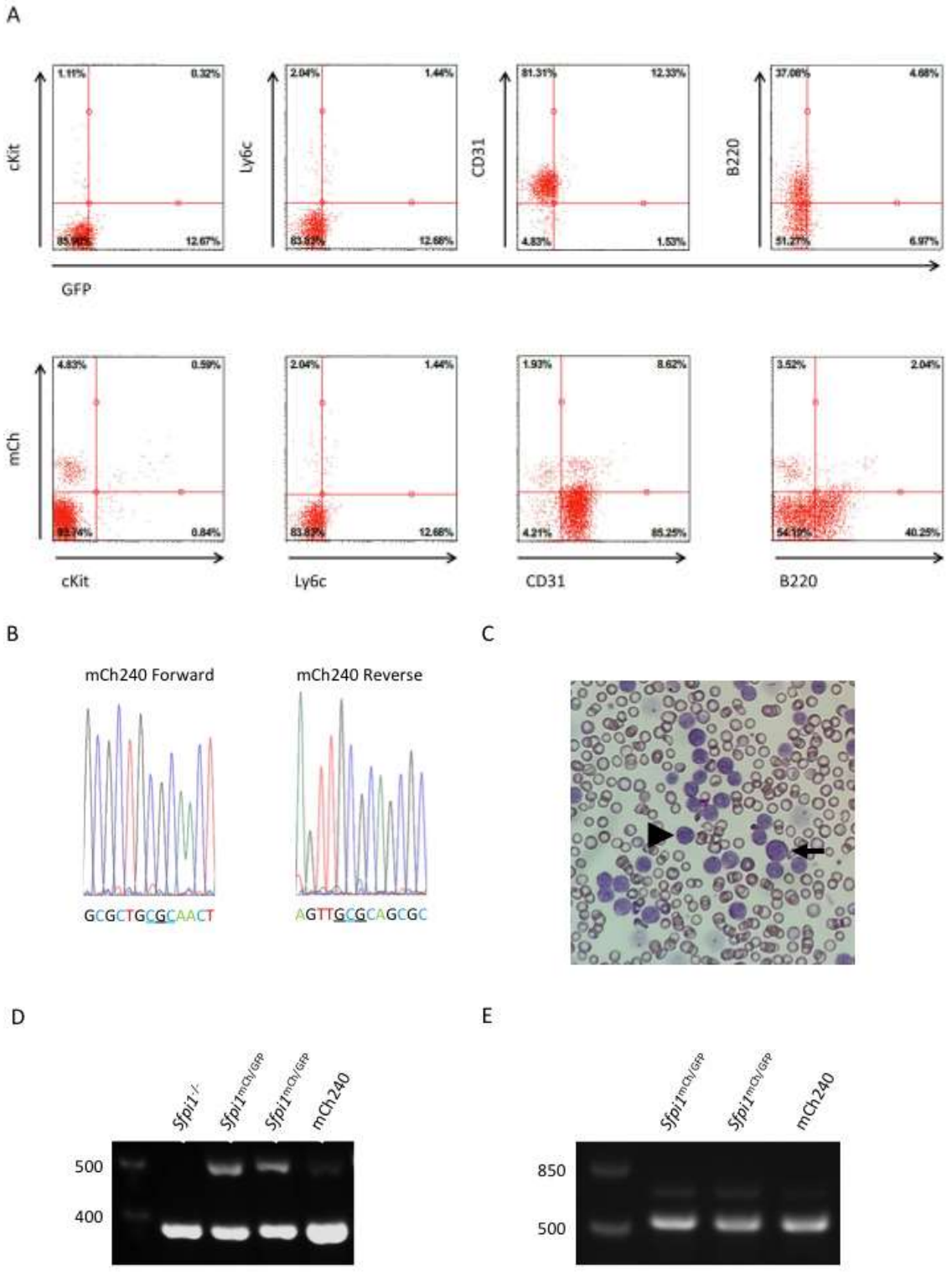



**Figure 3.33 mCh240 rAML characterisation**

At seventeen months following radiation exposure, *Sfpi1*$^{mch/GFP}$ mouse mCh240 presented with outward physical signs of AML and was sacrificed. (A) A single cell spleen suspension was prepared, and cells were labelled with antibodies conjugated with PE. mCherry, GFP and cell surface marker expression were analysed by flow

cytometry. (B) DNA was isolated from the spleen and exon 5 of the *Sfpi1* gene was amplified by PCR. The PCR product was sent for sequencing by Source BioScience (University of Oxford, UK). The exon 5 *Sfpi1* DNA sequence of mouse mCh240 is zoomed in on the CGC sequence known to exhibit a point mutation (point mutation are always confined to the underlined CGC sequence). (C) Peripheral blood smear. WBCs had a round nucleus and a very high nucleus to cytoplasm ratio (arrowhead and arrow). (D) DNA was isolated from the spleen and a PCR was performed amplifying the region containing the Rosa26-mCherry construct. The PCR product was run on an agarose gel (control DNA was obtained from a wild-type mouse and two sham-irradiated *Sfpi1*$^{mch/GFP}$ mice). (E) A PCR was also performed amplifying the region containing the GFP construct (control DNA was obtained from two sham-irradiated *Sfpi1*$^{mch/GFP}$ mice, left and middle lane).

DNA isolated from the spleen was also used in a PCR to amplify the region containing the Rosa26-mCherry construct. Whereas DNA obtained from *Sfpi1*$^{-/-}$ mice (i.e. mice not carrying the construct) only revealed a wild-type allele (383 bp; Figure 3.33D, left lane), DNA obtained from sham-irradiated *Sfpi1*$^{mCh/GFP}$ mice revealed both the Rosa26-mCherry allele (510 bp) and wild-type allele (Figure 3.33D, two middle lanes). As anticipated from the flow cytometry data, DNA obtained from the mouse mCh240 revealed only a wild-type allele (and a faint Rosa26-mCherry allele, most likely due to contaminating non-AML DNA present in the leukaemic spleen; Figure 3.33D, right lane), indicating that the spleen cells had lost the Rosa26-mCherry construct. DNA isolated from the spleen was also used in a PCR to amplify the region containing the GFP construct. In contrast with the flow cytometry data, DNA obtained from mouse mCh240 showed that the GFP allele had a similar intensity as the sham-irradiated GFP allele (512 bp), indicating that the GFP construct was still present. A faint wild-type allele could be detected, most likely due to contaminating non-AML DNA present in the leukaemic spleen (680 bp, Figure 3.33E). In summary, mouse mCh240 was diagnosed with an increased WBC count and had a latency of 17 months following radiation exposure. The chromosome 2 homologue carrying the Rosa26-mCherry

construct was deleted, and the remaining chromosome 2 homologue retained the GFP construct and did not have a point mutation in exon 5 of the *Sfpi1* gene. As the GFP construct was still detectable by PCR and as the leukaemic cells did not express GFP by flow cytometry (i.e. *Sfpi1* downregulation upon commitment towards the lymphoid lineage), mouse mCh240 developed most likely leukaemia with a lymphoid phenotype.

Similar to what we described for the female mouse mCh240 which developed leukaemia in which the Rosa26-mCherry construct was deleted, *Sfpi1*$^{mCh/GFP}$ mice can also develop leukaemia following loss of the GFP construct on the other chromosome 2 homologue. We will discuss this further by looking into detail at the female mouse mCh68. At 14 months following radiation exposure, peripheral blood analysis revealed a lower percentage of lymphocytes compared with age-matched mice (Figure 3.34A).

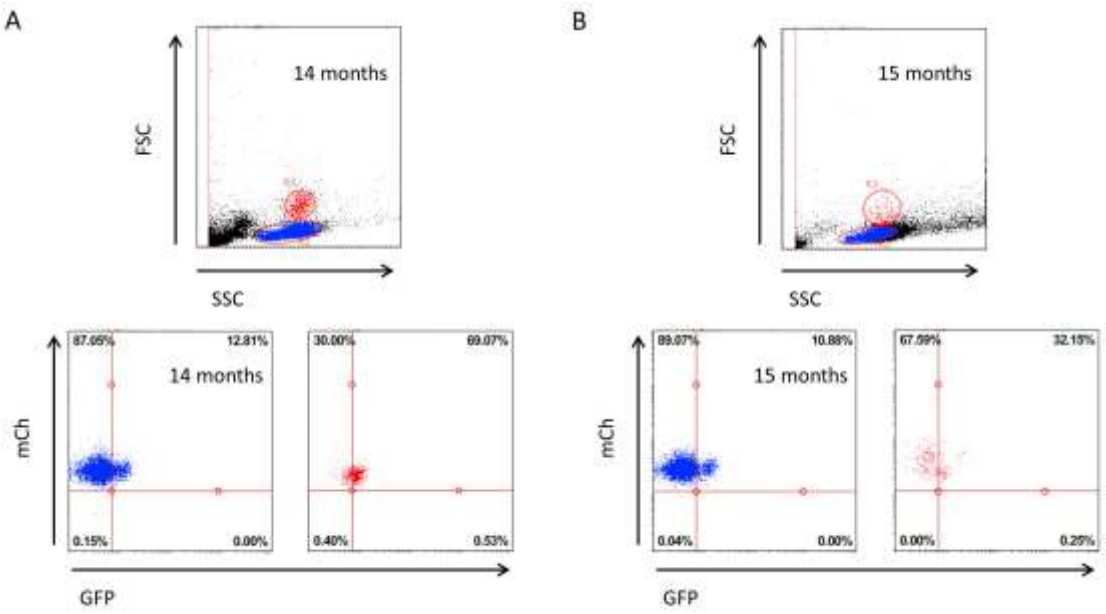



**Figure 3.34 Decreased lymphocytes in the peripheral blood of mouse mCh68**

Tail vein blood samples were collected from *Sfpi1*$^{mCh/GFP}$ mouse mCh68 at 14 and 15 months following radiation exposure, and mCherry and GFP expression were analysed by flow cytometry (A and B, respectively).

One month later, the number of lymphocytes had decreased further, and a change in the FSC/SSC plot could be detected (i.e. merging of the granulocytes and monocytes; Figure 3.34B), changes similar to those observed in mCh240 (Figure 3.32). Three weeks later (i.e. 16 months following radiation exposure), the mouse presented with outward physical signs of AML (i.e. decreased activity and hunched posture). This mouse was then sacrificed and severe hepatosplenomegaly was detected upon opening the abdominal cavity (spleen weight 1,330 mg). The spleen was extracted and a single cell spleen suspension prepared, after which cells were labelled with antibodies conjugated with PE, and mCherry, GFP and cell surface marker expression analysed by flow cytometry. Similar to flow cytometry data from the peripheral blood, all spleen cells expressed mCherry. However, they did not express GFP (Figure 3.35A). Immunophenotyping of the spleen cells of this mouse showed that mCherry+GFP- spleen cells had a very similar expression profile as observed for mCh240: cells did not express all expected immaturity cell surface markers. Whereas they had CD31 and minor cKit expression, they did not express Sca1 and Ly6c. On the other hand, these cells did not express mature, lineage-committed cell surface markers (CD3-, Mac1-, and Gr1-), except for high B220 expression (Figure 3.35A)(summarised in Table 6 and Table 7, at the end of this section). To assess the point mutation status of the *Sfpi1* copy on the remaining chromosome 2 homologue carrying the Rosa26-mCherry construct, we isolated DNA from the spleen and amplified exon 5 of the *Sfpi1* gene by PCR. The mCh68 DNA sequence revealed a **T**GC sequence (compared with a **C**GC sequence in a sham-irradiated mouse; Figure 3.35B). This point mutation replaced the amino acid residue arginine 235 (R235) with cysteine (R235C).

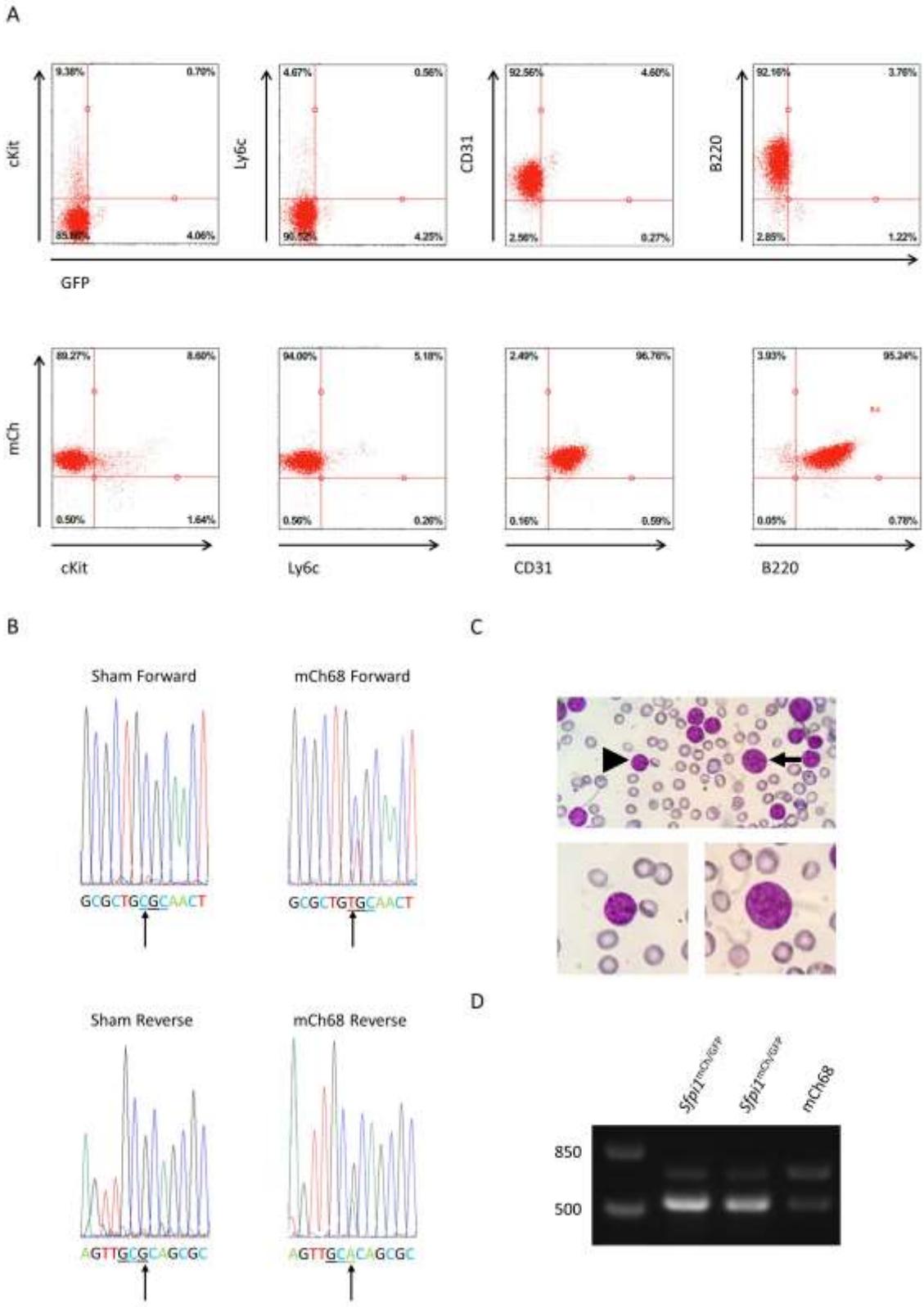



**Figure 3.35 mCh68 rAML characterisation**

At sixteen months following radiation exposure, *Sfpi1*$^{mch/GFP}$ mouse mCh68 presented with outward physical signs of AML and was sacrificed. (A) A single cell spleen suspension was prepared, and cells were labelled with antibodies conjugated with PE. mCherry, GFP and cell surface marker expression were analysed by flow cytometry.

(B) DNA was isolated from the spleen and exon 5 of the *Sfpi1* gene was amplified by PCR. The exon 5 *Sfpi1* DNA sequence of a sham-irradiated and mCh46.1 mouse is zoomed in on the CGC sequence known to exhibit a point mutation (left panels and right panels, respectively; point mutation are always confined to the underlined CGC sequence and the arrow indicates the point mutation in mCh46.1 where C is substituted for T, compared with the non-mutated CGC in a sham-irradiated mouse). (C) Peripheral blood smear. WBCs had a round nucleus and a very high nucleus to cytoplasm ratio (arrowhead and arrow). (D) DNA was isolated from the spleen and a PCR was performed amplifying the region containing the GFP construct. The PCR product was run on an agarose gel (control DNA was obtained from two sham-irradiated *Sfpi1*$^{mch/GFP}$ mice).

A peripheral blood smear was also prepared. Nucleated cells were two-fold larger than red blood cells and had a homogeneous appearance. The vast majority of cells had a round nucleus and a very high nucleus to cytoplasm ratio (indicated by an arrow and arrowhead, Figure 3.35C). Overall, this blood smear had a very similar appearance to the one from mouse mCh240. DNA isolated from the spleen was also used in a PCR to amplify the region containing the GFP construct. As anticipated from the flow cytometry data, DNA obtained from mouse mCh68 revealed a reduced intensity of the GFP allele and an increased intensity of the wild-type allele (the presence of a faint GFP allele can most likely be explained by contaminating non-AML DNA present in the leukaemic spleen; Figure 3.35D, right lane), indicating that the leukaemic spleen cells had lost the GFP construct. In summary, mouse mCh68 was diagnosed with an increased WBC count (144 x $10^6$ cells/ml) and had a latency of 16 months following radiation exposure. The chromosome 2 homologue carrying the GFP construct was deleted, and the remaining homologue retained the Rosa26-mCherry construct but had a point mutation in exon 5 of the *Sfpi1* gene. Similar to mCh240, this mouse developed most likely leukaemia with a lymphoid phenotype.

Interestingly, we also observed these leukaemias with a lymphoid phenotype in female *Sfpi1*$^{mCh/GFP}$ mice which do not harbour a chromosome 2 deletion. We will discuss this further by looking into detail at the female mouse mCh27. At 13 months following radiation exposure, peripheral blood analysis revealed a very low percentage of granulocytes and monocytes (i.e. mCherry+GFP+ cells), compared with age-matched mice (Figure 3.36A). One month later, we could only observe a homogenous population of mCherry+GFP- cells (Figure 3.36B). Two weeks later (i.e. 14.5 months following radiation exposure), the mouse presented with outward physical signs of AML (i.e. hunched posture). This mouse was then sacrificed and moderate hepatosplenomegaly was detected upon opening the abdominal cavity (spleen weight 320 mg).

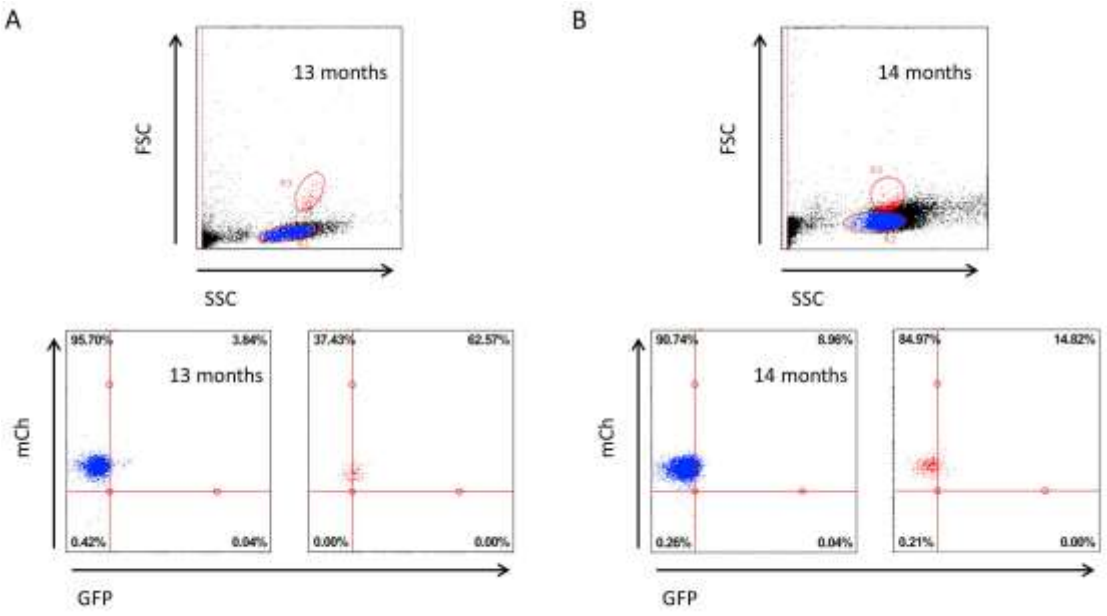



**Figure 3.36 Tail vein blood sampling detects rapid WBC size change in mouse mCh27**

Tail vein blood samples were collected from *Sfpi1*$^{mCh/GFP}$ mouse mCh27 at 13 and 14 months following radiation exposure, and mCherry and GFP expression were analysed by flow cytometry (A and B, respectively).

Similar to flow cytometry data from the peripheral blood, all spleen cells expressed mCherry. However, they did not express GFP (Figure 3.37A). Immunophenotyping of the spleen cells of this mouse showed that mCherry+GFP- spleen cells had a very similar expression profile as observed for the two previous discussed female leukaemic mice. Cells did not express all expected immaturity cell surface markers. Whereas they had CD31, high cKit and moderate Sca1 expression, they did not express Ly6c. On the other hand, these cells did not express mature, lineage-committed cell surface markers (CD3-, Mac1-, and Gr1-), except for high B220 expression. Remarkably, and in contrast with all previously described leukaemias in this thesis, all cells stained positive for the cell surface marker Flt3 (Figure 3.37A)(summarised in Table 6 and Table 7, at the end of this section).

To assess the point mutation status of the *Sfpi1* copy, we isolated DNA from the spleen, and amplified exon 5 of the *Sfpi1* gene by PCR. The mCh27 DNA sequence revealed a **T**GC sequence (compared with a **C**GC sequence in a sham-irradiated mouse; Figure 3.37B). This point mutation replaced the amino acid residue arginine 235 (R235) with cysteine (R235C).

A peripheral blood smear was also prepared. Nucleated cells were two-fold larger than red blood cells and had a homogeneous appearance. The vast majority of cells had a round nucleus and a very high nucleus to cytoplasm ratio (indicated by an arrow and arrowhead, Figure 3.37C). Overall, this blood smear was very similar to those from the two previously described female leukaemias.

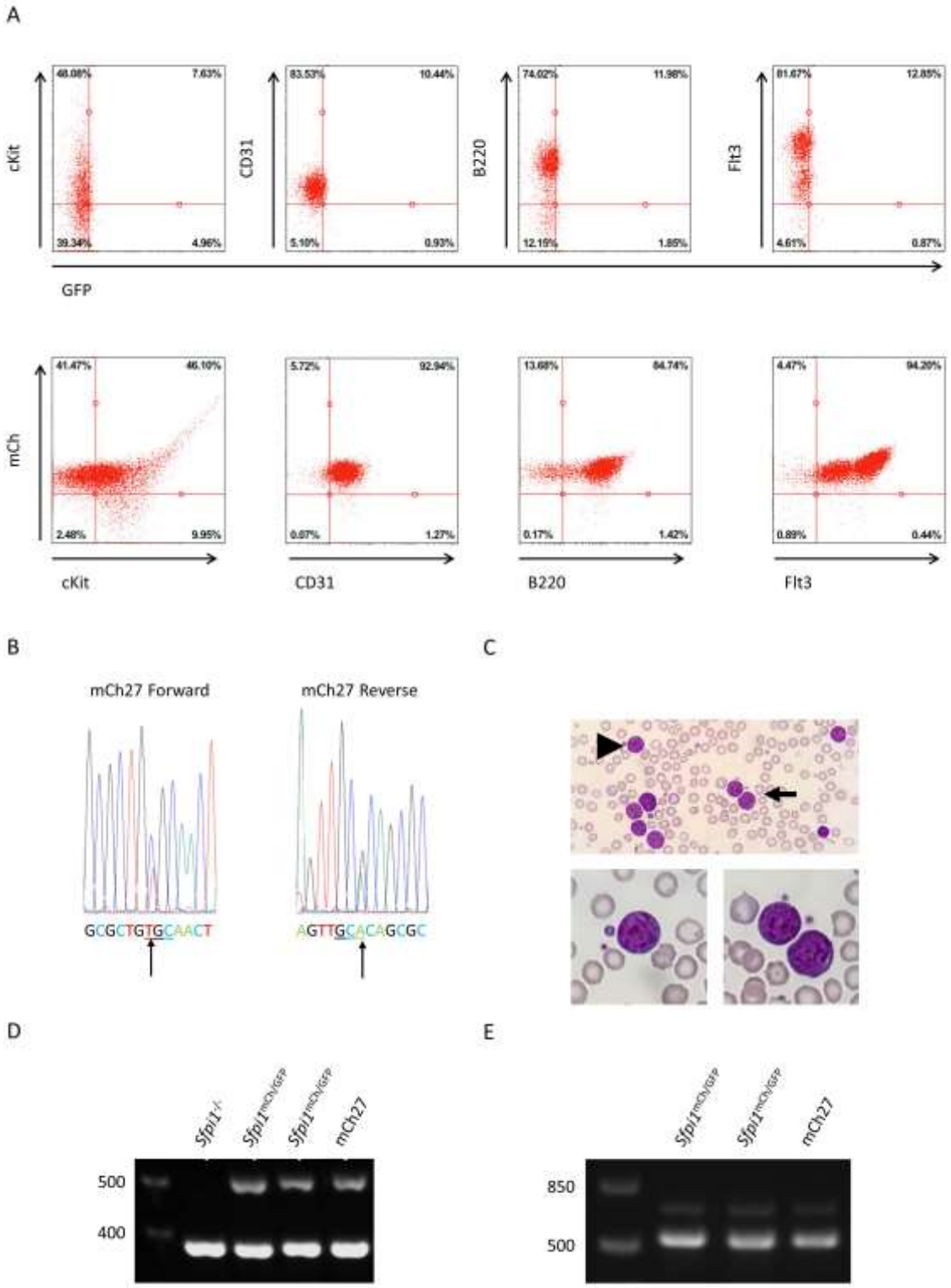



**Figure 3.37 mCh27 rAML characterisation**

At 14.5 months following radiation exposure, *Sfpi1*$^{mch/GFP}$ mouse mCh27 presented with outward physical signs of AML and was sacrificed. (A) A single cell spleen suspension was prepared, and cells were labelled with antibodies conjugated with PE. mCherry, GFP and cell surface marker expression were analysed by flow cytometry.

(B) DNA was isolated from the spleen and exon 5 of the *Sfpi1* gene was amplified by PCR. The exon 5 *Sfpi1* DNA sequence of mouse mCh27 is zoomed in on the CGC sequence known to exhibit a point mutation (point mutations are always confined to the underlined CGC sequence). (C) Peripheral blood smear (WBCs had a round nucleus and a high nucleus to cytoplasm ratio, indicated by arrowhead and arrow). (D) DNA was isolated from the spleen and a PCR was performed amplifying the region containing the Rosa26-mCherry construct. The PCR product was run on an agarose gel (control DNA was obtained from a wild-type mouse and two sham-irradiated *Sfpi1*$^{mch/GFP}$ mice). (E) A PCR was also performed amplifying the region containing the GFP construct (control DNA was obtained from two sham-irradiated *Sfpi1*$^{mch/GFP}$ mouse, left and middle lane).

DNA isolated from the spleen was also used in a PCR to amplify the region containing the Rosa26-mCherry construct. As anticipated from the flow cytometry data, DNA obtained from the mouse mCh27 revealed both a wild-type allele and a Rosa26-mCherry allele, Figure 3.37D, right lane), indicating that the spleen cells had retained the Rosa26-mCherry construct.

DNA isolated from the spleen was also used in a PCR to amplify the region containing the GFP construct. In contrast with the flow cytometry data, DNA obtained from mouse mCh27 showed that the GFP allele had a similar intensity as the sham-irradiated GFP allele (512 bp), indicating that the GFP construct was present as well (Figure 3.37E). In summary, mouse mCh27 was diagnosed with an increased WBC count (170 x $10^6$ cells/ml) and had a latency of 14.5 months following radiation exposure. Both the chromosome 2 homologue carrying the GFP construct and the homologue carrying the Rosa26-mCherry construct were retained, and a point mutation in exon 5 of the *Sfpi1* gene was identified. Similar to mCh240 and mCh68, this mouse developed most likely leukaemia with a lymphoid phenotype. In contrast with all previously described leukaemia's in this thesis, spleen cells of this mouse stained highly positive for the cell surface marker Flt3.

Thus far, we reported on the large rAML induction experiment where we exposed fifty female 10 week old *Sfpi1*$^{mCh/GFP}$ mice to a single acute 3 Gy whole body X-irradiation, and that seven out of eight female leukaemias had a lymphoid phenotype (i.e. CD31 and B220 expression by flow cytometry) with an average latency of 13 months follow radiation exposure. However, one female mouse presented with myeloid leukaemia following radiation exposure. We will discuss this further by looking into detail at the female mouse mCh82. At five months following radiation exposure, this mouse presented with outward physical signs of rAML (i.e. decreased activity and pallor). This mouse was then sacrificed and severe hepatosplenomegaly was observed upon opening the abdominal cavity (spleen weight 1,680 mg). Peripheral blood analysis showed a highly increased WBC count (420 x $10^6$ cells/ml), and a WBC population with increased size (i.e. higher FSC value) and increased granularity (i.e. higher SSC value) was observed by flow cytometry (Figure 3.38A; cells expressed mCherry and GFP).

A peripheral blood smear was also prepared. Nucleated cells were two-fold larger than red blood cells and had a varying degree of differentiation. Undifferentiated blast cells with several nucleoli were identified (Figure 3.38B, arrowhead), aside of neutrophilic myelocytes with a typical ringed nucleus (Figure 3.38B, arrow). Neutrophils were also present (Figure 3.38B, asterisk). Immunophenotyping of the spleen cells of this mouse showed that mCherry+GFP+ spleen cells expressed immaturity cell surface markers (i.e. cKit, Ly6c and CD31). Interestingly, the cells also expressed some mature, lineage-committed cell surface markers, such as Mac1 and Gr1 (Figure 3.38C), but not CD3 and B220 (summarised in Table 6 and Table 7, at the end of this section).

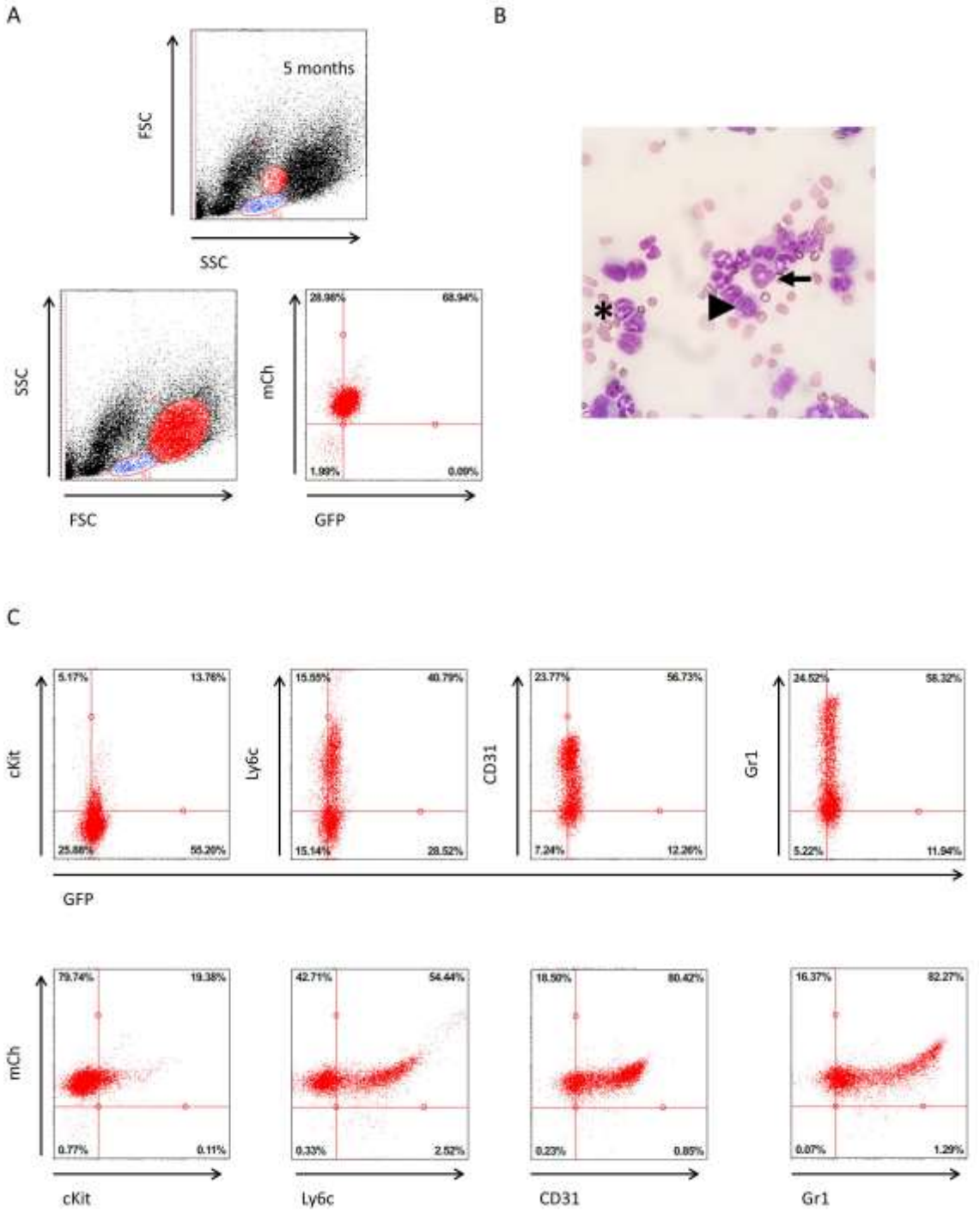



**Figure 3.38 mCh82 rAML characterisation**

At five months following radiation exposure, *Sfpi1*$^{mch/GFP}$ mouse mCh82 presented with outward physical signs of rAML and was sacrificed. (A) A single cell WBC suspension was prepared, and mCherry and GFP expression analysed by flow cytometry. (B) Peripheral blood smear. Undifferentiated blast cell with several nucleoli (arrowhead). Neutrophilic myelocyte with typical ringed nucleus (arrow). Neutrophil (asterisk). (C) A single cell spleen suspension was prepared, and cells were labelled with antibodies conjugated with PE. mCherry, GFP and cell surface marker expression were analysed by flow cytometry.

The point mutation status of *Sfpi1* exon 5 could not be assessed as the spleen was not stored properly. Similarly, the presence of the constructs by PCR was not assessed. To this end, frozen spleen cells of this mouse will have to be transplanted into CBA/Ca mice, and upon rAML presentation, the spleen could be used for DNA extraction.

**Table 6. Summary of leukaemic mice described above**

| | **mCh46.1** | **mCh50** | **mCh240** | **mCh68** | **mCh27** | **mCh82** |
|---|---|---|---|---|---|---|
| Gender | M | M | F | F | F | F |
| Latency (months) | 10.5 | 15.5 | 17 | 16 | 14.5 | 5 |
| WBC count ($x10^6$) | 90 | 41 | 270 | 144 | 170 | 420 |
| Spleen weight (mg) | 880 | 900 | 640 | 1,330 | 320 | 1,680 |
| Fluorescence loss? | mCherry | GFP | mCherry | GFP | no | no |
| Point mutation? | **T**GC | C**A**C | no | **T**GC | **T**GC | nd |

nd, not determined

**Table 7. Spleen cell surface marker expression of leukaemic mice**

| | **mCh46.1** | **mCh50** | **mCh240** | **mCh68** | **mCh27** | **mCh82** |
|---|---|---|---|---|---|---|
| Sca1 | - | - | - | + | + | - |
| cKit | + | + | - | + | + | + |
| Flt3 | - | - | - | - | + | - |
| Gr1 | - | - | - | - | - | + |
| Ly6c | + | + | - | - | - | + |
| Mac1 | - | - | - | - | - | + |
| CD31 | + | + | + | + | + | + |
| CD3 | - | - | - | - | - | - |
| B220 | - | - | + | + | + | - |

+, positive expression; -, no expression

### 3.4.4. Discussion

Exposure to high dose radiation exposure has been directly linked with increased AML incidence. However, the underlying mechanisms and the target cell for rAML development remain unidentified. Using the CBA mouse model, we assessed the changes taking place in the peripheral blood, from the time of radiation exposure until physical presentation with radiation-induced leukaemia. The CBA mouse strain was used because of its very low background leukaemia incidence, reproducible rAML induction (~20%) and the histopathological similarities with human myeloid leukaemia (Major, 1979). We used our newly engineered Chr2MDR$^{mCh}$ mice which have been generated on a CBA background and carry a Rosa26-mCherry construct on chromosome 2 within the MDR following radiation exposure. These mice were then crossed with homozygous *Sfpi1*$^{GFP}$ mice to generate offspring (*Sfpi1*$^{mCh/GFP}$ mice) that carry the GFP construct on one chromosome 2 homologue and the Rosa26-mCherry construct on the other homologue, allowing the detection of an interstitial deletion on either chromosome 2 homologue.

Firstly, we demonstrated by longitudinal blood sampling, that sham-irradiated *Sfpi1*$^{mCh/GFP}$ mice expressed mCherry in all peripheral blood WBCs and retained this expression throughout life. As GFP expression is under control of the *Sfpi1* promotor, lymphocytes did not express GFP (mCherry+GFP- cells) but myeloid cells did (mCherry+GFP+ cells). Interestingly, whereas the percentage of mCherry+GFP- cells decreased with age, the percentage of mCherry+GFP+ cells increased, indicating a decreased presence of lymphoid cells in the peripheral blood of ageing mice. This can be attributed to the fact that aged HSCs exhibit a markedly decreased output of lymphoid lineage cells, whereas the myeloid output of aged HSCs is maintained or

even increased compared with young HSCs (Pang et al., 2011). Sham-irradiated *Sfpi1*$^{mCh/GFP}$ mice had an average lifespan of 21 months and is similar to what has been previously reported for the CBA mouse strain (Storer, 1966).

Male *Sfpi1*$^{mCh/GFP}$ mice were exposed to single acute 3 Gy whole-body X-irradiation [i.e. the optimal rAML induction dose (Major and Mole, 1978)]. Tail vein blood samples were collected monthly [as recommended in the '*Bethesda proposals for classification of non-lymphoid haematopoietic neoplasms in mice*' (Kogan et al., 2002)], and mCherry and GFP expression was determined by flow cytometry. At 9 months following radiation exposure, one in three mice had mCherry- clonal expansion detectable in the peripheral blood. The percentage of mice with mCherry- clonal expansion increased further with time (46% at 18 months), and is in line with previously reported percentages of mice with a chromosome 2 aberrant clone in the bone marrow following 3 Gy radiation exposure (Bouffler et al., 1997). At 9 and 12 months following radiation exposure, all mice presenting with mCherry- clonal expansion in the peripheral blood had mCherry- myeloid and mCherry- lymphoid cells, indicating that the chromosome 2 deletion most likely occurred in a primitive haematopoietic cell type which can give rise to both lymphoid and myeloid progeny, such as the HSC or MPP population. We then confirmed our hypothesis that if both mCherry- lymphoid and mCherry- myeloid cells could be detected in the peripheral blood, the chromosome 2 interstitial deletion occurred in a haematopoietic stem cell, rather than in a lineage-committed haematopoietic cell type. To this end, we used the SLAM markers to identify HSCs (LSK CD48-CD150+; Kiel et al., 2005). A clearly identifiable mCherry- LSKCD48-CD150+ cell population in the haematopoietic stem and progenitor

fraction in the bone marrow can be detected in mice with mixed lineage mCherry- clonal expansion in the peripheral blood. It was also shown that these mice have mCherry- myeloid progenitors and mCherry- lymphoid progenitors in the bone marrow, based on differential CD127 expression in these cells (Kondo et al., 1997; Akashi et al., 2000), indicating that the HSC in which the chromosome 2 deletion occurred, gave rise to mCherry- daughter HSCs and also to more lineage-committed progeny, such as mCherry- CLPs and mCherry- CMPs.

However, at 15 months following radiation exposure, seven out of seventeen mice presenting with mCherry- clonal expansion in the peripheral blood, had mCherry- cells of the lymphoid lineage only, indicating that the chromosome 2 deletion in these mice most likely occurred in a haematopoietic cell type which can only give rise to lymphoid progeny, such as the common lymphoid progenitor. These mice had a different presentation in the haematopoietic stem and progenitor fraction, compared with mice with mixed lineage mCherry- clonal expansion. Although there was always a substantial percentage of mCherry- lymphoid cells in the peripheral blood, the percentage of mCherry- cells in the haematopoietic stem and progenitor fraction was only slightly higher than observed in sham-irradiated mice. Almost all mCherry- haematopoietic stem and progenitor cells were Sca1-cKit-, and no mCherry- HSCs/MPP were detectable, indicating that the chromosome 2 deletion most likely occurred in a lymphoid lineage-committed haematopoietic cell. We also assessed the cell surface marker expression on mCherry- peripheral blood WBCs and confirmed that these cells had a similar expression as mCherry+ WBCs, and did not express immaturity cells surface markers, such as Sca1 and cKit, indicating they have a normal WBC phenotype.

As the *Sfpi1* gene is located within the MDR following radiation exposure (Brown et al., 2015), and as an *Sfpi1* exon 5 point mutation is identified in the majority of murine rAMLs (Verbiest et al., 2015), we were interested to assess the *Sfpi1* expression on the intact chromosome 2 homologue upon deletion of the homologue carrying the Rosa26-mCherry construct. We were able to detect changes in *Sfpi1* expression as the GFP construct was designed in such a way that GFP expression was reflective of the *Sfpi1* expression (Nutt et al., 2005). We observed that GFP expression in mCherry- peripheral blood myeloid cells was 1.4-fold higher compared with GFP expression in mCherry+ cells, remained increased throughout life and was observed in each mouse with mCherry- peripheral blood granulocytes. As GFP expression is under control of the *Sfpi1* promotor, the increased GFP expression can be directly linked to increased activity of the *Sfpi1* promotor, indicating autoregulation of the *Sfpi1* expression (i.e. decreased *Sfpi1* levels are detected following chromosome 2 deletion, resulting in upregulation of the *Sfpi1* promotor). It has been reported previously that both the proximal promotor of *Sfpi1* and the URE have binding sites for *Sfpi1* itself (Chen et al., 1995; Okuno et al., 2005). Interestingly, the GFP expression of mCherry+ peripheral blood WBCs increased over time, indicating that the *Sfpi1* expression in peripheral blood myeloid cells increases when mice age. Autoregulation of *Sfpi1* expression was also observed in mCherry- haematopoietic stem and progenitor cells (i.e. increased GFP expression in bone marrow cells which lost the chromosome 2 homologue carrying the Rosa26-mCherry construct).

However, in some *Sfpi1*$^{mCh/GFP}$ mice with mCherry- clonal expansion in peripheral blood WBCs, the autoregulation of *Sfpi1* expression became dysregulated at some point

following radiation exposure. Whereas GFP expression in mCherry- WBCs was initially 1.4-fold increased, it decreased gradually over the course of several months, finally resulting in a GFP expression of mCherry- WBCs equal to GFP expression in mCherry+ cells. Interestingly, at this stage, no changes in the FSC/SSC plot of the peripheral blood could be detected, indicating the cells did not change in size or granularity. However, four weeks following GFP expression in mCherry- cells reaching background levels (i.e. no longer upregulated expression compared with mCherry+ cells, so no increased *Sfpi1* promotor activity anymore), the percentage of mCherry- peripheral blood WBCs had increased dramatically and a change in the FSC/SSC plot could be detected. Two weeks later, the vast majority of peripheral blood WBCs were mCherry-, and the mouse presented with outward physical signs of rAML. The time from appearance in the peripheral blood to the mouse becoming moribund was less than four weeks and is consistent with the defining criteria for non-lymphoid leukaemia's set out in the '*Bethesda proposals for classification of non-lymphoid haematopoietic neoplasms in mice*' (Kogan et al., 2002). Similarly, immunophenotyping showed that mCherry- spleen cells had an immature phenotype consistent with myeloid leukaemia presentation, and myeloblasts and myelocytes were observed on peripheral blood smear examination. We also confirmed that the Rosa26-mCherry construct was physically lost in mCherry- leukaemic spleen cells, and that the *Sfpi1* copy on the other chromosome 2 homologue carried a point mutation replacing the amino acid arginine 235 with cysteine [C to T substitution, the most common *Sfpi1* point mutation observed in murine rAMLs (Steffen et al., 2013)]. Our experimental observations are consistent with the two-hit model of murine radiation leukaemogenesis in which the first irreversible mutational hit (i.e. interstitial deletion of one *Sfpi1* gene on

chromosome 2) creates intermediate cells that have a growth advantage, but are not fully malignant. Subsequently, intermediate cells acquire a second mutational hit (i.e. point mutation in the remaining *Sfpi1* copy), resulting in the formation of a malignant cell which undergoes further clonal expansion and eventually develops into cancer (Dekkers et al., 2011). However, it remains to be determined at what time after irradiation this point mutation takes place. It could be hypothesised that the point mutation occurs at the time when the GFP levels start to return to 'normal' levels (i.e. as in mCherry+ cells), possibly linking the occurrence of the point mutation with loss of *Sfpi1* autoregulation. Preliminary data obtained from terminal peripheral blood samples of six irradiated mice with mCherry- peripheral blood WBCs, revealed that all six mice had the point mutation present in the peripheral blood (4 – 18% of WBCs had the C to T substitution). In contrast, terminal blood samples of irradiated mice without mCherry- peripheral blood WBCs did not harbour the point mutation. Similarly, terminal blood samples of sham-irradiated mice had no detectable C to T substitution. In addition, we detected the point mutation in the mCherry- haematopoietic stem and progenitor cell fraction of the bone marrow of mice with mCherry- peripheral blood WBCs, but not in the mCherry+ haematopoietic stem and progenitor cell fraction of the bone marrow of these mice. These observations link, for the first time, the occurence of the point mutation to a prior presence of the chromosome 2 deletion.

There are data suggesting that the point mutation probably leads to complete abolition of *Sfpi1* activity (Metcalf et al., 2006). This is further supported by our preliminary finding that genetically engineered mice carrying a *Sfpi1* point mutation on both alleles die during late gestation (substitution with thymine of the first cytosine of

the CGC sequence in exon 5, replacing the amino acid residue arginine 235 with cysteine), indicating the importance of the DNA binding domain in *Sfpi1* functioning (unpublished observations). Similarly, we observed rAMLs which had an interstitial deletion of the chromosome 2 homologue carrying the GFP construct. The overall male rAML incidence was 17% (11 rAMLs out of 64 male irradiated *Sfpi1*$^{mCh/GFP}$ mice) with an average latency of 13 months following radiation exposure, which is consistent with previous work in male CBA mice (Major, 1979; Weil et al., 2009; Olme et al., 2013b).

We also investigated the leukaemia progression and incidence in female *Sfpi1*$^{mCh/GFP}$ mice. At 12 months following radiation exposure, one in three female mice presented with mCherry- clonal expansion of peripheral blood WBCs, a similar number as we observed in male mice. Similar to male mice as well, the percentage of female mice with mCherry- clonal expansion increased further over time, to reach 100% 21 months following radiation exposure. However, a clear difference in the cell of origin of the mCherry- clonal expansion was detectable. At 12 months following radiation exposure, 33% of the female mice with mCherry- clonal expansion had mCherry- lymphoid WBCs only, this percentage increased further to 100% at 21 months following radiation exposure. In contrast, the majority of male mice developed mixed lineage mCherry- clonal expansion (i.e. both mCherry- myeloid and mCherry- lymphoid cells) following radiation exposure.

Eight of the forty-eight female mice developed leukaemia following radiation exposure (17%, a similar percentage compared to male mice). Also the average latency was similar to that observed in male mice (i.e. 13 months following radiation exposure). In contrast with 100% of leukaemia's in male mice being of myeloid origin (i.e. AML), only

one of the eight female leukaemia's had a myeloid phenotype, the other seven female mice had leukaemia with a lymphoid phenotype (i.e. CD31 and B220 expression by flow cytometry). Interestingly, the female mouse with rAML had a much shorter latency compared with male rAMLs (5 and 13 months following radiation exposure, respectively) and it did not exhibit a chromosome 2 deletion, as assessed by flow cytometry for loss of GFP or mCherry expression. It could therefore be hypothesised that the target cell differs between male and female mice (HSC and CLP, respectively). Interestingly, Iwasaki and colleagues reported that *Sfpi1*-knockout in lymphoid progenitors did not alter the maturation or proliferation of B-cells (Iwasaki et al., 2005), which could possibly explain why female leukaemia's have a mature B-cell phenotype (i.e. B-cell expression by flow cytometry; Table 7). On the other hand, *Sfpi1*-knockout in myeloid progenitors inhibited their maturation but not their proliferation, and is consistent with the immature myeloid phenotype observed in our male AMLs.

Although the female leukaemia's phenotypically differ from male mice (i.e. only one out of eight female leukaemia's is of myeloid origin), the underlying mechanism of radiation leukaemogenesis in female mice does not seem to differ from the one observed in male leukaemic mice (i.e. one chromosome 2 homologue has an interstitial deletion with *Sfpi1* loss and the other homologue carries a *Sfpi1* point mutation). Similar to the leukaemia's observed in male mice, we observed female leukaemia's with an interstitial deletion on the chromosome homologue carrying the Rosa26-mCherry construct, and also female leukaemia's with a deletion on the homologue carrying the GFP construct. We also identified one female leukaemia were both the GFP construct and Rosa26-mCherry construct were retained, indicating no

interstitial chromosome 2 deletion occurred. In male mice, a minority of rAMLs do not carry a chromosome 2 deletion (Rithidech et al., 1993; Bouffler et al., 1996; Hirouchi et al., 2008; Steffen et al., 2013). Our group previously identified that 43% of rAMLS without a chromosome 2 deletion and without a *Sfpi1* point mutation, present with *Flt3*-ITD mutations (Finnon et al., 2012). However, we did not identify Flt3-ITD mutations in this mouse.

Similar to our findings, reported AML incidences are higher among irradiated male mice than irradiated female mice (Upton et al., 1960; Yoshida et al., 1993; Di Majo et al., 1996; Olme et al., 2013b). As an intrinsic radiosensitivity difference in male versus female haematopoietic cells is highly unlikely, sex hormones might play a pivotal role in gender differences in leukaemogenesis. This hypothesis is further supported by the finding that castration does not affect the rAML incidence, whereas ovariectomy resulted in a two-fold increase in leukaemia incidence. Interestingly, gonadectomy did not alter leukaemia incidence in unexposed mice (Upton, 2008). It was also shown that binding of oestrogen to the HSC oestrogen receptor α enhances HSC self-renewal by upregulation of cell cycle gene expression (Nakada et al., 2014). Similarly, the follow-up of the atomic bomb survivors reported the baseline AML rate for Japanese women to be approximately 40% of this of men, and male atomic bomb survivors displayed a more rapid rate of increased AML incidence with attained age (Hsu et al., 2013), but beyond this, the effect of sex hormones on leukaemogenesis is not clearly understood.

In conclusion, by assimilating the experimental data presented here, it is possible to suggest a schematic representing the different pathways (Figure 3.39 and Figure 3.40).

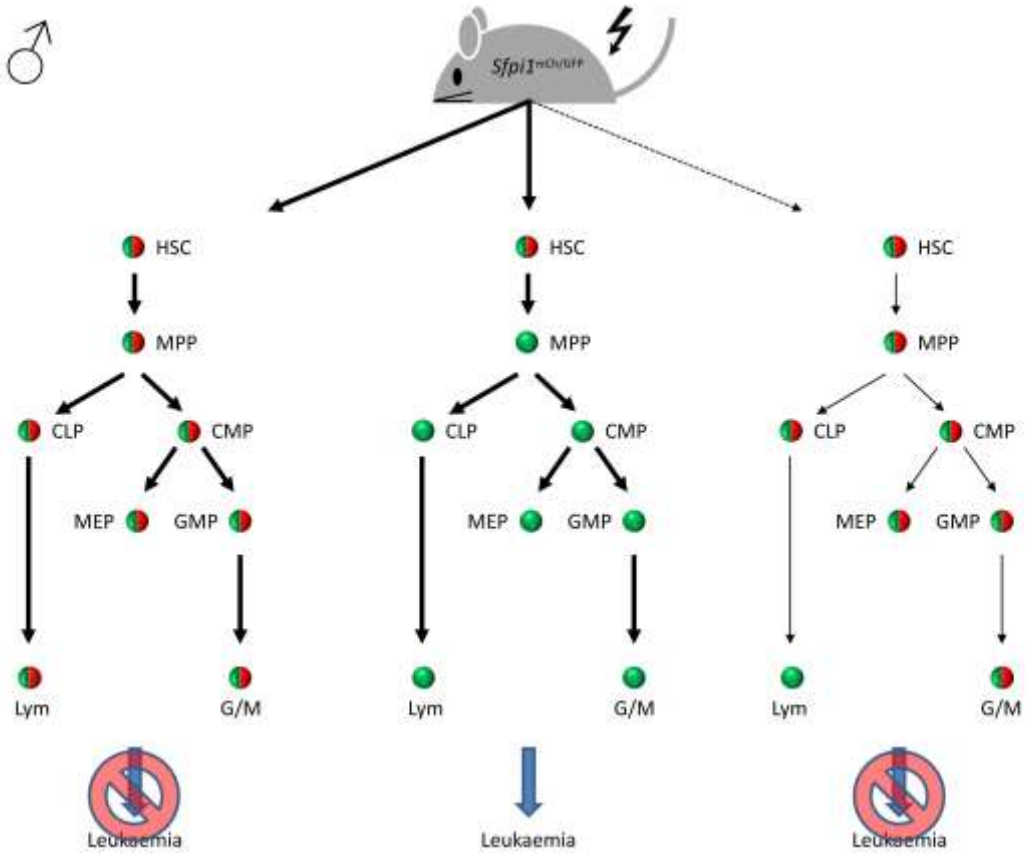



**Figure 3.39 Different pathways observed in male mice following radiation exposure**

Following 3 Gy whole-body X-irradiation of male *Sfpi1*$^{mCh/GFP}$ mice, two main pathways could be observed: mice which retained mCherry expression in all haematopoietic cells, and never developed leukaemia (left panel), and mice which lost mCherry expression in a HSC, resulting in mCherry- peripheral blood granulocytes (G), monocytes (M) and lymphocytes (Lym). Some of these mice developed leukaemia later in life (middle panel). A minority of mice lost mCherry expression in a CLP, resulting in mCherry- peripheral blood lymphocytes. Interestingly, these mice never developed leukaemia (right panel).

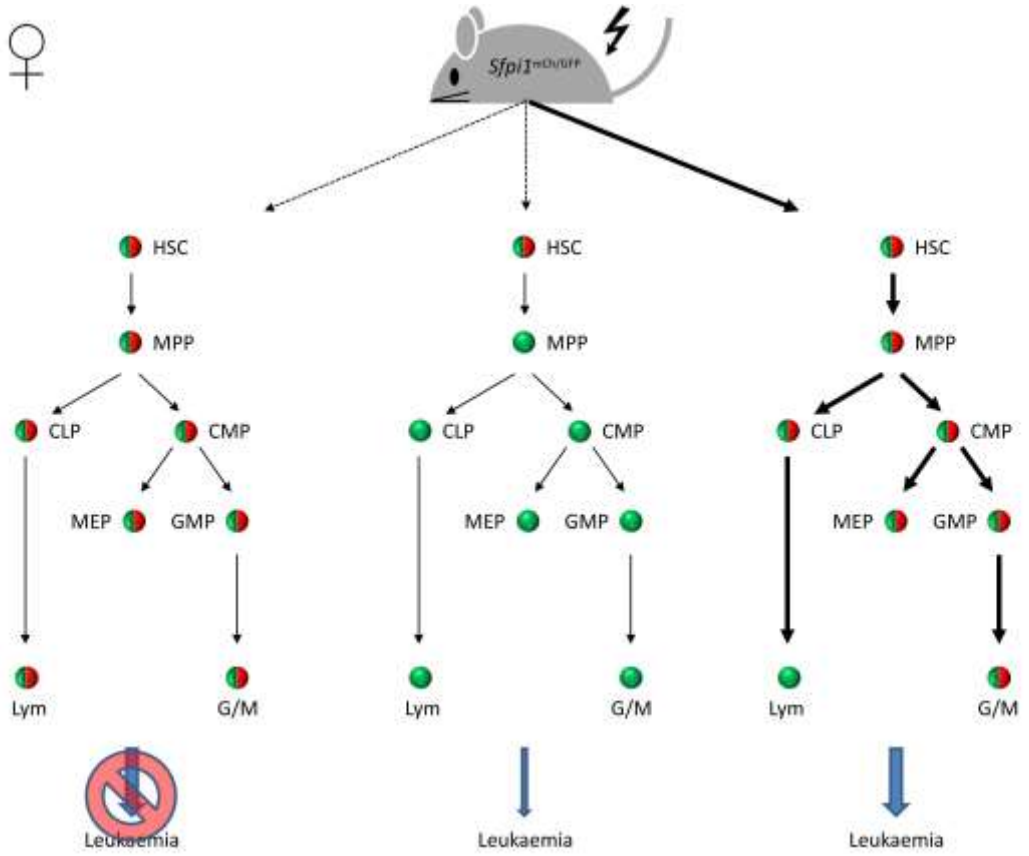



**Figure 3.40 Different pathways observed in female mice following radiation exposure**

Following 3 Gy whole-body X-irradiation of female *Sfpi1*$^{mCh/GFP}$ mice, the vast majority of mice lost mCherry expression in a CLP, resulting in mCherry- peripheral blood lymphocytes (Lym). Some of these mice developed leukaemia later in life (right panel). The remaining mice either retained mCherry expression in all haematopoietic cells throughout life, and never developed leukaemia (left panel), or lost mCherry expression in a HSC, resulting in mCherry- peripheral blood granulocytes (G), monocytes (M) and lymphocytes. Only one of these mice developed leukaemia (middle panel).

# CHAPTER 4

*General discussion and conclusion*

# 4. General discussion and conclusion

## 4.1. General discussion

Over the past three decades, low dose radiation exposure in humans increased nearly two-fold, and can be mainly attributed to a six-fold increase in exposure from medical sources (Brenner and Hall, 2007). Whereas it has long been acknowledged that moderate to high dose radiation exposure significantly increases cancer incidence, both for leukaemia and solid cancer, estimating carcinogenic risk following low dose exposure remains problematic. However, over the past five years, a variety of epidemiological studies of human cohorts exposed to low dose ionising radiation, provided clear evidence for a direct association between low dose radiation exposure and leukaemia. Firstly, it was reported that the overall cancer incidence was 24% greater for people exposed to computed tomography scans in their childhood than for unexposed children. The incidence rate ratio increased significantly for leukaemia and many types of solid cancer (Mathews et al., 2013). Another study into low dose medical radiation exposure reported that computed tomography scans in children delivering cumulative doses of approximately 50 mGy almost tripled the risk of developing leukaemia later in life (Pearce et al., 2012). Similarly, positive associations between protracted low dose radiation exposure and leukaemia have been reported in radiation-monitored workers (Leuraud et al., 2015) and human cohorts born in areas with high natural background radiation (Kendall et al., 2013; Spycher et al., 2015). Although a clear association is postulated, the currently available experimental models (such as bone marrow transplantation assays following prior conditioning) do not allow a detailed assessment of the effects of low dose radiation exposure on haematopoiesis in a biologically relevant microenvironment.

Following the observation of an intrinsic defect in the maintenance of *scid* HSCs which facilitated allogeneic HSC transplantation without prior conditioning (Qing et al., 2012), we hypothesised that NSG mice, a strain not susceptible to thymic lymphoma development but also harbouring the *scid* mutation (Ishikawa et al., 2005), could prove a suitable novel experimental mouse model to study the long-term effects of low dose radiation exposure on HSCs. Initially, we showed that six months following transplantation of *Sfpi1*$^{GFP}$ haematopoietic stem and progenitor cells into nonmyeloablated NSG mice, multilineage chimerism can be observed in peripheral blood, spleen and bone marrow. The fact that from five months following transplantation, haematopoiesis is entirely dependent on long-term HSC activity (Marusyk et al., 2009), led us to conclude that transplanted HSCs competed for the niches in the nonmyeloablated NSG bone marrow compartment and that the nonmyeloablated NSG bone marrow microenvironment was capable of supporting allogeneic long-term HSC engraftment and differentiation.

This first time observation of NSG mice being permissive to allogeneic HSC transplantation without prior conditioning could be a valuable tool to study the molecular basis of HSC transplantation in a more biologically relevant microenvironment and could prove useful to quantify the effects of environmental factors (such as benzene exposure), drug interactions, etc on the efficiency of bone marrow transplantation without the need for prior conditioning and the subsequent profound alterations to the bone marrow microenvironment. Similarly, it can also be applied in experiments to test novel strategies to increase the engraftment efficiency following HSC transplantation.

GFP expression in the *Sfpi1*$^{GFP}$ mouse model is under control of the *Sfpi1* promotor (Nutt et al., 2005) which results in GFP$^{neg}$ T-cell and GFP$^{low}$ B-cell progeny of transplanted GFP$^{high}$ HSCs, therefore, using GFP as a marker of chromosome 2 presence is not ideal. To overcome this, we designed a novel mouse model where the fluorescent marker mCherry is under control of the Rosa26 promotor and is located within the MDR following radiation exposure (i.e. Chr2MDR$^{mCh}$ mice). mCherry was constitutively expressed in all haematopoietic Chr2MDR$^{mCh}$ cell types, from primitive HSCs to terminally-differentiated lymphocytes and monocytes, and expression was retained throughout life.

The novel Chr2MDR$^{mCh}$ mouse model has proven to be of use to assess the long-term effects of *in vivo* low and high dose radiation exposure on haematopoiesis following transplantation of Chr2MDR$^{mCh}$ haematopoietic stem and progenitor cells into nonmyeloablated NSG mice. Six months following transplantation, a dose-dependent decrease in mCherry chimerism in peripheral blood and bone marrow was detectable. Interestingly, within the mCherry+ haematopoietic stem and progenitor cells, a dose-dependent Sca1 upregulation was detectable. In contrast, Sca1 expression in host NSG cells remained unchanged for all doses. Sca1 upregulation following radiation exposure has been previously reported, however Sca1 expression returned to pre-exposure levels 7 days following radiation exposure (Simonnet et al., 2009; Vazquez et al., 2015). Six months following secondary transplantation of mCherry+Sca1 haematopoietic stem and progenitor cells, mCherry+ multilineage chimerism was only detected in secondary NSG mice injected with cells obtained from primary NSG mice transplanted with 0 or

0.01 Gy irradiated cells, but not in secondary NSG mice injected with cells obtained from primary NSG mice injected with 0.1 or 1 Gy irradiated cells.

Radiation exposure did not alter the percentage of HSCs at the time of primary transplantation, except for 1 Gy irradiated Chr2MDR$^{mCh}$ mice which led us to postulate that following low dose radiation exposure the underlying mechanism of reduced donor HSC contribution had to be identified at a cellular level. We did not identify changes in HSC mitochondrial mass, mitochondrial ROS levels or mitochondrial membrane potential at seven days following low dose radiation exposure. However, mitochondrial ROS levels were significantly enhanced seven days following 1 Gy radiation exposure which is in line with a previous study were the persistent decline in HSC fitness following 5 Gy radiation exposure could partially be attributed to a persistent induction of reactive oxygen species (Marusyk et al., 2009). *Gadd45* gene expression, which has been linked with increased HSC differentiation following genotoxic stress (Wingert et al., 2016), was not significantly different for any of the doses at seven days following radiation exposure. Similarly, *Sfpi1* gene expression did not differ. The LSK cell cycle was not altered either, with the vast majority of cells residing in a quiescent state.

We propose to verify our finding of reduced mCherry+ chimerism following low dose radiation exposure by transplanting mCherry+ CD27+CD201+ HSCs (rather than mCherry+ haematopoietic stem and progenitor cells) and assessing the number of mCherry+ CD27+CD201+ HSCs at six months following transplantation. If a dose-dependent reduction in the number of mCherry+ HSCs can be detected at six months, a compromised HSC homing could be at the basis of our observation of reduced

chimerism following low dose radiation exposure. However, if a similar number of mCherry+ HSCs can be detected six months following transplantation, independent of the radiation dose, a radiation-induced intrinsic HSC defect is more likely.

We also assessed the changes taking place in the haematopoietic system between radiation exposure and the physical presentation with leukaemia. Previously, mice had to be sacrificed and bone marrow cells fixed after which *Sfpi1* loss could be assessed by FISH (Bouffler et al., 1997; Peng et al., 2009), resulting in a substantial use of mice and a loss of valuable information as it did not allow longitudinal tracking of chromosome 2 deleted cells over time. Using the *Sfpi1*$^{mCh/GFP}$ mouse model, we could for the first time detect an interstitial chromosome 2 deletion in live haematopoietic cells and track these cells over time, as the Rosa26-mCherry construct or GFP construct was deleted simultaneously, and a change in fluorescence was detectable.

Monthly blood sampling of 3 Gy irradiated male *Sfpi1*$^{mCh/GFP}$ mice provided novel insights into leukaemia progression and presentation following radiation exposure. Firstly, it was observed that the percentage of mice with mCherry- clonal expansion in peripheral blood WBCs increased with time and reached 100% at 21 months following radiation exposure. Interestingly, the phenotype of the mCherry- clonal expansion changed over time: whereas at 9 months mice presented with mixed lineage mCherry- clonal expansion only, the percentage of mice with lymphoid mCherry- clonal expansion increased over time to reach 100% of mice having lymphoid mCherry- clonal expansion at 21 months following radiation exposure. Longitudinal blood sampling allowed for the first time a continuous assessment of the changes following chromosome 2 deletions and the progression to overt leukaemia. We detected an

increased GFP expression following radiation-induced deletion of the Rosa26-mCherry construct which led us to postulate that *Sfpi1* expression is autoregulated, and is in line with previous reports that both the proximal promotor of *Sfpi1* and the URE have binding sites for *Sfpi1* itself (Chen et al., 1995; Okuno et al., 2005). Only when *Sfpi1* expression was no longer upregulated (i.e. detected as identical GFP levels in mCherry- cells compared to mCherry+ cells), changes in WBC size and granularity could be detected in the peripheral blood. These changes in peripheral blood could be detected each time two to four weeks before the mouse presented with outward physical signs of AML. Only acute myeloid leukaemias were observed with an average latency of 13 months between radiation exposure and rAML presentation (17% of mice). Notably, these numbers are subject to change as the remaining 37 male mice age and potentially develop leukaemia (or are humanely sacrificed). The myeloid leukaemias we observed in our study were consisted with the two-hit model previously postulated (Dekkers et al., 2011): firstly an interstitial chromosome 2 deletion occurs accompanied by loss of *Sfpi1* and the Rosa26-mCherry or GFP construct, followed by a point mutation in the remaining *Sfpi1* copy.

The vast majority of leukaemia induction experiments have been performed using male mice only (Major, 1979; Mole et al., 1983; Di Majo et al., 1986; Rithidech et al., 1993; Alexander et al., 1995; Fennelly et al., 1995; Rithidech et al., 2002; Cook et al., 2004; Hirouchi et al., 2008; Steffen et al., 2013). The very limited number of studies which did include female mice, consistently reported a lower AML incidence in female mice (Upton et al., 1960; Yoshida et al., 1993; Olme et al., 2013b). However, an increased leukaemia incidence for both men and women is reported in the atomic

bomb survivors (Hsu et al., 2013). Therefore, we similarly assessed the changes taking place in the haematopoietic system between radiation exposure of female *Sfpi1*$^{mCh/GFP}$ mice and the physical presentation with leukaemia.

We identified female mice with lymphoid mCherry- clonal expansion as early as 9 months following radiation exposure, and from 15 months, the number of female mice with lymphoid mCherry- clonal expansion was greater than the number of female mice with mixed lineage mCherry- clonal expansion. In line with the above-mentioned studies, we diagnosed only one female mouse with rAML. Our first time observation that the majority of female mice has lymphoid, rather than mixed lineage mCherry- clonal expansion provides a partial explanation for the lower rAML presentation observed in female mice compared with male mice. However, seven female mice developed leukaemia with a lymphoid phenotype. A potential explanation lies within the observation that in mice with mixed lineage mCherry- clonal expansion, mCherry- HSCs were consistently observed. However, in mice with lymphoid mCherry- clonal expansion, although all HSCs had retained mCherry expression, mCherry- common lymphoid progenitors could be identified. Possibly a gender-specific radiation-induced chronic expression of pro-inflammatory cytokines is involved. For example, it was previously reported that interleukin-1 drives HSCs towards myeloid differentiation at the expense of self-renewal (Pietras et al., 2016).

## 4.2. Conclusion

The overall aim of the doctoral research presented here was to identify and characterise the haematopoietic stem and progenitor cells at risk for leukaemia development following radiation exposure. In the first part of the thesis, the main objective was to identify a novel experimental mouse model with a biologically relevant microenvironment which would allow a detailed assessment of the haematological risks associated with low dose radiation exposure. We demonstrated for the first time that allogeneic HSCs from a different inbred strain can compete for the niches in the bone marrow compartment of nonmyeloablated NSG mice and that the nonmyeloablated NSG bone marrow microenvironment is capable of supporting allogeneic long-term HSC engraftment and differentiation. Following the generation of a novel genetically engineered mouse model (i.e. Chr2MDR$^{mCh}$ mice) where the fluorescent marker mCherry is under control of the Rosa26 promotor and is located within the MDR following radiation exposure, we established that *in vivo* exposure to 0.1 Gy radiation exposure (i.e. the equivalent of four positron emission tomography – computed tomography scans) significantly reduces the contribution of irradiated HSCs towards long-term haematopoiesis in nonmyeloablated NSG mice.

The second part of the thesis reports on the changes taking place in the haematopoietic system following high dose radiation exposure up until the moment of overt AML presentation. We identified that upon an interstitial deletion of chromosome 2 including one copy of *Sfpi1*, the activity of the remaining *Sfpi1* promotor increases in both peripheral blood and bone marrow cells. However, this autoregulatory mechanism becomes occasionally dysregulated several months

following radiation exposure (possibly at the time where the point mutation occurs), after which changes in size and granularity become detectable in the peripheral blood WBCs and mice eventually present with leukaemia. Interestingly, progression towards radiation-induced leukaemia occurred in a gender-dependent manner. Whereas male mice developed acute myeloid leukaemia, only a small subset of female mice developed leukaemia with a myeloid phenotype. The vast majority of female mice which developed leukaemia had a lymphoid phenotype which was consistent with the observation that the majority of female mice had lymphoid rather than mixed lineage mCherry- clonal expansion in the peripheral blood. Future studies should take advantage of this difference to further uncover the underlying molecular mechanisms of radiation-induced leukaemia.

# CHAPTER 5

*Future directions*

## 5. Future directions

It will be of utmost importance to confirm the finding that *in vivo* exposure to low dose radiation exposure significantly reduces the contribution of irradiated HSCs towards long-term haematopoiesis in nonmyeloablated NSG mice and to identify the underlying mechanisms, especially in the light of the increased exposure to low dose radiation from medical sources (such as computed tomography scans). Similarly, it is needed to determine if there is a lower limit at which a reduction can still be detected, as we observed reduced contribution following radiation exposure as low as 0.01 Gy (although not statistically different from sham-irradiated mice). Although 0.1 Gy is considered the highest 'low dose' exposure, the effective dose protracted from a chest computed tomography scan is just under 0.01 Gy (i.e. 7 mGy)(McCollough et al., 2015). From a radiation protection perspective, it is therefore advised to carry on adhering to the 'As Low As Reasonably Achievable' radiation safety principle.

The *Sfpi1*$^{mCh/GFP}$ mouse model allowed a detailed investigation of the initiating step of radiation leukaemogenesis, and revealed a gender-dependent progression following radiation exposure. However, the vast majority of rAMLs has, aside of the interstitial chromosome 2 deletion, a point mutation in the remaining *Sfpi1* copy, which was previously postulated as the two-hit model (Dekkers et al., 2011). The design of our study did not allow to determine at what time after radiation the point mutation occurs, and warrants further investigation. As we observed a dysregulation of *Sfpi1* upregulation following chromosome 2 deletion several months before progression to overt leukaemia, it will be of great use to assess whether the point mutation is already present at that time or only occurs at a much later stage. As terminal blood samples of

each *Sfpi1*$^{mCh/GFP}$ mouse have been stored at -80 °C, we could determine if the point mutation is present in aged sham-irradiated mice. Similarly, we could compare the point mutation status in samples with mixed lineage clonal expansion and samples with lymphoid clonal expansion, and this at various stages of progression. Finally, the observation of a gender-dependent leukaemia progression following radiation exposure warrants further investigation.

To further define how *Sfpi1* functions as a tumour suppressor in rAML, our group recently generated a *Sfpi1* point mutation mouse model. The *Sfpi1* point mutation (*Sfpi1*$^{pm}$) comprises a C to T substitution in the PU.1 DNA binding domain (R235) and is the most common base transition observed in murine rAML. Preliminary results show that homozygous *Sfpi1*$^{pm}$ mice die during late gestation, indicating the importance of the DNA binding domain in *Sfpi1* functioning. Interestingly, heterozygous *Sfpi1*$^{pm}$ mice develop spontaneous AML (unpublished observations). In-depth analysis is on-going to investigate the impact of this point mutation on haematopoiesis and (radiation) leukaemogenesis. Furthermore, gene expression analysis in pre-leukaemic and AML populations of *Sfpi1*-knock-down models would aid deciphering the specific changes leading to leukaemia. Consequently, analysis of global PU.1 DNA binding via ChIP-sequencing in normal haematopoietic progenitors and AML cells would further clarify the impact of reduced PU.1 activity on target gene regulation. The identification of biomarkers for PU.1 downregulation would greatly aid our understanding of how this event facilitates leukaemogenesis. Therefore, we suggest that, in future studies, the levels of PU.1 expression in human primary and therapy-related AML are carefully monitored.

# CHAPTER 6

*References*

## 6. References


Akashi, K., Traver, D., Miyamoto, T., Weissman, I.L., 2000. A clonogenic common myeloid progenitor that gives rise to all myeloid lineages. Nature 404, 193–197. doi:10.1038/35004599

Alexander, B.J., Rasko, J.E., Morahan, G., Cook, W.D., 1995. Gene deletion explains both in vivo and in vitro generated chromosome 2 aberrations associated with murine myeloid leukemia. Leukemia 9, 2009–2015.

Azzam, E.I., Jay-Gerin, J.P., Pain, D., 2012. Ionizing radiation-induced metabolic oxidative stress and prolonged cell injury. Cancer Lett. 327, 48–60. doi: 10.1016/j.canlet.2011.12.012

Ban, N., Kai, M., 2009. Implication of replicative stress-related stem cell ageing in radiation-induced murine leukaemia. Br. J. Cancer 101, 363–371. doi:10.1038/sj.bjc.6605135

Basova, P., Pospisil, V., Savvulidi, F., Burda, P., Vargova, K., Stanek, L., Dluhosova, M., Kuzmova, E., Jonasova, A., Steidl, U., Laslo, P., Stopka, T., 2013. Aggressive acute myeloid leukemia in PU.1/p53 double-mutant mice. Oncogene. doi:10.1038/onc.2013.414

Bonadies, N., Neururer, C., Steege, A., Vallabhapurapu, S., Pabst, T., Mueller, B.U., 2010. PU.1 is regulated by NF-kappaB through a novel binding site in a 17 kb upstream enhancer element. Oncogene 29, 1062–1072. doi:10.1038/onc.2009.371

Bonadies, N., Pabst, T., Mueller, B.U., 2010. Heterozygous deletion of the PU.1 locus in human AML. Blood 115, 331–334. doi:10.1182/blood-2009-03-212225

Bouffler, S.D., Meijne, E.I., Huiskamp, R., Cox, R., 1996. Chromosomal abnormalities in neutron-induced acute myeloid leukemias in CBA/H mice. Radiat. Res. 146, 349–352.

Bouffler, S.D., Meijne, E.I., Morris, D.J., Papworth, D., 1997. Chromosome 2 hypersensitivity and clonal development in murine radiation acute myeloid leukaemia. Int. J. Radiat. Biol. 72, 181–189.

Brehm, M.A., Racki, W.J., Leif, J., Burzenski, L., Hosur, V., Wetmore, A., Gott, B., Herlihy, M., Ignotz, R., Dunn, R., Shultz, L.D., Greiner, D.L., 2012. Engraftment of human HSCs in nonirradiated newborn NOD-scid IL2rγ null mice is enhanced by transgenic expression of membrane-bound human SCF. Blood 119, 2778–2788. doi:10.1182/blood-2011-05-353243

Brenner, D.J., Hall, E.J., 2007. Computed Tomography — An Increasing Source of Radiation Exposure. N. Engl. J. Med. 357, 2277–2284. doi:10.1056/NEJMra072149

Brown, N., Finnon, R., Manning, G., Bouffler, S., Badie, C., 2015. Influence of radiation quality on mouse chromosome 2 deletions in radiation-induced acute myeloid leukaemia. Mutat. Res. Genet. Toxicol. Environ. Mutagen. 793, 48–54. doi:10.1016/j.mrgentox.2015.07.012

Brown, N.L., Finnon, R., Bulman, R.A., Finnon, P., Moody, J., Bouffler, S.D., Badie, C., 2011. Sfpi1/PU.1 mutations in mouse radiation-induced acute myeloid leukaemias affect mRNA and protein abundance and associate with disrupted transcription. Leuk. Res. 35, 126–132. doi:10.1016/j.leukres.2010.06.015

Cancer Genome Atlas Research Network, 2013. Genomic and epigenomic landscapes of adult de novo acute myeloid leukemia. N. Engl. J. Med. 368, 2059–2074. doi:10.1056/NEJMoa1301689

Carotta, S., Dakic, A., D'Amico, A., Pang, S.H.M., Greig, K.T., Nutt, S.L., Wu, L., 2010. The transcription factor PU.1 controls dendritic cell development and Flt3 cytokine receptor expression in a dose-dependent manner. Immunity 32, 628–641. doi:10.1016/j.immuni.2010.05.005

Chen, H., Ray-Gallet, D., Zhang, P., Hetherington, C.J., Gonzalez, D.A., Zhang, D.E., Moreau-Gachelin, F., Tenen, D.G., 1995. PU.1 (Spi-1) autoregulates its expression in myeloid cells. Oncogene 11, 1549–1560.

Chua, H.L., Plett, P.A., Sampson, C.H., Joshi, M., Tabbey, R., Katz, B.P., MacVittie, T.J., Orschell, C.M., 2012. Long-Term Hematopoietic Stem Cell Damage in a Murine Model of the Hematopoietic Syndrome of the Acute Radiation Syndrome: Health Phys. 103, 356–366. doi:10.1097/HP.0b013e3182666d6f

Cleary, H., Boulton, E., Plumb, M., 2001. Allelic loss on chromosome 4 (Lyr2/TLSR5) is associated with myeloid, B-lympho-myeloid, and lymphoid (B and T) mouse radiation-induced leukemias. Blood 98, 1549–1554.

Cook, W.D., McCaw, B.J., Herring, C., John, D.L., Foote, S.J., Nutt, S.L., Adams, J.M., 2004. PU.1 is a suppressor of myeloid leukemia, inactivated in mice by gene deletion and mutation of its DNA binding domain. Blood 104, 3437–3444. doi:10.1182/blood-2004-06-2234

Corces-Zimmerman, M.R., Majeti, R., 2014. Pre-leukemic evolution of hematopoietic stem cells: the importance of early mutations in leukemogenesis. Leukemia 28, 2276–2282. doi:10.1038/leu.2014.211

Curik, N., Burda, P., Vargova, K., Pospisil, V., Belickova, M., Vlckova, P., Savvulidi, F., Necas, E., Hajkova, H., Haskovec, C., Cermak, J., Krivjanska, M., Trneny, M., Laslo, P., Jonasova, A., Stopka, T., 2012. 5-azacitidine in aggressive myelodysplastic syndromes regulates chromatin structure at PU.1 gene and cell differentiation capacity. Leukemia 26, 1804–1811. doi:10.1038/leu.2012.47

Dahl, R., Walsh, J.C., Lancki, D., Laslo, P., Iyer, S.R., Singh, H., Simon, M.C., 2003. Regulation of macrophage and neutrophil cell fates by the PU.1:C/EBPalpha ratio and granulocyte colony-stimulating factor. Nat. Immunol. 4, 1029–1036. doi:10.1038/ni973

Dakic, A., Metcalf, D., Di Rago, L., Mifsud, S., Wu, L., Nutt, S.L., 2005. PU.1 regulates the commitment of adult hematopoietic progenitors and restricts granulopoiesis. J. Exp. Med. 201, 1487–1502. doi:10.1084/jem.20050075

Dakic, A., Wu, L., Nutt, S.L., 2007. Is PU.1 a dosage-sensitive regulator of haemopoietic lineage commitment and leukaemogenesis? Trends Immunol. 28, 108–114. doi:10.1016/j.it.2007.01.006

Darakhshan, F., Badie, C., Moody, J., Coster, M., Finnon, R., Finnon, P., Edwards, A.A., Szluinska, M., Skidmore, C.J., Yoshida, K., Ullrich, R., Cox, R., Bouffler, S.D., 2006. Evidence for complex multigenic inheritance of radiation AML susceptibility in mice revealed using a surrogate phenotypic assay. Carcinogenesis 27, 311–318. doi:10.1093/carcin/bgi207

Dekkers, F., Bijwaard, H., Bouffler, S., Ellender, M., Huiskamp, R., Kowalczuk, C., Meijne, E., Sutmuller, M., 2011. A two-mutation model of radiation-induced

acute myeloid leukemia using historical mouse data. Radiat. Environ. Biophys. 50, 37–45. doi:10.1007/s00411-010-0328-7

Di Majo, V., Coppola, M., Rebessi, S., Bassani, B., Alati, T., Saran, A., Bangrazi, C., Covelli, V., 1986. Dose-response relationship of radiation-induced harderian gland tumors and myeloid leukemia of the CBA/Cne mouse. J. Natl. Cancer Inst. 76, 955–966.

Di Majo, V., Coppola, M., Rebessi, S., Saran, A., Pazzaglia, S., Pariset, L., Covelli, V., 1996. The influence of sex on life shortening and tumor induction in CBA/Cne mice exposed to X rays or fission neutrons. Radiat. Res. 146, 81–87.

Duran-Struuck, R., Dysko, R.C., 2009. Principles of bone marrow transplantation (BMT): providing optimal veterinary and husbandry care to irradiated mice in BMT studies. J. Am. Assoc. Lab. Anim. Sci. JAALAS 48, 11–22.

Durual, S., Rideau, A., Ruault-Jungblut, S., Cossali, D., Beris, P., Piguet, V., Matthes, T., 2007. Lentiviral PU.1 overexpression restores differentiation in myeloid leukemic blasts. Leukemia 21, 1050–1059. doi:10.1038/sj.leu.2404645

Fennelly, J., Crabtree, G., Macdonald, D., Lorimore, S., Laval, S., Proffitt, J., Boyd, Y., Wright, E., Plumb, M., 1995. Complex Y chromosome aberrations are a recurrent secondary event in radiation-induced murine acute myeloid leukaemia. Leukemia 9, 506–512.

Finnon, R., Brown, N., Moody, J., Badie, C., Olme, C.-H., Huiskamp, R., Meijne, E., Sutmuller, M., Rosemann, M., Bouffler, S.D., 2012. Flt3-ITD mutations in a mouse model of radiation-induced acute myeloid leukaemia. Leukemia 26, 1445–1446. doi:10.1038/leu.2011.377

Fuks, Z., Strober, S., Bobrove, A.M., Sasazuki, T., McMichael, A., Kaplan, H.S., 1976. Long term effects of radiation of T and B lymphocytes in peripheral blood of patients with Hodgkin's disease. J. Clin. Invest. 58, 803–814. doi:10.1172/JCI108532

Futrega, K., Lott, W.B., Doran, M.R., 2016. Direct bone marrow HSC transplantation enhances local engraftment at the expense of systemic engraftment in NSG mice. Sci. Rep. 6, 23886. doi:10.1038/srep23886

Genik, P.C., Vyazunova, I., Steffen, L.S., Bacher, J.W., Bielefeldt-Ohmann, H., McKercher, S., Ullrich, R.L., Fallgren, C.M., Weil, M.M., Ray, F.A., 2014. Leukemogenesis in Heterozygous PU.1 Knockout Mice. Radiat. Res. 140730122200006. doi:10.1667/RR13738.1

Ghisletti, S., Barozzi, I., Mietton, F., Polletti, S., De Santa, F., Venturini, E., Gregory, L., Lonie, L., Chew, A., Wei, C.-L., Ragoussis, J., Natoli, G., 2010. Identification and characterization of enhancers controlling the inflammatory gene expression program in macrophages. Immunity 32, 317–328. doi:10.1016/j.immuni.2010.02.008

Guo, C.-Y., Luo, L., Urata, Y., Goto, S., Huang, W.-J., Takamura, S., Hayashi, F., Doi, H., Kitajima, Y., Ono, Y., Ogi, T., Li, T.-S., 2015. Sensitivity and dose dependency of radiation-induced injury in hematopoietic stem/progenitor cells in mice. Sci. Rep. 5, 8055. doi:10.1038/srep08055

Heinz, S., Benner, C., Spann, N., Bertolino, E., Lin, Y.C., Laslo, P., Cheng, J.X., Murre, C., Singh, H., Glass, C.K., 2010. Simple combinations of lineage-determining transcription factors prime cis-regulatory elements required for macrophage and B cell identities. Mol. Cell 38, 576–589. doi:10.1016/j.molcel.2010.05.004

Hirouchi, T., Akabane, M., Tanaka, S., Braga-Tanaka, I., Todate, A., Ichinohe, K., Oghiso, Y., Tanaka, K., 2011. Cell surface marker phenotypes and gene expression profiles of murine radiation-induced acute myeloid leukemia stem cells are similar to those of common myeloid progenitors. Radiat. Res. 176, 311–322.

Hirouchi, T., Takabatake, T., Yoshida, K., Nitta, Y., Nakamura, M., Tanaka, S., Ichinohe, K., Oghiso, Y., Tanaka, K., 2008. Upregulation of c-myc gene accompanied by PU.1 deficiency in radiation-induced acute myeloid leukemia in mice. Exp. Hematol. 36, 871–885. doi:10.1016/j.exphem.2008.01.015

Hsu, W.-L., Preston, D.L., Soda, M., Sugiyama, H., Funamoto, S., Kodama, K., Kimura, A., Kamada, N., Dohy, H., Tomonaga, M., Iwanaga, M., Miyazaki, Y., Cullings, H.M., Suyama, A., Ozasa, K., Shore, R.E., Mabuchi, K., 2013. The incidence of leukemia, lymphoma and multiple myeloma among atomic bomb survivors: 1950-2001. Radiat. Res. 179, 361–382. doi:10.1667/RR2892.1

Ishikawa, F., Yasukawa, M., Lyons, B., Yoshida, S., Miyamoto, T., Yoshimoto, G., Watanabe, T., Akashi, K., Shultz, L.D., Harada, M., 2005. Development of functional human blood and immune systems in NOD/SCID/IL2 receptor {gamma} chain(null) mice. Blood 106, 1565–1573. doi:10.1182/blood-2005-02-0516

Iwasaki, H., Somoza, C., Shigematsu, H., Duprez, E.A., Iwasaki-Arai, J., Mizuno, S.-I., Arinobu, Y., Geary, K., Zhang, P., Dayaram, T., Fenyus, M.L., Elf, S., Chan, S., Kastner, P., Huettner, C.S., Murray, R., Tenen, D.G., Akashi, K., 2005. Distinctive and indispensable roles of PU.1 in maintenance of hematopoietic stem cells and their differentiation. Blood 106, 1590–1600. doi:10.1182/blood-2005-03-0860

Jawad, M., Cole, C., Zanker, A., Lo, P., Fitch, S., Plumb, M., 2006. Evidence for clustered tumour suppressor gene loci on mouse chromosomes 2 and 4 in radiation-induced acute myeloid leukaemia. Int. J. Radiat. Biol. 82, 383–391. doi:10.1080/09553000600784161

Kamath, M.B., Houston, I.B., Janovski, A.J., Zhu, X., Gowrisankar, S., Jegga, A.G., DeKoter, R.P., 2008. Dose-dependent repression of T-cell and natural killer cell genes by PU.1 enforces myeloid and B-cell identity. Leukemia 22, 1214–1225. doi:10.1038/leu.2008.67

Kaplan, H., Malmgren, J., DeRoos, A., 2012. Increased risk of MDS/AML post radiation treatment for breast cancer: Analysis of SEER data 2001-2008. J. Clin. Oncol. 30, suppl; abstr 6560.

Kayser, S., Döhner, K., Krauter, J., Köhne, C.-H., Horst, H.A., Held, G., von Lilienfeld-Toal, M., Wilhelm, S., Kündgen, A., Götze, K., Rummel, M., Nachbaur, D., Schlegelberger, B., Göhring, G., Späth, D., Morlok, C., Zucknick, M., Ganser, A., Döhner, H., Schlenk, R.F., German-Austrian AMLSG, 2011. The impact of therapy-related acute myeloid leukemia (AML) on outcome in 2853 adult patients with newly diagnosed AML. Blood 117, 2137–2145. doi:10.1182/blood-2010-08-301713

Kendall, G.M., Little, M.P., Wakeford, R., Bunch, K.J., Miles, J.C.H., Vincent, T.J., Meara, J.R., Murphy, M.F.G., 2013. A record-based case-control study of natural background radiation and the incidence of childhood leukaemia and other cancers in Great Britain during 1980-2006. Leukemia 27, 3–9. doi:10.1038/leu.2012.151

Kiel, M.J., Yilmaz, O.H., Iwashita, T., Yilmaz, O.H., Terhorst, C., Morrison, S.J., 2005. SLAM family receptors distinguish hematopoietic stem and progenitor cells and reveal endothelial niches for stem cells. Cell 121, 1109–1121. doi:10.1016/j.cell.2005.05.026

Kogan, S.C., Ward, J.M., Anver, M.R., Berman, J.J., Brayton, C., Cardiff, R.D., Carter, J.S., de Coronado, S., Downing, J.R., Fredrickson, T.N., Haines, D.C., Harris, A.W., Harris, N.L., Hiai, H., Jaffe, E.S., MacLennan, I.C.M., Pandolfi, P.P., Pattengale, P.K., Perkins, A.S., Simpson, R.M., Tuttle, M.S., Wong, J.F., Morse, H.C., Hematopathology subcommittee of the Mouse Models of Human Cancers Consortium, 2002. Bethesda proposals for classification of nonlymphoid hematopoietic neoplasms in mice. Blood 100, 238–245.

Kondo, M., Weissman, I.L., Akashi, K., 1997. Identification of clonogenic common lymphoid progenitors in mouse bone marrow. Cell 91, 661–672.

Krebs, C., Rask-Niehlsen, H.C., Wagner, A., 1930. The Origin of Lymphosarcomatosis and Its Relation to other Forms of Leucosis in White Mice: LYMPHOMATOSIS INFILTRANS LEUCEMICA ET ALEUCEMICA. Acta Radiol. 10, 1–72. doi:10.1177/0284185130011S1001

Krestinina, L.Y., Davis, F.G., Schonfeld, S., Preston, D.L., Degteva, M., Epifanova, S., Akleyev, A.V., 2013. Leukaemia incidence in the Techa River Cohort: 1953-2007. Br. J. Cancer 109, 2886–2893. doi:10.1038/bjc.2013.614

Kueh, H.Y., Champhekar, A., Nutt, S.L., Elowitz, M.B., Rothenberg, E.V., 2013. Positive Feedback Between PU.1 and the Cell Cycle Controls Myeloid Differentiation. Science 341, 670–673. doi:10.1126/science.1240831

Leuraud, K., Richardson, D.B., Cardis, E., Daniels, R.D., Gillies, M., O'Hagan, J.A., Hamra, G.B., Haylock, R., Laurier, D., Moissonnier, M., Schubauer-Berigan, M.K., Thierry-Chef, I., Kesminiene, A., 2015. Ionising radiation and risk of death from leukaemia and lymphoma in radiation-monitored workers (INWORKS): an international cohort study. Lancet Haematol. 2, e276–e281. doi:10.1016/S2352-3026(15)00094-0

Major, I.R., 1979. Induction of myeloid leukaemia by whole-body single exposure of CBA male mice to x-rays. Br. J. Cancer 40, 903–913.

Major, I.R., Mole, R.H., 1978. Myeloid leukaemia in x-ray irradiated CBA mice. Nature 272, 455–456.

Marusyk, A., Casas-Selves, M., Henry, C.J., Zaberezhnyy, V., Klawitter, J., Christians, U., DeGregori, J., 2009. Irradiation Alters Selection for Oncogenic Mutations in Hematopoietic Progenitors. Cancer Res. 69, 7262–7269. doi:10.1158/0008-5472.CAN-09-0604

Mathews, J.D., Forsythe, A.V., Brady, Z., Butler, M.W., Goergen, S.K., Byrnes, G.B., Giles, G.G., Wallace, A.B., Anderson, P.R., Guiver, T.A., McGale, P., Cain, T.M., Dowty, J.G., Bickerstaffe, A.C., Darby, S.C., 2013. Cancer risk in 680 000 people exposed to computed tomography scans in childhood or adolescence: data linkage study of 11 million Australians. BMJ 346, f2360–f2360. doi:10.1136/bmj.f2360

McCollough, C.H., Bushberg, J.T., Fletcher, J.G., Eckel, L.J., 2015. Answers to Common Questions About the Use and Safety of CT Scans. Mayo Clin. Proc. 90, 1380–1392. doi:10.1016/j.mayocp.2015.07.011

Mcculloch, E.A., Till, J.E., 1960. The radiation sensitivity of normal mouse bone marrow cells, determined by quantitative marrow transplantation into irradiated mice. Radiat. Res. 13, 115–125.

McIntosh, B.E., Brown, M.E., Duffin, B.M., Maufort, J.P., Vereide, D.T., Slukvin, I.I., Thomson, J.A., 2015. Nonirradiated NOD,B6.SCID Il2rγ-/- Kit(W41/W41) (NBSGW) mice support multilineage engraftment of human hematopoietic cells. Stem Cell Rep. 4, 171–180. doi:10.1016/j.stemcr.2014.12.005

McKercher, S.R., Torbett, B.E., Anderson, K.L., Henkel, G.W., Vestal, D.J., Baribault, H., Klemsz, M., Feeney, A.J., Wu, G.E., Paige, C.J., Maki, R.A., 1996. Targeted disruption of the PU.1 gene results in multiple hematopoietic abnormalities. EMBO J. 15, 5647–5658.

Metcalf, D., Dakic, A., Mifsud, S., Di Rago, L., Wu, L., Nutt, S., 2006. Inactivation of PU.1 in adult mice leads to the development of myeloid leukemia. Proc. Natl. Acad. Sci. U. S. A. 103, 1486–1491. doi:10.1073/pnas.0510616103

Mizuki, M., Schwable, J., Steur, C., Choudhary, C., Agrawal, S., Sargin, B., Steffen, B., Matsumura, I., Kanakura, Y., Böhmer, F.D., Müller-Tidow, C., Berdel, W.E., Serve, H., 2003. Suppression of myeloid transcription factors and induction of STAT response genes by AML-specific Flt3 mutations. Blood 101, 3164–3173. doi:10.1182/blood-2002-06-1677

Mohrin, M., Bourke, E., Alexander, D., Warr, M.R., Barry-Holson, K., Le Beau, M.M., Morrison, C.G., Passegué, E., 2010. Hematopoietic stem cell quiescence promotes error-prone DNA repair and mutagenesis. Cell Stem Cell 7, 174–185. doi:10.1016/j.stem.2010.06.014

Mole, R.H., Papworth, D.G., Corp, M.J., 1983. The dose-response for x-ray induction of myeloid leukaemia in male CBA/H mice. Br. J. Cancer 47, 285–291.

Moreau-Gachelin, F., Tavitian, A., Tambourin, P., 1988. Spi-1 is a putative oncogene in virally induced murine erythroleukaemias. Nature 331, 277–280. doi:10.1038/331277a0

Mueller, B.U., Pabst, T., Fos, J., Petkovic, V., Fey, M.F., Asou, N., Buergi, U., Tenen, D.G., 2006. ATRA resolves the differentiation block in t(15;17) acute myeloid leukemia by restoring PU.1 expression. Blood 107, 3330–3338. doi:10.1182/blood-2005-07-3068

Mueller, B.U., Pabst, T., Osato, M., Asou, N., Johansen, L.M., Minden, M.D., Behre, G., Hiddemann, W., Ito, Y., Tenen, D.G., 2002. Heterozygous PU.1 mutations are associated with acute myeloid leukemia. Blood 100, 998–1007.

Nakada, D., Oguro, H., Levi, B.P., Ryan, N., Kitano, A., Saitoh, Y., Takeichi, M., Wendt, G.R., Morrison, S.J., 2014. Oestrogen increases haematopoietic stem-cell self-renewal in females and during pregnancy. Nature 505, 555–558. doi:10.1038/nature12932

Nakanishi, M., Tanaka, K., Shintani, T., Takahashi, T., Kamada, N., 1999. Chromosomal instability in acute myelocytic leukemia and myelodysplastic syndrome patients among atomic bomb survivors. J. Radiat. Res. (Tokyo) 40, 159–167.

Nikkilä, A., Erme, S., Arvela, H., Holmgren, O., Raitanen, J., Lohi, O., Auvinen, A., 2016. Background radiation and childhood leukemia: A nationwide register-based case-control study. Int. J. Cancer 139, 1975–1982. doi:10.1002/ijc.30264

Nugent, S.M.E., Mothersill, C.E., Seymour, C., McClean, B., Lyng, F.M., Murphy, J.E.J., 2007. Increased mitochondrial mass in cells with functionally compromised

mitochondria after exposure to both direct γ radiation and bystander factors. Radiat. Res. 168, 134_142. doi:10.1667/RR0769.1

Nutt, S.L., Metcalf, D., D'Amico, A., Polli, M., Wu, L., 2005. Dynamic regulation of PU.1 expression in multipotent hematopoietic progenitors. J. Exp. Med. 201, 221–231. doi:10.1084/jem.20041535

O'Connell, R.M., Rao, D.S., Chaudhuri, A.A., Boldin, M.P., Taganov, K.D., Nicoll, J., Paquette, R.L., Baltimore, D., 2008. Sustained expression of microRNA-155 in hematopoietic stem cells causes a myeloproliferative disorder. J. Exp. Med. 205, 585–594. doi:10.1084/jem.20072108

Okuno, Y., Huang, G., Rosenbauer, F., Evans, E.K., Radomska, H.S., Iwasaki, H., Akashi, K., Moreau-Gachelin, F., Li, Y., Zhang, P., Göttgens, B., Tenen, D.G., 2005. Potential autoregulation of transcription factor PU.1 by an upstream regulatory element. Mol. Cell. Biol. 25, 2832–2845. doi:10.1128/MCB.25.7.2832-2845.2005

Olme, C.-H., Brown, N., Finnon, R., Bouffler, S.D., Badie, C., 2013a. Frequency of acute myeloid leukaemia-associated mouse chromosome 2 deletions in X-ray exposed immature haematopoietic progenitors and stem cells. Mutat. Res. 756, 119–126. doi:10.1016/j.mrgentox.2013.04.018

Olme, C.-H., Finnon, R., Brown, N., Kabacik, S., Bouffler, S.D., Badie, C., 2013b. Live cell detection of chromosome 2 deletion and Sfpi1/PU1 loss in radiation-induced mouse acute myeloid leukaemia. Leuk. Res. 37, 1374–1382. doi:10.1016/j.leukres.2013.05.019

Pang, W.W., Price, E.A., Sahoo, D., Beerman, I., Maloney, W.J., Rossi, D.J., Schrier, S.L., Weissman, I.L., 2011. Human bone marrow hematopoietic stem cells are increased in frequency and myeloid-biased with age. Proc. Natl. Acad. Sci. 108, 20012–20017. doi:10.1073/pnas.1116110108

Pearce, M.S., Salotti, J.A., Little, M.P., McHugh, K., Lee, C., Kim, K.P., Howe, N.L., Ronckers, C.M., Rajaraman, P., Craft, A.W., Parker, L., Berrington de González, A., 2012. Radiation exposure from CT scans in childhood and subsequent risk of leukaemia and brain tumours: a retrospective cohort study. The Lancet 380, 499–505. doi:10.1016/S0140-6736(12)60815-0

Pedersen-Bjergaard, J., Andersen, M.K., Andersen, M.T., Christiansen, D.H., 2008. Genetics of therapy-related myelodysplasia and acute myeloid leukemia. Leukemia 22, 240–248. doi:10.1038/sj.leu.2405078

Peng, Y., Brown, N., Finnon, R., Warner, C.L., Liu, X., Genik, P.C., Callan, M.A., Ray, F.A., Borak, T.B., Badie, C., Bouffler, S.D., Ullrich, R.L., Bedford, J.S., Weil, M.M., 2009. Radiation leukemogenesis in mice: loss of PU.1 on chromosome 2 in CBA and C57BL/6 mice after irradiation with 1 GeV/nucleon 56Fe ions, X rays or gamma rays. Part I. Experimental observations. Radiat. Res. 171, 474–483. doi:10.1667/RR1547.1

Pietras, E.M., Mirantes-Barbeito, C., Fong, S., Loeffler, D., Kovtonyuk, L.V., Zhang, S., Lakshminarasimhan, R., Chin, C.P., Techner, J.-M., Will, B., Nerlov, C., Steidl, U., Manz, M.G., Schroeder, T., Passegué, E., 2016. Chronic interleukin-1 exposure drives haematopoietic stem cells towards precocious myeloid differentiation at the expense of self-renewal. Nat. Cell Biol. 18, 607–618. doi:10.1038/ncb3346

Prochazka, M., Gaskins, H.R., Shultz, L.D., Leiter, E.H., 1992. The nonobese diabetic scid mouse: model for spontaneous thymomagenesis associated with immunodeficiency. Proc. Natl. Acad. Sci. U. S. A. 89, 3290–3294.

Qing, Y., Lin, Y., Gerson, S.L., 2012. An intrinsic BM hematopoietic niche occupancy defect of HSC in scid mice facilitates exogenous HSC engraftment. Blood 119, 1768–1771. doi:10.1182/blood-2011-05-350611

Radivoyevitch, T., Sachs, R.K., Gale, R.P., Molenaar, R.J., Brenner, D.J., Hill, B.T., Kalaycio, M.E., Carraway, H.E., Mukherjee, S., Sekeres, M.A., Maciejewski, J.P., 2016. Defining AML and MDS second cancer risk dynamics after diagnoses of first cancers treated or not with radiation. Leukemia 30, 285–294. doi:10.1038/leu.2015.258

Rithidech, K., Dunn, J.J., Roe, B.A., Gordon, C.R., Cronkite, E.P., 2002. Evidence for two commonly deleted regions on mouse chromosome 2 in gamma ray-induced acute myeloid leukemic cells. Exp. Hematol. 30, 564–570.

Rithidech, K.N., Bond, V.P., Cronkite, E.P., Thompson, M.H., 1993. A specific chromosomal deletion in murine leukemic cells induced by radiation with different qualities. Exp. Hematol. 21, 427–431.

Rithidech, K.N., Cronkite, E.P., Bond, V.P., 1999. Advantages of the CBA mouse in leukemogenesis research. Blood Cells. Mol. Dis. 25, 38–45. doi:10.1006/bcmd.1999.0225

Rivina, L., Schiestl, R., 2013. Mouse models for efficacy testing of agents against radiation carcinogenesis—a literature review. Int. J. Environ. Res. Public. Health 10, 107–143. doi:10.3390/ijerph10010107

Rosenbauer, F., Wagner, K., Kutok, J.L., Iwasaki, H., Le Beau, M.M., Okuno, Y., Akashi, K., Fiering, S., Tenen, D.G., 2004. Acute myeloid leukemia induced by graded reduction of a lineage-specific transcription factor, PU.1. Nat. Genet. 36, 624–630. doi:10.1038/ng1361

Scott, E.W., Fisher, R.C., Olson, M.C., Kehrli, E.W., Simon, M.C., Singh, H., 1997. PU.1 functions in a cell-autonomous manner to control the differentiation of multipotential lymphoid-myeloid progenitors. Immunity 6, 437–447.

Scott, E.W., Simon, M.C., Anastasi, J., Singh, H., 1994. Requirement of transcription factor PU.1 in the development of multiple hematopoietic lineages. Science 265, 1573–1577.

Shao, L., Feng, W., Li, H., Gardner, D., Luo, Y., Wang, Y., Liu, L., Meng, A., Sharpless, N.E., Zhou, D., 2014. Total body irradiation causes long-term mouse BM injury via induction of HSC premature senescence in an Ink4a- and Arf-independent manner. Blood 123, 3105–3115. doi:10.1182/blood-2013-07-515619

Shore, R.E., 2014. Radiation Impacts on Human Health: Certain, Fuzzy, and Unknown. Health Phys. 106, 196–205. doi:10.1097/HP.0000000000000021

Shultz, L.D., Lyons, B.L., Burzenski, L.M., Gott, B., Chen, X., Chaleff, S., Kotb, M., Gillies, S.D., King, M., Mangada, J., Greiner, D.L., Handgretinger, R., 2005. Human lymphoid and myeloid cell development in NOD/LtSz-scid IL2R gamma null mice engrafted with mobilized human hemopoietic stem cells. J. Immunol. Baltim. Md 1950 174, 6477–6489.

Silver, A., Moody, J., Dunford, R., Clark, D., Ganz, S., Bulman, R., Bouffler, S., Finnon, P., Meijne, E., Huiskamp, R., Cox, R., 1999. Molecular mapping of chromosome 2 deletions in murine radiation-induced AML localizes a putative tumor

suppressor gene to a 1.0 cM region homologous to human chromosome segment 11p11-12. Genes. Chromosomes Cancer 24, 95–104.

Simonnet, A.J., Nehmé, J., Vaigot, P., Barroca, V., Leboulch, P., Tronik-Le Roux, D., 2009. Phenotypic and Functional Changes Induced in Hematopoietic Stem/Progenitor Cells After Gamma-Ray Radiation Exposure. Stem Cells 27, 1400–1409. doi:10.1002/stem.66

Spangrude, G.J., Brooks, D.M., 1993. Mouse strain variability in the expression of the hematopoietic stem cell antigen Ly-6A/E by bone marrow cells. Blood 82, 3327–3332.

Spycher, B.D., Lupatsch, J.E., Zwahlen, M., Röösli, M., Niggli, F., Grotzer, M.A., Rischewski, J., Egger, M., Kuehni, C.E., 2015. Background Ionizing Radiation and the Risk of Childhood Cancer: A Census-Based Nationwide Cohort Study. Environ. Health Perspect. doi:10.1289/ehp.1408548

Staber, P.B., Zhang, P., Ye, M., Welner, R.S., Levantini, E., Di Ruscio, A., Ebralidze, A.K., Bach, C., Zhang, H., Zhang, J., Vanura, K., Delwel, R., Yang, H., Huang, G., Tenen, D.G., 2014. The Runx-PU.1 pathway preserves normal and AML/ETO9a leukemic stem cells. Blood 124, 2391–2399. doi:10.1182/blood-2014-01-550855

Staber, P.B., Zhang, P., Ye, M., Welner, R.S., Nombela-Arrieta, C., Bach, C., Kerenyi, M., Bartholdy, B.A., Zhang, H., Alberich-Jordà, M., Lee, S., Yang, H., Ng, F., Zhang, J., Leddin, M., Silberstein, L.E., Hoefler, G., Orkin, S.H., Göttgens, B., Rosenbauer, F., Huang, G., Tenen, D.G., 2013. Sustained PU.1 Levels Balance Cell-Cycle Regulators to Prevent Exhaustion of Adult Hematopoietic Stem Cells. Mol. Cell 49, 934–946. doi:10.1016/j.molcel.2013.01.007

Steffen, L.S., Bacher, J.W., Peng, Y., Le, P.N., Ding, L.-H., Genik, P.C., Ray, F.A., Bedford, J.S., Fallgren, C.M., Bailey, S.M., Ullrich, R.L., Weil, M.M., Story, M.D., 2013. Molecular characterisation of murine acute myeloid leukaemia induced by 56Fe ion and 137Cs gamma ray irradiation. Mutagenesis 28, 71–79. doi:10.1093/mutage/ges055

Steidl, U., Rosenbauer, F., Verhaak, R.G.W., Gu, X., Ebralidze, A., Otu, H.H., Klippel, S., Steidl, C., Bruns, I., Costa, D.B., Wagner, K., Aivado, M., Kobbe, G., Valk, P.J.M., Passegué, E., Libermann, T.A., Delwel, R., Tenen, D.G., 2006. Essential role of Jun family transcription factors in PU.1 knockdown-induced leukemic stem cells. Nat. Genet. 38, 1269–1277. doi:10.1038/ng1898

Storer, J.B., 1966. Longevity and gross pathology at death in 22 inbred mouse strains. J. Gerontol. 21, 404–409.

Suraweera, N., Meijne, E., Moody, J., Carvajal-Carmona, L.G., Yoshida, K., Pollard, P., Fitzgibbon, J., Riches, A., van Laar, T., Huiskamp, R., Rowan, A., Tomlinson, I.P.M., Silver, A., 2005. Mutations of the PU.1 Ets domain are specifically associated with murine radiation-induced, but not human therapy-related, acute myeloid leukaemia. Oncogene 24, 3678–3683. doi:10.1038/sj.onc.1208422

Travis, L.B., Andersson, M., Gospodarowicz, M., van Leeuwen, F.E., Bergfeldt, K., Lynch, C.F., Curtis, R.E., Kohler, B.A., Wiklund, T., Storm, H., Holowaty, E., Hall, P., Pukkala, E., Sleijfer, D.T., Clarke, E.A., Boice, J.D., Stovall, M., Gilbert, E., 2000. Treatment-associated leukemia following testicular cancer. J. Natl. Cancer Inst. 92, 1165–1171.

Turkistany, S.A., DeKoter, R.P., 2011. The transcription factor PU.1 is a critical regulator of cellular communication in the immune system. Arch. Immunol. Ther. Exp. (Warsz.) 59, 431–440. doi:10.1007/s00005-011-0147-9

Upton, A.C., 2008. Studies on the Mechanism of Leukaemogenesis by Ionizing Radiation, in: Wolstenholme, G.E.W., O'Connor, M. (Eds.), Novartis Foundation Symposia. John Wiley & Sons, Ltd., Chichester, UK, pp. 249–273.

Upton, A.C., 1986. Radiation carcinogenesis. Elsevier, New York.

Upton, A.C., Odell, T.T., Sniffen, E.P., 1960. Influence of Age at Time of Irradiation on Induction of Leukemia and Ovarian Tumors in RF Mice. Exp. Biol. Med. 104, 769–772. doi:10.3181/00379727-104-25982

Vangala, R.K., Heiss-Neumann, M.S., Rangatia, J.S., Singh, S.M., Schoch, C., Tenen, D.G., Hiddemann, W., Behre, G., 2003. The myeloid master regulator transcription factor PU.1 is inactivated by AML1-ETO in t(8;21) myeloid leukemia. Blood 101, 270–277. doi:10.1182/blood-2002-04-1288

Vazquez, S.E., Inlay, M.A., Serwold, T., 2015. CD201 and CD27 identify hematopoietic stem and progenitor cells across multiple murine strains independently of Kit and Sca-1. Exp. Hematol. 43, 578–585. doi:10.1016/j.exphem.2015.04.001

Verbiest, T., Bouffler, S., Nutt, S.L., Badie, C., 2015. PU.1 downregulation in murine radiation-induced acute myeloid leukaemia (AML): from molecular mechanism to human AML. Carcinogenesis 36, 413–419. doi:10.1093/carcin/bgv016

Walter, M.J., Park, J.S., Ries, R.E., Lau, S.K.M., McLellan, M., Jaeger, S., Wilson, R.K., Mardis, E.R., Ley, T.J., 2005. Reduced PU.1 expression causes myeloid progenitor expansion and increased leukemia penetrance in mice expressing PML-RARalpha. Proc. Natl. Acad. Sci. U. S. A. 102, 12513–12518. doi:10.1073/pnas.0504247102

Weil, M.M., Bedford, J.S., Bielefeldt-Ohmann, H., Ray, F.A., Genik, P.C., Ehrhart, E.J., Fallgren, C.M., Hailu, F., Battaglia, C.L.R., Charles, B., Callan, M.A., Ullrich, R.L., 2009. Incidence of acute myeloid leukemia and hepatocellular carcinoma in mice irradiated with 1 GeV/nucleon (56)Fe ions. Radiat. Res. 172, 213–219. doi:10.1667/RR1648.1

Welch, J.S., Ley, T.J., Link, D.C., Miller, C.A., Larson, D.E., Koboldt, D.C., Wartman, L.D., Lamprecht, T.L., Liu, F., Xia, J., Kandoth, C., Fulton, R.S., McLellan, M.D., Dooling, D.J., Wallis, J.W., Chen, K., Harris, C.C., Schmidt, H.K., Kalicki-Veizer, J.M., Lu, C., Zhang, Q., Lin, L., O'Laughlin, M.D., McMichael, J.F., Delehaunty, K.D., Fulton, L.A., Magrini, V.J., McGrath, S.D., Demeter, R.T., Vickery, T.L., Hundal, J., Cook, L.L., Swift, G.W., Reed, J.P., Alldredge, P.A., Wylie, T.N., Walker, J.R., Watson, M.A., Heath, S.E., Shannon, W.D., Varghese, N., Nagarajan, R., Payton, J.E., Baty, J.D., Kulkarni, S., Klco, J.M., Tomasson, M.H., Westervelt, P., Walter, M.J., Graubert, T.A., DiPersio, J.F., Ding, L., Mardis, E.R., Wilson, R.K., 2012. The origin and evolution of mutations in acute myeloid leukemia. Cell 150, 264–278. doi:10.1016/j.cell.2012.06.023

Wingert, S., Thalheimer, F.B., Haetscher, N., Rehage, M., Schroeder, T., Rieger, M.A., 2016. DNA-damage response gene GADD45A induces differentiation in hematopoietic stem cells without inhibiting cell cycle or survival. Stem Cells Dayt. Ohio 34, 699–710. doi:10.1002/stem.2282

Wright, J.D., St Clair, C.M., Deutsch, I., Burke, W.M., Gorrochurn, P., Sun, X., Herzog, T.J., 2010. Pelvic radiotherapy and the risk of secondary leukemia and multiple myeloma. Cancer 116, 2486–2492. doi:10.1002/cncr.25067

Yakes, F.M., Van Houten, B. 1997. Mitochondrial DNA damage is more extensive and persists longer than nuclear DNA damage in human cells following oxidative stress. Proc. Natl. Acad. Sci. 94, 514–519.

Yoshida, K., Nemoto, K., Nishimura, M., Seki, M., 1993. Exacerbating factors of radiation-induced myeloid leukemogenesis. Leuk. Res. 17, 437–440.

Youle, R.J., van der Bliek, A.M. 2012. Mitochondrial fission, fusion, and stress. Science. 337, 1062–1065. doi:10.1126/science.1219855

Yu, G.-P., Schantz, S.P., Neugut, A.I., Zhang, Z.-F., 2006. Incidences and trends of second cancers in female breast cancer patients: a fixed inception cohort-based analysis (United States). Cancer Causes Control CCC 17, 411–420. doi:10.1007/s10552-005-0338-y

# CHAPTER 7

*Appendix*

## 7. Appendix

OXFORD

*Carcinogenesis*, 2015, Vol. 36, No. 4, 413–419

doi:10.1093/carcin/bgv016
Advance Access publication March 6, 2015
Review

REVIEW

# PU.1 downregulation in murine radiation-induced acute myeloid leukaemia (AML): from molecular mechanism to human AML

Tom Verbiest[1,2], Simon Bouffler[1], Stephen L.Nutt[3,4] and Christophe Badie[1,*]

[1]Biological Effects Department, Centre for Radiation, Chemical and Environmental Hazards, Public Health England, Didcot OX11 ORQ, UK, [2]CRUK & MRC Oxford Institute for Radiation Oncology, Department of Oncology, University of Oxford, Oxford OX3 7DQ, UK, [3]Walter and Eliza Hall Institute of Medical Research, 1G Royal Parade, Parkville, Victoria 3052, Australia and [4]Department of Medical Biology, University of Melbourne, Parkville, Victoria 3010, Australia

*To whom correspondence should be addressed. Tel: +441235825088; Fax: +441235833891 Email: christophe.badie@phe.gov.uk

## Abstract

The transcription factor PU.1, encoded by the murine *Sfpi1* gene (*SPI1* in humans), is a member of the Ets transcription factor family and plays a vital role in commitment and maturation of the myeloid and lymphoid lineages. Murine studies directly link primary acute myeloid leukaemia (AML) and decreased PU.1 expression in specifically modified strains. Similarly, a radiation-induced chromosome 2 deletion and subsequent *Sfpi1* point mutation in the remaining allele lead to murine radiation-induced AML. Consistent with murine data, heterozygous deletion of the *SPI1* locus and mutation of the −14 kb *SPI1* upstream regulatory element were described previously in human primary AML, although they are rare events. Other mechanisms linked to PU.1 downregulation in human AML include *TP53* deletion, *FLT3*-ITD mutation and the recurrent AML1-ETO [t(8;21)] and PML-RARA [t(15;17)] translocations. This review provides an up-to-date overview on our current understanding of the involvement of PU.1 in the initiation and development of radiation-induced AML, together with recommendations for future murine and human studies.

## Introduction

Just over a decade following the discovery of X-rays by Wilhelm Roentgen in 1895, the first cases of leukaemia were suspected in medical radiation workers (1). Over the past 70 years, a variety of epidemiological studies provided support for an increased leukaemia incidence after both high and low dose radiation exposure (radiotherapy and CT-scan, respectively). The continuing epidemiological survey of the Japanese atomic bomb survivors estimates that ~50% of all leukaemia cases observed in survivors exposed to >5 mGy, are associated with radiation exposure. Remarkably, over the last 15 years of this follow-up, acute myeloid leukaemia (AML) became the pre-dominant radiation-associated leukaemia, accounting for ~80% of excess leukaemia cases (2). Although a clear association between radiation exposure and leukaemia development is acknowledged, today, 80 years since two-time Nobel Prize winner Marie Curie died of radiation-induced leukaemia, the underlying mechanisms remain unidentified. Elucidating the cytogenetic and molecular alterations in murine radiation-induced AML (rAML) should provide further insight in the genetic basis of human radiation leukaemogenesis. Here we provide an overview on our current understanding of the involvement of the haematopoietic transcription factor PU.1 in the initiation and development of murine rAML, and seek to further define its involvement in human primary and therapy-related AML (tAML).

## Murine modelling of rAML

Since 99% of human protein-coding genes are also present in mice and given the power of murine genetic interventions (including gene knock-in/-down), the use of murine models remains the most representative and ethical option available to study the cytogenetic and molecular mechanisms underlying radiation leukaemogenesis. The CBA mouse strain is regarded

Received: November 18, 2014; Revised: February 4, 2015; Accepted: February 24, 2015

© The Author 2015. Published by Oxford University Press.
This is an Open Access article distributed under the terms of the Creative Commons Attribution Non-Commercial License (http://creativecommons.org/licenses/by-nc/4.0/), which permits non-commercial re-use, distribution, and reproduction in any medium, provided the original work is properly cited. For commercial re-use, please contact journals.permissions@oup.com